University of Bath

UNIVERSITY OF BATH

PHD

Thermodynamic Analysis of Air Source Heat Pumps and Micro Combined Heat and Power Units Participating in a Distributed Energy Future

Cooper, Sam

Award date:
2013

Awarding institution:
University of Bath

Link to publication

THERMODYNAMIC ANALYSIS OF AIR SOURCE HEAT PUMPS AND MICRO COMBINED HEAT AND POWER UNITS PARTICIPATING IN A DISTRIBUTED ENERGY FUTURE

Samuel J. G. Cooper

A thesis submitted for the degree of Doctor of Philosophy

University of Bath

Department of Mechanical Engineering

April 2013

Contents overview

Detailed contents list

Tables

Figures

Acknowledgements

Many people have contributed to the completion of this research and I am grateful to them all.

Many thanks to my supervisors: Geoff Hammond and Marcelle McManus for your help, direction, patience and encouragement. Also, many thanks to Irene Turner for the numerous insightful suggestions which have helped shaped this thesis from a jumble of thoughts into a legible piece of work.

Thank you to everyone in the Sustainable Energy Research Team for your time, friendship, edible treats and for making my time here very enjoyable.

Finally, thank you to Carolyn. You have shown me so much patience and unwavering support throughout this study. You are the best and I love you.

Abstract

Achieving the reductions in carbon dioxide emissions which are necessary will require improvements in the way in which domestic space heating is supplied. Air Source Heat Pumps and micro-Combined Heat and Power units both have the potential to reduce emissions while using primary energy resources more efficiently. The performance which these technologies can achieve is fundamental to fulfilling this potential and yet it is still subject to some uncertainty. This thesis analyses the performance of Air Source Heat Pumps and micro-Combined Heat and Power units in terms of their energy and exergy requirements and in terms of the carbon dioxide emissions associated with their operation.

A review of the literature identified that it was appropriate to develop a novel modelling approach. Models of many components currently exist and these are adopted and extended wherever possible within this modelling approach. However, it is the unique way in which this research combines these models and adds additional components which delivers performance data relating to a wider range of conditions at a greater level of detail than that which was previously available. The model which was developed can dynamically simulate the heating and power demands in many dwellings simultaneously, facilitating meaningful study of effects which are dependent upon the sum of their power flows. Consideration of the effect of operating conditions includes permutations of climate, control systems (including those which engage with demand side management), grid generation mixes and building properties.

Efficient Air Source Heat Pumps units have the potential to make energy and carbon emissions savings at present but their performance is sensitive to the conditions studied. In particular, appropriate control of the units can yield energy savings of around 25%. Additionally, the carbon emissions intensity of the grid is an important consideration which is explored in depth.

Currently, energy requirements and carbon emissions can be reduced by the use of micro-Combined Heat and Power units. Their potential to further reduce carbon emissions diminishes if the grid is predominantly decarbonised but units with high electrical efficiencies can still save energy. The effect of the control approach which is adopted is also significant and has different effects on fuel-cell based units compared to combustion-based units.

The key contribution of this work is the analysis of performance data for a selection of units operating under a range of conditions, calculated with a consistent, accurate methodology. Comparison is made between the technologies and between the effects of different operating conditions. A second significant contribution of this work is the development of the model which was used to generate the performance results. These advances allow more detailed comparative analysis of performance data in a wider range of conditions than previously possible.

Abbreviations

A nomenclature of symbols used in diagrams and equations in provided as Appendix B.

ASHP	Air Source Heat Pump
BoP	Balance of Plant
CC	Central Coordination, name of a hypothetical future grid generation scenario.
CCGT	Ground Source Heat Pump
CCS	Carbon Capture and Storage
CEF	Mean Carbon Emissions Factor
CHP	Combined Heat and Power
CO_2	Carbon Dioxide
DCLG	Department For Communities And Local Government
DECC	Department for Energy and Climate Change
DER	Dwelling Emissions Rate, refers to building standards / SAP
EC	European Community
ECBCS	Energy Conservation in Buildings and Community Energy
EST	Energy Saving Trust
EPSRC	Engineering and Physical Sciences Research Council
HHV	Higher Heating Value, enthalpy of combustion of fuel including energy released as water vapour product is condensed.
GCV	Gross Calorific Value, i.e. HHV
GSHP	Ground Source Heat Pump
GT	Gas Turbine
GWP	Global Warming Potential, measured relative to CO_2
ICE	Internal Combustion Engine
IEA	International Energy Agency
LHV	Lower Heating Value, enthalpy of combustion of fuel excluding energy released as water vapour product is condensed.
mCHP	Micro Combined Heat and Power
MEF	Marginal Carbon Emissions Factor
MR	Market Rules, name of a hypothetical future grid generation scenario.
NCV	Net Calorific Value, i.e. LHV
ORC	Organic Rankine Cycle
PEMFC	Polymer Electrolyte (or Proton Exchange) Membrane Fuel Cell
PER	Primary Energy Requirement
PMV	Predicted Mean Vote, a measure of thermal comfort.
PV	(solar) Photovoltaic
SAP	Standard Assessment Procedure, a standardised steady-state assessment of building energy performance
SE	Stirling Engine
SOFC	Solid Oxide Fuel Cell
TER	Target Emissions Rate, refers to building standards / SAP
TF	Thousand Flowers, name of a hypothetical future grid generation scenario.
UKERC	UK Energy Research Council

1. Introduction

1.1 Analysis of Air Source Heat Pumps and micro Combined Heat and Power units.

There is a clear requirement to reduce Carbon Dioxide (CO_2) emissions (IPCC 2007; Stern 2006). In the UK this requirement has been formalised as a legislative obligation to achieve an 80% reduction in CO_2 emissions rates (relative to 1990 rates) by 2050 (HM Government 2008). Achieving this will require a substantial change to the way in which domestic space heating is provided. Although options such as the use of biomass and improvements in the insulation of dwellings are likely to fulfil some of this requirement, most proposals include the electrification of heating with decarbonised electricity (DECC 2012; Boardman 2007b; DECC 2009b).

Air Source Heat Pumps (ASHP) and micro-Combined Heat and Power (mCHP) units both have the potential to contribute to achieving a low-carbon society and so it is necessary to understand the ways in which operating conditions may affect their performance. Their performance characteristics are of particular interest given that both technologies have significant electrical power flows associated with them in addition to heat flows. Field trials (e.g. Carbon Trust 2011; Lipp 2012; Energy Saving Trust 2010) and modelling (e.g. Kelly & Cockroft 2011; Dorer & Weber 2009) have demonstrated that a range of performances might be achieved by the units, depending upon both the characteristics of the units themselves but also the conditions in which they are operated. A wider study of the relative effect that these factors have is therefore justified. A range of technologies is available and so it will be more relevant to investigate the trends which occur rather than the performance of specific devices under specific circumstances. In particular, as it is possible that the technologies will see much wider adoption in the future, the conditions in which the units may operate in the future are arguably more relevant. Consideration of these conditions should include both the factors seen at present (e.g. variations in climate) and those not (e.g. the potential influence of demand side management systems).

1.2 Preliminary Aim

The general aim of this study is therefore to evaluate the thermodynamic and CO_2 emissions performance of ASHP and mCHP units in the context of the range of conditions they may experience over the period of the next 40 years. The specific range of conditions to be considered and the ways in which this should be achieved are explained in more detail in the Aims (page 66).

1.3 Layout of thesis

The background to the study (chapter 2) will review the literature and introduce the technologies being analysed (Figure 1). It starts by demonstrating that there is a significant need for low carbon domestic heating and that both ASHP and mCHP units have the potential to make important contributions. ASHP and mCHP systems are then described in more detail and the state of the current development of each technology is examined. The chapter goes on to provide some considerations which are relevant regarding the metrics used to analyse the performance of the technologies (energy, exergy and CO_2 emissions). Finally, the relevant comparable modelling studies which are documented in the literature are reviewed; in particular, the approaches taken are discussed and additional needs are identified.

The aims of this work are then presented in chapter 3; in light of the potential significance of these systems, which aspects of their performance does this research seek to explore?

This leads to a full description of the modelling approach developed within this research (chapter 4); aiming to address these requirements and enable analysis of the performance of the units in a way which fulfills the objectives of the study.

Results are presented in chapter 5; considering and discussing the effect of each aspect of the scenarios in which the units may operate. Key observations are then summarised and conclusions are drawn regarding their relevance and application in chapter 6. The ways in which these findings address the objectives of the study and contribute to the field of knowledge are highlighted at the end of the chapter. The thesis ends with recommendations and suggestions for further research (chapter 7).

Background
- *The need for low-carbon heating*
- *Introducing the technologies*
- *How their performance will be assessed*
- *Consideration of previous modelling*

Aims
- *Detailed, identified aims of this research. Parameters to consider when generating results and requirements for modelling*

Modelling
- *Overview of the modelling approach which was developed*
- *Description of each component of the model and the parameters used to generate results*

Results
- *Results, illustrating the effect of different parameters and operating conditions on the performance of the selected units*

Conclusions
- *Summary of key findings*
- *Conclusions – how the study has met its aims and made a contribution*
- *Recommendations for future study*

Figure 1: Layout of thesis

2.   Background to study

This chapter firstly considers the need for low carbon domestic heating and demonstrates that it is appropriate to consider the role which ASHP and mCHP units may play in fulfilling this need. The technologies are then examined before a description of the way in which metrics of their performance are used in this study. Previous modelling work is reviewed leading to conclusions regarding the requirements for modelling if it is to contribute to this field of knowledge.

2.1 The need for low carbon domestic heating

2.1.1   Emissions reductions requirements

By 2050, the UK will need to reduce emissions of CO_2 by 80% in order to fulfil obligations laid out under the Climate Change Act (HM Government 2008). In the shorter term, a reduction of 34% is required by 2020 (both relative to 1990 emissions). In addition, 15% of our energy will need to be supplied from renewable resources and it is intended that part of this obligation will be met by a tenfold increase in the supply of renewable heating (DECC 2007).

The imperative to reduce CO_2 emissions is firmly established. The Intergovernmental Panel on Climate Change's Fourth Assessment report (AR4) (IPCC 2007) builds upon previous studies in presenting evidence for anthropogenic climate change, noting that current CO_2 concentration is almost 40% higher than before the Industrial Revolution and that there has been an average temperature rise of approximately 0.75ºC since 1900. In order to have a 50% probability of temperatures not rising more than 2ºC above pre-industrial levels, a maximum atmospheric CO_2 concentration of 450ppm is suggested, implying a worldwide reduction in the rate of CO_2 emissions before 2020 and a reduction to 50% of 1990 emissions rates by 2050.

At the same time, economic studies have presented the potential costs of climate change to the economy. It is estimated that, without mitigation, a 5ºC average temperature rise is feasible over the next century and that this will cost the world economy the equivalent of 5% – 20% of its gross product (Stern 2006). Given that the cost of stabilising CO_2 concentration at 450 – 550ppm is estimated at 1% - 2% of gross global product, there is a clear impetus for action.

Depleting conventional fossil fuel reserves may lead to reduced energy security and the potential for higher and more volatile fuel prices (Sorrell et al. 2010; Fantazzini et al. 2011). The extent to which the increasing use of unconventional reserves is likely to alleviate this is not yet clear. In any case there is motivation to reduce dependence on fossil fuels, through substitution or improved efficiency, especially in roles such as space heating where high quality energy vectors are not inherently necessary.

The UK Low Carbon Transition Plan (DECC 2009b) presents the policies that are intended to deliver the shorter term emissions targets. Principally, it is intended that there will be an increase in the share of electricity generated from low carbon sources to 40%, driven by extensions to the Renewables Obligations (Secretary of State 2010) and the retirement of some coal plant in 2016 due to the Large Combustion Plant Directive (EC 2001). This is likely to reduce the carbon emissions factor (CEF) of grid supplied electricity to around 340 g_{CO2}/kWh to 360g_{CO2}/kWh. This analysis has recently been supplemented by the 2050 Pathways analysis (DECC 2010a) looking further ahead to consider possible scenarios.

In parallel, the EU directive on use of Renewable Energy (EC 2009) commits to 20% of energy in the EU being supplied by renewables by 2020. In response to this, the UK is committed to 15% of energy being supplied by renewables. Interim targets are 7.5% by 2016 and then 10% by 2018. In addition to electrical generation and transport, it is intended that a large part of this will be met by a tenfold increase of renewable heating from 7.7TWh in 2008 to 72TWh in 2020 (DECC 2007).

Various scenarios have been investigated by different academic groups in support of this planning. The UKERC "Pathways to a Low Carbon Economy" project has modelled possible scenarios using the MARKAL economic optimisation modelling tool (Anandarajah et al. 2009). Under the SUPERGEN consortium, supply side modelling has been combined with the UK Domestic Carbon Model demand side model to produce scenarios for use in exploring the effect of extensive penetration of decentralised generation (Supergen HDPS 2006; Jardine & Ault 2008). The EPSRC "Transition Pathways to a Low Carbon Economy" project considers the ways in which this transition may take place (Foxon 2013; Foxon et al. 2010). Because of the detail available on these "Transition Pathways" scenarios, they are used as background to some of the analysis presented later in this work (see chapter 4, section 4.6.3). Although the various scenarios vary in details and in underlying assumptions, they all include significant decarbonisation of the supply of heat to the domestic sector. This is mainly achieved through decarbonisation of the electricity sector along with increased electrification of heating.

2.1.2   Overview of domestic energy use and carbon emissions

The Low Carbon Transition Plan (DECC 2009b) aims for a 29% reduction in the direct CO_2 emissions from the domestic sector by 2020. This is necessary given that 12% of the UK's CO_2 emissions are direct emissions from domestic space heating and hot water (DHW) systems with an additional 10% attributable to the generation of the electricity used in homes (Figure 2 illustrates the proportions of these emissions within the domestic sector). Every realistic proposed scenario for achieving a significant reduction in CO_2 emissions includes a reduction in the emissions associated with both of these energy demands. In fact, to achieve an 80%

reduction in CO_2 emissions, domestic heat demand may need to be entirely decarbonised (DECC 2012).
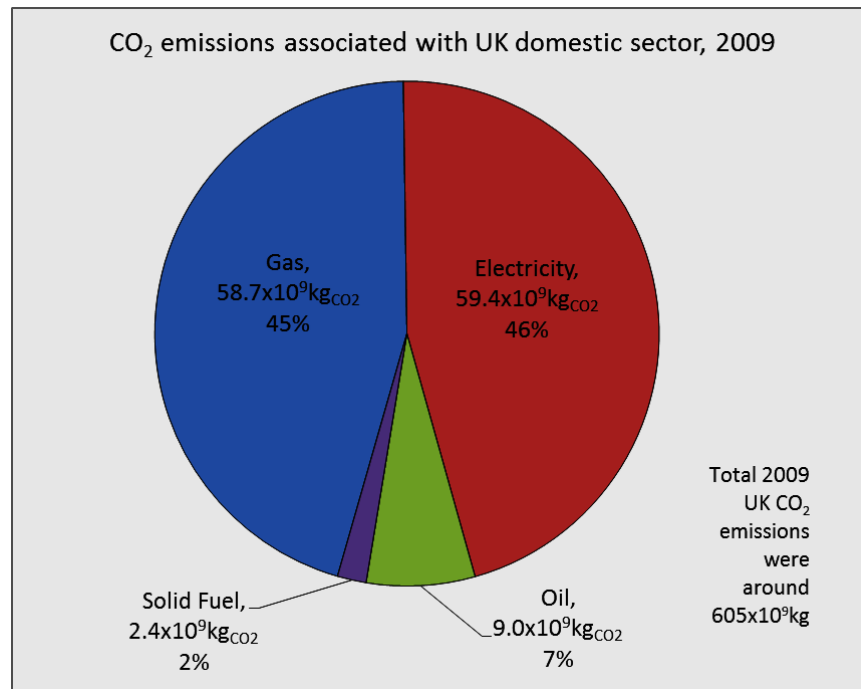
Figure 2: CO_2 emissions associated with domestic sector by fuel. Adapted from Palmer & Cooper (2011) & DECC (2009b)

Figure 3 illustrates the proportions of average energy consumption relating to each type of domestic demand.
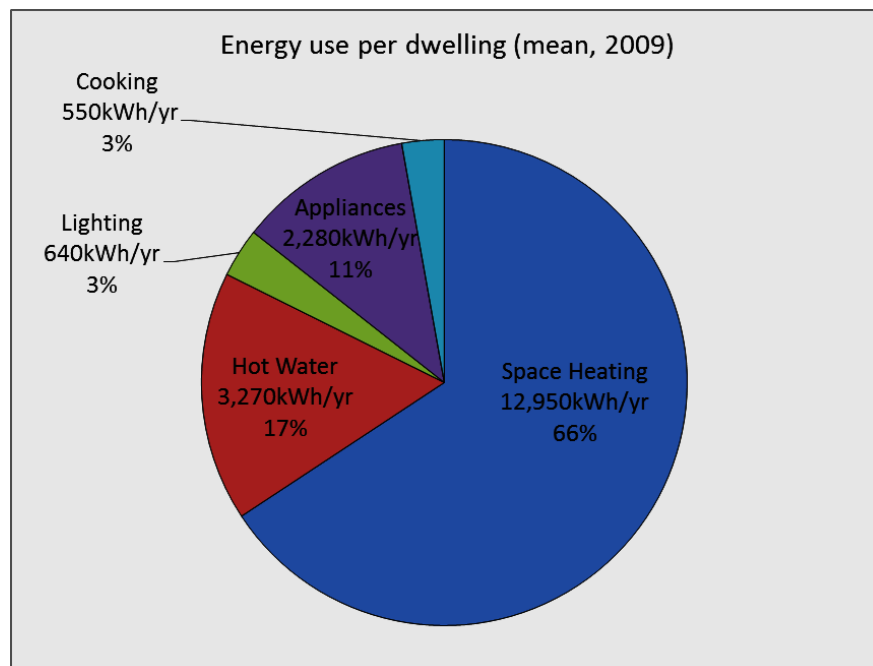
Figure 3: Average energy use in 2009 dwellings. Adapted from Palmer & Cooper (2011)

In 2009, energy use in the 25.6 million dwellings of the domestic sector was 500TWh, just over 28% of UK end-use consumption (Palmer & Cooper 2011). Although this is an increase of around 17% since the 1970s, the housing stock has increased and so there has been a slight reduction in the energy use per household from over 22,200kWh/yr in 1970 to just under 19,690kWh/year in 2009 but the annual variation is relatively high compared to this (up to almost 1,000kWh/year). Space heating dominates the end-use consumption; in fact even though it has reduced by about 10% since 2004 it is still slightly higher (per dwelling) than it was in 1970.

2.1.3 Proposals for reducing domestic energy demand and associated emissions.

A range of proposals have been suggested in the literature, each aiming to demonstrate how some or all of the required reductions in CO_2 emissions associated with the domestic sector might be achieved. These proposals invariably involve a combination of energy demand reduction (improving the efficiency of appliances and insulation in buildings) and decarbonisation of the energy sources (i.e. low carbon generation of electricity and heat). However, the balance between these approaches and the technologies preferred for low carbon heating varies somewhat between proposals. This section will provide an overview of some of these proposals before considering some of the specific suggestions in more detail in the following sections. It should be noted that each proposal includes some use of electrified heating (i.e. using Air Source Heat Pumps, ASHP) with decarbonised electricity and several proposals include the use of micro-Combined Heat and Power (mCHP) units.

The potential reduction in domestic heating demand which could be achieved by 2020 by continuing to improve insulation levels (using newer technologies such as solid wall insulation alongside established technologies) has been assessed to be 27TWh/yr by DECC (2012). Although significant, this saving is only 6.6% of current domestic heating demand. It was therefore assumed that some form of low carbon heating will be required across the building stock in order to meet future decarbonisation targets. A variety of sources of low carbon heating including district heating networks (DHNs), biogas injection and individual dwelling solutions (e.g. ASHP, mCHP and biomass) have the potential to form part of the solution. This is supported by earlier analysis by Radov et al. (2009) on the potential supply of renewable heating in the UK. Their study concluded that 25TWh/yr of renewable heating could be available to the UK by 2020 with no additional cost and that this increases to between 46TWh/yr and 66TWh/yr if an additional cost of £0.10/kWh is accepted (including both domestic and non-domestic heat). Because the study found supply-side limitations to be a key constraint in the period up to 2020, it was suggested that it is unlikely that this supply of

renewable heating could be significantly increased, even at much higher costs. The large share of biomass heating which was suggested is sensitive to the low potential costs given by E4Tech (2009). The proposed mix of heating sources also included a significant contribution from ASHPs (in both domestic and non-domestic buildings) and a slightly smaller contribution from Ground Source Heat Pumps (GSHP), (mostly in non-domestic properties). Public responses to the DECC consultation report highlighted the need to consider the infrastructure required to meet the implied electrical demands; accurate assessment of this challenge is clearly still required.

In an earlier study, Shorrock et al. (2005) investigated the effect of applying a series of efficiency measures to the dwellings they are applicable to and concluded that savings of around $81Mt_{CO2}$/yr are technically feasible, with reductions of between $33Mt_{CO2}$/yr and $64Mt_{CO2}$/yr (24% to 46% relative to 2001 emissions) possible at no net cost. The measures considered were all based around reducing energy demand (with addition of solar PV) rather than using low carbon heating systems; however the implication is that both approaches will be necessary in order to achieve the more extensive emissions reductions which are required. Both the Royal Academy of Engineering (2012) and Clarke et al. (2008) acknowledged the need for a range of approaches in reducing emissions from domestic heating. They suggested that improved insulation and construction, heat pumps, CHP with district heating networks, mCHP and biomass heating all have a part to play but no quantitative analysis of their relative contributions was presented.

Boardman (2007b) built upon earlier work (Boardman et al. 2005; Boardman 2007a) to propose strategies to reduce domestic carbon emissions by 80% by 2050 across the domestic sector. The study considered sociological aspects of changes, improvements in appliance and lighting efficiency, building fabric improvements and the use of low carbon technologies. Relatively limited decarbonisation of grid supplied electricity (with the CEF remaining at 440g/kWh after 2020) was conservatively assumed. This lead to a preference for mCHP devices over heat pumps although the use of both was suggested and low carbon technologies contribute around one third of the overall savings proposed. Controversially, a fourfold increase in the demolition rate (currently less than 0.1%) of the worst performing stock was proposed in order to reduce the average space heating demand in dwellings, given that the retrofit options considered feasible would not achieve the required reduction on their own. Even with this rate of demolition, the reports concluded that between 80% and 87% of the housing stock in 2050 would consist of buildings that have already been built. The analysis indicated that an average heat demand of 6,800kWh/yr should then be feasible by reducing heat demand in pre-1996 dwellings to around 9,000kWh/yr and achieving an average heat demand of 2,000kWh/yr in dwellings built between 1996 and 2050. This is around seven times the 27TWh/yr saving by 2020 suggested by DECC (2012). CO_2 emissions associated with the current in-use phase of

current buildings' lives were shown to be considerably higher than the embodied CO_2 attributable to their construction (it is suggested that the CO_2 emissions avoided by an efficient new home compared to the current stock average outweigh the CO_2 released due to the new construction after around 13 years).

Conversely, Lowe (2007) summarised and built upon modelling work described by Johnston et al. (2005) to present a set of options for decarbonisation and argued that extensive demolition is not necessary. The studies made slightly more optimistic assumptions about the reduction in space heating that is possible and assumed more extensive decarbonisation of the electricity grid (with the CEF reduced to around half the present levels). They proposed that a mixture of internal and external insulation could be used on solid wall properties as the majority of their exposed wall area is actually at the back of them (making external insulation more aesthetically acceptable). In combination with measures such as upgrading doors and windows, this could reduce heat demand to between 33% and 50% of current levels. A large role for low carbon heating was envisioned with a preference for heat pumps over mCHP units as the CEF of grid generated electricity decreases. The Sustainable Development Commission (2006) made a similar case against demolition, with analysis indicating that it is possible to reduce carbon emissions from the domestic sector by 33 to 73Mt_{CO2}/yr by 2020 (i.e. 24% to 52% relative to 2006).

The significance of occupant behaviour and appropriate control systems is noted in many of these studies and should not be underestimated, given the wide range of energy consumptions observed in otherwise similar properties with occupants from similar demographic groups. For example, annual gas consumption was found to range from 7,450kWh to 15,644kWh in 12 almost identical properties within the same housing development using the same heating (in this case a mCHP unit as part of a Carbon Trust (2007) field trial). The Royal Academy of Engineering (2012) reported that ranges of three-to-one have been observed elsewhere.

In order to achieve the proposed reduction in CO_2 emissions, the CO_2 emissions from the domestic sector will need to be drastically reduced. A combination of approaches including energy reduction and the adoption of low carbon energy resources is likely to be required in order to achieve this.

2.1.4   Contribution from building fabric improvements

Most suggestions for the reduction of CO_2 emissions from the domestic sector have involved some improvement of the average performance of the building stock. This typically involves both better standards for future construction and improvements to current buildings.

The Department For Communities And Local Government's (DCLG) (2007c) green paper: "Homes for the future: more affordable, more sustainable" presented policy for future building stock. Plans are laid out in order to comply with the EU directive on the Energy Performance of Buildings (EC 2002) in the 240,000 new homes per year that the government aims to see built (i.e. three million in the period to 2020). Building Regulations will be systematically improved until 2016 (DCLG 2007a), using energy performance standards given in the Code for Sustainable Homes (DCLG 2009). The criteria for compliance with the Building Regulations is expressed as a Target Emissions Rate (TER) which the actual Dwelling Emission Rate (DER) must be lower than. Table 1 summarises the relationship between the year that these standards are due to be implemented, the Code for Sustainable Homes level and the relative change to the TER:

Table 1: Building emissions reductions requirements

Year	TER relative to 2006	Code for Sustainable Homes level
2002	+25% (i.e. 2006 is 20% lower)	N/A
2006	0	N/A
-	*-10%*	*1*
-	*-18%*	*2*
2010	-25%	3
2013	-44%	4
-	*-100%*	*5*
2016	NZC (approx. -150%)	6

The TER and DER are calculated using the Standard Assessment Procedure (SAP) 2009 (BRE 2010); a methodology adopted from BRE's Domestic Energy Model. The SAP2009 methodology is used with the dimensions of the dwelling and either reference values supplied in SAP2009 Appendix R to calculate the TER (for 2002) or the actual property values in order to calculate the DER. From 2016, all new housing will have to achieve net zero carbon emissions (NZC). This includes emissions associated with electrical appliances (which are not included in the DER) so actually represents a reduction of approximately 150% relative to the 2006 standard.

Buildings built to standards equivalent to Code for Sustainable Homes level 4 are not unprecedented. Many buildings have been constructed in continental Europe meeting the Passivhaus Standard; this requires that space heating demand is less than 15kWh/year per m² of useable floor area and that total non-renewable demand is less than 120kWh/year-m². Similarly, the BEDZED development in London includes 82 homes built using Passivhaus concepts with a 130kWe wood-chip burning CHP unit rather than individual boilers (though this has subsequently ceased operating) and 700m² of solar photovoltaic (PV) panels (Marsh 2002). An extensive refurbishment in a conservation area was reported on by Parker (2009). The terraced property in London was refurbished with much improved airtightness, insulation, mechanical ventilation and heat recovery, and solar PV reducing its overall energy demand by 80% (space heating demand reduced from 24,000kWh/yr to 2,160kWh/yr). Carbon emissions were reduced from 6,542kg$_{CO2}$/yr to 2,146kg$_{CO2}$/yr (or 1,630kg$_{CO2}$/yr including the emissions offset by the use of PV panels). Although the home would achieve Code for Sustainable Homes level 4, the refurbishment undertaken was extensive and unlikely to fall into the "cost effective" category of broader studies referred to earlier. A case study of 14 new build homes in Norfolk was used by Monahan & Powell (2010) in order to compare the energy and carbon implications of different energy systems in them. The most successful measures were solar thermal and solar photo-voltaic (PV) panels. Solar thermal panels provided 65% - 89% of the domestic hot water demand and PV panels 14% - 41% of the electrical demand at the homes to which they were fitted, achieving a carbon payback period of approximately 3 years.

However, economically achieving the Code for Sustainable Homes level 5 and especially the level 6 standards are likely to be much harder. Banfill & Peacock (2007) have expressed concern about the 2016 net-zero carbon requirement, arguing that efforts to reduce the energy consumption of existing stock may be more cost effective. In particular, although effective technological solutions exist for low carbon heating, economic net-zero carbon electricity generation through solar PV panels or micro-wind turbines is much more problematic and likely to incur significant costs. They recommended that the low-carbon generation of heat and electricity are treated separately.

Significantly, the policy only affects current building stock when extensive refurbishment is carried out. Boardman (2007b) estimated that at least 80% of the 2050 housing stock is already built and also suggested policy to target emissions associated with these. As noted in the previous section, there is debate over the extent to which reductions in heat demand of current stock can be economically achieved but estimates vary between one-third and two-thirds. It is appropriate that these studies do not hypothesise the use of materials and methods which have not been proved. However, it should also be noted that several materials are under development which are likely to facilitate the upgrade of "hard-to-treat" dwellings and may make even

greater savings feasible (Jelle 2011). Vacuum insulation materials and nano-insulation materials are being developed that demonstrate thermal conductivities of 4-5mW/mK, around a quarter that of polyurethane panels (which are twice as effective as rock wool). Unlike vacuum insulated panels, they are sufficiently robust for construction use and show potential for good longevity. On the other hand, Dowson et al. (2012) pointed out that in practice there are challenges in encouraging sufficient uptake of measures to building fabric and that the actual savings achieved are often overestimated; it appears unlikely that the current incentives in the UK will achieve all of the improvements that are technically feasible.

In considering the future performance of low carbon heating systems, it is important to consider the effect of building fabric improvements on the mix of the types of energy demanded. Borg et al. (2010) presented work in support of the SUPERGEN HiDEF consortia's research, focussing on the probable characteristics of the energy demands of future building stock. Notably, (and consistent with Johnston et al., 2005) the effect of measures to reduce energy consumption were shown to considerably reduce the space heating load but are less effective in reducing the domestic hot water (DHW) load or electrical demands, see Figure 4. For example the consistency of DHW heating demand compared to the seasonal fluctuation in space heating demand may prove to be favourable to mCHP if suitably sized units with a sufficiently high power to heat ratio become available.
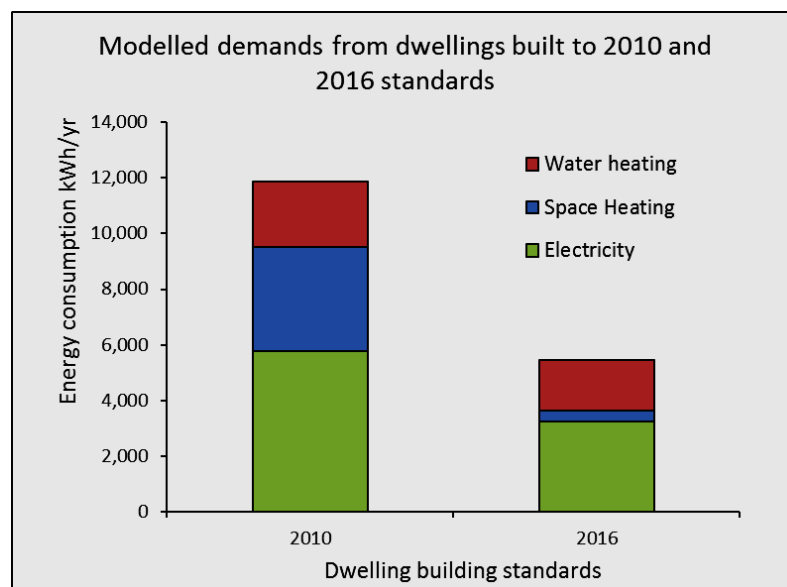
Figure 4: Relative energy demands for base case (2010) building and zero carbon (2016) building. Adapted from Borg et al. (2010)

Although improvements to the fabric of buildings are likely to reduce their heat demand, low-carbon heating will be needed in order to achieve the reductions in CO_2 emissions which are required.

2.1.5 Other low carbon approaches to heating

A range of low carbon micro-generation technologies are available for integration with buildings including solar PV panels, solar thermal panels, micro-wind generators, mCHP units, biomass boilers and heat pumps (Staffell et al. 2010). Of these, heat pumps and mCHP units are the two micro-generation technologies which have both significant thermal and significant electrical characteristics to consider. This work focuses on the performance of mCHP and ASHP units, complementing Allen's (2009) study which focussed on solar and wind micro-generation technologies. Solar thermal panels have the potential to make an energy efficient contribution to domestic heating demands (Allen & Hammond 2010) but demonstrate somewhat seasonal performance in the UK and are generally considered to be a secondary heating source.

Before considering the performance of ASHP and mCHP units in more detail, district heating and biomass heating will be briefly discussed.

2.1.5.1 District heating networks

District heating networks (DHNs) are used to supply a large proportion of heat demand in many northern European cities and there are some smaller schemes in larger cities in the UK. Analysis by Davies and Woods (2009) indicated that DHNs are likely to be economically viable in locations with a heat demand density greater than $3,000kWh/km^2yr$. Although subsequent heat demand mapping produced by DECC indicated that this criteria currently applies to almost 50% of heat demand in England (DECC 2012), additional barriers limit the likely uptake of DHNs to far less than this. The main barriers identified by Davies and Woods (2009) were the high capital cost of such schemes and the variety of project risks involved in their development. If a discount rate of 3.5% is assumed (i.e. developments are effectively de-risked) and the shadow cost of carbon is fully accounted for then they suggested that DHNs have the potential to supply between approximately 3 and 8 million households and a total of 5.8% to 13.9% of the UK's building heating demand. However, if a more realistic rate of 6% is used, then this potential drops to 300,000 households and 0.6% of the UK's building heat demand. Although the analysis took account of the potential for reductions in domestic space heating in terms of demand, it is not clear whether the possible reduction in heat distribution efficiency associated with this was considered. Given the sensitivity of the economic potential of DHN future capacity to the selection of an appropriate discount rate (effectively representing the perceived risk in projects), it is likely that their widespread development would require government-led initiatives rather than relying on a solely market based approach.

DHN have a key advantage in terms of flexibility. Once the infrastructure is in place, heat can be generated from a variety of sources; optimising the best source of heat as conditions change

and potentially replacing heat sources as lower carbon options become available. DHNs act as an enabler for low-carbon technologies including large scale heat pumps, CHP plants, waste heat from other processes, geothermal plants and biomass boilers (DECC 2010b). Speirs et al. (2010) developed this argument to suggest some reconsideration of the extent to which CHP plant should be considered as potential future generation (in contrast to the extensive electrification of domestic heating typical in most current low-carbon energy scenarios). Their analysis suggested that if DNHs are constructed to supply 14% of UK building heat demand then a 5% reduction in primary energy requirements could be achieved by using conventional CHP plant as an intermediate solution before replacing it with CHP with carbon capture and storage (CCS) in place of other fossil plant with CCS.

If the barriers to their development can be overcome, it is possible that DHNs will supply a significant part of domestic heat demand in the UK. However, heating systems for individual dwellings are almost certain to dominate the total domestic heat supply, especially in areas with lower heat demand density.

2.1.5.2   Biomass

Biomass has the potential to supply a large quantity of energy. The potential supply from the UK is estimated to be just over 110TWh/yr at present (i.e. equivalent to over a quarter of current domestic heating demand). The potential supply has been forecast to rise to between 140TWh/yr and 210TWh/yr by 2030 depending upon the price which is available and the extent to which constraints which are overcome (AEA Consulting et al. 2011). If 10% of internationally traded biomass is assumed to be available, a high price (£0.036/kWh) is accepted and most constraints are overcome then the potential supply was estimated to increase from around 300TWh/yr at present to 1800TWh/yr by 2030. The majority of the current UK biomass potential is in the form of landfill gas and waste wood residues. It is likely that landfill gas availability will decrease but that the supply from waste wood residues, anaerobic digestion, energy and biofuel crops, and dry agricultural residues can increase between now and 2030. The majority of the additional fuel available from international markets is likely to be woody biomass.

Although there is relatively little competition between energy sectors for these energy resources at present (as they tend to use different feedstocks) this is likely to change. For example, the development of technologies to create biofuels from lignocellulose opens a range of the solid feedstocks to potential use in the transport sector. Bio-methane (from either landfill gas or anaerobic digestion) could be used in Combined Cycle Gas Turbine (CCGT) power plants, injected into the gas grid or used in the transport sector (as either liquefied compressed gas or processed to liquid fuel).

Solid biomass from wood waste, forest residues and energy crops could be used to generate electricity. There are several options available for this (Pihl et al. 2010). The fuels can be fired to supply heat to a steam cycle although high temperature corrosion issues usually limit the maximum cycle temperature and correspondingly the efficiency to around 25% to 30% (relative to net calorific value, NCV of fuel). To relieve this constraint, biomass is more commonly co-fired with coal (10% to 15% biomass), achieving efficiencies of around 39% to 40% (NCV). CCGT configurations can be used in different ways. For example, the biomass could either supply heat to the bottoming cycle of the power plant, or, a gasifier could be used with the biomass in order to feed the products directly into the CCGT (as a mixture with at least 35% to 50% natural gas). Comparing these options, Pihl et al. (2010) found that the gasification option is likely to achieve the highest overall efficiency (around 45% in a CCGT conventionally achieving 52% efficiency, GCV). The hybrid combined cycle option could also achieve a higher efficiency than a stand-alone biomass fired steam plant (up to 37%, GCV, compared to 34%). However, the marginal efficiency of the energy supplied by the biomass is fairly consistent across the options at around 28% to 33% and, in fact, slightly better in the stand-alone plants. Waste heat from these power plants could be used to supply other heat demands but is also well suited to the drying of additional biomass, saving energy upstream.

In order to supply domestic heating, this electricity could be used to drive heat pumps. However, it is probably simpler for the fuels to be burnt, supplying the heat directly. This could be done in either individual burners or a remote biomass fired boiler connected to a DHN. The prominence of biomass fuelled heating in DECC's (2012) proposals demonstrates that it has potential to meet a large proportion of future domestic heating demand, despite the competing demands outlined above. However, it is unlikely to fulfill all heating demands. The combustion and emissions characteristics of several fuel types make them less suitable to domestic heating (see, for example, Rabaçal et al., 2013). It is possible that poorly designed burners will emit methane with large implications for their global warming potential (Johansson et al. 2004). Additionally, other constraints such as fuel supply and storage logistics may limit their application in densely populated areas.

Biomass and District Heating Networks have the technical potential to supply a significant proportion of domestic heating. However, given the constraints upon their application, it is highly unlikely that they will supply all of it. Technologies to provide heating at an individual dwelling level with convenient supply logistics (to the consumer) will almost certainly be needed and could continue to dominate the sector.

2.1.6 Demand side management of electrical loads and distributed power generation

Demand Side Management (DSM) is the process of influencing consumers' electrical demands (and possibly generation) rather than varying only central generation in order to balance the generation and consumption of electricity. For example, electrical heating could be co-ordinated to operate at times when other electrical demands are low rather than matching the peak demand with additional generation. DSM has several potential advantages and was suggested as a part of the "Smart Grid" envisioned by DECC (2009b) and the Electricity Networks Strategy Group, (2009). More efficient plant could be operated with a higher load factor, a lower plant margin might be acceptable (decreasing the need for generating plant to meet peaks), investment in network infrastructure could be used more efficiently, the integration of both intermittent large scale renewable generation and distributed micro-generation could be facilitated (Strbac 2008).

Interest in DSM is closely linked to the possible extensive deployment of distributed micro-generation (which might or might not be centrally coordinated). Micro-generation has attracted widespread attention (e.g. Degner et al., 2006), primarily because of its potential to reduce transmission and distribution losses and to reduce the requirement for additional network infrastructure investment.

Many hypothetical scenarios of the future electrical power system in the UK anticipate that DSM could affect a significant proportion of domestic electrical demands and a large number of micro-generation systems. For example, Barton et al., (2012a) calculated that DSM has the potential to achieve a 10GW reduction in the peak dispatchable electrical demand experienced in each of the scenarios generated by the Transition Pathways project. It should be noted that there is a significant difference between measures to alter peaks in demand (which generally follow a diurnal pattern) and measures to maximise the use of intermittent renewable generation (which has a less regular profile and often a period of several days). Pudjianto et al., (2013) used a different method to generate demand profiles based upon the same scenarios and considered the relative reduction in distribution infrastructure which could be achieved through the use of DSM applied to heat pumps and electric vehicles. Measured heat demand data was used as the counterfactual case and it was suggested that a reduction in the peak electrical demand of around 39GW could be achieved relative to it by rescheduling the heating and electric vehicle charging. It was estimated that this would result in a saving of £20 billion to £25 billion in the cost of network reinforcements between now and 2050. In addition, it was suggested that DSM of micro-generation could provide ancillary support services such as system reserve, secondary frequency control and voltage control; in a scenario investigated by Pudjianto & Strbac (2012) these services generated revenues worth 20% of the value of the electricity generated.

Several studies consider the effect on local distribution infrastructure that different quantities of mCHP units might have if used to supply domestic heating. Peacock & Newborough (2006) compared the impacts that different penetrations of two generic mCHP units (representing a SE-mCHP unit and a SOFC-mCHP unit) might have on local power flows when they are not centrally coordinated. It was concluded that if all dwellings used the SE-mCHP unit modelled, peak winter demand could be reduced by around 44%. Using the SOFC-mCHP unit, however, reverse power flows occur in winter when more than 15% of dwellings are fitted with them. This work was developed by Peacock & Newborough (2007) to include the effect on local power flows when DSM is used. The study assumed that Whispergen SE-mCHP units were fitted in all dwellings. The analysis suggested that the peak demand per dwelling could be reduced from 2kW to 1.2kW without DSM control and down to 0.9kW if DSM control is used.

Modelling by Burt et al. (2008) investigated the power flows which might be expected in a distribution system with a variety of mCHP, micro-wind and solar PV micro generation feeding into it. In some of the circumstances considered, exports of a few tens of kW were observed from the 11kV to the 33kV network but it was concluded that the scenarios presented are unlikely to pose significant problems. The study modelled dwellings with the various types of micro generation for a typical week in spring using ESP-r and then the resulting demand profiles were transformed (in time and amplitude) to generate a diversified set of profiles. Network branches supplying various combinations of dwellings were then modelled by using these profiles. Thomson & Infield (2008) reached a similar conclusion; even if all dwellings are fitted with SE-mCHP units (generically modelled as 1kW electrical and 9kW thermal output) it is unlikely that power export from a network (modelled as 1262 dwellings) will occur. If mCHP units with 1kW electrical and 3kW thermal output are fitted in all houses (representative in this case of ICE-mCHP units though PEMFC units could share similar characteristics) then power export might occur but is unlikely to cause any problems. However, if units with a higher electrical output (e.g. larger ICE-mCHP units or SOFC-mCHP units) are used then significant (potentially problematic) reverse power flows will occur. The modelling required a diverse set of mCHP operating profiles which were derived by applying a distribution to an average heat demand profile. Sulka & Jenkins (2008) reported power exports of up to 50kW from a modelled housing estate of 150 dwellings using mCHP units. A simple thermal model was used with a mix of occupancy patterns and two models of non-modulating SE-mCHP units shared between them (10% electrical efficiency). The on-off switching pattern of the units was then determined along with the net power flow in the system. If ASHPs are using in combination with mCHP units, net power demands can be reduced as electrical generation and demand will both increase with heat demand. Indicative analysis by Hawkes et al. (2011) suggested that a 50:50 mix of ASHP and SOFC-mCHP has the potential to reduce peak power demands associated with their operation by around 80%.

More recently, the modelling developed as part of this work was used to investigate the coincidence of the additional generation and demand caused at a neighbourhood level by combinations of ASHP and mCHP units operating without DSM control (Rogers et al. 2013). The study showed that the number of units which can be installed in a neighbourhood supplied by the existing distribution infrastructure increases when a combination of devices is used and that this reduces the total associated CO_2 emissions more than is possible with just one type of micro-generation. However, imbalances still occur and so it is likely that yet more micro-generation could be installed if DSM is employed.

The concepts of micro-grids, cells, and virtual power plants have been developed by several research groups in order to assist with the planning and control of distributed generation (Pudjianto et al. 2008). Aggregating the control attributes and output of groups of micro-generators brings several advantages. Control can be decentralised and lends itself to an agent based approach, reducing communication overheads and improving flexibility. The aggregated output of a cell might feasibly participate in the electricity market. It is possible that other electrical supply services can be provided, including frequency response and regulation, immediate reserve, peak lopping and local voltage support. Roossien et al. (2008) described a field trial demonstrating the virtual power plant concept with 10 mCHP units in which electrical demand peak was reduced by 30% to 50% when the control mechanism was in operation. A similar concept for DSM control of heat pumps has also been demonstrated in field trials (Warmer et al. 2007). An agent based control system ("PowerMatcher") was used to minimise the cost of running heat pumps primarily supplied by a wind farm with exposure to the Dutch balancing market. Underproduction from the wind farm (compared to the contracted, predicted output) could usually be partially compensated for but there were periods in which it could not be compensated for at all. Overproduction could generally be completely compensated for.

The suitability of direct electric heating and electric heat pumps for participation in DSM has been investigated by several researchers. Hong et al. (2012) assessed the flexibility of heat pump operation using detailed thermal models created in ESP-r. Time shifts of one or two hours in the operation of heating are possible without seriously impacting the thermal comfort of residents in current average housing. However, in improved housing with thermal buffering, this could be extended to around six hours. In the study, heat pumps were controlled using an on-off function aiming to achieve thermal comfort at specific times of active occupancy in the dwelling rather than controlled using a modulating function. Moreau (2011) concluded that (in the context of Canada) the electric demands associated with domestic hot water heating can be largely shifted away from times of peak electrical demand.

DSM may be used to facilitate the successful integration of any future deployment of large numbers of low carbon domestic heating systems if they have significant supply electrical

implications. It is also feasible that any electrical demands or potential generation which can be time shifted to some extent (for example, those providing heat to systems with significant thermal inertia) could be used to assist in the integration of intermittent renewable generation onto the electrical grid. Any consideration of the future performance of ASHP and mCHP units should therefore consider the effect that interaction with DSM might bring.

2.2 Heat Pumps

2.2.1   Introduction to heat pumps

Heat pumps take heat from a low temperature source such as the outside air, ground or water and deliver it to heat emitters at a higher temperature (Berntsson 2002). In the domestic setting, this is usually achieved through a vapour compression cycle with an electrically driven compressor (see Figure 5).
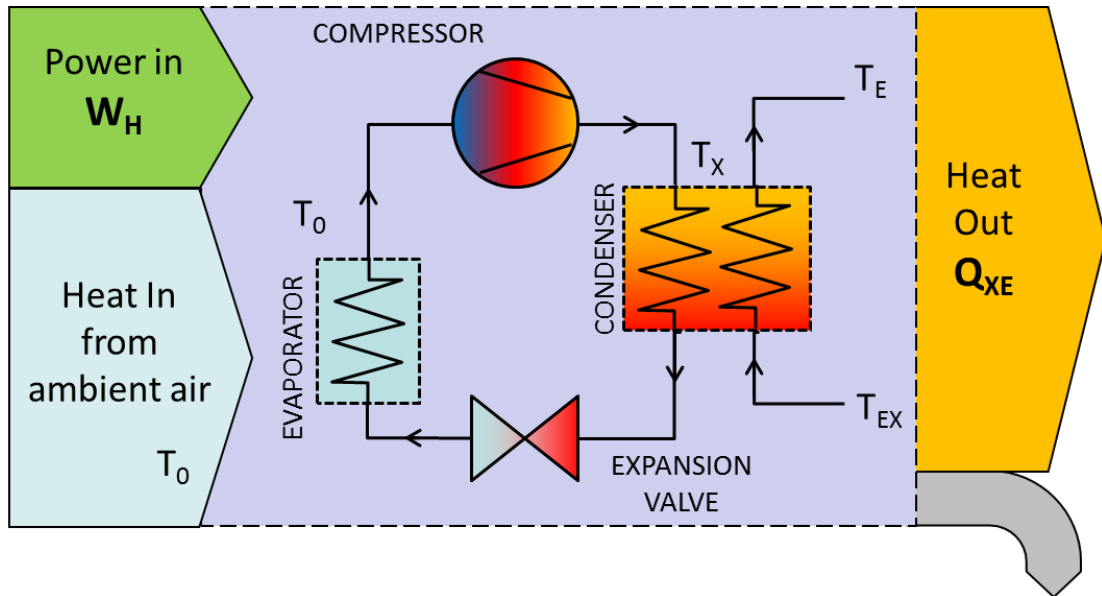
Figure 5: Heat Pump Vapour Compression Cycle

Carnot and Kelvin both devised the concept of a heat pump but the first patent for a practical device was issued to TGN Haldane in 1927. Heat Pumps were installed in the Equitable Building, Portland, Oregon, as early as 1948 but have only been widely commercially available since the 1970's (Hepbasli & Kalinci 2009).

The majority of the analysis presented here will relate to ASHPs. Ground Source Heat Pumps (GSHPs, heat pumps using the ground as a heat source) tend to perform more efficiently than ASHPs because the ground offers a more stable heat source temperature (Rawlings & Sykulski 1999). However, they are more constrained than ASHPs in terms of appropriate locations for installation (Energy Saving Trust 2007), requiring up to 600m^2 for a heat collector (Berntsson 2002). ASHPs are considered to be an easier retrofit option, replacing boilers (Cockroft & Kelly 2006). Additionally, the capital costs of GSHPs are usually higher, the Energy Saving Trust (2012) suggests prices of £6,000 to £10,000 for an installed ASHP compared to £9,000 to £17,000 for a GSHP. Excluding installation costs, low quality ASHP units can be purchased for around £1,000 or around £2,500 for a small mid-range unit (AirconWarehouse Ltd 2012).

Modern ASHP usually use either rotary or scroll compressors, typically operating between around 0.6MPa and 2.5MPa. Historically, chlorofluorocarbon (CFC) or hydrochlorofluorocarbon (HCFC) based refrigerants such as R22 ($CHClF_2$) have been used but these are being phased out in favour of hydrofluorocarbon (HFC) based refrigerants such as R32 (CH_2F_2) and R134a (CH_2FCF_3) due to their lower ozone depletion potential. Mixtures of HFCs are commonly used in order to improve their properties (e.g. R410A, an almost-azeotropic mixture of R32 and R125 or R407C, a mixture of 23% R32, 25% R125 and 52% R134a). Propane (R290) has reasonable properties as a refrigerant and low global warming potential but there are concerns regarding its flammability. R744 (CO_2) is used in some heat pumps but employs a different thermodynamic cycle (the Lorentzen cycle) in which most of the heat rejection takes place with the refrigerant in the supercritical state.

2.2.2 Performance of heat pumps

Heat pumps use work, typically supplied by electricity, to drive compressors and other ancillary components. Depending upon their performance and the efficiency of the electrical generation, the primary energy consumed may be more or less than alternative heating options. The coefficient of performance (COP), k_{WQ}, for a heat pump is given by:

$$k_{WQ} = \frac{Q_{XE}}{W_H}$$

Equation 1

where Q_{XE} is heat delivered and W_H is the electrical energy consumed.

The COP of heat pumps varies with operating conditions; notably the performance decreases as the difference between the source and sink temperatures that it operates between increases (see Figure 6). In addition to thermodynamic constraints requiring a greater work input as the temperature difference increases, frost can form on the air heat exchanger / evaporator component of an ASHP if its temperature drops below the local dew point. This further reduces performance as the thermal conduction of the heat exchanger is temporarily reduced and defrosting is required (Hepbasli & Kalinci 2009). Measures such as larger or more effective heat emitters and improved insulation in a building will decrease the outlet flow temperature which the heating system needs to supply and thereby improve the performance of a heat pump; these effects are studied further in the Modelling and Results chapters.

Heat pump performance measurement is standardised in BS EN14511:2007. This supersedes BS EN255-2:1997 for space heating applications but BS EN255-3:1997 is still valid for the heating of domestic hot water (DHW). Power input to pumps only includes that used within the unit (e.g. power supplied to circulate hot water outside the pump is excluded). The standard has

been adapted by European Heat Pump Association (2009) for testing to achieve their quality label. The testing procedure defined by BS EN255-3:1997 includes measurement of COP but the conditions and method are different to those in BS EN14511:2007. Significantly, the hot water temperature is generally higher (at least 40ºC) and the water inlet temperature is lower so the heat exchanger potentially operates with a greater temperature range.

Testing to BS EN14511:2007 is conducted at defined operating conditions, including ambient air and outlet temperatures, as defined by tables provided in BS EN14511-2:2007 (see Table 2). The standard rating of ASHPs is determined with a dry-bulb air temperature of 7ºC and supplying heat to water with a flow temperature of 35ºC and a return temperature of 30ºC. Additional test conditions use the same flow rate as the standard test (i.e. the ambient air and the heat exchanger's inlet temperatures are defined and the water return temperature varies accordingly).

Table 2: ASHP test conditions to EN14511-2:2007

Test condition	Air temperature	Water temperature
A-15/W35	-15°C	35°C
A-7/W35	-7°C	35°C
A2/W35	2°C	35°C
A-15/W45	-15°C	45°C
A-7/W45	-7°C	45°C
A2/W45	2°C	45°C
A-7/W55	-7°C	55°C
A7/W55	7°C	55°C

The test has initial precondition and equilibrium periods before the data collection period used to determine the heat pump's performance. If the heat pump operates within tolerances and without a defrost cycle, it is defined as "steady state operation" and the data collection period lasts 35 minutes. If the heat pump's performance varies outside tolerances or it undergoes defrost cycles under the defined operating conditions, it is defined as "transient operation", the test is extended to at least 3 hours and the average performance (including defrost cycles) is taken into account.

Performance data for seven ASHP units is given in Table 3. Modelling results in this study will relate to these units and a hypothetical eighth unit (ASHP H) achieving a performance around 10% higher than ASHP A, representing what may be the state-of-the-art in a few years. For the first four of these units, the variation in the COP with temperature difference is illustrated in Figure 6:
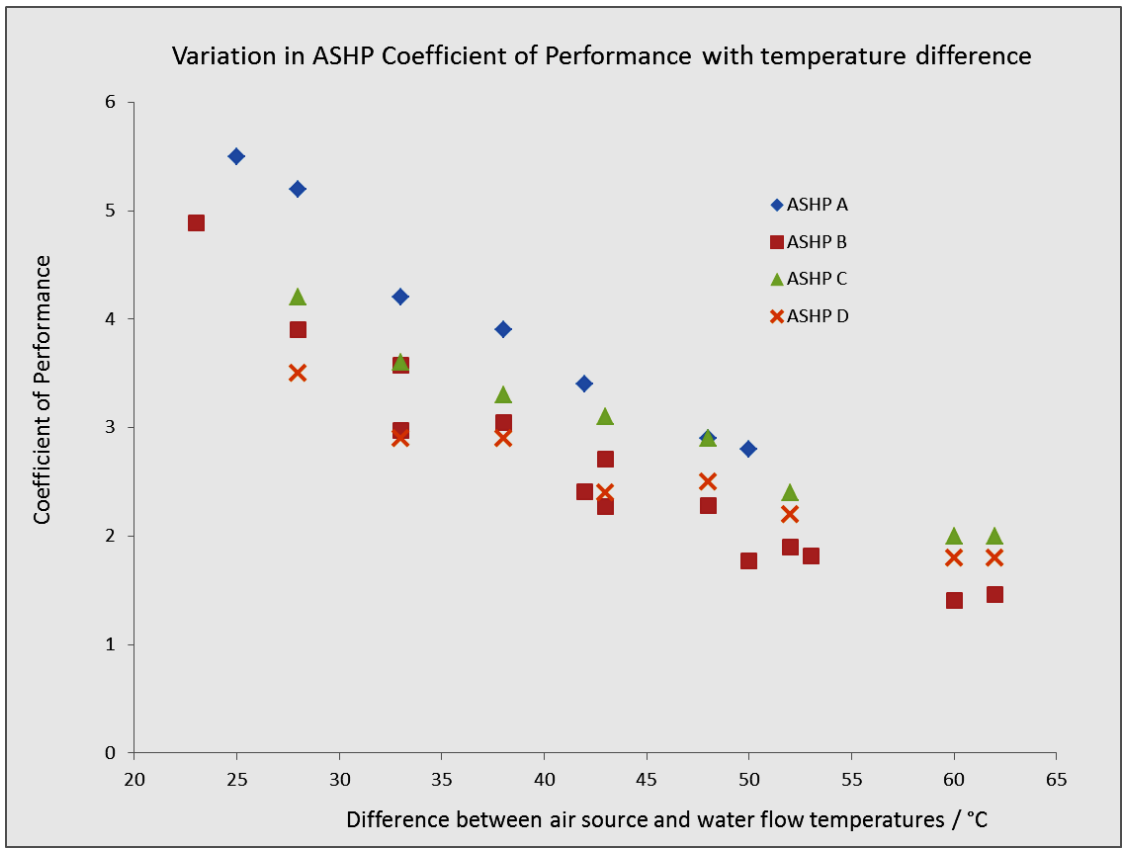
Figure 6: ASHP performance with variation in operating temperature. Data adapted from Butler & Hyde 2007; Warmepumpen-Testzentrum 2013; Energimyndigheten 2012.

Table 3: ASHP COPs measured under test conditions

	ASHP A	ASHP B	ASHP C	ASHP D	ASHP E	ASHP F	ASHP G	ASHP H
Reference for data:	*1*	*3*	*2*	*2*	*1*	*1*	*3*	*N/A*
Air / water temp. (°C)	Heliotherm HP10L-WEB	Mitsubishi Ecodan W85	Viessman Vitocal 300-A	Bosch EHP 8 AW	Daikin ERHQ014	Oscher GMLW14	Mitsubishi Ecodan W140	Future model
A-15/W35	2.80	1.77			2.20	2.80	1.97	
A-15/W45		1.41	2.00	1.80			1.40	
A-7/W35	3.40	2.41			2.70	3.60	2.32	
A-7/W45		1.90	2.40	2.20			1.95	
A-7/W55		1.46	2.00	1.80	1.50	2.50	1.62	
A2/W35	4.20	2.97	3.60	3.50	3.40	4.40	2.70	4.6
A2/W45		2.27	3.10	2.40			2.27	
A2/W55		1.82					1.80	
A7/W35	5.20	3.90	4.20	3.50	4.50	5.00	4.22	
A7/W45	3.90	3.05	3.30	2.90	3.50	4.10	3.20	
A7/W55	2.90	2.28	2.90	2.50	2.60	3.30	2.36	
A10/W35	5.50					5.30		
A12/W35		4.89						
A12/W45		3.58						
A12/W55		2.71						
A20/W55	4.00				3.30	4.00		
Rated thermal output at A7/W35	12.5kW	9.0kW	9.9kW	7.1kW	14.9kW	15.1kW	14.0kW	
Thermal output at A2/W35	10kW	8.5kW	8.3kW	5.8kW	10.3kW	13.2kW	14.0kW	10kW

(References, 1: Warmepumpen-Testzentrum 2010; 2: Energimyndigheten 2012; 3: Butler & Hyde 2007)

Major field-trials of heat pumps have been conducted in Germany (Miara 2008) and the UK (Energy Saving Trust 2010), demonstrating a wide range of performances and the importance of appropriate installation practice.

The German field trial was conducted by the Fraunhofer Institute for Solar Energy Systems in Germany, involving 78 heat pump installations (56 GSHP, 15 ASHP, 7 Water source heat

pumps) and was run over a period of two heating seasons. For the GSHPs, a seasonal average system COP of 3.72 was calculated with 87% of the output being used for space heating and 3% of the electricity consumed by electric backup heaters. For the ASHPS, an average COP of 2.99 was calculated with 72% of output used for space heating (remainder used for hot water). Only 1% of electricity consumed was used in backup electrical resistive heaters.

The Energy Saving Trust (EST) (2010) trial included approximately 80 ASHP and GSHP units representing 15 different heat pump manufacturers, installed at sites across the UK. Six ASHPs were installed and tested by a manufacturer and achieved an average COP of 2.75 with a range of COPs (averaged across the year) from 2.4 to 3.0. The remaining 22 ASHPs achieved an average COP of 1.82 with a range from 1.2 to 2.2 observed between installations. Further analysis was undertaken by DECC and EST to investigate the reasons for this large variation in the COP which was observed (Dunbabin & Wickins 2012). The largest factor in causing underperformance was found to be under-sizing of some of the units; this caused a large proportion of heat demand to be met by backup electrical resistive heating. In other cases, the units were over-sized and not capable of modulated operation (i.e. they had one output level). A third, significant issue was that the flow temperatures which were used were higher than necessary with "weather compensated" control being disabled in one case. The relative influence of this last issue is explored further in the Modelling and Results chapters, below.

A trend for improvement in the performance of heat pump units being manufactured was noted by Rawlings and Sykulski, (1999) and can be observed by looking at actual test data. Figure 7 shows the COP of various heat pumps against the year in which they were tested (Butler & Hyde 2007; DeLonghi n.d.; Warmepumpen-Testzentrum 2010; Warmepumpen-Testzentrum 2013; Danfoss 2012; Viessmann 2009; Energimyndigheten 2012). The COPs are given for air at 2°C and with a flow temperature of 35°C. Because earlier data was measured with a larger heat exchanger temperature difference (in accordance with EN255-3:1997), these COPs have been reduced by 7.5%; this is the difference in COP which a Carnot cycle would exhibit between the conditions and approximately compensates for the difference but direct comparison is not possible. Despite some variation, there is a trend in the COP of the best performing units. The four labelled ASHPs ("A", "B", "C" and "D") relate to the units in Figure 6 and Table 3.
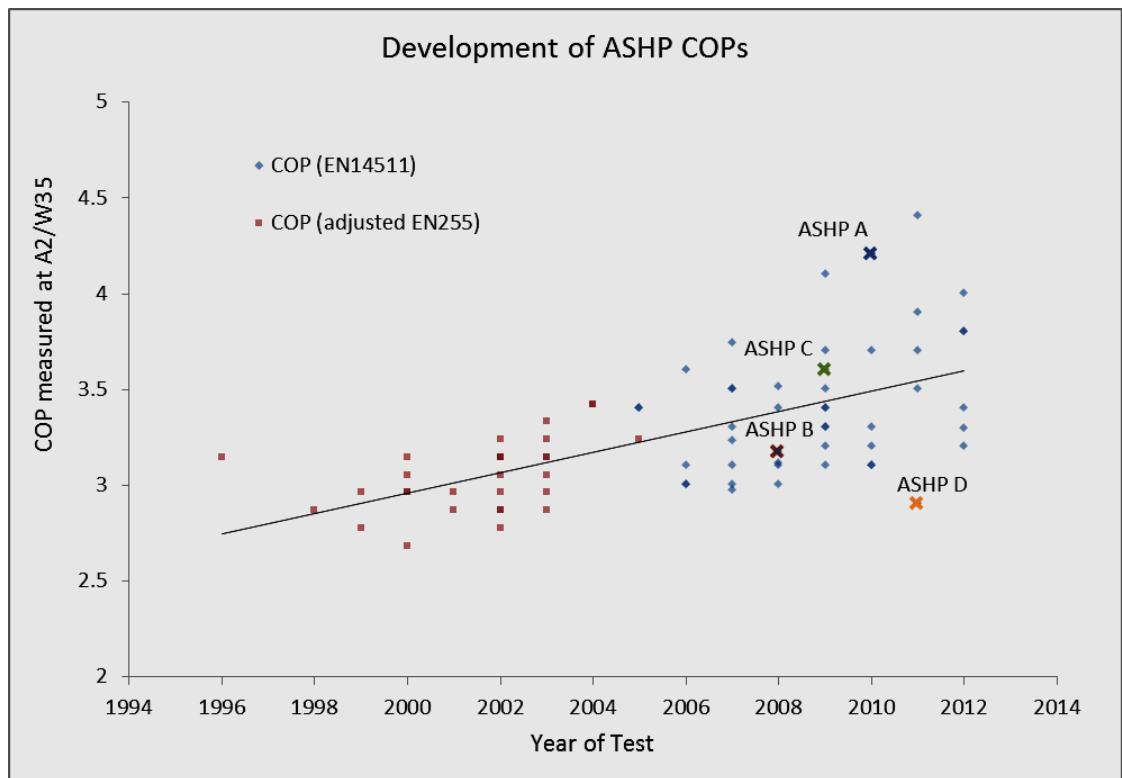
Figure 7: Representative COP of ASHPs Adapted from data by Butler & Hyde 2007; DeLonghi n.d.;
Warmepumpen-Testzentrum 2010; Warmepumpen-Testzentrum 2013; Danfoss 2012; Viessmann 2009;
Energimyndigheten 2012

2.2.3   Developments in heat pumps

Other improvements in the performance of heat pumps are possible. Exergy analyses of heat pumps completed by Hepbasli & Akdemir (2004) and Bi et al. (2009) identified the motor-compressor sub-system as the main source of exergy loss and therefore potential for improvement in heat pump designs. There are several ways in which this can be accomplished. The introduction of scroll compressors (made possible by improved manufacturing tolerances) achieves approximately 10% higher efficiency than the reciprocating piston compressors they replace. Suction and discharge processes are separate (reducing heat transfer to incoming refrigerant), the process is much smoother (i.e. less torque fluctuation) and does not require the use of valves. Additionally, cooling the compressor and motor assembly to a constant temperature has been shown to reduce compression work by about 16% (Chua et al. 2010). Scroll compressors are now used by many manufacturers (Energimyndigheten 2012; Warmepumpen-Testzentrum 2013).

Multistage compressors can be used to optimise designs for fixed pressure ratios, reduce pressure ratios and also improve heat recovery. In an experimental study of an ASHP with a two-stage compressor, Wu et al. (2012) found that overall performance can be improved (by

around 8%) by using both compressor stages when the temperature difference between source to sink is high and then switching to just one stage as the temperature difference decreases. Many manufacturers now use inverter driven motors, providing soft-start and stepped operation (Mitsubishi Electric Europe 2008; Viessmann 2009; Energimyndigheten 2012).

The second largest source of exergy losses is generally the heat exchanger. Two-stage evaporators have been suggested as they can extract heat from air more effectively (35% more effectively in one study, Chua et al., 2010). Operating at two pressures and therefore two temperatures, the evaporators are arranged such that warm air first passes the high pressure evaporator and then passes the low pressure evaporator.

Although the exergy losses in the expander are proportionally small in a conventional heat pump cycle, it is possible to reduce them. Various improvements to the expansion valve assembly are used to optimise the flow characteristics and some manufacturers use capillary tubes for this function. A more significant improvement could be achieved through the use of an expander turbine or similar device but the additional complexity involved means that this does not appear to have been pursued to date. A simpler alternative is the use of an ejector and gas-liquid separator in place of the expansion valve. The ejector allows a higher pressure to be maintained at the inlet to the compressor while the evaporator still operates at a lower pressure such that adequate evaporation (and associated heat transfer) can occur. In reviewing their use, Sarkar (2012) noted that studies have indicated that COP improvements between 7% and 24% could be expected through the use of an ejector compression cycle. Although the design details of the highest performing domestic ASHPs are not publically available, promotional material hints that some recovery of the energy loss in the expander takes place so it is possible that ejector compression cycles are already used.

At low ambient temperatures, frost can accumulate on the outside heat exchanger of an ASHP. This inhibits the transfer of heat from the outside air and is typically removed using a defrost cycle which uses a reversal of the heat flows in the heating cycle. Alternatives configurations have been suggested in order to expedite this process (e.g. by bypassing hot gasses from the compressor, Choi et al., 2011) or to better control it in order to reduce energy consumption (Wang et al., 2011). The hot gas bypass defrosting method is used in some commercially available ASHPs.

Changes in refrigerant can improve performance. Compressors using R410A tend to run cooler and use less power. R433A has recently been shown to offer further improvement potential (order of 5 – 7% improvement in COP over equivalent R22 system) (Chua et al. 2010).

Perhaps more significantly, the use of R744 (CO_2) has been suggested as a replacement for HFC based refrigerants, primarily because of its lower global warming potential (Austin & Sumathy 2011). However, CO_2's relatively low critical temperature (31.1ºC) makes it more suited to a trans-critical compression cycle. The critical pressure of CO_2 is 7.37MPa so heat pumps operating with this cycle (the Lorentzen cycle) require higher operating pressures (typically 8MPa to 13MPa for isobaric supercritical heat rejection and around 2MPa to 4MPa in evaporator). That is, heat is primarily rejected as sensible cooling of the working fluid (with associated temperature glide) rather than primarily as it condenses (relatively limited temperature glide). It is therefore more suited to applications in which the heat sink has a large temperature differential, such as domestic hot water brought up to temperature from a cold mains inlet (Austin & Sumathy 2011; Tian et al. 2009). This is an advantage in dwellings in which improved insulation has significantly reduced the space heating demand and Stene (2007) observed that heat pumps using CO_2 tend to outperform their HFC equivalents when the fraction of heat used for domestic hot water is above 50% to 60%.

Compressor efficiency is reduced with an increased pressure ratio (Jingying et al. 2010) and has been a limiting factor in the performance of these units. However, on-going improvements in scroll compressor design and manufacturing tolerances will inevitably improve performance. Exergy analysis by Sarkar et al. (2005) indicated that expansion losses are significant; they are proportionally higher in a transcritical cycle than a subcritical cycle. This suggests that there is more merit in using an ejector compression cycle to recover some of the work which is available (Sarkar 2012). A study by Yari and Sirousazar, (2007) suggested a 21% improvement in the COP is possible in this way (cooling of compression stage was also used) and that further improvements can be expected if two-stage compression is also used. Even if an expander is not used, it is likely that using capillary tube expansion can result in performance improvements in the order of 10% to 20% (Austin & Sumathy 2011) or that improvements in the order of 10% can be achieved by using an additional heat exchanger before the expansion valve (Fernandez et al. 2010).

Because the performance of a transcritical heat pump depends not only on the temperature of the heat source and sink used but also on the configuration of the heat exchangers used, it is not appropriate to use the same model as that employed for subcritical heat pumps. A new model would need to be developed. It is likely that heat pumps using R744 will become increasingly significant but the relative resistance to change in the overall energy demand profile of the building stock makes it likely that HFC based heat pumps will remain dominant. Because of this, this research will focus on the performance of HFC based, subcritical heat pumps but it is recommended that further work should include R744 based transcritical heat pumps.

2.2.4 Alternative heat pump configurations

Several studies have undertaken to consider the effect of combining a heat pump with other renewables such as solar collectors. The heat pump's evaporator can be coupled to a solar collector in order to increase the temperature of the evaporator and therefore improve the heat pump's performance. The coupling can either be indirect (e.g. hot water is generated by the solar collector and this is used as heat source) or direct (in which case the evaporator and solar collector are a single unit). Using an experimental direct expansion unit, Ito et al. (1999) achieved a COP of 5.3 (ambient air temperature 8ºC, heating water from 25ºC to 40ºC) but the insolation level was higher (Japan) than that likely to be experienced in the UK. Various modelling exercises (Freeman et al. 1979; Biaou & Bernier 2008; Chandrashekar et al. 1982) and experimental work (Comakli et al. 1993; Ozgener & Hepbasli 2005; 2007) have considered the effect of using different configurations when using solar collectors. In most cases, a simpler "parallel" configuration (i.e. the solar collector and heat pump supply hot water independently) achieved greater efficiency than the "series" configuration described above.

An interesting alternative is to couple the heat pump's evaporator to a solar PV array, given that the efficiency of PV units decreases when their temperature increases. Chow et al. (2010) described such a system being trialled and achieving an average COP of 5.4, while improving modelled PV efficiency from 8.7% to 12.1% in Hong Kong. However, again, it is unlikely that this could be achieved in the UK given the lower solar insolation experienced.

For larger applications, Lian et al. (2005) demonstrated that there is potential for large improvements in primary energy efficiency by using an internal combustion engine to drive the compressor of the heat pump (and, of course, recovering "waste" heat from it). However, given the scale the systems available (multi-MW in the example considered but 100kW to 1MW in other systems (Hepbasli et al. 2009)) it seems that the concept has limited scope for application to the UK domestic sector, unless combined with a district heating network.

Adsorption and absorption heat pumps are driven by higher temperature heat flows (rather than a compressor) in order to supply more heat at a lower temperature. This potentially makes them an attractive option as a replacement for gas boilers as the high temperature heat can be supplied by burning gas; only minimal electrical power flows are required (Critoph & Metcalf 2012). Although some emissions are inevitable unless the gas supply is decarbonised, their operation will emit less CO_2 than a conventional boiler. However, the performance which can be achieved with them is currently limited to COPs below 1.4 (with zeolite adsorbent / water as working fluid, Demir et al., 2008) and so although some units have been developed (e.g. Viessmann 2011), they have not attracted the same attention as other devices for this application, being

used primarily in applications where waste heat is available but cooling is required (e.g. industrial processes and trigeneration plants).

The operation of the two types of heat pump are similar in principle but vary in the selection of either a solid (e.g. zeolite) that absorbs the refrigerant (e.g. water) in an adsorption cycle or a fluid (e.g. water) which the refrigerant (e.g. ammonia) is soluble in, in an absorption cycle. In its simplest conceptual form, the cycle is as follows:

1. The process of the vaporised refrigerant being absorbed is exothermic and occurs at low pressure (e.g. 6 – 10mbar(a) for water / ammonia mix), rejecting heat which can be used.

2. Higher temperature heat is then applied to the absorbent causing the refrigerant to be released as a vapour at a higher pressure (e.g. 40 – 80mbar(a) for water / ammonia mix) and move to a second volume. The absorbent remains in the first volume.

3. The refrigerant vapour condenses in the second volume, rejecting heat which can be used (still at the higher pressure with high temperature heat continuing to be applied to the absorbent).

4. The higher temperature heat source is removed from the absorbent and the pressure drops. This causes the refrigerant to evaporate; cooling and receiving heat in the second volume (supplied from either the environment or a volume to be chilled).

5. The low pressure, vaporised refrigerant is then reabsorbed by the absorbent and the cycle repeats.

In a practical arrangement, the two volumes could each be split into a volume for receiving heat and a volume for rejecting heat. This could be achieved by introducing a pump between the volumes in which the absorbent / refrigerant mixture rejects and receives heat and an expansion valve between the volumes in which the refrigerant rejects and receives heat.

In a hypothetical grid mix with a large proportion of wind generation, it is possible that an adsorption heat pump could be combined with electrical storage heating as its high temperature heat source in order to store energy at times that the wind generation would otherwise need to be constrained. This system is somewhat more hypothetical than those being analysed in this study but remains an interesting possibility.

2.3 Micro Combined Heat and Power

2.3.1   Introduction to micro Combined Heat and Power units

Combined Heat and Power (CHP) units combine the generation of power (typically electrical generation) with provision of heat. Because the heat supplied is generally that rejected during the power generation and would otherwise be wasted, CHP units can achieve high total efficiencies. Although any CHP plant with an electrical output of less than 50kW is defined as micro-CHP (mCHP) (EC 2004), in practice mCHP usually refers to CHP plant with an electrical output of less than 15kW as these can be realistically installed in a single dwelling (Simader et al. 2006).

Various types of mCHP unit can be categorised by the way they generate electricity. This is either with a heat engine driving an electrical generator or a fuel cell. The heat engines used, to date, in commercialised units are Stirling engines (SE), internal combustion engines (ICE) and gas turbines (GT). The fuel cells used in commercialised units are either polymer electrolyte (or "proton exchange") membrane fuel cells (PEMFC) or solid oxide fuel cells (SOFC).

Internal Combustion Engine (ICE) mCHP units have seen the most commercial success to date. They achieve reasonable electrical efficiencies (typically 20% to 30%, more detail on performance is given in the next section) and a rapid electrical response (De Paepe et al. 2006). The Senertec Dachs is widely used for small commercial baseload heating but with a 5.5kW electrical output (HKA5.5 model) and a 12.5kW thermal output, it is too large for most dwellings. Its cost is reported to be around £10,000 to £14,000 (Staffell et al. 2010) or €13,750 (De Paepe et al. 2006). Yanmar Energy Systems Co. have developed 5kW, 10kW and 35kW electrical output ICE units. Kinoshita (2011) has suggested various operating strategies based upon these units operating together in order to achieve maximum cost effectiveness and efficiency but their size makes this more appropriate for small to medium commercial applications. The Valliant EcoPower (also marketed as PowerPlus or Marathon) unit has a similar capacity and price as the Dachs HKA5 (1.3kW to 4.7kW electrical, 4kW to 12.5kW thermal, around £11,000 (Staffell et al. 2010) or €11,750 (De Paepe et al. 2006)). However, its ability to modulate generation increases its flexibility and makes it more suitable to domestic heating. The EcoWill ICE-mCHP (branded as FreeWatt in the USA) uses a smaller, 163cc ICE manufactured by Honda and has an electrical output of around 1kW with 2.8kW heat output but does not modulate in order to avoid operating at lower efficiency (Roselli et al. 2011). Over 50,000 had been sold by July 2007 (Honda Motor Co. Ltd. 2007) with a list price of 900,000 yen (i.e. around £6,000, Nichi Gas 2012).

Stirling Engines (SE) have the potential to provide reliable operation, fuel flexibility, good emission characteristics and quiet operation. Solo Stirling 161 microKWK units have a similar capacity to the Senertec and EcoPower ICE units and are capable of modulating their output from 2kW to 9.5kW electrical output with 8kW to 26kW thermal output. They operate with helium as their working fluid, pressurised to between 30bar and 130bar. De Paepe et al. (2006) report their installed price to be around €25,000. The Whispergen and Baxi EcoGen SE-mCHP units are smaller and, being more suited to individual dwellings, have attracted more attention in the UK. The Baxi Ecogen also uses helium as its working fluid but at lower pressure than the Solo Stirling unit (up to 23bar). It is capable of varying its electrical output from 300W to 1kW output and its thermal output between 3.4kW and 6.4kW. The Whispergen uses Nitrogen as its working fluid (Aliabadi et al. 2010) and costs around €9000 installed. It has an electrical output of around 750W with a thermal output of just over 7kW (De Paepe et al. 2006). The Whispergen has a standby power consumption of around 9W, increasing to 100W when operating (Whispergen Ltd 2006).

Although GT-mCHP units are currently limited to lower electrical efficiencies than ICE units, it is likely that they have the potential to achieve lower CO and NOx emissions and greater reliability (Simader et al. 2006). At local district heat network scale, GT-CHP units with reasonable electrical efficiencies are possible; for example Ristic et al. (2008) consider the optimum dispatch profile for a 635kWe GT-CHP unit achieving 31% electrical efficiency. GT-mCHP units that could achieve 15% mechanical efficiency with less than 1kW output, have been suggested (e.g. Clay & Tansley 2010) but apparently not yet commercialised. A GT-mCHP with 3kW electrical output and 15kW thermal output has been developed (Visser et al. 2011) and is due to enter field trials in early 2013 with commercialisation planned for 2014 (MTT 2013).

Fuel Cells have several advantages over other prime movers including high electrical efficiency, quiet operation and low emissions (Hawkes et al. 2011). Cruden et al. (2008) also noted their relatively modular nature (that is, their efficiency is not as dependent upon their size as it is for other prime movers). Fuel cells operate by combining reactants across an electrolyte, directly creating an electrical current. Ions migrate across the electrolyte to complete the reaction whilst electrons carrying the same charge are released at the anode to generate the current. Depending upon the nature of the electrolyte either positive ions (e.g. H^+ ions) are transferred from the anode to the cathode or negative ions (e.g. O^{2-} ions) are transferred from the cathode to the anode. Because electrons flow to the cathode (the same as in electrolysis), it is the positive terminal relative to external measurement (unlike electrolysis). The reactants most commonly used are hydrogen (to the anode) and oxygen (to the cathode) producing water as the product, see Figure 8.
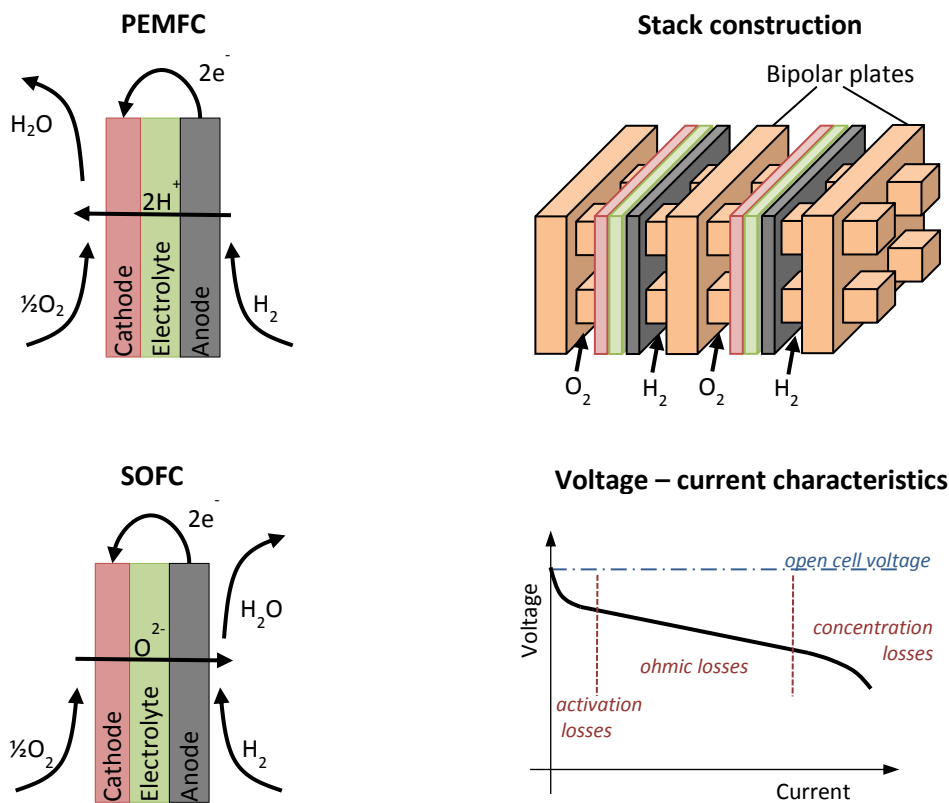
Figure 8: Introduction to fuel cells

Each cell produces a voltage of typically 0.8V and so cells are arranged in series in a stack, separated by bipolar plates in order to provide more useful voltages. Larminie & Dicks (2003) described three losses that reduce the voltage across cells (proportional to efficiency as current is directly related to fuel consumption rate): activation losses, ohmic losses and concentration losses. Activation losses occur due to the energy required for the electrochemical reaction to start; lower losses occur at higher temperatures, higher losses occur as the logarithm of the current density (i.e. the rate of reaction) increases. Ohmic losses are due to the resistance of the electrodes, electrolyte, bipolar plates and interconnections. Concentration (Nernstian) losses are due to an effective reduction in the partial pressure of the reactants due to insufficient flow of fuel relative to the current density. As these losses increase with current density the maximum power output occurs at less than the maximum current density of the stack.

Several different types of fuel cells can be distinguished depending upon the electrolyte used. PEMFCs and SOFCs are the ones which have attracted most interest for application as mCHP. Other types include alkaline fuel cells, phosphoric acid fuel cells, molten carbonate fuel cells and methanol fuel cells.

PEMFCs use a polymer electrolyte that transfers H+ ions. Advantages include low temperature (70ºC) operation, compact and relatively rugged construction with no corrosive fluids. The

polymer most commonly used is nafion (sulphonated PTFE). In order to operate at lower temperatures, a catalyst (platinum) is deposited on the electrodes. Electrodes are either constructed from a porous conductive sheet such as carbon paper with carbon particles supporting the platinum, or the carbon particles are fixed directly to the polymer electrolyte. Operation of the electrolyte depends upon the presence of some humidity but too much will adversely affect the overall operation and so this must be maintained between 80% and 100% relative humidity. The Balance of Plant (BoP) for a PEMFC is relatively complex, especially in the case that the fuel is not hydrogen (methane being the most convenient fuel for domestic applications). This BoP would typically include fuel reforming to hydrogen and scrubbing to remove carbon monoxide and other compounds as these poison the catalyst. A 700W electrical output PEMFC-mCHP unit has been listed for 3.5M Yen (i.e. around £25,000 excluding installation, Nichi Gas 2012) with an observed learning rate of (i.e. decrease in costs associated with doubling of production) around 20% (Staffell 2009).

SOFCs use a ceramic oxide electrolyte that transfers cations. Steam reforming of methane occurs can occur internally at the operating temperatures within a SOFC stack. Although this reduces the BoP required, it still usually includes pre-heating of reactants to reduce thermal loading, the removal of sulphur compounds and either an afterburner or alternative use for fuel which has not been utilised in the stack (fuel utilisation rates of around 80% are typical). Yttria-stabilised zirconia oxide (YSZ) has been used as the electrolyte but in order to conduct the oxygen ions it must be maintained at above 800ºC and thin. In order to reduce stack temperature from 1000ºC to 800ºC the electrolyte thickness must be reduced from 200µm to 20µm (Milewski & Miller 2006), alternative electrolyte materials at this thickness can theoretically improve the stack efficiency by over 15% (e.g. 45% to 60%). Intermediate temperature SOFC units (operating at 500°C to 750°C) have attracted attention at this scale as they have several advantages: below 600ºC, stainless steels can be used for elements of the construction, start-up times are reduced and thermal stresses are reduced (Bove 2007). For these intermediate temperatures, ceria-gandolinium oxide (CGO) is an option for the electrolyte if it is thin enough (15µm) but must be supported. Within a SOFC, excess air is generally supplied to the cathode side in order to provide cooling. A 1.5kW – 2kW electrical output SOFC-mCHP is listed at £19,950 excluding installation (Fuel Cell Today 2012) and it has been suggested that the learning rate may be as high as 35% for similar SOFC units (Rivera-Tinoco et al. 2012).

The open cell voltage of the cell is proportional to the Gibbs energy of the reaction which occurs. The Gibbs energy of the reaction is a function of the relative concentration of the reactants and products and of the temperature at which the reaction occurs (shown in Figure 9 for the formation of water). This means that the open cell voltage of a SOFC will be lower than that of a PEMFC (as it is at a higher temperature). In practice, however, the reduction in

activation losses more than compensates for this and so the electrical efficiency of a SOFC is typically higher than that of a PEMFC.
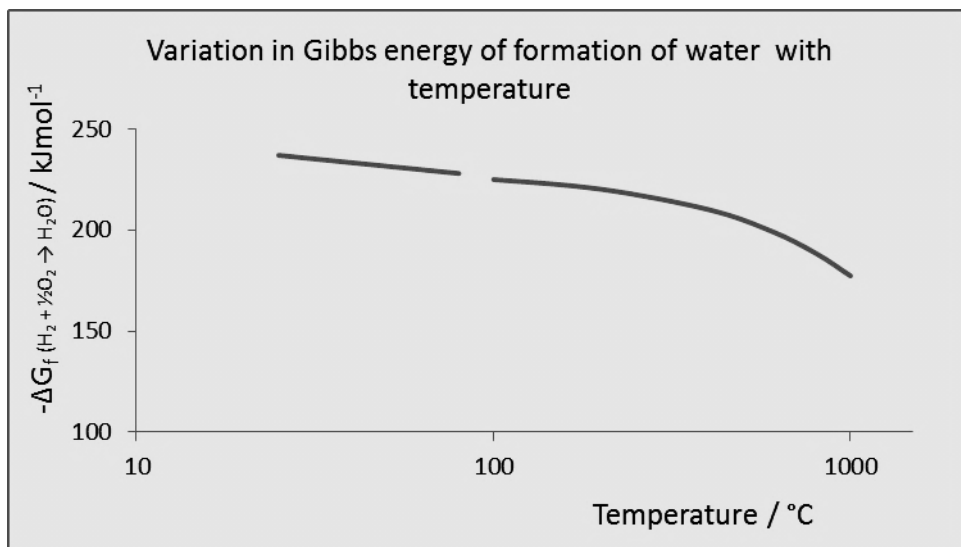
Figure 9: Variation in Gibbs free energy of formation of water. Data from Larminie & Dicks (2003). N.B. below 100°C, water is condensed.

Despite the optimum stack efficiency occurring at less than full load, the response of the fuel reformer often results in lower fuel utilisation and therefore system efficiency. Vijay et al. (2010) observed that maintaining constant fuel utilisation achieves a good approximation to optimum efficiency; effectively maintaining the fuel mass inlet rate proportional to the current density from the cells. SOFC stacks are sensitive to thermal cycling and have typical warm up and cool down cycles of 12 – 24h with operational ramp rates of around 0.05kW/min. PEMFC units can react faster but still require at least one hour to warm up and exhibit a typical maximum ramp rate of around 0.2kW/min (Hawkes et al. 2009). Both PEMFC and SOFC units have a practical minimum turn-down ratio (typically around 20%) as below this, the parasitic loads from auxiliary systems and the need to maintain the temperature of the unit require the majority of the energy output.

2.3.2 mCHP performance

The potential efficiency of mCHP units has attracted considerable attention and so performance data is available from several sources including laboratory testing and field trials. A range of efficiency data is presented in Figure 10. The data is intended to illustrate the range of performances which are generally achieved by these technologies. Most data points relate to steady-state operation of the units but the approximate range of efficiencies encountered in field trials is also illustrated by the three ellipses. Efficiencies are relative to the Gross Calorific

Value (GCV) of the fuel. Some data points relate to the same unit under different conditions or test facilities.
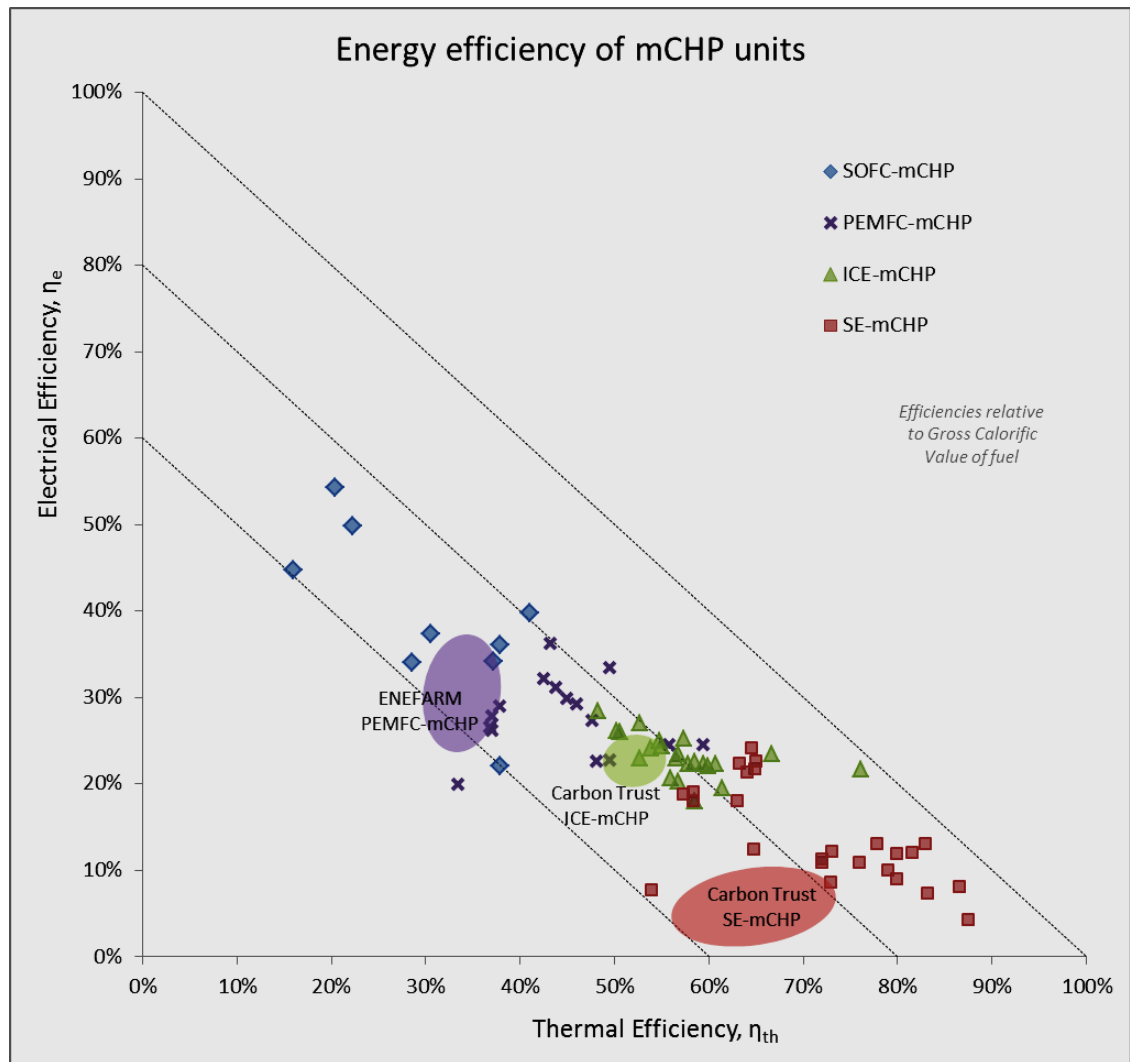
Figure 10: Energy efficiency of mCHP units. (Data adapted from Carbon Trust 2011; Thomas 2008; Yamada & Nishizaki 2009; Aliabadi et al. 2010; De Paepe et al. 2006; Bianchi et al. 2011; Beausoleil-Morrison, Arndt, et al. 2007; Dorer & A. Weber 2009; Thorsteinson et al. 2011; Payne et al. 2009; Love et al. 2009; Magri et al. 2012; Roselli et al. 2011; Staffell 2009)

Almost all total efficiencies exceed 60% and are, of course, limited to less than 100% although some SE-mCHP units can approach this. The total efficiency tends to increase in the units with a higher heat to power ratio. Changing the temperature that heat is supplied at affects thermal efficiency primarily as a function of whether heat can be recovered through the condensing of exhaust gasses. The electrical efficiency of SE-mCHP is generally more affected by the temperature of heat recovery than ICE-mCHP units; for example the Solo's electrical efficiency decreases from 26.8% to about 24.5% when the flow temperature is increased from 40ºC to 65ºC (Thomas 2008).

The high performance of the BlueGen SOFC-mCHP unit manufactured by Ceramic Fuel Cells Ltd (2008) merits further description. The unit is apparently capable of achieving a net electrical efficiency of 54% (GCV). This is achieved at an electrical output of 75% of its rated power (i.e. at 1.5kW electrical output), with 77% total efficiency. The unit's output can be varied from 0 – 100% but requires relatively long start-up and cool-down periods (20hr & 36hr respectively). Payne et al. (2009) and Love et al. (2009) describe the unit in more detail. Achieving a high fuel utilisation rate (85%) is a key enabler of the performance and therefore a driver for the careful design of the stack components. At this fuel utilisation, the stack layer voltage is 0.83V and DC efficiency is 61% (GCV). The majority of voltage drop is due to polarisation at the anode-electrolyte interface and ohmic losses; relatively small (~10mV) losses are due to concentration despite the high fuel utilisation. Other aspects of the design such as the balance of plant also require care in order to minimise heat losses (to 200W in this unit).

The Carbon Trust (2007) reported on a large scale field trial of mCHP units conducted in the UK. 87 mCHP units were monitored in detail for periods between 2005 and 2007. Most of these (72) were SE-mCHP units in domestic dwellings (mostly Whispergen Mk4 & Mk5 units), but the trial also included 15 larger ICE-mCHP units in commercial buildings. In the winter, 85% of the SE-mCHP units achieved a thermal efficiency of 64% - 76%, with 38% in the centre band of 68 – 72% (GCV, including parasitic losses while in standby). Electrical efficiencies ranged from about 3% to 8% with a mode of about 6% in the heating season but were typically 3 – 4% lower in the summer. The importance of a large consistent heat load to the performance of these units is a consistent theme also seen in studies using modelling and so merits the further exploration given it in the modelling chapter. A smaller trial of four Baxi Ecogen SE-mCHP units demonstrated higher efficiencies but used dwellings with large heat demands (around 30,000kWh/ year) and large buffer tanks (Lipp 2012).

The largest trials of mCHP units, to date, have taken place in Japan under the ENEFARM programme. This primarily involved ICE-mCHP and PEMFC-mCHP units with more limited testing of other types such as SOFC-mCHP units. Tokyo Gas conducted a field trial of 166 PEMFC-mCHP units from 2008, making them commercially available from May 2009 (Yamada & Nishizaki 2009). The units can generate 300W to 1kW electricity and have design efficiencies of 33% for electricity and 47% for heat (both relative to GCV). However, in operation some units performed slightly better (exceeding 36% electrical efficiency in some cases). The electrical output is variable from 300W to 1kW. Heat is supplied at 60°C and the units are generally supplied with a 200 litre hot water tank. Ecowill 1kWe ICE-mCHP units were tested in 70 dwellings between 2001 and 2003 (Iwata 2004). The units were controlled by a predictive, heat-led algorithm, using excess electricity to increase heating when it is not needed locally. Run times of 1,327 to 3,160 hours / year were observed with carbon emissions

savings of up to 1,220kg /year (against a grid carbon emissions factor of $0.69kg_{CO_2}$/kWh). Because electrical export is not permitted in Japan, Maeda et al. (2010) suggested an improved control logic based on this including the use of excess electricity for heating.

The performance characteristics of 12 mCHP units are used in the main modelling exercise conducted during this research. A summary of the main characteristics of these units is provided in Table 4. The units have been selected to represent the range of performance and capacities which are available. In particular, this included modulating and non-modulating heat engine units as well as undersized and oversized units. Because of the high performance but small size of the CFCL unit ("SOFC A"), a second hypothetical unit ("SOFC B"), comprising three SOFC A units in parallel, has been considered. This is modelled as a hypothetical, larger unit rather than three smaller units; that is, the potential to achieve high efficiency at low loads by turning off two of the units has not been considered here. Although some of the units have auxiliary gas burner modules, these are considered separately in the modelling so that the contribution from each subsystem is apparent.

Table 4: Characteristics of mCHP units investigated

Unit designation	Based upon	Electrical capacity	Thermal capacity	Electrical efficiency[1]	Thermal efficiency[1]
SE- mCHP A	Whispergen Mk0	0.75W[2]	6.5kW[2]	10.8%[3]	76%[3]
SE- mCHP B	Baxi Ecogen	0.17kW – 1kW[4]	3.5kW – 6.8kW[4, 5]	4.2% - 12%[4]	88% - 80%[4]
SE- mCHP C	Solo Stirling 161	1.3kW – 8kW[2]	6.9kW – 24.3kW[2]	12% - 21%[2]	64%[2]
ICE- mCHP A	Senertec Dachs HKA 5.5	5.5kW[6]	12.5kW[6]	25%[6]	55%[6, 7]
ICE- mCHP B	Powerplus EcoPower e4.7	1.2kW – 4.4kW[2]	3.8kW – 12.1kW[2]	20% - 22%[2]	62% - 60%[2]
ICE-mCHP C	EcoWill / FreeWatt	1kW[3]	2.8kW[3]	20%[3]	57%[3]
PEMFC A	(Confidential)	1.5kW – 4.6kW[2]	3.0kW – 9.1kw[2]	17% - 24%[2]	61% - 45%[2]
PEMFC B	(Confidential)	1.1kW - 4.5kW[2]	1.6kW – 7.7kW[2]	17% - 24%[2]	30% - 45%[2]
PEMFC C	Hyteon prototype	0.54kW - 1kW[8]	0.69kW – 1.5kW[8]	46% - 42%[8]	29% - 32%[8]
SOFC A	CFCL Bluegen	0.5kW - 2kW[9]	0.3kW - 1kW[9]	37% - 54% - 51%[9]	25% - 21% - 29%[9]
SOFC B	3 x CFCL Bluegen units	1.5kW - 6kW[9]	0.9kW - 3kW[9]	37% - 54% - 51%[9]	25% - 21% - 29%[9]
SOFC C	FCT	3kW – 3.7kW[2]	*4.6kW – 6.1kW[2, 10]*	24%[2]	*50% - 52%[2, 10]*
Notes. Ranges relate to modulating behaviour of units. 1: Efficiencies relative to GCV of fuel; 2:Beausoleil-Morrison, Arndt, et al. (2007); 3: Roselli et al. (2011); 4: Magri et al. (2012); 5: excludes auxiliary burner; 6: Thomas (2008); 7: Without additional condenser unit; 8: Thorsteinson et al. (2011); 9: Payne et al. (2009); 10: Thermal output based upon assumption of 100% effective heat recovery rather than measured data.					

2.3.3 Alternative configurations

The use of other sources of heat in mCHP units has been suggested by several researchers. The use of biomass has the potential to reduce overall CO_2 emissions and could be achieved with various prime movers: a gasifier with an IC engine, an Organic Rankine cycle (ORC), an indirectly fired gas turbine, a Stirling engine or biofuel IC engines. These systems are feasible at the 30kW – 1MW electrical output, with analysis suggesting that a 100kW gas turbine unit could achieve around 20% electrical efficiency (Wood & Rowley 2011). ORC devices have been proposed due to the relatively high output that they can achieve from heat supplied at moderate temperatures; a 2kW electrical output device achieving a theoretical efficiency of almost 17% has been modelled by H. Liu et al. (2011). Several ORC-based biomass CHP units

are commercially available with sizes of around 400kW electrical output and typically achieving 20% electrical efficiency but there do not appear to be any commercially available at mCHP scales (Dong et al. 2009). An interesting alternative to biomass is the use of a solar collector in combination with a gas boiler to supply heat to an ORC, as reported by Yagoub et al. (2006). A unit was developed and installed in an office building in the UK. A 25kW solar thermal collector was used with a gas boiler to drive a 1.5kW turbine operating using an ORC cycle. An electrical efficiency of 7.5% was achieved, feeding into an average daily demand of 28kWh; however the solar fraction of the heat supplied was estimated to be only 14%.

An alternative form of biomass supply is the combination of a fuel cell CHP with an anaerobic digester. The potential market for this is clearly smaller and units would probably not be feasible at mCHP scales but the concept has still attracted some interest. For example, the Greenhouse Gas Technology Centre Southern Research Institute (2004) reported on the operational performance of a 200kW Phosphoric Acid Fuel Cell CHP unit combined with an anaerobic digester. The unit achieved 35% - 40% (average 37.5%) efficiency with anaerobic digester gas which is processed to remove hydrogen sulphide, other sulphur and volatile organic compounds.

Increasing the pressure of reactants in a fuel cell increases its efficiency and power output (e.g. increasing the pressure from 1bar to 3bar caused a 15% increase in output in an example described by Singhal 2000). In the case of SOFC units, this leads to a potential synergy with gas turbines; the SOFC and afterburner are used in place of the combustion chamber (Choudhury et al. 2013). The performance of hybrid systems based upon available GT and SOFC units (30kW to 100kW and 160kW to 260kW outputs, respectively) has been modelled by Bakalis & Stamatis (2012) with results suggesting that electrical efficiency could be improved from 49% to 60% in some configurations.

Larger SOFC units could be combined with coal gasification and provision for carbon capture. In fact, several synergies are possible, minimising the performance penalty (Li et al. 2011): hot, decarbonised and humidified anode exhaust gas can be recycled back to the hydro-gasifier; the gasifier can produce methane-rich syngas rather than hydrogen as this will be reformed within the SOFC; pressurisation necessary for the operation of the gasifier also increases SOFC efficiency and allows the use of an additional gas turbine

2.4 Performance metrics

2.4.1 Energy analysis

The energy flows which are considered in this analysis are notionally illustrated by Figure 11. Energy flows will occur at each of the four stages. In most cases, the Primary Energy Requirement (PER, stage 1 in Figure 11) and the end use energy demand (stage 4) will be most relevant. However, comparison with the energy delivered to the unit (stage 2) and delivered by the unit (stage 3) will sometimes yield interesting observations, for example in the cases where supplementary burners are used with mCHP units.
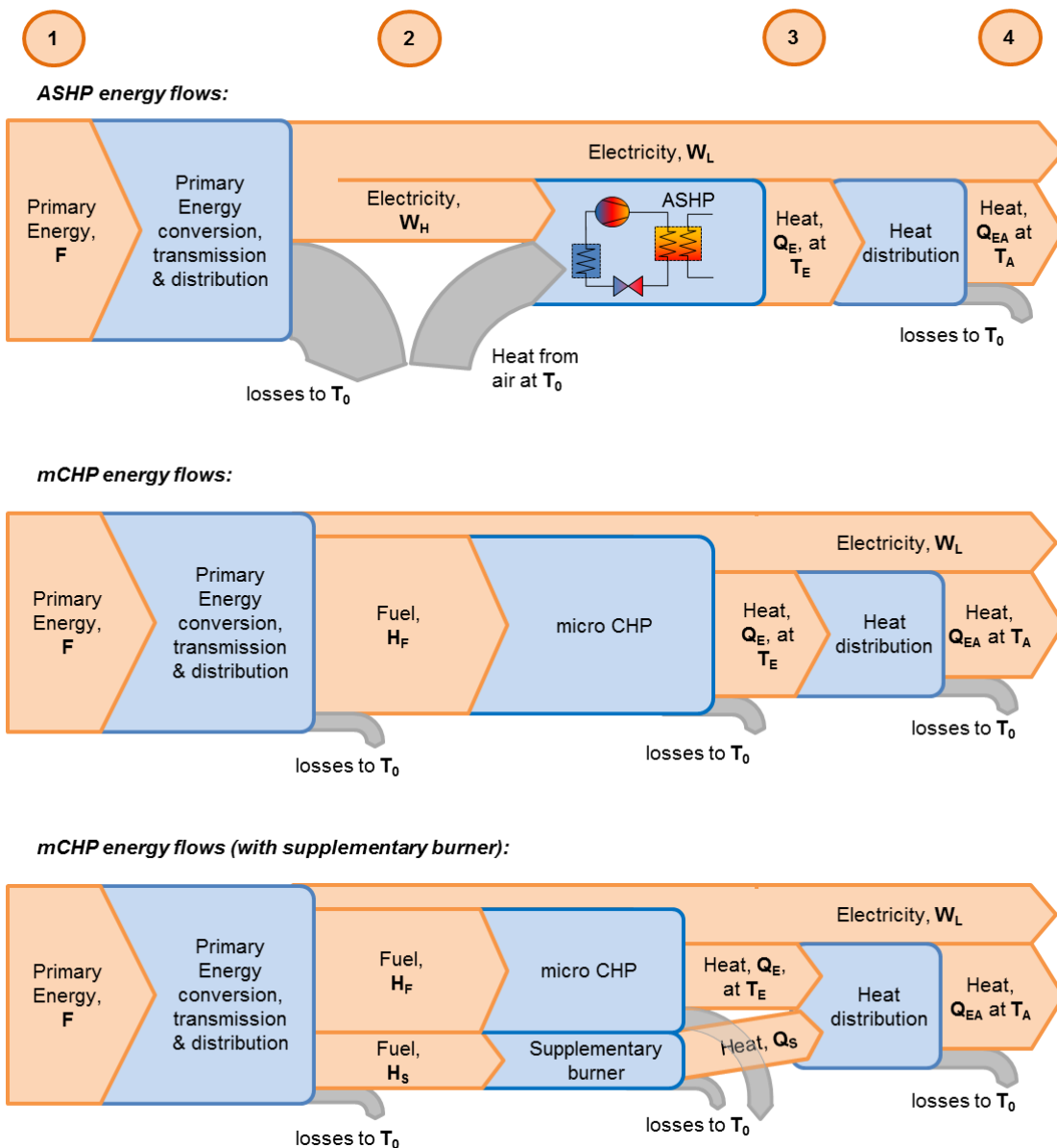
Figure 11: Whole system energy flows associated with ASHP and mCHP units

Upstream energy use associated with the extraction and processing of fuels is not included; that is the initial boundary is delivery to power stations for primary energy supplied for the generation of electricity. The renewable energy consumption of renewable generation is not included in their PER but life-cycle energy requirements associated with construction, operation and maintenance are. Energy associated with the construction, operation and maintenance of other types of power generation are included but are relatively low in the case of fossil fuel plant; around 1.5% in the case of CCGT (Spath & Mann 2000; Odeh & Cockerill 2008). All values of fuel energy content (enthalpy of combustion, H) are converted to gross calorific value (GCV, i.e. higher heating value, including the latent heat of vaporisation of water formed during combustion).

The values for Energy Requirement for Energy given in Table 5 are used to calculate PERs (see chapter 4, section 4.6.5).

For nuclear power stations, the convention for thermal efficiency employed by DECC (2011) has been followed with additional allowance for construction energy. It should be noted that reliable figures for this were difficult to obtain. The figure of 2.62 consists of a thermal energy input of 2.56 (DECC 2011) and an additional 0.06 corresponding to construction (AEA Energy & Environment 2008).

The figures for biomass and CHP are sensitive to assumptions made regarding the mix of generation technologies, the fuel for the CHP plant and the source of the biomass. However, the contribution from them is low in the Transition Pathways scenarios used as background to this study apart from in the "Thousand Flowers" scenario which postulates high penetration of CHP (see Table 18). The selected values reflect those selected for LCA work within the project (O'Grady 2012, personal communication) consistent with the assumption of primarily thermal-based CHP using low carbon biomass.

Losses from natural gas pumping, leakage and other operator activities amounted to 2% of the total natural gas energy input in 2010 with a resultant PER for natural gas supplied to mCHP units of 1.02 per unit of energy (i.e. GCV of fuel) supplied (DECC 2011). Losses upstream from input to the national transmissions system (e.g. extraction and processing) are not included in this study.

Table 5: Average energy requirement for energy associated with different generating plant types

Generating plant type, *L*	Energy Requirement for Energy	Notes
Gas CCGT	2.22	(Odeh & Cockerill 2008)
Gas CCGT with CCS	2.59	(Odeh & Cockerill 2008)
Subcritical pulverised coal	2.98	(Odeh & Cockerill 2008)
Coal IGCC	2.83	(Odeh & Cockerill 2008)
Coal IGCC with CCS	3.29	(Odeh & Cockerill 2008)
CHP	3.31	(Ecoinvent 2010)
Thermal renewables (e.g. biomass)	1.64	(Ecoinvent 2010)
Wind	0.13	(Ecoinvent 2010)
Tidal	0.06	(Douglas et al. 2008)
Nuclear	2.62	(increased by 0.05 in 2010 due to maintenance) (AEA Energy & Environment 2008; DECC 2011).
Hydro	0.07	(Ecoinvent 2010)
Figures considering only energy content of fuel:		
Coal	2.77	(2.79 in 2009) (DECC 2011)
Gas (CCGT)	2.10	(2.15 in 2009)(DECC 2011)
CCGT	2.02	(Hammond & Ondo Akwe 2007)
CCGT with CCS	2.56	(Hammond & Ondo Akwe 2007)
State of art CCGT	1.85	(Siemens AG 2010)
Other non-renewable thermals	3.13	(DECC 2011)

2.4.2 Exergy analysis

Exergy analysis is concerned with the quality of the energy flows in a system (in terms of the theoretical work which could be extracted from them). As such, exergy has been suggested as a measure of the value and potential environmental impact of a process or activity. Rosen & Dincer (2001) argued that "a thorough understanding of exergy and the insights it can provide into the efficiency, environmental impact and sustainability of energy systems, are required for the engineer or scientist working in the area of energy systems and the environment". Szargut (2007) discusses the use of the "Cumulative Exergy Consumption" as an alternative to

Cumulative Energy Consumption when considering the impact of a product or service. However, in terms of sustainability, exergy analysis does not provide the whole picture and other measures such as LCA are also required (Hammond 2004b).

As a measure of the irreversibilities in a process, exergy analysis is more widely used to identify the potential improvement in a system and the components or sub-systems which might show the greatest efficiency gains when they are improved. This has been applied to various heat pump systems, generally resulting in the motor-compressor sub-assembly being identified as the largest source of exergy destruction (e.g. 56% in a study of GSHPs by Hepbasli & Akdemir (2004), 36% in a study by Bi et al. (2009)). Although some authors (Hepbasli 2008, Koroneos et al. 2003) have analysed the exergy efficiency of renewable systems, most take the approach of considering the exergy output of these systems to be the same as their input when analysing the overall energy system.

Because exergy recognises that work and heat can have different values, it has been used as a performance metric for the comparison of CHP plant with other technologies. This has been applied to mCHP units but is not perfect and other concepts such as marginal efficiency may be useful, depending upon the scenario under analysis (Aliabadi et al. 2010).

The boundaries for the exergy analysis in this study will be the same as those used with the energy analysis. However, the property is perhaps less familiar than energy and additional processes are required in order to calculate its value. A more thorough discussion of exergy is therefore included here.

For a heat engine, the exergy (i.e. the potential work) which can be extracted from a heat flow between two fixed temperatures is limited by the requirement that the total entropy of the (isolated) system cannot decrease, that is:

$$dS = \frac{Q_E}{T_E} - \frac{Q_{out}}{T_0} \geq 0$$

Equation 2

where dS is the change of entropy within the engine occurring during the (cyclic) process, Q_E is the heat entering the system at absolute temperature T_E and Q_{out} is the minimum heat which must leave the system at absolute temperature T_0. This constrains the minimum value of Q_{out}. Rearranging Equation 2 and substituting it into the equation for the conservation of energy leads to Carnot's familiar expression for the maximum amount of work which can be extracted, E:

$$E = Q_E - Q_{out,min} = Q_E - Q_E \cdot \frac{T_0}{T_E} = Q_E (1 - \frac{T_0}{T_E})$$

Equation 3

This has the effect of decreasing the exergy content of thermal energy as the temperature at which the energy is supplied decreases relative to the ambient temperature (Figure 12).
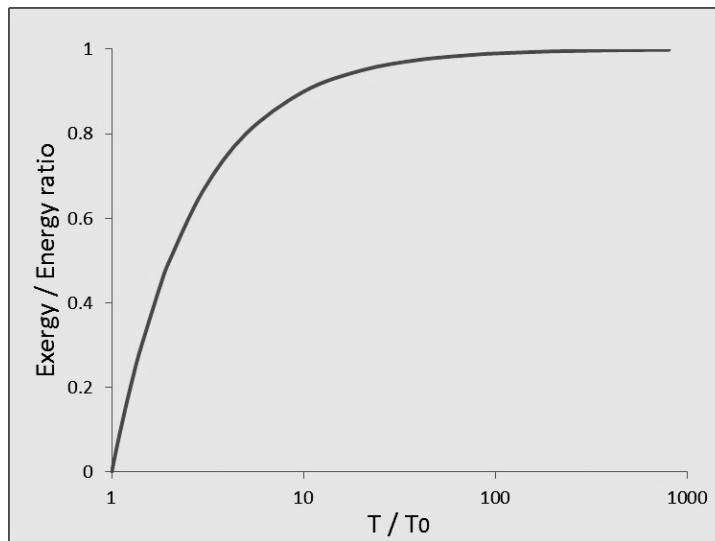
Figure 12: Variation of exergy content of heat flow with temperature

In applying exergy techniques to the UK's energy system, Hammond & Stapleton (2001) discussed the effect of employing different reference ambient temperatures, noting that the different conventions used by various authors (e.g. 25ºC, 10ºC, -1ºC) will have a large effect on any exergy analysis of low-temperature heat demands. In order to address this potential ambiguity, the approach used in the present study is to calculate all exergy flows during each time-step using the temperatures which occur during that time-step. The low exergy value of thermal energy used for space heating generally results in poor exergy efficiencies for domestic heating systems; for example, Hepbasli & Akdemir (2004) found an overall exergy efficiency of approximately 4% when analysing a heating system. This is recognised by Schmidt (2009) who discusses the importance and application of the exergy concept to domestic energy consumption. Schmidt has described the work within the International Energy Agency Energy Conservation in Buildings and Community Systems (IEA ECBCS) Annex 49 on the "LowEx" approach. This suggests that energy saving measures should be prioritised according to exergy saved rather than just energy.

The exergy value of heat transferred across a boundary for which temperature is not constant (as is the case in a heat exchanger in which the temperature of the receiving working fluid increases as it absorbs heat) is given by integrating the exergy value at each temperature. Equation 3 becomes:

$$E = \int_{T_{EX}}^{T_E} (1 - \frac{T_0}{T}) dQ = Q_E - \int_{T_{EX}}^{T_E} cm \left(\frac{T_0}{T}\right) dT \qquad \text{Equation 4}$$

where T_{EX} is the return absolute temperature. For a domestic heating system, the fluid receiving heat is typically water. Given that the heat capacity of water remains approximately constant for the temperature range encountered (20ºC to 85ºC), Equation 4 can be evaluated to:

$$E = Q \left[1 - \frac{T_0}{T_E - T_{EX}} ln \left(\frac{T_E}{T_{EX}}\right) \right] \qquad \text{Equation 5}$$

The exergy efficiency (ψ) of a process or system is given as the ratio of useful exergy outputs to exergy inputs (Kotas et al. 1995), that is:

$$\psi = \frac{\sum E_{out}}{\sum E_{in}} \qquad \text{Equation 6}$$

Figure 13 illustrates the same underlying heat pump performance data as those plotted in Figure 6 but using exergy efficiency rather than COP to measure performance. Although Figure 6 shows that the COP decreases with an increasing temperature difference between the heat source and heat sink, it is clear that the exergy efficiency does not vary as much (the average standard deviation per unit is only 2.1% of the mean). This is a useful result which is used to facilitate the modelling of the units (see section 4.4.4.2 on page 97).
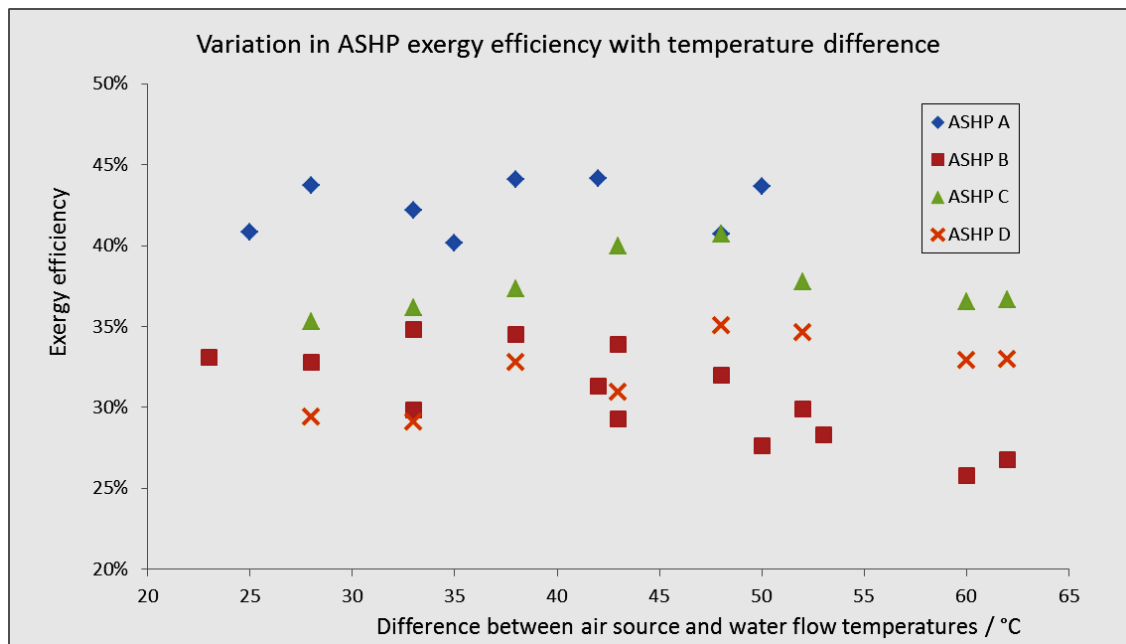
Figure 13: ASHP exergy efficiency with variation in operating temperatures. Data adapted from Butler & Hyde 2007; Warmepumpen-Testzentrum 2013; Energimyndigheten 2012.

For domestic systems involving both electricity (work) and space heating (e.g. heat pumps and combined heat and power units), the system exergy efficiency will depend upon the ratio between heat and electricity being demanded, the efficiency of electrical generation and also the exergy value of the space heating which will depend upon the temperature of the dwelling and the ambient temperature. This is illustrated in Figure 14 which shows the relationship between a system's total exergy efficiency, total energy efficiency, electrical (or other work) efficiency and its power fraction (that is, the proportion of useful output that is in the form of electrical energy). In this example, the dwelling is heated to 20°C with an ambient (outside) temperature of 10°C. If the power fraction is low (i.e. the heat to electrical energy ratio is high) then the exergy efficiency of the system will be limited to low values unless its energy efficiency exceeds 100%.
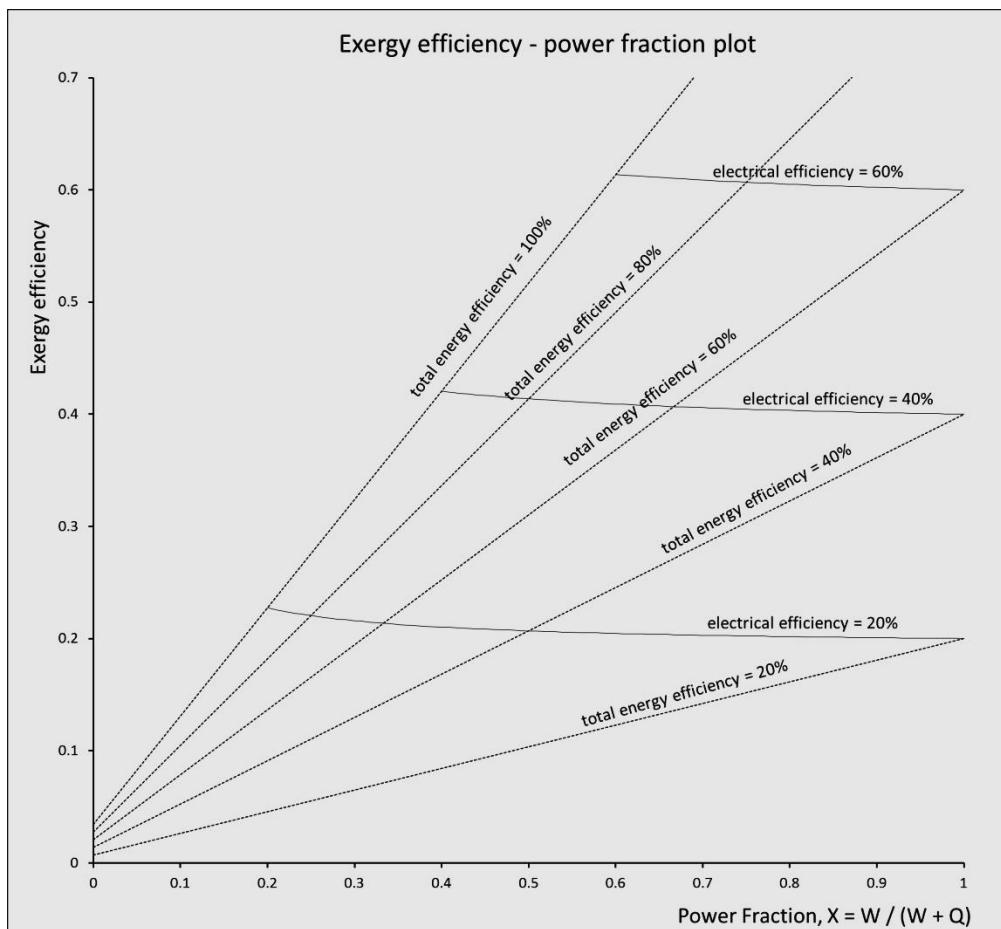
Figure 14: Effect on exergy efficiency of variation in power fraction

It is convenient to consider the exergy content of a substance as the sum of its kinetic and potential energy (E_{KE} and E_{PE}, both interchangeable with work), its physical exergy (i.e. related to temperature and pressure, E_{ph}) and its chemical exergy, E_0:

$$E = E_{KE} + E_{PE} + E_{ph} + E_0 \qquad \text{Equation 7}$$

This form is used by Kotas (1986). The value of the physical and chemical exergy components can be evaluated separately by considering hypothetical reversible processes that extract work as the substance is returned first to ambient conditions and then to reference substances. For steady flow conditions, the physical exergy rate is given by:

$$\dot{E}_{ph} = \dot{m}[(h - h_0) - T_0(s - s_0)] \qquad \text{Equation 8}$$

where h and s are the specific enthalpy and entropy of the substance and $\dot{m}$ is its mass flow rate (assuming all are measured in consistent units). The subscript, 0, denotes values at ambient conditions.

Kotas (1980) noted that the chemical exergy of a substance, E_0, is the sum of both the work available as the substance is reacted isothermally to form reference compounds at standard conditions and also the work available as it is reduced to the partial pressure which reflects its normal concentration in the environment. By comparison with the equivalent expressions for the chemical exergy of the elements that make up the substance, it can be shown that this is the same as the sum of the Gibbs function of formation for the substance(s) and the sum of the chemical exergies of the constituent elements:

$$E_0 = \sum_f N_f \tilde{g}_{f0} + \sum_e N_e E_{e0} \qquad \text{Equation 9}$$

where E_{e0} is the standard chemical exergy of element e, N_f is the number of moles of reactant substance f (i.e. the substances being evaluated), $\tilde{g}_{f0}$ is the molar Gibbs function of formation for substance f at standard conditions. Equation 9 is a useful result as, for gaseous reactions, certain elements (C, O_2, H_2) will appear for a large number of reactant substances and it is convenient to tabulate the value of their standard chemical exergies, facilitating the calculation of the standard chemical exergy of other substances.

Van Gool (1998) has discussed the selection of reference substances; criticising previous methodologies for the variation in the exergy of a gas with its concentration in the air and suggesting an alternative methodology for deriving the chemical exergy of elements. The methodology presented by Van Gool does provide more consistency than others but, in practice, the difference in values obtained for common substances is small. The molar chemical exergy value for methane is found to vary from 836kJ/kmol (Kotas 1980) to 831kJ/kmol for a source

quoted by Van Gool to 815kJ/kmol using Van Gool's methodology. This is almost entirely attributable to the reduction in chemical exergy associated with the concentration of CO_2. Additionally, for fuels which comprise a mixture of chemical compounds, it is difficult to determine an exact exergy content using the analytical methods above. Kotas (1986) notes that Szargut and Styrylska determined the ratio between chemical exergy and net calorific value for hydrocarbon fuels, finding good correlation for fuels with similar atomic ratios. Similar values are adapted from Kotas and supplied by Allen (2009) in order to compare the exergy performance of micro-generators with the fossil fuel based systems that they could replace. Table 6 gives typical ratios of exergy to gross calorific value for fossil fuels ($\phi = E_0/H$ where H is the Higher Heating Value, i.e. the Gross Calorific Value of the fuel).

Table 6: Exergy content of fossil fuels relative to gross calorific value (adapted from Allen 2009)

Fuel	ϕ
Coal	1.027
Fuel Oil	1.009
Natural Gas	0.937

The Gibbs function for a reaction is the maximum work that can be extracted from it (for isothermal, isobaric conditions). As the entropy of reactants and products is generally different for a fixed state, the ordered energy (e.g. work) available from the reaction will vary from the enthalpy of the reaction by the heat rejection required to maintain the total entropy of the system. That is:

$$-\Delta G = \Delta H - T\Delta S \qquad\qquad \text{Equation 10}$$

Note that, by convention, the change in Gibbs function is negative for a reaction in which work is available (i.e. it actually represents the energy which is absorbed by the reaction). For a reaction in which the entropy of products is less than the entropy of reactants, the Gibbs function will therefore have a lower magnitude than the enthalpy of reaction (in gaseous reactions, this will usually occur if there are less moles of product than reactant, e.g. $2H_2 + O_2$ → $2H_2O$). The quantity $T\Delta S$ could be thought of as the minimum quantity of heat that must be rejected by the reaction (and is therefore unavailable to perform work) in order to maintain the total entropy of the system. For such a reaction, the maximum work output is available when $T = T_0$. This is significant for the design of fuel cells operating with hydrogen as fuel; their theoretical maximum work output reduces as temperature increases (Larminie & Dicks 2003).

However, as the temperature increases the work which can be performed by a heat engine using the rejected heat increases and so the total work theoretically available from the fuel remains the same:

$$E = -\Delta G + E_{ph}$$ Equation 11

$$= (\Delta H - T\Delta S) + Q\left(1 - \frac{T_0}{T}\right)$$

$$= \Delta H - T_0\Delta S = -\Delta G_0$$

Finally, of significance to the analysis of fuel cells, it should be noted that the molar Gibbs function for a substance is also known as its chemical potential, μ_{i0}. Chemical potential, measured in Volts, is a third driving force with pressure and temperature. A substance in a mixture in membrane equilibrium with its surroundings will have the same partial chemical potential as the substance on its own outside.

2.4.3 Environmental analysis

This work focuses upon the energetic, exergy and CO_2 emissions performance of ASHP and mCHP units. However, it is important that results are considered in conjunction with other aspects of the relative merits of the units in order to form a complete assessment of their sustainability and suitability (Hammond 2004a; Hammond 2004b). Although it is necessary to give consideration to environmental impacts from each life stage of the units (not just the in-use stage), previous Life Cycle Assessment studies have shown that the majority of impacts associated with ASHP and mCHP units occur during their operation.

Using Ecoinvent2007 data, Johnson (2010) concluded that the production of ASHP units accounts for between 2% and 4% of their global warming impacts. Although Rey Martínez et al. (2011) have suggested a higher proportion (around 9%), this was due to the fact that the heat pump was assumed to supply a small cooling load requiring less than 20% of the electrical consumption typical in comparable studies. The study found that the most significant impacts are those to human health, associated with the emission of respiratory inorganics due to electricity generation. This was using the Eco-indicator'99 methodology and is clearly specific to the source of the electricity. An LCA conducted by Blom et al. (2010) found that the impacts from an ASHP are higher than those from a gas boiler system. Fresh water toxicity and terrestrial toxicity were indicated to be the largest impacts, around five times as significant as other impact categories. The terrestrial toxicity is largely associated with the supply of

electricity while the fresh water toxicity is associated with the manufacture of the ASHP units; unfortunately the sources of these impacts were not identified or discussed further.

The total equivalent warming impact (developed at Oak Ridge National Laboratory) concept is used in the "Der blaue engel" standard to include the effect of HFCs released during the life and disposal of heat pumps (Forsen 2005). They have a significant effect; Johnson (2010) concluded that the global warming potential (GWP) of the refrigerants released during the manufacture, use and maintenance of ASHPs probably contributes around 15% to 18% of the total GWP impacts associated with them. If the generation of electricity is decarbonised or the average COP is improved, this proportion will increase. It is possible that this will further drive the adoption of R744 (CO_2) as a refrigerant given the high GWP of HFCs; R407C has a GWP of 1610 CO_2-equivalent, slightly less than R410A with a GWP of 2088 CO_2e (IPCC 2007).

The proportion of GWP impacts associated with manufacturing is even lower for mCHP units. Cradle to grave LCAs on SOFC units (Karakoussis et al. 2001) and on a range of mCHP units (Pehnt 2008) both concluded that the impacts from manufacturing are around 1% of total in-use impacts. The relative contribution to other environmental impact categories from the manufacturing stage of the SOFC lifecycle is higher but this reflects the fact that operational impacts are low; emissions associated with manufacturing the BoP are likely to be higher than those from manufacturing the actual stack. Pehnt (2008) noted that the effect of unburnt methane emissions is unknown; estimates of emissions vary from 20mg to 500mg per MJ of fuel consumed with the higher estimates relating to ICE-mCHP units. Emissions of NOx were also observed to be considerably higher for ICE-mCHP units compared to other mCHP units or centralised power plants (due to better emission control) but are unlikely to be sufficient to cause local air quality issues.

Any unburnt methane will increase the GWP associated with the operation of a unit. Given that methane has a 100yr-GWP of 25 CO_2e (IPCC 2007) the 500mg/MJ estimate for ICE-mCHP units is equivalent to around $15g_{CO2}$/kWh. Perhaps a more significant problem, overall, is the leakage of gas from the national transmission system. This is officially estimated at approximately 0.5% but other studies have suggested it could be much more and potentially up to 10% (Mitchell et al. 1990). It is not clear how this may have changed over the last 20 years or how this should be attributed to natural gas use (marginal changes in natural gas use will not cause same change in leakage rate). However, even if only 0.5% leakage were attributed to the operation of devices using natural gas it would increase the GWP associated with them by almost 5% (remembering that burning 1kg of CH_4 will release 2.75kg of CO_2). Taking this effect into account along with the energy requirement for energy of 1.02 for natural gas distribution referred to in section 2.4.1, leads to a carbon emission factor of $190g_{CO2}$/kWh for gas at the point of use (relative to GCV of fuel).

Various grid average carbon emissions factors (CEF) are available (Table 7) and could be applied by multiplying by the relevant electrical consumption to approximate the associated carbon emissions. However, given the sensitivity in any assessment of the relative environmental impacts of mCHP and ASHP units to the CEF (Dorer & Weber 2009; Healy 2012), a more detailed approach has been taken in this research, using the CEF for each generating plant type given in Table 8. The methodologies are described in chapter 4, section 4.6

Table 7: Selection of UK average carbon emissions factors (CEF)

CEF g_{CO_2}/kWh	Notes	Source
485	2009, five year rolling average of $523g_{CO_2}$/kWh excluding indirect emissions	(DEFRA 2011)
594	Five year rolling average including indirect emissions	(DEFRA 2011)
545	Point of use, five year rolling average from data similar to (DEFRA 2011)	(Carbon Trust 2010a)
517	Electricity supplied	SAP 2009 (BRE 2010)
529	Electricity displaced	SAP 2009 (BRE 2010)
568	Electricity displaced	SAP 2005 (BRE 2010)
458	"Supplied" (i.e. excluding transmission & distribution losses)	DUKES 2011 (DECC 2011)
356	CCGT achieving 60% (NCV) efficiency with 7% transmission and distribution losses	(Siemens AG 2010)
690	marginal factor, 2002 to 2009	(Hawkes 2010)

In this context, a marginal impact factor (e.g. CO_2 emissions or PER) at a given instant is the impact factor that can be attributed to an increase or decrease in demand for electricity at that moment. If the marginal impact factor is consistent, it is usually the appropriate factor to use in considering the effect of using one technology relative to an alternative (i.e. appropriate to *consequential* LCA studies). However, an average impact factor is usually more appropriate for *attributional* LCA studies. That is, in comparing the effect of an action in the context of the range of concurrent activities, it is generally appropriate to assign each of them the mean impact factor, given that they all contribute towards the impact and that increasing or decreasing the demand from any of them will have the same effect.

Under the marginal methodology, the emissions associated with the use of the ASHPs are taken to be those from the generating plant which is likely to be operated to meet the additional demand due to the operation of the ASHPs. Conversely, the avoided emissions attributed to the electricity generated by the mCHP units are also assumed to be those which would have been emitted by the generating plant which is likely to cease operating. Large increases in the baseload demand which would occur, for example, if there were widespread adoption of ASHPs are likely to affect the case for investment in different generating plant types it is not clear that it would be appropriate to use the marginal emissions factors under all scenarios. Similarly, the effect of widespread mCHP adoption (especially if it is operated continuously as SOFC-mCHP units might be) is likely to affect the generation mix in the longer term.

Table 8: Carbon emissions factors (CEF) by fuel type.

Generating plant type, L	CEF $\left[\frac{\dot{c}}{\dot{W}}\right]_L$ / g.kWh^{-1}	Notes
Gas CCGT	488	(Odeh & Cockerill 2008)
Gas CCGT with CCS	200	(Odeh & Cockerill 2008)
Subcritical pulverised coal	984	(Odeh & Cockerill 2008)
Coal IGCC	861	(Odeh & Cockerill 2008)
Coal IGCC with CCS	167	(Odeh & Cockerill 2008)
CHP	30	(Ecoinvent 2010)
Thermal renewables (e.g. biomass)	38	(Ecoinvent 2010)
Wind	13	(Ecoinvent 2010)
Tidal	15	(Douglas et al. 2008)
Nuclear	7	(AEA Consulting 2009)
Estimates of direct emissions for comparison:		
Coal	909	(DECC 2011)
Gas (CCGT)	398	(DECC 2011)
CCGT	397	(Hammond & Ondo Akwe 2007)
CCGT with CCS	51	(Hammond & Ondo Akwe 2007)
State of art CCGT	356	(Siemens AG 2010)
Other non-renewable thermals	653	(DECC 2011)
Comparison to carbon emissions factor for burning natural gas directly		
Natural gas (typical UK composition)	190	Assumptions outlined above (section 2.4.1)

The figures relating to biomass and CHP in Table 8 are very sensitive to assumptions made regarding the mix of generation technologies, the fuel for the CHP plant and the source of the biomass. However, the contribution from them is low in the Transition Pathways scenarios used as background to this study apart from in the "Thousand Flowers" scenario which postulates high penetration of CHP (see Table 18, page 118). The selected values reflect those selected for LCA work within the project (O'Grady 2012, personal communication) consistent with the assumption of largely thermal based CHP using low carbon biomass.

2.5 Limitations in previous modelling

Various modelling studies from the literature were reviewed and several models were created by the author during preliminary studies as part of this research. In each case, the modelling approach which was selected was chosen in order to investigate a specific question or problem. However, limitations (either in the level of detail, the scope of study or the accuracy and reliability of the results) were identified in each case. This motivated the development of the model used to calculate the majority of results presented in this thesis. The main modelling approach is described in chapter 4 below, but the preliminary research undertaken by the author and the modelling approaches found in the literature will be reviewed first.

2.5.1 Case study: The Old Schoolhouse

The performance of an installed ASHP was investigated by the author as a case study. Although this provided useful information regarding the operation of the unit, it was not possible to draw general conclusions from the study. The lack of control over operating conditions highlighted the potential usefulness of a modelling approach.

Electricity and fuel consumption data were recorded by the residents of a property near to Bath, UK (Figure 15). These data were recorded for a period of over 14 years, including a period of approximately 12 years in which oil-fired heating was used and then two years after it was replaced by an ASHP. In order to account for fluctuations in the heating demand at the property it was necessary to correlate it with historic climate records. It was assumed that the heating demand was proportional to the degree-days experienced (Carbon Trust 2010b). However, several factors made it unlikely that the conventional balance point temperature for UK residential properties (15.5°C) would be appropriate (Layberry 2008; 2009). The property is relatively old, has a high thermal inertia, a secondary solar hot water system, an open fire and an AGA stove that heats some of the rooms. The best fit between recorded monthly heating oil consumption and the degree-days in that month was found with a balance point temperature of 14.5°C. This was used to estimate the heat supplied by the ASHP since its installation and the oil which would have been consumed to generate it.

Figure 15: The Old Schoolhouse

The electrical consumption of the ASHP was estimated in two ways. Firstly, by considering the difference in monthly electrical consumption relative to the average for those months before the installation of the ASHP (although this was based on less than 2 years of data). Secondly, as the sum of the heat demand at each outside air temperature encountered divided by the COP at that temperature. The performance of the ASHP at each outside air temperature (divided into finite intervals of 1°C) was found by interpolating from performance data (from Butler & Hyde 2007) measured under standardised test conditions (BSI 2007a). The latter method suggested larger savings with the introduction of the ASHP; a 40% reduction in the CO_2 emissions associated with the heating.

The study provided a useful illustration of the practical working of an ASHP and the methods which can be used to calculate their power consumption if steady-state assumptions are made. However, with relatively low-resolution data and a large number of uncontrolled variables it was not possible to draw clear conclusions regarding the actual performance of the unit. In order to gain useful insights regarding the performance of the ASHP it must be possible to control and vary the conditions under which it operates. This is a task which modelling is well suited to. The following sections will consider the level of detail which is appropriate.

2.5.2 Steady-state modelling.

The primary factors affecting the energy flows associated with the ASHP and mCHP units do not vary dynamically; for example the steady-state performance of the units and the temperature of the ambient air used as a heat source by ASHPs. Additionally, although the accuracy of

steady-state methods for calculating the heating demands of dwellings is subject to simplifications, these methods have been noted to produce consistent results (Kokogiannakis et al. 2008). Therefore, for some applications, the performance of the units can be determined to an acceptable level of accuracy by considering their performance under a finite set of conditions and then weighting this performance by the heat demand which occurs under each condition. This approach can be easily applied to a wide range of conditions and has a low computational overhead. It is therefore suited to providing a comparison between units operating under a wide range of conditions or scenarios.

For example, Young & Henderson (2008) used the "Standard Assessment Procedure" (SAP), (BRE 2010) to compare a wide range of heating options including biomass, mCHP, ASHP and GSHP as well as more conventional units by applying standard performance factors from SAP2005. A range of results were reported including the possibility that a 13% - 28% *increase* in CO_2 emissions could result from the use of ASHP units. Although the accuracy of SAP has been questioned (see Kelly et al., (2012) for a discussion of issues which have been raised), it does provide a recognised benchmark for comparative studies. It is difficult to draw firm conclusions from Young & Henderson's study because the assumptions inherent in the calculations are quite specific and not necessarily appropriate but their approach does give a broad overview of the heating options available.

Within SAP, the performance of the heat pumps considered is characterised as a Seasonal Performance Factor. This has been suggested as a benchmark for comparing ASHP performance by IEA Heat Pump Programme Annex 28; it is similar to the COP but is an annual average figure and includes some additional optional consumption such as electric-resistive backup heaters. The group's final report (IEA Heat Pump Programme Annex28 2006) and associated publications, such as (Wemhoener et al. 2008), outline their proposed methodology which has since been taken forward to form the basis of BS EN15316-4-2:2008. Hayton (2010) has explained the "SAP2009 Appendix Q" approved procedure for assessing the performance of heat pumps for inclusion in the calculation of SAP ratings, based upon BS EN15316-4-2:2008 but with small changes to some definitions. Standardised methods for assessing the average performance of heat pumps can be inaccurate (for example, where actual domestic hot water demand is more than allowed for, Bourke & Bansal 2010) but they do provide convenient and well used metrics for comparison between units.

Despite its limitations, the Seasonal Performance Factor is a useful tool for assessing the relative heat pump performance which has been used in several comparative studies and so the method for calculating it will be described in more detail here. The main factor influencing ASHP performance which is considered is the ambient air temperature. Additionally, the system boundary is extended relative to BS EN14511:2007 (i.e. standardised definition of COP) to

include circulation pumps / fans for heat collectors (e.g. ground heat exchanger), backup heaters, DHW storage and thermal buffers used by the heat pump, but does not include circulation pumps for the heat emitter system. Performance variation with ambient air temperature is accounted for by using temperature "bins". Hourly climate data representative of the heat pump's location is used to calculate the number of hours within temperature "bins" of, ideally, 1°C. That is, the number of hours in the year when the temperature is between 1ºC and 2ºC, the number of hours between 2ºC and 3ºC, between 3ºC and 4ºC and so on (see Figure 16).
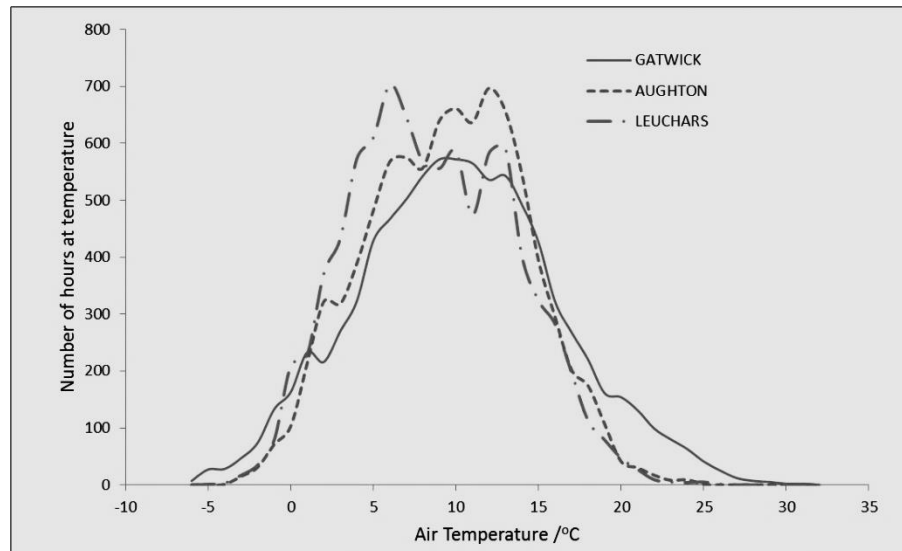
Figure 16: Example of 1°C bins for three UK locations

Space heating demand is assumed to follow a Time-Temperature Difference model, i.e. the rate of heat loss is assumed to be proportional to the difference between ambient air temperature and the balance point temperature for the building. DHW heating demand is assumed to be constant and is added to the space heating demand. For each of the "bins", a COP is assigned to the heat pump based upon the midpoint temperature and operating temperature for the heat emitter system at that ambient temperature. If the heat demand within the "bin" is higher than the rated capacity of the heat pump in those conditions, a backup electric heater is assumed to be used, reducing the effective system COP. From the rate of heat demand in each bin, the number of hours within each bin and the representative COP for that bin, electrical power consumption can be calculated and summed to give a total for the year. See Equation 12.

$$SPF = \frac{\Sigma Q}{\Sigma W} \qquad \qquad \textit{Equation 12}$$

$$= \sum_{T_0 = T_{0min}}^{T_{A0}} [k_{A0}(T_{A0} - T_0).t(T_0)] \Bigg/ \sum_{T_0 = T_{0min}}^{T_{A0}} \left[\frac{k_{A0}(T_{A0} - T_0).t(T_0)}{k_{WQ}(T_0)} \right]$$

Where T_0 is the average outside air temperature for each bin, T_{A0} is the balance-point temperature being assumed, k_{A0} is the effective total heat loss coefficient for the building (though assuming that it is a constant, it drops out of the calculation), $t(T_0)$ is the total time in the year when the temperature is within the bin and $k_{WQ}(T_0)$ is COP of the ASHP as a function of ambient temperature, T_0 (note that the COP will also depend upon its outlet flow temperature which is a function of both T_0 and of the heat emitter system used).

An alternative to SAP is the Tarbase Domestic Model (Jenkins et al. 2012) which has been developed as a tool for the assessment of the energy performance of buildings and measures to improve it. A steady-state modelling approach is employed because of the identified need to assess the performance of a range of buildings but the limitations are also discussed. Additional modelling at a higher level of detail was required in order to accurately assess the performance of mCHP and ASHP units, prior to their inclusion.

Similar methodology was used by the author to analyse a range of ASHP and mCHP units (Cooper et al. 2011a; 2011b). The use of this methodology allowed a large number of units to be modelled under a relatively wide range of conditions. By adapting the SPF methodology detailed above, it was possible to calculate the average (weighted by heat demand) exergy efficiency of the units; enabling consideration of their performance potential and the usefulness of the energy processes within the units. Additionally, by selecting synthetic climate data which includes the modelled effect of climate change (Eames et al. 2010), the range of future potential performances could be estimated. Although it cannot provide reliable prediction of the heat or power demands of a specific installation, the approach does facilitate comparison across the range of units and conditions; highlighting the factors which have the greatest influence on the energetic performance of the units.

2.5.3 Static performance maps with dynamic load profiles.

A more detailed approach was used by Peacock & Newborough (2005) in order to investigate the effect that using SE-mCHP and FC-mCHP units might have on CO_2 emissions from the domestic sector. An elegant, hybrid approach was adopted where measured demand profiles

were taken as the demand, fixed performance characteristics were assumed for the heating units and a buffer tank was used as the intermediate supply / demand for the loads. This approach facilitates efficient study of the overall performance of the units at a reasonable level of detail, making it feasible to consider the effect on performance of a larger number of permutations.

Similar methodology was used by Jenkins et al. (2009) to model the performance of a GSHP. The model was quite detailed, including measured demand profiles and a performance map for the GSHP (as Peacock & Newborough 2005) but also allowing for the variation in ground temperature, brine temperature and the part-load performance of the GSHP. The effect of flow temperature, the GSHP capacity and the CEF of the grid were all considered but the study focused on the effect that defined variations in these parameters would have, rather than providing a broader exploration of what would be necessary to cause them.

A variation on this approach was used in Cockroft & Kelly's (2006) study comparing the performance of an ASHP unit with SE-mCHP, ICE-mCHP and SOFC-mCHP units. Rather than using measured demand profiles, detailed models of three dwelling types were created using ESP-r for 2005 and 2020 scenarios (involving reduction of UK grid CEF and improvement to the insulation levels in the dwellings). Some predictions such as the need for large heat loads for effective SE-mCHP operation have subsequently been observed elsewhere (e.g. Carbon Trust 2011). However, the study was not able to investigate effects associated with the dynamic behaviour of the units as only static performance maps were available. Additionally, it was noted that without a clear understanding of the way in which grid electrical generation is dispatched, it is hard to assess the impacts associated with the export of surplus electricity generated by mCHP units. Lohani & Schmidt (2010) took a similar approach in comparing ASHP and GSHP units to a gas boiler but focussed on the exergy flows involved rather than the change of conditions which is expected. Detailed thermal modelling was used with fixed temperature emitters and performance maps of the heat pumps. The exergy analysis illustrates the need for the appropriate use of energy vectors at each stage of the energy system but does not explore the ways in which the results could change under a wider range of scenarios.

Although the methodology adopted by Barbieri et al. (2011) assumed dynamic operation of the heating units, the simplifications used (no thermal dissipation, on-off operation, heat-led operation) mean that the main contribution relative to steady-state modelling is the use of the auxiliary heating system. Comparisons between a good range of units (representing ICE-mCHP, SE-mCHP, mGT-mCHP, Organic Rankine Cycle and Thermo-Photovoltaic technologies) were made but the analysis of the factors affecting the energetic performance is not extensive. Similarly, although Dorer et al. (2005) used dynamic thermal building models in evaluating the performance of SOFC-mCHP and PEMFC-mCHP units, the dynamics of the units are assumed

to be limited. However, the study did investigate a wider range of configurations including grid mix, building insulation levels and the addition of solar thermal water heating.

The accuracy of these studies is adequate as a standard comparison between units but it can be improved upon. In particular, the performance indicated by simulations of mCHP units is dependent upon the time-step used being sufficiently fine; it should be less than 10 minutes (Hawkes & Leach 2005). The effect of this limitation can be overcome to some extent by assuming ideal installation conditions and thermal buffering but in doing so, the effect of varying these important factors is ignored. Another factor which is ignored to some extent by steady-state modelling assumptions is the control methodology used by the heating system. This is an important aspect of the system performance but requires consideration of the dynamic interactions between the heating unit and the building it is installed in and within the heating units itself. There is clearly merit in using more detailed, dynamic models to investigate these effects.

2.5.4   Detailed thermal modelling of units

Several researchers have developed models of mCHP and ASHP units based upon the fundamental principles governing each component. The models are useful for incorporating into other studies or to inform the design of other models but in most cases the studies reporting them stop short of using the models to assess the way that the performance of the units will vary in actual use. Component type models have been developed for a heat pump with buffer tank (Kim et al. 2004), a gas-engine heat pump (Yang et al. 2013), an ASHP (Fardoun et al. 2011), an ICE-mCHP unit (Yun et al. 2013) and a PEMFC-mCHP unit (Barelli et al. 2011); no doubt amongst many more. These models can identify effects which are relevant to modelling the systems in their wider context; for example it was indicated that the PEMFC-mCHP is likely to require around 25 seconds to respond to a change in electrical loading and that the average performance of the ASHP is likely to be better if it is heating a larger reservoir. However, without empirical results to compare these findings to and to calibrate them, their usefulness in this regard is limited. They are well suited to investigations refining design proposals or exploring the ways in which the performance of a unit can be improved but a modelling approach based on empirically derived performance characteristics is likely to be more appropriate for investigations in which the objective is to determine the performance which is likely to be achieved.

To evaluate the performance of a Senertec Dachs ICE-mCHP unit, Voorspools & D'haeseleer (2002) used data obtained from experimental testing of the transient behaviour of the unit in order to model it through the year. Although the unit operates at full electrical output almost immediately, there is a considerable thermal lag. From cold, the unit takes 5 to 10 minutes

before heat is produced, 30 minutes to achieve 65% of the rated heat output and 60 minutes to achieve 80% of the rated thermal output. This delay will vary depending upon the temperature of the engine block at the point that it starts operating so the use of an effective thermal inertia seems appropriate.

This approach has been adopted by Annex 42 of the International Energy Agency (IEA) Energy Conservation in Buildings and Community Systems (ECBCS) Programme, in order to formalise a modelling structure for mCHP units. In fact, the model specification (Beausoleil-Morrison, Weber, et al. 2007) includes tnetswo thermal capacitances in order to capture the fast thermal transients and the slower transfers to other systems which can occur. The model is designed to be suitable for detailed modelling of housing; more precise than average efficiencies but not too computationally complex for year-long simulations. The model was calibrated and validated against experimental data from a 2003 Canadian Centre for Housing Technology (CCHT) evaluation of a Whispergen SE-mCHP unit and a 2006, Forschungsstelle f˙ur Energiewirtschaft (FfE) evaluation of a Dachs ICE-mCHP unit. The group's report (Beausoleil-Morrison, Arndt, et al. 2007) included details of these two calibrations along with information regarding testing of other mCHP units including Whispergen SE, Solo Stirling 161, Power Plus Ecopower, Senertec Dachs and prototype PEMFC and SOFC devices.

IEA ECBCS Annex 42's research provides a well-established prototype for modelling mCHP units at an appropriate level of detail and valuable data to apply it to some units. ASHP units can be simulated with the same model structure but a different set of performance characteristics (e.g. a performance map of COP can be used to determine power demand as a function of heat generation for a given set of conditions). However, in order to gain insights into the real world performance of the units and how this could vary under different circumstances, it is necessary to use these models within thermal models relating to building thermal demands in defined scenarios.

2.5.5 Studies incorporating thermal models of heat demands.

The SE-mCHP unit model developed by IEA ECBCS Annex 42 has been used by Kelly et al. (2008) to investigate its performance in different dwellings. With increased insulation, the mCHP efficiency tended to decrease (although overall energy consumption reduced) with parasitic and cycling losses becoming more significant. The modelling also indicated that the unit would be able to react to an external on-off signal (and therefore contribute to a DSM system) for over 90% of the time. With a 200l tank, the unit could be turned "on" for 1 to 200 minutes or "off" for 1 minute to 800 minutes without affecting occupant comfort. Similar analysis was presented by Beyer & Kelly (2008) to include an ICE-mCHP unit. The performances of the two units were simulated with four building types, different occupancy

patterns, and four thermal buffer sizes (nil, 200l, 500l and 750l). A lack of thermal buffering resulted in thermal efficiency penalties of up to 15% for the ICE-mCHP unit and up to 25% for the SE-mCHP unit. However, this was mostly thermal efficiency; electrical efficiency was largely unaffected. The performance of two SE-mCHP units, two ICE-mCHP units, a PEMFC-mCHP unit and a SOFC-mCHP unit were modelled by Dorer & Weber (2009) using the IEA ECBCS Annex 42 models and experimental data. The study actually involved a reasonably wide range of parameters; two building types (each with three levels of demand) were considered in the context of two grid mixes. However, the importance of the time-varying CEF of the grid was noted and the suggestion made that further work should take this into account.

Similar modelling approaches based on alternative data sources have been taken by some researchers. Boait et al. (2011) used data from a field trial to calibrate a simple dynamic model of a heat pump in a dwelling and use it to investigate the effect of incorporating night-time set-back into the programmed temperature profile. The approach taken is actually similar to that taken within this research, albeit on a smaller scale and with less variation in the options considered. Peacock & Newborough (2008) expanded upon the method used in their 2005 study in order to consider the effect of reduced heat demands on the performance of mCHP units. Rather than using a thermal inertia approach to take delays in heat production into account, a start / stop delay was incorporated into the models of the heating units and (as before) a predetermined demand profile was used and then adapted. This method appears to be effective and efficient, facilitating the use of a large number of simulations to cover the permutations considered, though it is not clear that it would cope as well with modulating heating units. To compare the performance of several mCHP units, De Paepe et al. (2006) also used models of the mCHP units with time functions rather than relying on a thermal inertia approach. However, in contrast to Peacock & Newborough (2008), they used dynamic simulation of the buildings (a terraced dwelling and a detached dwelling, both modelled in DOE2.5) in order to derive the heat demands that the mCHP units satisfy. Recognising the significance of the CEF of the grid, results were presented for three generation options (CCGT, average Belgian mix and average Belgian fossil fuel plant mix).

The performance of ASHPs in buildings has been the subject of numerous studies using detailed thermal modelling. Jenkins et al., (2008) used ESP-r to analyse the performance of an ASHP in an office block with conditions (gains, climate and insulation) typical of 2005 and 2030. Kelly and Cockroft, (2011) also used ESP-r to model the performance of an ASHP unit but this time in a terraced dwelling. Good agreement was achieved between the simulation results and those from a field trial of eight installed units (once appropriate controllers were employed). These studies present results which are likely to be representative of real conditions (e.g. Energy Saving Trust 2010). However, they do not necessarily identify the relative contribution that

different changes in conditions have on the ASHP performances. For example, Kelly and Cockroft, (2011) noted that not using weather-compensated control probably reduced the COP from around 3.5 to 3.0 when the ambient air temperature was 10°C but did not explore the sensitivity of this interesting observation. In each case, mean emissions factors (CEFs) are used rather than marginal carbon emissions factors (MEFs).

These studies provide a detailed level of modelling and it is expected that their results will exhibit good fidelity to the systems which they simulate. However, the results are generally specific to the particular cases being considered; although there are general trends, there is also some variation between studies reflecting the range of input variables which are assumed. Because the detailed models are computationally intense, it would be hard to repeat them with the wide range of parameters necessary to understand the sensitivity of the results to the range of conditions that the units might operate within. Additionally, the models are designed to provide detailed simulation of the conditions within each building and heating unit but are not designed to simulate changing electrical grid conditions. This limitation prevents them from being used to consider the effect of dynamically changing grid conditions (relating, for example to variations in MEFs as intermittent renewable generation occurs) or to the effect of DSM measures which might be applied in a hypothetical future scenario. The CEF and MEF of the grid-supplied electricity used to power heat pumps is significant to the results and varies considerably across Europe. Even within the UK, a range of CEFs have been used (see, for example, Table 8, page 53) so a good understanding of this effect is important.

2.5.6 Network modelling

In addition to the performance and impacts associated with the use of individual mCHP or ASHP units, there is interest in the effect that the operation of large numbers of these units may have on network electrical power flows. Studies of these power flows have been undertaken and are reviewed in chapter 2, page 15, (Burt et al. 2008; Peacock & Newborough 2006; 2007; Sulka & Jenkins 2008; Thomson & Infield 2008). There are several ways in which this work can be extended, however. In some studies the number of dwellings simulated was unlikely to model the diversity which should be expected, in other cases no DSM of loads was attempted (i.e. the study relates to the flows which would be expected without DSM). Various combinations of unit types and the control methodologies which best suit them (for example if they are capable of modulated output) should be analysed. Additionally, the effect that any such interventions on the performance of the units has not been investigated elsewhere.

2.5.7 Simplified dynamic modelling approach

In order to address these limitations and to facilitate the study of the effect of factors such as the control methodology on the performance of the heating units, a dynamic model was developed in a preliminary study as part of this research (Cooper et al. 2012b).

The dynamic model uses a single lumped-capacitance approach for thermal flows, similar to that taken by others (e.g. Danov et al. 2012; Sulka & Jenkins 2008; Boait et al. 2011). Additionally, a dynamic model of the electrical grid was developed based upon historic grid generation data for the UK (Elexon 2012). This allowed consideration of the effect of different levels of non-dispatchable renewables to be considered.

Building thermal characteristics were estimated based upon the average dimensions and thermal properties of the building stock in the UK (Utley & Shorrock 2008; Hong et al. 2010). This simplification was considered to be acceptable for the preliminary study for two reasons. Primarily, because the objective of the study was to investigate the relative effect of measures on the performance of the heating units rather than the absolute heat and power demands. Secondarily, because in practice, a wide variation in energy consumption is observed even for identical dwellings; attributable to occupant behaviour and preferences (e.g. more than a factor of two for similar buildings (Hiller 2012; Carbon Trust 2007)). However, the accuracy of these characteristics was subsequently refined for the final modelling approach used (see below).

This model was also used to investigate the effect of changing the control algorithm on the performance of the heating unit. Results were used to inform the selection of test conditions used with the final model. A general trend for improved performance with consistent but accurate control of ASHPs was observed. This suggests that it may be hard to achieve reductions in CO_2 emissions by adjusting the operation of the unit to be weighted towards times when grid MEF is lower or external air temperature is higher and so this was investigated further in the main body of research (see chapter 5.11).

The model was then developed by the author to include the consideration of DHW demand (this affects the flow minimum temperature requirements) and the adoption of a model for the heating units which was compatible with that suggested by IEA ECBCS Annex 42 (Beausoleil-Morrison, Arndt, et al. 2007). In this form, the model was used to produce a set of results comparing the performance of a range of ASHP and mCHP units (Cooper et al. 2012a), reproduced in Appendix C.

In this state, the integrated approach within the model facilitated studying the effect of a wide range of factors which are dependent upon each other and vary dynamically; an improvement on

other approaches which focus detail on a few aspects of the system and assume that other aspects are independent or steady-state. However, it still lacked any consideration of either local electrical demands, network constraints or of the thermal comfort of occupants; limiting some of the investigations which could be performed with it. Adding these elements and improving the accuracy of the other elements resulted in the final model described in chapter 4.

2.6 Conclusion to background - the significance of ASHP and mCHP performance

Reducing the CO_2 emissions with the UK domestic sector will require a range of actions including the reduction of heating and power demand and also the provision of low carbon, efficient heating. This low-carbon heating requirement will be met by a combination of different technologies but it is likely that ASHP and mCHP units will have a role to play.

The widespread installation of either of these types of units will have significant implications in terms of both energy consumption and CO_2 emissions and in terms of the demands placed upon electrical distribution infrastructure. In order to inform decisions regarding these technologies and to direct future research, it is necessary to understand not just the performance of the units under specific circumstances but also the trends that could be expected under a range of scenarios representative of the present and the future.

The relative performance of mCHP and ASHP units is therefore of interest and value in terms of planning future energy systems and in furthering the field of knowledge. Although many studies have investigated the performance of these technologies under specific conditions or as an overview, it is possible to identify a need for a consistent comparison of the technologies under a range of operating conditions and at a suitable level of detail.

3. Aims

The general aim of this research is to evaluate the thermodynamic and CO_2 emissions performance of ASHP and mCHP units. However, specific aims can now be identified. There are two overall aims; the first aim is to derive the results which are necessary to assess the performance of the technologies. The second aim is to develop a suitable model which both facilitates the first aim but also forms a contribution in its own right as a tool to enable further research.

3.1 Investigation of effect of various factors on performance of units.

This research will analyse the effect of the following list of factors on the performance of the heating technologies. A consistent approach will be taken in analysing the effect of these factors. Some of the individual factors have been investigated elsewhere, but a unique contribution of this research will be to present analysis which is comprehensive and comparable across all the factors. Where appropriate, the mean and marginal PER, exergy and CO_2 emissions associated with the units will be used as metrics to assess their performance. The factors to be varied are:

1. The heating unit and its properties. The eight ASHPs detailed in Table 3 and the 12 mCHP units detailed in Table 4 will be considered. These cover the range of types of unit and the range of nominal performances which are available. Some will use supplementary gas burners whereas others will not.

2. The properties of the buildings which are being heated. Analysis will include the effect of varying the nominal heat load and relative gains of the dwelling as well as the effectiveness of the heat emitter system within the building. Several sizes of buffer tank will be considered for some permutations.

3. The control system used by the heating system. Investigation will be given to the effect of the methodologies used to determine the heat output from the units, the effect of different temperature programmes and the effect of any alternative control system methodologies which are suggested during the course of the investigation.

4. The climate which the units operate within. This will be varied spatially across locations in the UK and temporally across historic climate data and future modelled climate datasets.

5. The electrical supply mix. The performance of the units in the context of both the present supply mix and modelled future mixes will be analysed.

6. Alterations to the operating profile which may result from DSM interventions will be investigated. This will include different levels of DSM interventions based upon both grid generation considerations (e.g. the MEF of generation at a given instant) and upon local distribution considerations (e.g. limiting total power flows).

3.2 Development of a model which enables results to be generated and which facilitates future research

A model will be developed to enable this research and to facilitate future research. It will:

- Include dynamic and appropriately detailed models of the ASHP and mCHP units, calibrated to a range of real units which represent the current range which is commercially available.

- Generate data regarding the energy and exergy flows at each point, including electrical power, heat and fuel flows. Grid generation data should be disaggregated by plant type to enable impacts such as CO_2 emissions and PER relating to grid generated electricity to be calculated. This data will be calculated using both mean and marginal methodologies.

- Include thermal models of dwellings. As different operating regimes will be used with the heating units, it is not sufficient to use static heating profiles. The models need to be sufficiently detailed and calibrated to provide realistic heating demands to the heating system models but do not need to be extremely accurate in calculating the absolute value of total heating demands. If possible, the models should not present a large computational overhead on the simulations.

- Allow the range of factors listed in section 3.1 (above) to be varied and to respond realistically to these different conditions. For example, temperatures which form part of a control algorithm need to be explicitly, dynamically modelled; elements such as heat emitters which affect flow temperatures need to be modelled in sufficient detail; requirements such as DHW demand which limit low temperature operation of the heating need to be considered.

- Model the diversity of heating demands and local electrical demands as the sums of the demands from multiple, independent, simultaneously simulated dwellings.

- Simulate a DSM system. The architecture of this system does not have to be modelled realistically but the effect which it has on the operation of the devices should possess magnitude and temporal properties which are representative of a realistic system.

- Be constructed in a way which is as transparent as possible in order to facilitate future development or adaptation by other researchers.

4.   Modelling

A modular approach has been adopted in order to deal with the complexity of the modelling in a way that facilitated improvement as it became possible or necessary. Various systems are modelled along with the interactions between them (see Figure 17, page 72). In this way, the modelling of each system can be refined as appropriate. The choice of systems selected for modelling was dependent upon the parameters to be varied, as listed in the aims.

Although models are available to analyse most of these aspects individually, it was necessary to construct a model which takes consideration of all of them in order to investigate the interactions which may take place. In particular, calculating the sum of power flows within a network necessitates summing the power flows from individually modelled dwellings (rather than simply applying a multiplier). If the effect of control feedback based on this sum of power flows is to be considered then the model must contain detail of each heating system and their interactions.

The first section of this chapter outlines the overall structure and flow within the model before subsequent sections describe each element in more detail. Where appropriate, the suitability of the model selected for each component is discussed within its subsection but additional examples of the outputs from the model are given in section 4.9.2 to verify that the model has been implemented appropriately.

4.1 Overview: Top level flows

A time-step approach is used; the majority of the processes iterate once per time-step and update their respective properties. By default the time-step is set at 60 seconds as this ensures modelling stability of the building temperatures. A 60 second time-step was also used in the active occupancy model adopted as this resolution captures the use of electrical appliances such as kettles. This is well below the maximum time-step of 5 to 10 minutes suggested by Hawkes and Leach, (2005). To ensure modelling stability, a much shorter time-step (0.5 seconds) is used when modelling the heat transfers within the heating units.
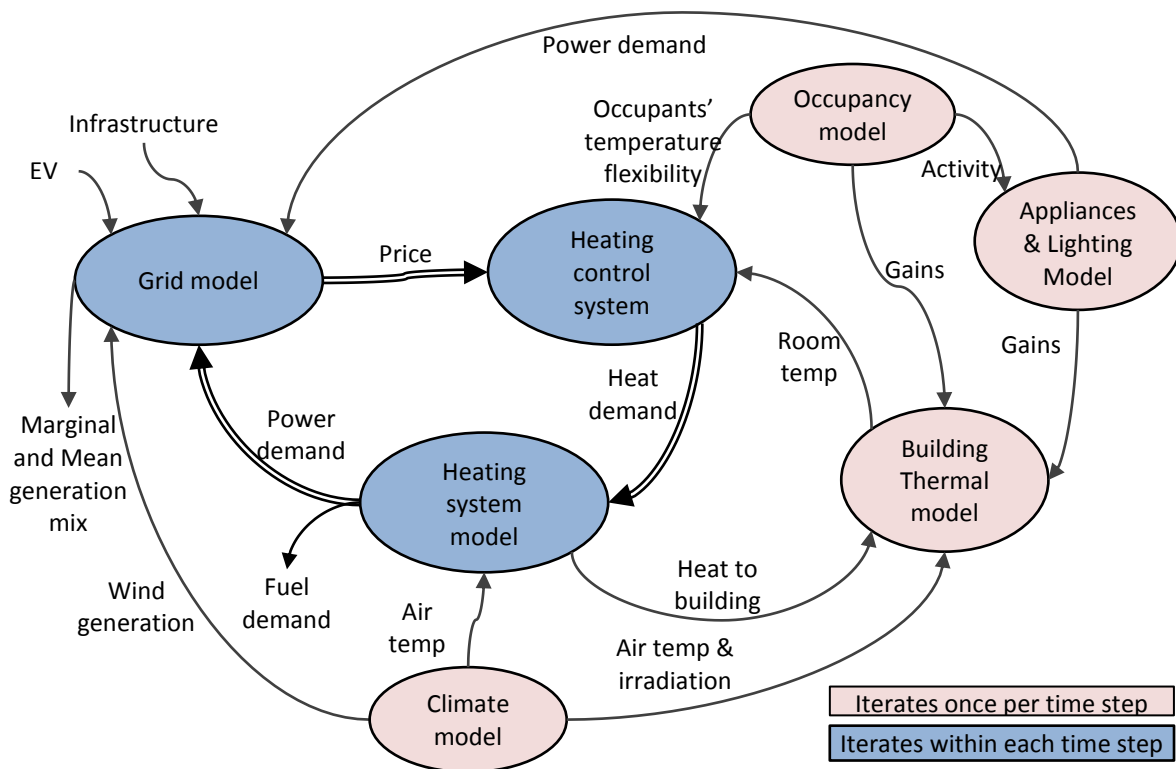
Figure 17: Top level flows in model

Within each time-step, there are several iterations of the grid model, heating control models and heating systems models (that is, the darker shaded systems in Figure 17, see Figure 29, page 108) in order to establish the level of demand side management (DSM) intervention that best suits the grid conditions and to establish the associated heating system power flows.

Once values for the "electricity price" and the associated heat and power demands are established by the iterations (see 4.6.2), the other flows and processes within that time-step take place, appropriate values are recorded and the model moves to the next time-step.

The model can be run for any period of time. For most of the results presented in this study, the model is run for a year, recording the values of the total energy and exergy flows within each dwelling, the total electrical generation required by each dwelling and metrics of thermal comfort within each dwelling. For one or more selected dwelling, values of the flows at each time-step (or averages for a longer recording period, e.g. hourly) can be recorded in order to study the interaction of the various systems.

It is important to take the diversity of demands into account. To achieve this, a number of dwellings are defined. Each dwelling definition consists of identifying the climate, heating system, heating control system, building type (i.e. thermal characteristics), appliance and lighting configuration, number of residents, domestic hot water (DHW) system and occupant behaviour characteristics associated with that dwelling. In this way, a collection of dwellings can be defined with a good level of diversity from a relatively small number of definitions of the relevant sub-systems. For example, 32 dwelling permutations would be possible with four building type definitions, four heating system definitions and two heating control system definitions (i.e. $4 \times 4 \times 2$). Additional diversity is built into most of the sub-system models as explained in their detailed descriptions.

Total grid-side power flows are assumed to be the sum of the power flows from all the dwellings; reactive power flows are not considered. The model is intended to enable the consideration of local network power flows (i.e. associated with approximately 100 to 200 dwellings) as a possible driver for demand side management (DSM) interventions (e.g. limiting power flows to the capacity of the local transformer). However, by using a large number of dwellings definitions and associating a multiplier with each definition it is possible to calculate indicative power demands for the whole domestic sector (Strbac, (2008) suggests that there are only minimal decreases in the coincidence factor of loads above 1000 dwellings). This enables DSM interventions associated with generation objectives (e.g. maximizing the use of power with a low MEF) to be considered.

The following sections describe the model components relating to the building thermal characteristics, the heating control system, the heating system, DHW consumption, the characteristics of the electrical grid, occupancy and appliance use and, finally, climate.

4.2 Building thermal model

4.2.1   Heat flows within building

The building thermal model is simplified to a lumped capacitance model. That is, it is assumed that the inside air and the building fabric can each be treated as a single thermal inertia with a mean temperature which is sufficiently representative of the entire mass. This is common in similar studies (e.g. Sulka & Jenkins 2008; Boait et al. 2011) where it is often justified by the large number of dwellings being considered. However, other studies have shown that good approximations to more detailed models can be achieved (Ramallo-González et al. 2013).

Here, additional justification for the simplification is found in the fact that the results of interest are the *relative* performances of the heating systems under investigation, not the absolute energy flows within the building at a given time. The air temperature is the parameter which is of most interest as it is the main input to the heating control system; it is the dynamics of a single temperature which determine when and relatively how much heating is required. Although little confidence should be placed in the ability of the model to produce accurate predictions of the total amount of heat required, this is of less significance as we are interested in the factors which affect the relative performance of the heating system in delivering it.   The model cannot simulate the heat flows between different spaces within the building but this is unnecessary if parameters can be selected that produce equivalent dynamics at the point where the control system would measure its input temperature. In practice, the simplified model will not demonstrate fully equivalent dynamics but a good approximation can be achieved (see section 4.2.2).

 The heat flows considered by the thermal model are presented in Figure 18.
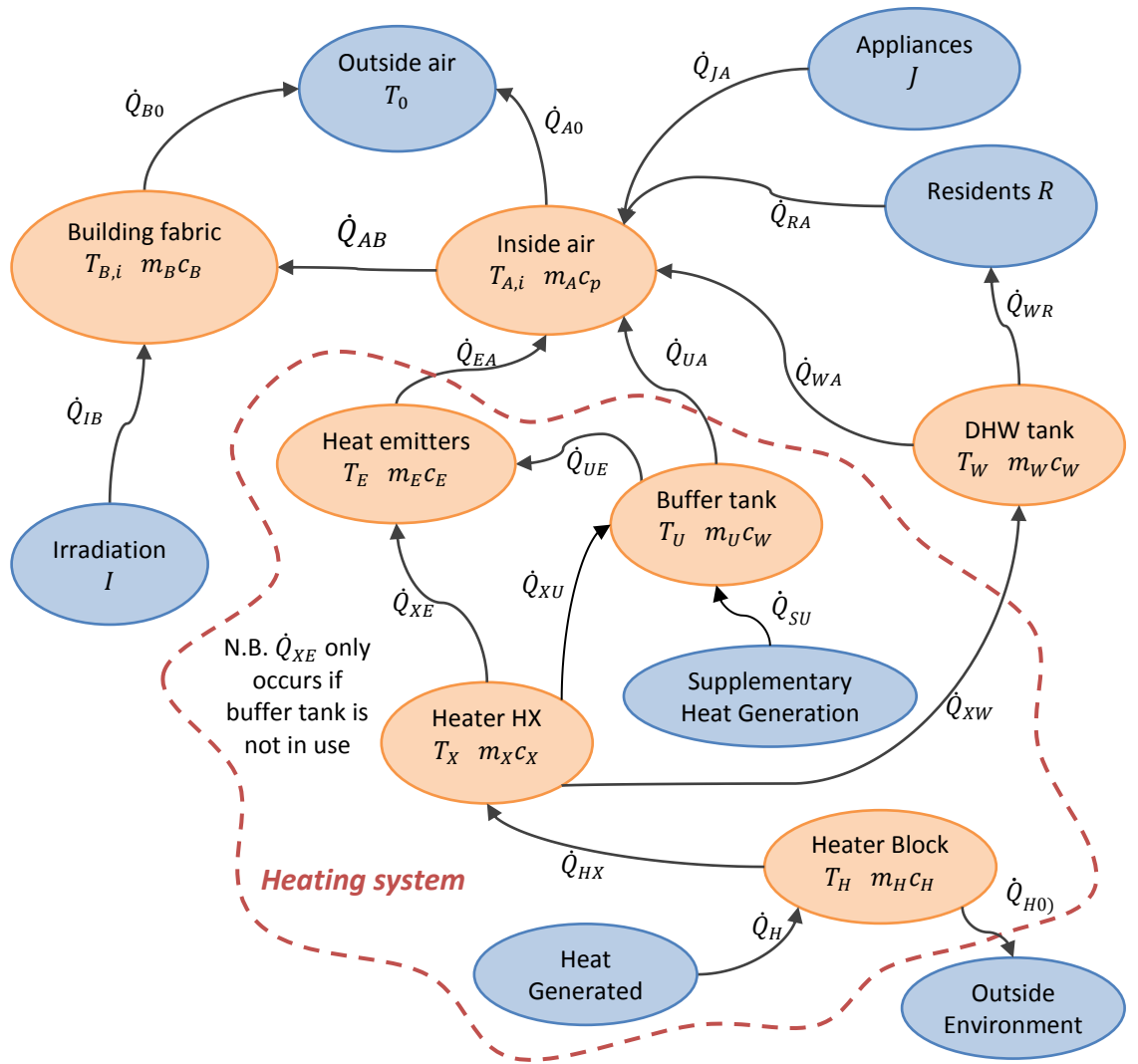
Figure 18: Representation of heat flows modelled

The heat flows and temperatures within the heating system are described in section 4.4. The heat flow rates and temperatures outside the heating system are as follows:

$$\dot{Q}_{A0} = (T_A - T_0)\dot{m}_A c_p \qquad\qquad Equation\ 13$$

$$\dot{Q}_{B0} = (T_B - T_O)k_{B0} \qquad\qquad Equation\ 14$$

$$\dot{Q}_{AB} = (T_A - T_B)k_{AB} \qquad\qquad Equation\ 15$$

$$\dot{Q}_{IB} = Ik_{IB} \qquad\qquad Equation\ 16$$

$$T_{A,i} = T_{A,i-1} + \frac{\left(\dot{Q}_{EA} + \dot{Q}_{LA} + \dot{Q}_{NA} + \dot{Q}_{UA} + \dot{Q}_{WA} - \dot{Q}_{A0} - \dot{Q}_{AB}\right)t}{m_A c_p}$$

Equation 17

$$T_{B,i} = T_{B,i-1} + \frac{\left(\dot{Q}_{AB} + \dot{Q}_{IB} - \dot{Q}_{B0}\right)t}{m_B c_B}$$

Equation 18

where:

$\dot{Q}_{A0}$ is the heat flow rate (all heat flow rates measured in Watts) from the inside air to the outside air due to infiltration rate $\dot{m}_A$ (kg/s), $\dot{Q}_{B0}$ is the heat flow rate from the building fabric to the outside air with heat transfer coefficient k_{B0} (W/K) and $\dot{Q}_{AB}$ is the heat flow rate from inside air to building fabric across heat transfer coefficient k_{AB} (W/K)

$\dot{Q}_{IB}$ is the rate of heat gains due to irradiation intensity I (W/m^2), acting on an effective solar area of k_{IB} (m^2).

$\dot{Q}_{JA}$, $\dot{Q}_{NA}$, $\dot{Q}_{UA}$ and $\dot{Q}_{WA}$ are the rates of internal gains to the inside air from appliances, occupants, and heat losses from the buffer tank and DHW tank. These are described in their relevant sections, below.

$T_{A,i}$ is the mean temperature of the inside air (all temperature in degrees Kelvin) at time-step i, t seconds after $i-1$ and $T_{B,i}$ is the mean temperature of the building fabric at time-step i. m_A and m_B are the effective thermal masses of the inside air and building fabric respectively (kg), c_p and c_B are the mean specific heat capacities of the inside air (at constant pressure) and building fabric respectively (J/(kgK)).

The rate of heat transfer from the emitter system into the inside air, $\dot{Q}_{EA}$, varies with the temperature difference between the heat emitters and the inside air. For the range of conditions encountered by domestic heat emitters (i.e. Rayleigh numbers less than 10^9), the heat transfer coefficient varies in proportion to the temperature difference to the power of 0.25 (Incropera & DeWitt 1985). To account for this, the heat transfer rate is expressed in terms of a nominal heat transfer coefficient k_{EA} (W/K), which occurs at a specified temperature difference, T_{DE}, (in this case, the characteristic temperature difference is 29K for radiator systems and 14K for enhanced / underfloor systems, see section 4.2.2).

$$\dot{Q}_{EA} = k_{EA} \left(\frac{T_E - T_A}{T_{DE}} \right)^{0.25} (T_E - T_A) \qquad \textit{Equation 19}$$

$$= \frac{k_{EA}}{T_{DE}^{0.25}} (T_E - T_A)^{1.25}$$

4.2.2 Selection of building parameters

Values for the heat transfer coefficients, effective irradiation area, inside air mass and building fabric thermal inertia for three different building types were derived by calibrating the results from the model against temperature profiles generated using ESP-r by Dr. Nick Kelly and Dr. Jun Hong at ESRU, University of Strathclyde. Although preliminary modelling work used values for these building properties calculated from real materials data, it is the effective heat transfers and thermal inertias which are of interest and so more accurate results are obtained using the calibrated properties.

The three buildings selected were based upon work previously conducted within the SUPERGEN HiDEF consortium to identify representative building types for the UK (Hong et al. 2010), based primarily upon work by DCLG (2007b) and Utley & Shorrock (2008), see Table 9.

Table 9: Typical building types

Building type	Floor area	Fraction of UK building stock	Average heat loss
	m^2	%	W / K
Semi-detached	87	28	265
Flat	56	16	167
Terraced	58	19	235

The resulting building characteristics are given in Table 10.

Table 10: Modelled building properties

Building Index	$m_A c_p$	$m_B c_B$	k_{B0}	k_{AB}	k_{IB}
#	kJ / K	kJ / K	W / K	W / K	m^2
1 (Semi-detached)	701	16570	386	339	13.0
2 (Flat)	748	15340	106	251	11.2
3 (Terraced)	785	13020	153	179	10.4
4 (Semi-detached with improved insulation)	701	16570	232	339	13.0

The modelled buildings were constructed with an assumed air infiltration rate of 0.5 air changes per hour. Examples of the resulting modelled temperature profiles are given in Figure 19 along with the temperature profiles generated by ESP-r that the building parameters were calibrated against. The overall fit is good with root mean squared errors of 0.45K, 0.59K and 0.52K for the three building types (less than 2% of the temperature range in the profiles).

To investigate the effect of improved insulation levels, a fourth building type was used with the same inertia properties but the external heat transfer coefficient reduced to 60% of the original value and the air infiltration rate reduced to 0.25 air changes per hour.

Notably, the best fit is in winter (when the majority of heat demand takes place) and so the effective error is actually less significant. The characteristic overshoot in the temperature profile for the heated periods produced by the simplified model (in contrast to the flat profile produced by ESP-r) is likely to be due to the lack of additional materials in each house providing a range of heat transfers as the heating is backed off. Additionally, the simplified model does not take account of orientation with respect to solar irradiation and so there is a larger midday effect from south facing windows in the ESP-r models. Both of these effects are specific to the detail of the buildings being modelled and so it is unlikely that a single set of parameters could adequately describe them for the population of dwellings.
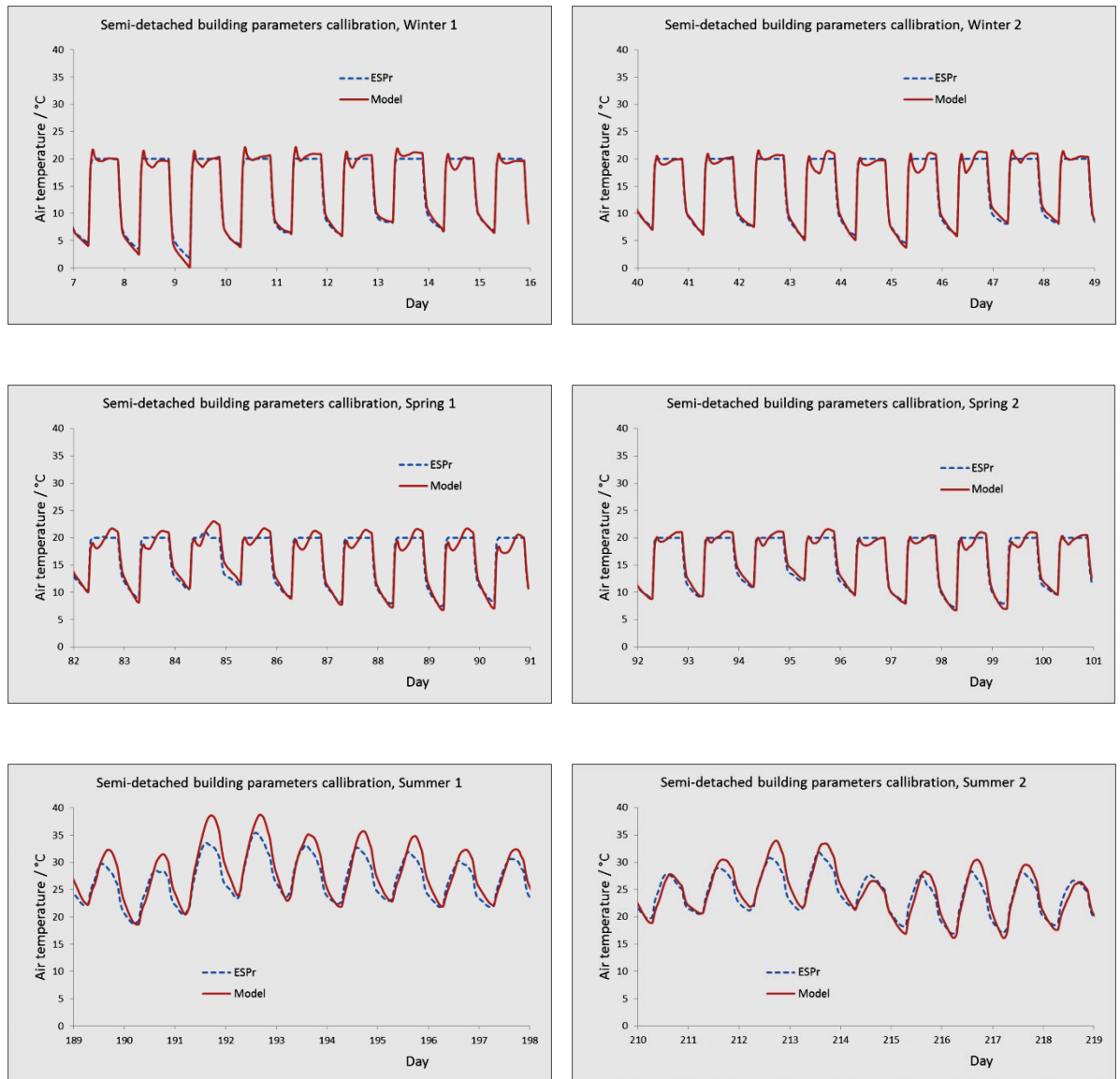
Figure 19: Modelled temperature profile in semi-detached house from ESP-r and simplified model

The nominal heat transfer coefficients for the emitter systems in the buildings (k_{EA}) were selected such that the rate of heat loss from the building (i.e. $\dot{Q}_A + \dot{Q}_B$) when the outside air temperature is -1°C and inside air temperature is 21°C is matched by the rate of heat delivered by emitters operating with a flow temperature of either 50°C (i.e. T_{DE} = 29K) in the case that "conventional" heat emitters are being modelled or 35°C (i.e. T_{DE} = 14K) if "enhanced" heat emitters (effectively, underfloor) are being modelled. Both of these ratings are calculated with an assumed return temperature 5°C lower than the flow temperature.

4.2.3 Exergy content of heat flows in building

In addition to the various energy (heat) flows, the exergy content of the energy flows into the heat emitter system and into the inside air are calculated and recorded at each time-step. It is assumed that the changes in the emitter temperature and the inside air temperature during each time-step are sufficiently small that Equation 3 can be used to calculate the exergy flows.

$$\dot{E}_{XE} = \dot{Q}_{XE}\left(1 - \frac{T_0}{T_E}\right)$$

Equation 20

$$\dot{E}_{EA} = \dot{Q}_{EA}\left(1 - \frac{T_0}{T_A}\right)$$

Equation 21

where $\dot{E}_{XE}$ and $\dot{E}_{EA}$ are the exergy flow rates (W) entering the emitter system and the inside air respectively. Here, the outside air temperature, T_0, (K) at that time is selected as the reference temperature. Given the sensitivity to changes in the selection of the ambient temperature it would be problematic to use an annual mean value of outside air temperature in this context.

4.3 Heating Control System

4.3.1   Control system temperature program

In the model, a programme of temperatures, T_{RA}, are preselected for each dwelling. In the simulations conducted, three programmes are used:

- 21°C continuously

- 21°C during the day, set back to 16°C between 22:00 and 07:00.

- 18°C continuously

The normal temperature (21°C) was selected to provide almost neutral thermal comfort levels and for consistency with SAP2009.

4.3.2   Thermal comfort – predicted mean vote

Occupant comfort is a complex subject which is not fully understood (De Dear 2011). It involves far more than just the air temperature; with practitioners moving away from the paradigm of still, dry air within an acceptable temperature range in the last decade (Borgeson & Brager 2011). Factors such as perceived air quality affect the acceptability of temperature variations and it is noted that occupant comfort tends to be fairly equal across a range of temperatures before reducing rapidly outside of it (Zhang et al. 2011). The range of acceptable temperatures can be extended considerably (in the order of 2ºC) by personal heating or cooling systems (for example, fans, radiating heating) before space heating or cooling is necessary. It is possible that alternative heating systems may provide the same comfort at lower temperatures, reducing energy requirements.

Given the large effect that the temperature of the building has on its heat demand, this temperature must be controlled for in some way. In order to provide some metric for comparison between buildings in different scenarios, a modified version of the "predicted mean vote" (PMV), a measure of thermal comfort proposed by Fanger (1973) is used. Despite the limitations outlined above, PMV is well used and the method for calculating it is formalised (ISO 7730:2005). The PMV can be related to the average thermal sensation experienced by a group of people on a seven-point thermal sensation scale (Table 11):

Table 11: Thermal sensation scale. From ISO 7730:2005

Vote	Sensation
+ 3	Hot
+ 2	Warm
+ 1	Slightly warm
0	Neutral
- 1	Slightly cool
- 2	Cool
- 3	Cold

Calculating the PMV requires the metabolic and work rates of the individual(s), the air temperature and effective radiant temperature, the level of clothing worn by the individual(s) and the vapour partial pressure of moisture in the atmosphere. The calculation requires iteration as it involves heat transfer coefficients and temperature which are functions of each other. However, if the other conditions are fixed, the function relating air temperature to PMV is effectively linear (Figure 20). These simplifications are adopted on the basis that the objective is to provide a metric which can be used to determine when comparison between the performance of units is being performed with approximately equivalent thermal comfort in each case. The objective is not to provide an exact measure of thermal comfort but rather one which is approximately consistent between simulations. This "pseudo-PMV" is calculated for each dwelling during each time-step. These are summed for each dwelling in each scenario. Because a PMV either side of 0 represents increasing thermal discomfort, only the negative values are summed as a measure of the total thermal discomfort due to cold.
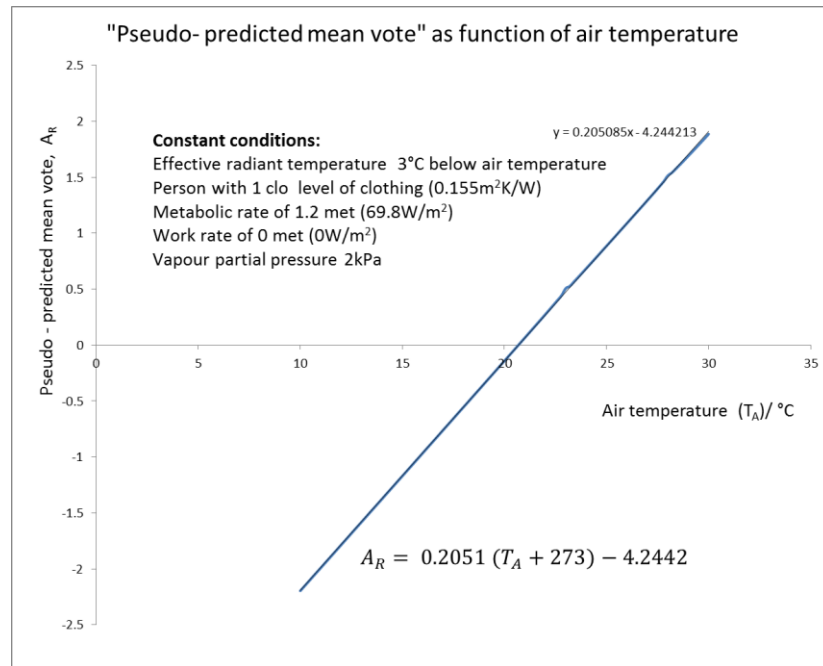
Figure 20: Predicted mean vote as function of air temperature

The conditions used for all calculation of the pseudo-PMV by the model are fixed and given in Table 12.

Table 12: Conditions used in calculation of pseudo-PMV

Effective radiant temperature:	3°C below air temperature
Level of clothing:	0.155m^{2}K/W (i.e. 1 "clo")
Metabolic rate:	69.8W/m^2 (i.e. 1.2 "met")
Work rate:	nil
Partial pressure of moisture:	2kPa

The resulting equation to calculate pseudo-PMV (A_R) is:

$$A_R = 0.2051 (T_A + 273) - 4.2442$$

Equation 22

4.3.3 Deviation from temperature program because of DSM signal

For the purposes of this model, it is necessary to assume that some relationship exists between occupant preference for thermal comfort and the price of achieving certain air conditions. It is assumed that occupants will accept some deviation from the program temperature and that this will depend upon both their preferences and the price of electricity at that instant. A two-part

sigmoid shaped function is used in order to provide a continuous function but also to reflect the reducing acceptability of temperature variations outside of a central range, noted above:

$$T_{ZC} = T_{Z0} \sin(\frac{\pi}{2}(1 - Z)) \;\; if \; Z < 1 \qquad \text{Equation 23}$$

$$T_{ZC} = T_{Zmax} \sin(\frac{\pi}{2}(Z - 1)/(Z_{max} - 1)) \;\; if \; Z \geq 1 \qquad \text{Equation 24}$$

where T_{ZC} is the change in the control system target temperature relative to the program temperature (K) and Z is the normalised price of electricity. T_{Z0} is the temperature change when electricity is free and T_{Zmax} is the temperature change when the normalised price of electricity is Z_{max}. For the sake of simplicity, it is assumed that Z is constrained to the range $0 \leq Z \leq Z_{max}$ where Z_{max} is taken to be 4.

For dwellings with ASHPs (i.e. where high electricity prices incentivise lower temperatures), the values of T_{Z0} and T_{Zmax} will be, respectively, the maximum increase (T_{Rhot}) and decrease (T_{Rcold}) to the target inside air temperatures which the occupants find acceptable. For dwellings with mCHP units (i.e. where high electricity prices incentivise higher temperatures), this is reversed; the values of T_{Z0} and T_{Zmax} will be, respectively, the minimum and maximum changes to target inside air temperatures which the occupants find acceptable.

The model is not designed to model the actual variation in price that would occur but rather the variation in heating demand that could reasonably be achieved by some signal such as price. Such a relationship is implicit in field trials reported by Warmer et al. (2007) and further work might better identify its characteristics but it is sufficient here to assume that some deviation from the program temperature could be incentivised. Some people will accept larger variations of temperature for a given incentive than others.

Nine different levels of flexibility are considered in this study; their associated values of T_{Rhot} and T_{Rcold} are given in Table 13. Four of these are illustrated by Figure 21.

Resident Flexibility	T_{Rhot}	T_{Rcold}
A – no flexibility	0°C	0°C
B	0°C	-1°C
C	0°C	-2°C
D	+1°C	-1°C
E	+1°C	-2°C
F	+1°C	-3°C
G	+2°C	-2°C
H	+2°C	-3°C
I	+3°C	-3°C
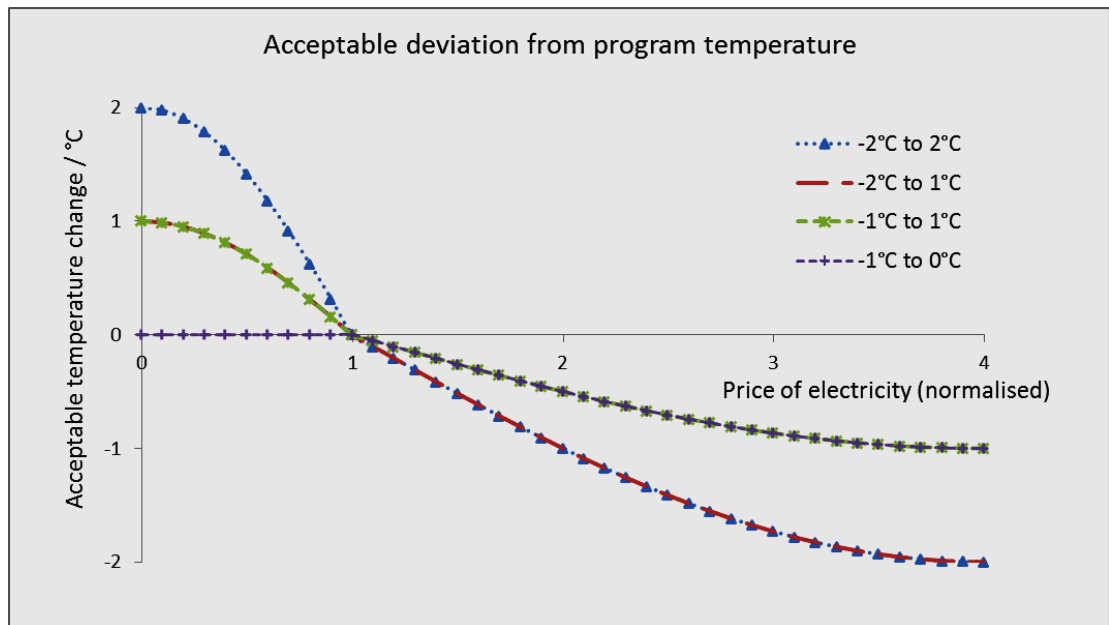
Figure 21: Variations in acceptable temperature deviation with price of electricity assumed in model

The target inside air temperature that the control system attempts to maintain, T_{CA}, is then given by Equation 25:

$$T_{CA} = T_{RA} + T_{ZC}$$

Equation 25

Using a signal to adjust the temperature at which the control system is aiming to maintain the inside air is a more robust system than attempting to adjust the electrical power demand of the heating system directly as the implications can be more readily understood and the non-linear

responses of heating system power demands to changes in heating demands do not need to be explicitly modelled in the control system.

It is important to maintain the temperature within a range which is still comfortable to the occupants. If the temperature were to drop too much because of direct control of the heating system (i.e. to reduce electrical demand) then it is likely that occupants would resort to using appliances which are not subject to direct DSM control to heat their homes. These would inevitably be less efficient and so the problem would be exacerbated as the direct DSM control becomes progressively tighter as a result.

4.3.4 Target heat generation

The model includes four algorithms for calculating the target heat generation. The first three relate to three different control methodologies, only one of these will be implemented in a particular dwelling. The fourth relates to the condition when the DHW tank temperature is too low.

4.3.4.1 Control system 1: Proportional control.

This is used without a buffer tank. The target heat generation is calculated using Equation 26.

$$\dot{Q}_C = k_C(T_{CA} - T_A)$$
<div align="right">Equation 26</div>

where $\dot{Q}_C$ is the target heat generation (W), T_A is the inside air temperature and T_{CA} is the target inside air temperature calculated using Equation 25. k_C is the control coefficient (W/K). To facilitate meaningful adjustment of the model parameters, this is given as the product of an adjustment factor, k_P, and the coefficient which would create a steady state inside air temperature of 20°C (i.e. 1°C below target of 21°C) when outside air temperature is -1°C.

Although proportional controllers are used in some heating systems, this particular system has not been observed and is included to investigate the possible improvements in performance that may be reasonably expected by matching the flow temperature to the minimum which is needed as closely as possible.

4.3.4.2 Control system 2: Variable temperature ("weather-compensated") control.

This is used with a buffer tank. It can be used with both units that are capable of modulating and those that are not. The control system aims to maintain the buffer tank at a temperature which is a function of the outside air temperature. In this study, for dwellings using conventional

radiators, the target buffer tank temperature is 55°C when the outside air temperature is -2°C, decreasing linearly to 25°C when the outside air temperature is 15°C. For dwellings using enhanced heat emitters (effectively equivalent to an underfloor system), the flow temperature when the outside air temperature is -2°C is reduced to 40°C (see Figure 22).
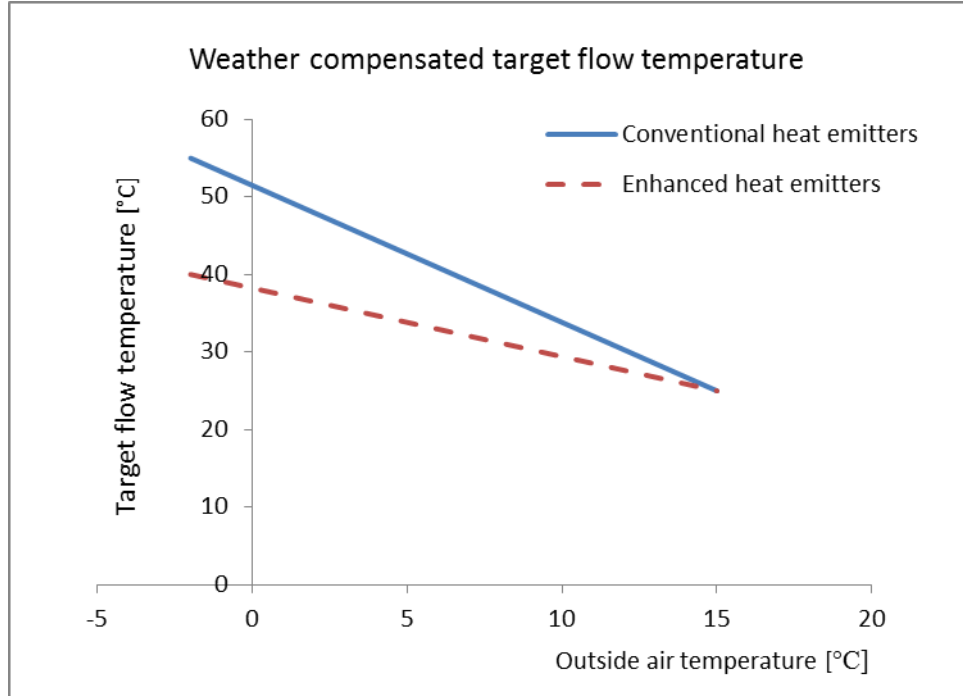
Figure 22: Variable-temperature control, target flow temperature

This system is used in several commercially available heat pump systems; it reduces the flow temperature when a lower rate of heat delivery is required.

The target buffer tank temperature (T_{CE}) is adjusted by the DSM signal in the same way as the target inside air temperature but with the range increased threefold relative to the ranges in Table 13. In the case that a modulating heating unit is used, a proportional controller is used to determine the target heat generation.

$$\dot{Q}_C = k_C(T_{CE} - T_U) \qquad \text{Equation 27}$$

where T_U is the actual buffer tank temperature.

In the case that a fixed-output heating unit is used, a dead-band (T_{UC}) of +4K / -4K (selected according to whether the heating system operated in the last time-period) is used relative to the target temperature to determine whether the heating unit is off or operating at full capacity ($\dot{Q}_{Hmax}$).

$$\dot{Q}_C = \dot{Q}_{Hmax}\langle T_{CE} - T_U + T_{UC}\rangle^0 \qquad\qquad \text{Equation 28}$$

Flow from the buffer tank to the heat emitters is controlled by a secondary thermostat system (see section 4.4.6).

4.3.4.3   Control system 3: Fixed Temperature, Flow control

This control system is similar to control system 2, but the system aims for a consistent buffer tank temperature rather than the weather-compensated temperature. In the case of this study, the target buffer tank temperature is 55°C in buildings which have conventional heat emitters and 40°C in buildings which have enhanced heat emitters. This control system is functionally similar to that used on the majority of condensing gas boilers and so the majority of consumers and installers are familiar with it.

4.3.4.4   DHW heating

Heat is delivered to the DHW tank according to Equation 48 whenever the heater heat-exchanger temperature is high enough, regardless of the heating control system. However, if the DHW tank temperature drops below its minimum acceptable temperature (in this study, 40°C), the control system stops heat from being fed to the heat emitters or buffer tanks so that the heater heat-exchanger temperature is increased and the rate of heat delivery to the DHW tank is increased. A dead-band (T_{WC}) of +5°C / -0°C is used to prevent unstable behaviour.

In this case, the target heat generation is calculated as:

$$\dot{Q}_C = \dot{Q}_{WR} + (T_{WC} + T_{ZC})\, m_W c_W / t_{WC} \qquad\qquad \text{Equation 29}$$

where t_{WC} is the nominal time for heat to be diverted solely to the DHW tank, set at 120 seconds by default.

4.4 Heating unit model

4.4.1   Heating system overview

Readers are referred to Table 3 and Table 4 for a list of the 8 ASHP units and 12 mCHP units referred to here as "ASHP x", "SE-mCHP y" and so on. The model is based on the standard model specifications for combustion-based mCHP units suggested by IEA ECBCS Annex 42 (Beausoleil-Morrison, Arndt, et al. 2007) and is illustrated in Figure 23 (a subset of the flows illustrated in Figure 18). This model has been shown to have good fidelity to measured performance where suitable calibration has taken place. Parameters for three units (SE-mCHP, ICE-mCHP and SOFC-mCHP) are available in the Annex's final report, with the possible caveat that condensing behaviour was not fully explored during the experimental testing used. Additional performance data are also included to facilitate calibration of appropriate parameters to other units. The same set of elements are also used for the ASHP units, following Kelly and Cockroft, (2011) and to facilitate comparison between them.
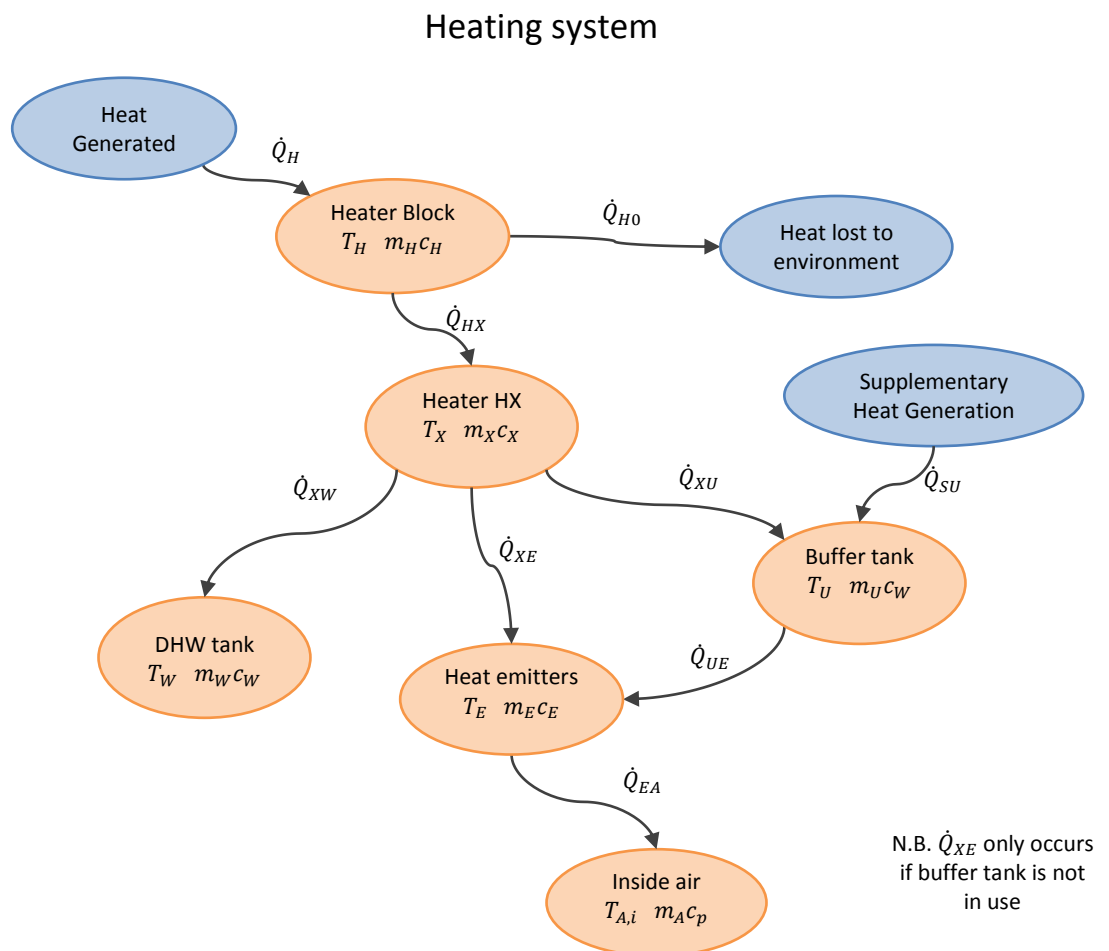
Heating system

Figure 23: Heating system thermal flows

The heat flows and temperatures assume a lumped-capacitance model. The heat flows within the heating system are calculated as follows:

$$\dot{Q}_{HX} = (T_H - T_X)k_{HX} \qquad\qquad \textit{Equation 30}$$

$$\dot{Q}_{H0} = (T_H - T_0)k_{H0} \qquad\qquad \textit{Equation 31}$$

$$T_{H,i} = T_{H,i-1} + \frac{(\dot{Q}_H - \dot{Q}_{HX} - \dot{Q}_{H0})t}{m_H c_H} \qquad\qquad \textit{Equation 32}$$

$$T_{X,i} = T_{X,i-1} + \frac{(\dot{Q}_{HX} - \dot{Q}_{XW} - \dot{Q}_{XE} - \dot{Q}_{XU})t}{m_X c_X} \qquad\qquad \textit{Equation 33}$$

where $\dot{Q}_{HX}$ is the heat flow rate (W) from heater block to the heater heat exchanger through heat transfer coefficient k_{HX} (W/K) and $\dot{Q}_{H0}$ is the heat flow rate from heater block to the outside air through heat transfer coefficient k_{H0}. $\dot{Q}_{XW}$ (heat flow to DHW tank) is described in section 4.5.

4.4.2   Actual heat generation

The heating control system will request the target heat generation ($\dot{Q}_C$) from the heating system but the actual heat generated ($\dot{Q}_H$) will also depend upon the performance of the heating system. In addition to limitations on the heat generation imposed by the performance of the heating system, the heat transferred to each component of the heating system (e.g. the DHW tank, buffer tank and / or heat emitter system) will depend upon the relative temperatures and thermal inertias of the elements within each component.

These two aspects (restrictions on the heat generated and the way that the heat generated is delivered) are treated separately. This has the advantage that the second, dynamic, part can be based upon the standard Annex 42 model specification. It also makes the code more efficient as the calculation of heat generated affects the power demanded from the grid and so needs to be included in the iterations of the price of electricity whereas the calculation of heat flows can happen once per time-step with the other heat flows.

The restrictions on heat generation applied to the heating systems are:

- Minimum heat generation. In the case of some SOFC-mCHP systems, the unit cannot be turned off as part of their usual operation.

- Minimum operational heat generation. In the case of other units, there is usually a minimum operating heat generation; that is, they cannot be operated with a lower heat output.

- Maximum heat generation. The maximum heating capacity of the unit. Some mCHP have an auxiliary gas boiler unit. The heat generation from these components is treated separately in this model.

- Modulation steps. Some units have only one operating level, (i.e. their minimum and maximum operational heat generation levels are the same). However, other units are capable of varying (modulating) their output between their minimum and maximum levels. Some of these can achieve continuously variable output between these extremes (e.g. (Heliotherm n.d.)) whereas other units have discrete operating steps (i.e. they can modulate between the minimum and maximum operating levels but only at predefined steps, e.g. some units have 8 modulation levels (Daikin n.d.). In the case of units with discrete operating levels, the heat output step equal to or above the target heat generation is selected.

- Maximum rate-of-change. Some units are constrained to a maximum rate-of-change of output. This is typical of high temperature SOFC-mCHP units and, to a lesser extent, PEMFC-mCHP units. The limitation is usually enforced by the unit's control system to prevent thermal fatigue of the stack components. If this limit is applied in the model, it is necessary to ensure that there is not a "minimum operating level" specified for the unit (or, if it is, that it is the same as the minimum heat generation level). Otherwise, the unit would be unable to turn on if a step increase from off to "minimum" is greater than the permitted rate-of-change.

- A supplementary burner is available within the model. This is modelled as a fixed efficiency unit, burning natural gas and supplying the heat generated ($\dot{Q}_{SU}$) directly to the buffer tank. This additional heating is only used with the units which have a thermal capacity of less than 4kW (i.e. ICE-mCHP B, PEMFC B, SOFC A, SOFC B and SOFC C). When operated, the supplementary heat generated is assumed to match any shortfall in the heat generated by the unit ($\dot{Q}_H$) relative to the target heat generation ($\dot{Q}_C$). That is, it behaves "perfectly" with no thermal lag and continuously variable output. The energy flows associated with this supplementary heat are accounted for separately in the results. Treating the supplementary heat separately means that the results can distinguish the performance of the heating unit from the system performance achieved with it.

The maximum heat output of a unit and its ability to modulate is generally given in its specification (see Table 3 and Table 4 for details of the 20 units considered in this research). For ASHPs with the ability to modulate, the minimum output level is assumed to 25% of the maximum output for ASHP units (consistent with that claimed by Mitsubishi Electric Europe, 2008b) unless it is specified. The maximum turn-down ratio for mCHP units is usually specified or can be inferred from test data and it is assumed that their modulation is continuous (i.e. not in discrete steps). Most of the ASHP units have stepped modulation and it is assumed that eight modulation steps are available unless further information is available. Sensitivity analysis was conducted with the model to determine whether the number of modulation steps used has a significant effect on the results from the model. Several ASHP units were simulated for a three-month period with different numbers of modulation steps available to them; the resulting performances are presented in Figure 24.
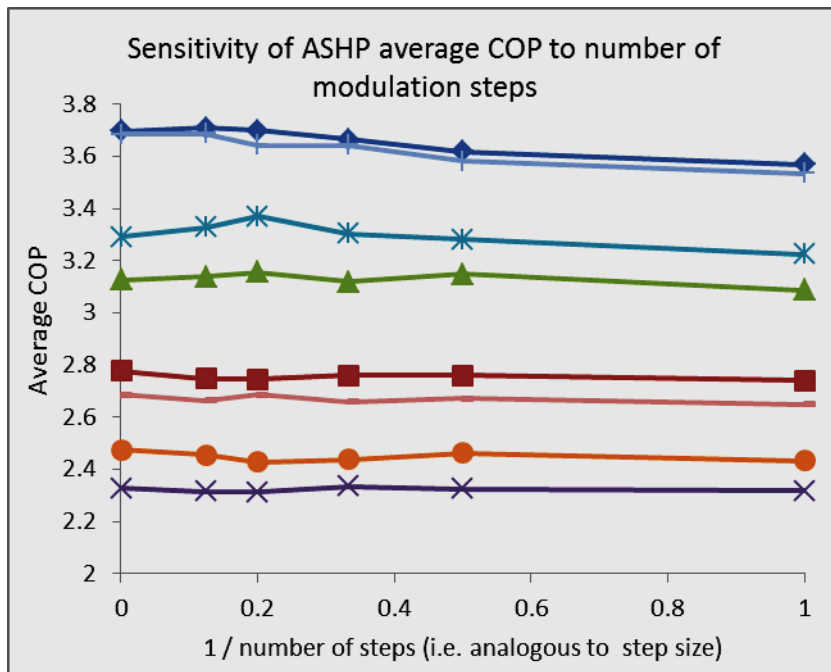
Figure 24: Sensitivity of modelled ASHP COP to number of modulation steps modelled (each plot relates to a different ASHP model)

The modelled performances of the ASHP units are insensitive to the number of modulation steps. The bottom four plots actually relate to cases with more buffering and so (unsurprisingly) the number of modulation steps has even less effect on them. There is usually a slight increase in performance as the number of modulation steps increases (i.e. at the lower values on the reciprocal x-axis scale) but there is minimal improvement (and, curiously, one case of minor performance degradation) when more than five steps are used (i.e. when the relative step size is less than 0.2).

4.4.3 Heating system fuel demand

4.4.3.1   Gas boilers

For both the gas boilers and the mCHP units, the fuel used is assumed to be natural gas with standard composition for the UK. In the case of gas boilers (including any supplementary heating systems), the thermal efficiency is assumed to remain constant at 90% (GCV). It is likely that the efficiency would vary (in particular, the flow temperature affects the viability of the condensing function) but the simplification has been used as condensing gas boilers are only included as a readily understandable benchmark to compare other results against.

4.4.3.2   mCHP

Because the model assumes some thermal losses from the heater block ($\dot{Q}_{H0}$, see Figure 23) thermal efficiency coefficients (k_{HH}) are used to characterise the relationship between heat generation within the units and fuel use. The values of these coefficients are slightly higher than the measured thermal efficiency of the units. They are calculated such that, under steady-state conditions, the useful heat flow from the heater (i.e. heat generation minus heat losses) corresponds to the steady-state thermal efficiency of the units.

The thermal efficiency for ICE-mCHP units is considered to be almost constant in the IEA ECBCS Annex 42 model, based upon the ICE-mCHP units used for calibration. However, other (generally, modulating) devices do show some variation in steady-state thermal efficiency between different heat outputs and so an additional linear interpolation is used in this model between the coefficients corresponding to the nearest conditions. Thermal efficiency coefficients are listed in Table 14. Thermal losses coefficients (i.e. k_{H0}) are listed with the other thermal characteristics of the units in Table 16.

Below its nominal operating temperature, T_{H0}, the Annex 42 model assumes that the thermal efficiency of SE-mCHP units is a function of their temperature as described by Equation 34:

$$\dot{m}_F \mathrm{h}_F = \frac{\dot{Q}_H}{k_{HH}} \left(1 + k_F \frac{T_{H0} - T_0}{T_H - T_0} \right) \qquad \textit{Equation 34}$$

where $\dot{m}_F$ and h_F are the fuel mass flow rate and specific enthalpy of combustion (in kg/s and J/kg). k_F is an empirically derived constant and T_H is the temperature of the heater block. For SE-mCHP A, the values of k_F and T_{H0} were empirically derived by Beausoleil-Morrison, Arndt, et al. (2007) to be 0.04 and 257°C respectively.

The other two SE-mCHP units considered are capable of modulating their power output (unlike SE-mCHP A) and so the function relating thermal efficiency to heater block temperature is not used. More accurate modelling of their characteristics can be achieved by adopting the interpolation approach used with ICE-mCHP units.

The Annex 42 model for FC- mCHP takes a different approach and models the energy content of the fuel, air and water flows through the stack, heat exchanger and ancillary systems. This approach has enabled a high fidelity model of a SOFC-mCHP to be calibrated but it is harder to implement within the overall model used here. This is for two reasons; firstly, because heat generation is a function of several other factors, it is not possible to use heat generation as a control variable. Secondly, although coefficients are available for the calibrated SOFC-mCHP unit, deriving them from the data available on other FC- mCHP units is unlikely to be possible.

The interpolation approach has therefore been taken for both types of FC- mCHP as well as the combustion based units. Variations in the steady-state thermal performance of some FC-mCHP units with the flow temperature have been accounted for by appropriate selection of heat loss coefficients. SOFC-mCHP C is the unit for which a calibrated model is provided by Beausoleil-Morrison, Arndt, et al. (2007); for this unit the maximum heat recovery which could be achieved by a perfect heat exchanger (after heat losses are accounted for) has been calculated for each performance point and these data are used to calculate the effective thermal efficiency coefficients. This is an optimistic approach but as the thermal efficiency for this unit does not represent the limit of the performance envelope under any conditions, it is considered a reasonable simplification.

Table 14: mCHP thermal efficiency coefficients

Unit	Thermal efficiency coefficients, k_{HH}. The heat generation rate ($\dot{Q}_H$) that each coefficient relates to is given below the coefficient.						
	1	2	3	4	5	6	7
SE- mCHP A	87.4% 7.29kW						
SE- mCHP B	100% 3.5kW	100% 3.7kw	92% 4kW	91% 4.3kW	92% 5.6kW	92% 6.8kW	
SE- mCHP C	70.5% 6.9kW	70.0% 24.3kW					
ICE- mCHP A	59.5% 13.45kW						
ICE- mCHP B	73.6% 3.8kW	65.7% 7.9kW	62.8% 12.1kW				
ICE-mCHP C	56.8% 2.8kw						
PEMFC A	75.3% 7.1kW	69.7% 8.4kW	70.9% 10.4kW	73.2% 12.7kW	69.4% 13.4kW		
PEMFC B	62.8% 1kW	63.9% 1.3kW	57.7% 1.9kW				
PEMFC C	42.9% 3.4kW	44.5% 4.7kW	47.7% 6.9kW	50.2% 8.9kW			
SOFC A	20.2% 320W	22.7% 370W	20.0% 400W	18.7% 520W	25.7% 1000W		
SOFC B	20.2% 960W	22.7% 1.1kW	20.0% 1.2kW	18.7% 1.5kW	25.7% 3kW		
SOFC C	49.8% 4.6kW	50.3% 4.8kW	50.7% 5.1kW	51.1% 5.3kW	52.0% 5.5kW	51.7% 5.7kW	52.1% 6.1kW

4.4.4   Heating system power flows

The heating systems will have electrical power flows (potentially negative, i.e. net generation, in the case of mCHP systems) associated with their operation.

Each unit has a standby power when not operating and an additional pumping power when operating. In most cases, the standby power is not specified and is assumed to be 10W, around the same as SE-mCHP A (Whispergen Ltd 2006).

4.4.4.1   mCHP units

The electrical efficiency of mCHP units is affected by their output power level, typically varying by +/- 5% across the operating range for an ICE-mCHP but by more for other types. The efficiency is linearly interpolated from known data points. These are given in Table 15.

Table 15: mCHP electrical efficiencies

Unit	Net Electrical Efficiency, η_e. The **heat generation** rate ($\dot{Q}_H$) that each efficiency relates to is given below it.						
	1	2	3	4	5	6	7
SE- mCHP A	8.4% 7.29kW						
SE- mCHP B	4.2% 3.5kW	7.4% 3.7kw	9.0% 4kW	10.1% 4.3kW	11.9% 5.6kW	12.1% 6.8kW	
SE- mCHP C	12.4% 6.9kW	21.3% 24.3kW					
ICE- mCHP A	24.3% 13.45kW						
ICE- mCHP B	19.7% 3.8kW	22.0% 7.9kW	22.3% 12.1kW				
ICE-mCHP C	20.3% 2.8kw						
PEMFC A	15.9% 7.1kW	20.9% 8.4kW	20.4% 10.4kW	20.2% 12.7kW	23.2% 13.4kW		
PEMFC B	32.0% 1kW	32.0% 1.3kW	29.0% 1.9kW				
PEMFC C	17.5% 3.4kW	22.0% 4.7kW	24.5% 6.9kW	24.4% 8.9kW			
SOFC A	12.6% 320W	36.9% 370W	45.1% 400W	54.1% 520W	51.4% 1000W		
SOFC B	12.6% 960W	36.9% 1.1kW	45.1% 1.2kW	54.1% 1.5kW	51.4% 3kW		
SOFC C	24.4% 4.6kW	24.2% 4.8kW	24.1% 5.1kW	24.0% 5.3kW	23.8% 5.5kW	23.8% 5.7kW	23.6% 6.1kW

As with thermal efficiency, the Annex 42 model for SE-mCHP power generation during unit warm-up is given as a function of the temperature of the heater engine block, T_H:

$$\dot{W}_H = \dot{W}_{Hmax}\left(\frac{T_H - T_A}{T_{H0} - T_A}\right) \qquad \qquad \textit{Equation 35}$$

For SE-mCHP A, the maximum net power generation, $\dot{W}_{Hmax}$, is 698W. The unit also has an average power consumption of 57.5W for 1500s after fuel supply is ceased (Beausoleil-Morrison, Arndt, et al. 2007).

The other two SE-mCHP units considered are both capable of modulating their output and so it is again more appropriate to model their power output independently of engine temperature, relying instead on interpolation of measured performance points (as per Magri et al. 2012). The potential inaccuracy of this approach is the overestimation of power generation during the unit's warm-up period (Beausoleil-Morrison, Weber, et al. 2007). However, testing of SE-mCHP B demonstrated that it is capable of achieving full power generation within around two minutes and that the overestimation of generation (around 10Wh) which would occur from assuming instantaneous production is almost exactly balanced by the power generation which continues to occur as the unit cools down after fuel supply ceases (Lipp 2012).

4.4.4.2   Heat Pumps

In order to calculate the power demand of the heat pump it is necessary to know its Coefficient of Performance (COP, k_{WQ}) under the conditions it is operating under (primarily the outside air temperature (T_0) and outlet flow temperature (T_X), both measured here in K) at that moment. As it is unlikely that these temperatures will match the temperatures that the unit has been tested under, the COP is calculated by interpolating from the COP measured under test conditions (specified by BS EN14511-2 2007), see Table 3. The interpolation is performed in four stages:

1. Four test conditions fulfilling different criteria are selected; one with a higher outside air temperature, one with a lower outside air temperature, one with a higher outlet flow temperature and one with a lower outlet flow temperature than the modelled conditions at that moment. The test conditions fulfilling each criteria with the lowest summed-square temperature difference (ΔT) to the modelled conditions are selected (see Figure 25). If a test condition meeting one of these criteria is not available, the remaining test condition performances are used.
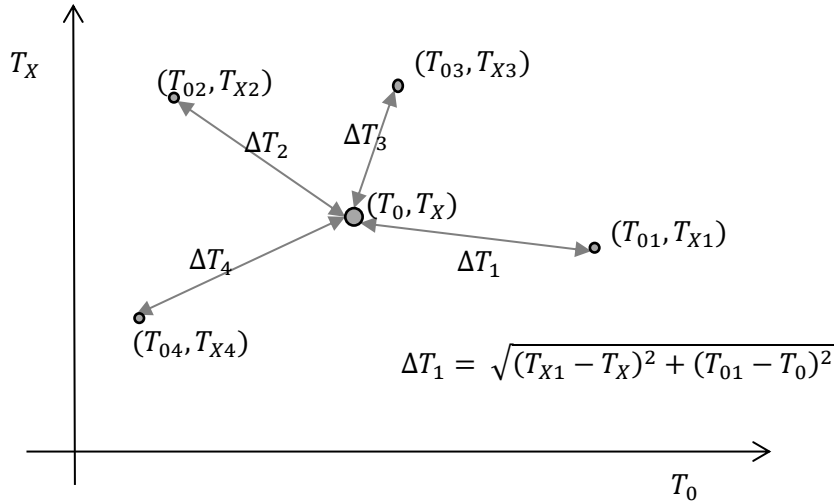
Figure 25: Selection and weighting of test COP measurements

2. The exergy efficiency of the ASHP under each test condition, ψ, is calculated, e.g.:

$$\psi_1 = k_{WQ1}\left(1 - \frac{T_{01}}{T_{X1}}\right)$$

Equation 36

3. The weighted average of these exergy efficiencies is calculated using the summed-squared differences:

$$\overline{\psi} = \frac{\Sigma(\frac{\psi}{\Delta T})}{\Sigma(\frac{1}{\Delta T})}$$

Equation 37

4. The average exergy efficiency is converted back into a COP:

$$k_{WQ} = \overline{\psi}\Big/\left(1 - \frac{T_0}{T_X}\right)$$

Equation 38

By using the exergy efficiency in this way it is possible to more accurately calculate the performance of ASHP units where fewer test measurements are known and extrapolation is therefore necessary. A similar comparison between COP and exergy efficiency is used by Ertesvåg (2011) to study the uncertainty in the performance measurement of ASHPs, concluding that the flow temperature tolerances permitted under testing can result in an error of up to 9% in the recorded COP. A 9% error is significant when attempting to predict the

performance of an individual specific unit but not when considering the range of performances available or the effect of different conditions on the performance of that ASHP.

The part-load efficiency of ASHP compressors is generally slightly higher than their full-load efficiency (Energimyndigheten 2012). This can be seen in specific test results (e.g. Butler & Hyde 2007) and it has been suggested that it may have been exploited to inflate the nominal performance achieved by an ASHP under standard test conditions (Ertesvåg 2011). Bettanini et al. (2003) suggest a modelling approach based upon results obtained from monitoring of the performance of a range of air chillers. A wide range of results are noted; however, the average performance above 40% load factor has a consistent range and an average value close to the full-load performance. Part-load factors are therefore not considered specifically in the model; it is assumed that the majority of the effect (if any) is accounted for in the range of standard test conditions tabulated above.

4.4.4.3   Exergy of power flows

By definition, the energy and exergy flows associated with electrical power flows are the same as each other.

4.4.5   Heating system thermal inertia

The thermal characteristics of the heating units are given in Table 16. For SE-mCHP A and ICE-mCHP A, these are taken directly from the values supplied by Beausoleil-Morrison, Arndt, et al. (2007). For other devices they were estimated from the available data as described below.

In the case of SE-mCHP B, the loss coefficient was selected to be the same as that for SE-mCHP A and then the other coefficients were adjusted in order to replicate the heat flow profile provided by Lipp (2012). A similar process was repeated for SE-mCHP C; heat losses were scaled up and then the thermal efficiency coefficients were determined at the appropriate flow temperatures before thermal inertias were determined by comparison with heat and temperature profiles in Beausoleil-Morrison, Arndt, et al. (2007).

The ICE-mCHP units were slightly harder to calibrate. Because no heat flow profiles relating to ICE-mCHP B could be obtained, the engine block thermal inertia and heat transfer coefficients for it were estimated based upon the properties of ICE-mCHP A. These were scaled by the engine volume for inertia and by the engine cross-sectional area for the heat transfer. For ICE-mCHP C, thermal efficiency coefficients were calculated at the three known operating conditions, based on a lower estimate for the heat loss coefficient than that for ICE-mCHP A as the total efficiency implied would otherwise exceed 100% in some cases. Although heat flow and temperature traces are available (again from Beausoleil-Morrison, Arndt, et al. 2007) there

is clearly internal control occurring as the unit waits until it can provide flow at a reasonable temperature before delivering any heat. This makes it hard to estimate the effective thermal properties. Instead, the engine block thermal inertia has been selected such that the energy content released after fuel flow ceases approximately matches between the model and the data available. Heat exchanger properties similar to those for an ASHP (see below) seem appropriate given the relatively rapid secondary fluctuations in heat delivery which occur.

As noted earlier, the dynamics of FC-mCHP units are dealt with differently by the Annex 42 model. The rate of change of output is usually constrained in these units by their control system to reduce the premature degradation of the stack and so the effect of the thermal inertia of the units on their dynamic behaviour is much less significant. Here, the limits on the rate of change of electrical generation are converted into limits regarding the rate of change of heat generation. Although the Annex 42 model does not take the thermal inertia of the FC-mCHP units into account, large thermal inertias are still used for the FC-mCHP units in this work in order to use a consistent heat flow model in each case. These are notionally based on the actual mass of the units (which would usually provide an upper limit on the effective thermal inertia) but the constraints on the rate of change of the output from the units renders their performance insensitive to this value.

ASHPs typically use plate heat exchangers. The properties of these were based upon the 4.6kg stainless steel heat exchanger used by ASHP B with surrounding structure bringing the total heated mass to around 8kg. At rated output, there is a 2°C temperature drop between the condenser and flow temperature of this device; as the return temperature is 5°C lower than the outlet flow temperature under these conditions, the average temperature difference across the heat exchanger is approximately 4.5°C (Mitsubishi Electric Europe 2008). The effective inertia and heat transfer coefficient for each unit is calculated based upon these conditions, scaled to the rated thermal output of the unit. The structure of ASHPs does not lend itself as well to the two lumped-capacitances model used with the mCHP units; heat transfers occur continuously within the working fluid as it moves around the cycle. However, by using the same thermal inertia and transfer coefficients as the heat exchanger component, the initial transient was found to be around two minutes which is consistent with observations (during defrost cycles, for example). In fact, the sensitivity of the model to variations in the values for the ASHP thermal inertias is limited. Figure 26 shows the effect of varying the thermal inertia of components from 37% to 400% of the values used on the average performance of two ASHPs operating under various conditions. It can be seen that there is little effect on the average performance of the units apart from some (still relatively minor) variation at low inertias.
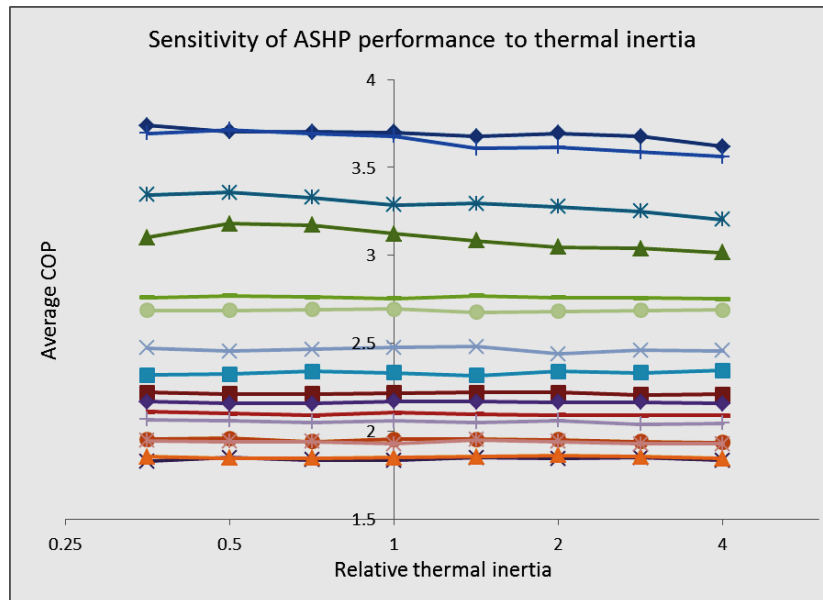
Figure 26: Sensitivity of ASHP model to assumptions regarding thermal inertia (each plot relates to a different ASHP unit).

Similarly, Figure 27 shows the sensitivity of the performance of two of the mCHP models to changes in their thermal inertia, under a range of different conditions. The graph shows that the effect of changing the thermal inertia is negligible in these cases. The sensitivity is lower than in the case of the ASHP units primarily because the nominal inertias are much higher. It should be noted that SE-mCHP A is likely to demonstrate a higher sensitivity given the additional equations governing its energy flows but this is of less concern as its characteristics are taken directly from the detailed calibration described by Beausoleil-Morrison, Arndt, et al. (2007).
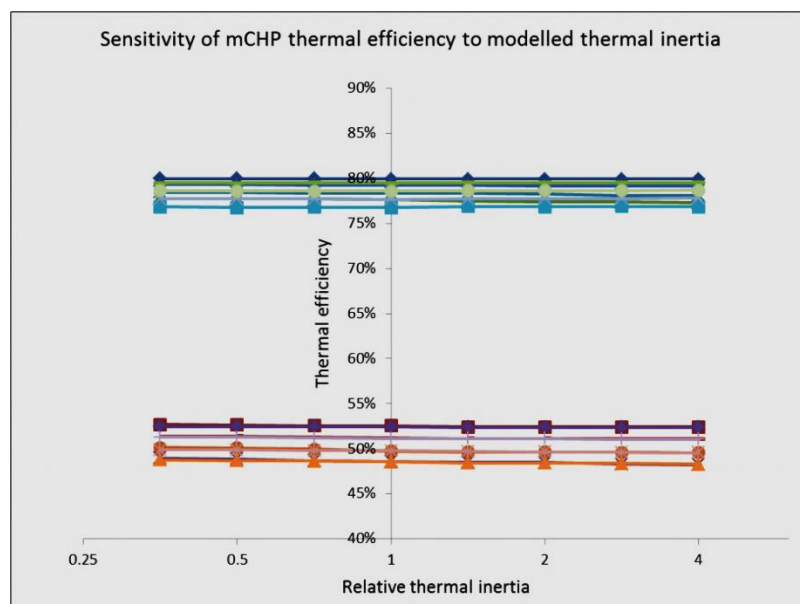
Figure 27: Sensitivity of mCHP model to assumptions regarding thermal inertia (each plot relates to a mCHP unit).

Table 16: Thermal properties of all modelled units

Unit	Heater Block Thermal Inertia $m_H c_H$ J / K	Block to Heat Exchanger Heat Transfer Coefficient k_{HX} W / K	Heat Exchanger Thermal Inertia $m_X c_X$ J / K	Heat Exchanger Heat Transfer Coefficient k_{XE} W / K	Thermal losses coefficient k_{H0} W / K	Heat generation maximum rate of change W / s
ASHP A	2260	890	2260	890	1	N/A
ASHP B	4800	1890	4800	1890	1	N/A
ASHP C	4690	1840	4690	1840	1	N/A
ASHP D	3280	1290	3280	1290	1	N/A
ASHP E	5820	2290	5820	2290	1	N/A
ASHP F	7450	2930	7450	2930	1	N/A
ASHP G	7900	3110	7900	3110	1	N/A
ASHP H	5650	2220	5650	2220	1	N/A
SE- mCHP A	18500	32	28100	1600	4.6	N/A
SE- mCHP B	7000	40	7000	1200	4.5	N/A
SE- mCHP C	30000	220	10000	2000	14	N/A
ICE- mCHP A	63606	741	1000	1600	13.7	N/A
ICE- mCHP B	45000	500	4000	1600	4	N/A
ICE-mCHP C	17906	318	4000	1600	0	N/A
PEMFC A	200000	1200	4800	1150	67	5
PEMFC B	100000	500	4800	500	15	1.6
PEMFC C	200000	250	4800	850	24	5
SOFC A	100000	1000	4800	1600	0	0.06
SOFC B	300000	1000	4800	1600	0	0.17
SOFC C	200000	1000	4800	1600	5	0.4

4.4.6   Heat transfers to heat emitter system and buffer tank

Some heating systems operate with a buffer tank whereas others feed heat directly to the heat emitters. For those with a buffer tank:

$$\dot{Q}_{UE} = (T_U - T_E)k_{UE}$$

Equation 39

if the heating thermostat is open. If the thermostat is closed:

$$\dot{Q}_{UE} = 0$$

Equation 40

where $\dot{Q}_{UE}$ is the heat flow rate from the buffer tank to the to the heat emitters system through heat transfer coefficient k_{UE}. A thermostat turns the supply of heat from the buffer tank to the heat emitters on or off if the temperature of the inside air is less or more (respectively) than the target temperature (taking DSM temperature adjustment into account as appropriate). A dead-band (T_{EC}) of +1K/-1K is used to prevent unstable operation. The temperature of the emitter system is given by:

$$T_{E,i} = T_{E,i-1} + \frac{(\dot{Q}_{UE} - \dot{Q}_{EA})t}{m_E c_E}$$

Equation 41

where the thermal inertia of the emitter system, $m_E c_E$, is based upon an estimated requirement of 14 litres per kW of rated capacity.

The heat flows to the buffer tank are given by:

$$\dot{Q}_{XU} = ((T_X + T_{UX})/2 - T_U)k_{XU}$$

Equation 42

$$\dot{Q}_{UA} = (T_U - T_A)k_{UA}$$

Equation 43

where $\dot{Q}_{XU}$ is the heat flow rate from heater heat exchanger to the buffer tank through heat transfer coefficient k_{XU}. In order to calculate the average temperature differences, it is necessary to know the return temperatures to the heat exchanger (T_{UX}). This is selected as the maximum of either the sink temperature (i.e. T_U) or the flow temperature minus the normal operating temperature difference across the heat exchanger (T_{DX}, taken here to be 5K). $\dot{Q}_{UA}$ is the rate of heat loss from the buffer tank through heat transfer coefficient k_{UA} to the inside air. k_{UA} and k_{XU} are selected to be consistent with the Hot Water Association's Thermal Store Specification (Hot Water Association 2010, p.49).

The temperature of the buffer tank, T_U, is given by:

$$T_{U,i} = T_{U,i-1} + \frac{(\dot{Q}_{XU} + \dot{Q}_{SU} - \dot{Q}_{UE} - \dot{Q}_{UA})t}{m_U c_w}$$

<div style="text-align: right">*Equation 44*</div>

where $\dot{Q}_{SU}$ is any heat generated by a supplementary system and fed to the buffer tank (see section 4.4.2).

For systems without a buffer tank, $\dot{Q}_{XU}$, $\dot{Q}_{UE}$ and $\dot{Q}_{UA}$ are all zero. In this case, the heat transfer to the emitter system ($\dot{Q}_{XE}$) is given by:

$$\dot{Q}_{XE} = ((T_X + T_{EX})/2 - T_E)k_{XE}$$

<div style="text-align: right">*Equation 45*</div>

where the return temperature from the heat emitters to the heater heat exchanger, T_{EX}, is again determined as the maximum of either the emitter temperature (T_E) or the heat exchanger flow temperature (T_X) minus the normal operating temperature difference across it (5K).

Because the systems without buffer tanks use a proportional control system (see section 4.3.4), no thermostat on-off function is necessary.

4.5 Domestic Hot Water Demand

Average Domestic Hot Water (DHW) demand, V_W, is taken to be (Energy Saving Trust 2008):

$$V_W = 40 + 28N_R \qquad\qquad \text{Equation 46}$$

where V_W is measured in litres per day and N_R is the number of occupants in the dwelling.

In the model, the 28 litres per person component is assumed to be distributed throughout the day with the weightings in Figure 28 multiplied by the active occupancy at that time. The additional 40 litres are assumed to be spread equally across the 24 hours.
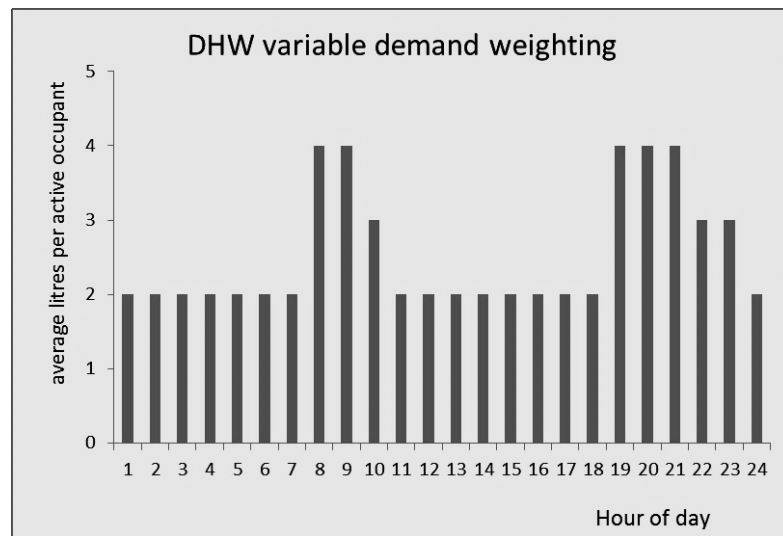
Figure 28: DHW demand weighting

The heat balance for the DHW tank is given by:

$$T_{W,i} = T_{W,i-1} + \frac{(\dot{Q}_{XW} - \dot{Q}_{WR} - \dot{Q}_{WA})t}{m_W c_W} \qquad\qquad \text{Equation 47}$$

where $T_{W,i}$ is the tank temperature at time i, $\dot{Q}_{XW}$ is rate of heat delivered to the tank, $\dot{Q}_{WR}$ is the rate of thermal energy leaving the DHW tank in hot water drawn by residents and $\dot{Q}_{WA}$ is the rate of heat loss from the tank to the inside air. $m_W c_W$ is the thermal inertia of the tank (i.e. product of the mass of water and the specific heat capacity of water, J/K). Variation in the size of the DHW tanks was not considered in this study; all DHW tanks were assumed to contain 70kg of water.

The heat flows are calculated as follows:

$$\dot{Q}_{XW} = ((T_X + T_{WX})/2 - T_W)k_{XW} \qquad \text{Equation 48}$$

where T_X is the heating system outlet flow temperature and T_{WX} is the return temperature. The return temperature is found as the maximum of either the tank temperature or the outlet flow temperature minus the normal temperature difference across the heat exchanger (T_{DX}, 5K by default). The DHW tank heat exchanger coefficient, k_{XW}, is taken to be 550W/K, consistent with the minimum in the Hot Water Association's Thermal Store Specification (Hot Water Association 2010).

$$\dot{Q}_{WR} = (T_W - T_{0W})\dot{m}_W c_W \qquad \text{Equation 49}$$

where $\dot{m}_W$ is the rate of DHW demand in kg/s. Cold water inlet temperature, T_C, is taken to be 10°C.

$$\dot{Q}_{WA} = (T_W - T_A)k_{WA} \qquad \text{Equation 50}$$

The heat loss from the DHW tanks, k_{WA}, is taken to be equivalent to 2.8W/K consistent with the same Thermal Store Specification (Hot Water Association 2010).

4.6 Grid model

4.6.1   Overview

The grid model has two main functions that are carried out during each time period:

- Iterate the "price" signal in order to adjust net demand, aiming for certain objectives.

- Calculate the generation from each type of generating plant (e.g. coal or gas) that is used to supply the demand due to the operation of the heating systems. Two sets of figures are derived; firstly using a methodology to calculate generation using the mean mix and, secondly, with a methodology using the marginal mix. For the mean generation mix, the mix of generation types meeting the demand is assumed to be the same as the total generation mix during that period. For the marginal generation mix, the change in the electricity generated from each plant type due to heating system demands is calculated, assuming the generation mix supplying all heating systems is the same.

These generation totals are given by:

$$W_{LH} = \sum_{i=1}^{n} \dot{W}_{GH,i} \frac{\dot{W}_{L,i}}{\dot{W}_{G,i}} t \qquad \text{Equation 51}$$

$$W_{LD} = \sum_{i=1}^{n} \dot{W}_{GH,i} \frac{\Delta \dot{W}_{L,i}}{\Delta \dot{W}_{G,i}} t \qquad \text{Equation 52}$$

where W_{LH} is total generation (in J) from plant type L, calculated with the mean generation methodology and W_{LD} is the corresponding total with the marginal methodology. $\dot{W}_{GH,i}$ is the power generation (in W) required to satisfy the heating power demand, $\dot{W}_{G,i}$ is the total power generation and $\dot{W}_{L,i}$ is the power generation by plant type L, during time period, i,

The total generation from each generating plant type (using both the "marginal" and the "mean" methodologies) is then used to calculate the PER, exergy and CO_2 emissions associated with the operation of the heating system. This is in contrast to calculating and recording the impacts across all the generating plants during each time-step and then summing them. This calculation order is used as it facilitates the consideration of additional environmental impacts or different emissions rates which are known for each generating plant type. Additional environmental impacts (e.g. metal resources depletion) have been considered in collaborative work using results based upon this model (McKenna et al. 2013).

4.6.2   Price Iteration

To model the implications of DSM signals on the performance and power flows associated with the heating systems, it is necessary to generate a realistic signal that will, in turn, be affected by the resulting changes in power demands. Rather than use a direct control signal (i.e. associated with a hypothetical system in which loads are directly, centrally, controlled), this model assumes that a signal representing the grid operators' intention that demands should reduce is used. Different systems such as heating can then react as appropriate to this signal. This signal is referred to here as "price" as it will follow the same approximate pattern as a price signal but it is stressed that the model does not represent actual prices, rather the relative strength that any such signal would need to take in one time period relative to another.

The model attempts to set a price which maximises the "profit" for the grid operator for that time period. This is calculated based upon the "cost" (to the operator) of electricity, the "price" to the consumer and the electrical demand during that time period. The maximum "profit" per unit of electricity is limited to prevent a situation where the overall maximum profit is achieved by combining a very high price and consequent low demand (in reality such a situation could occur if there was neither regulation nor a competitive market). For any given power demand, a representative cost to the grid operators can be calculated based upon factors such as the total dispatchable power demand at that time, the rate of change in dispatchable power demand, fuel and CO_2 emissions costs and local network power distribution constraints. These cost functions will be specific to the scenarios being simulated. The demand response to changes in price is described in section 4.3.3 above, but it is sufficient here to note that the magnitude of the effect will increase in some way as price increases (see Figure 29). This means that for the set of conditions during a particular time-period, there will be an optimum "price" that can be associated with achieving certain DSM objectives, expressed as the "cost" function.
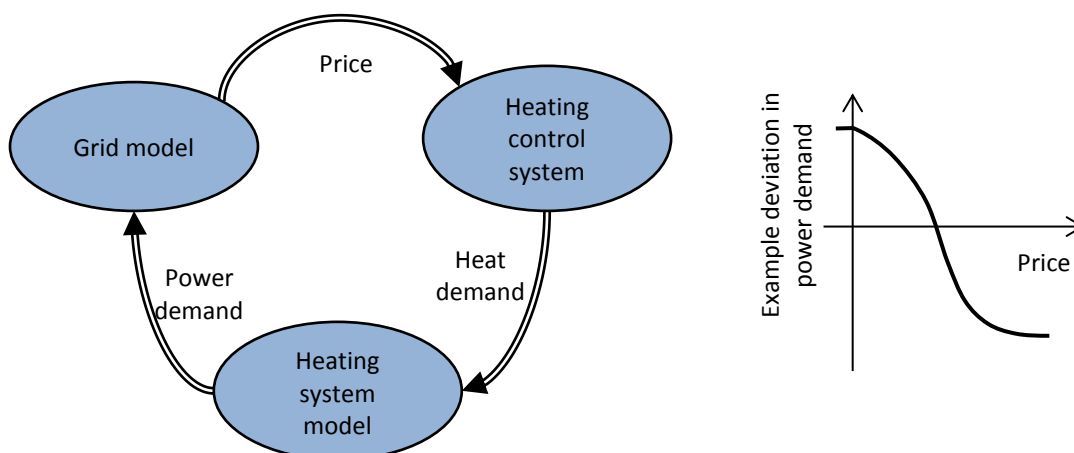

Figure 29: Iteration to determine price / power demand

Iterations are used within the time-period to determine this optimum "price" and the power demand associated with it:

- An initial price is assumed. For each dwelling, the occupants will have a particular reaction to the price of electricity in terms of the temperature that they would like their dwelling to be maintained at. For example, in some cases the occupants will be relative flexible and might accept a 2°C decrease in the target temperature if electricity is expensive while others might be less flexible (see section 4.3.1).

- Depending upon the other conditions associated with the dwelling during that time period and the control parameters relevant to the dwelling, a hypothetical heat demand is generated. The heating system signals a hypothetical power demand (potentially negative in the case of mCHP) relating to that heat demand but also constrained by the heating system performance.

- The sum of the hypothetical power demands from the heating systems of the population of dwellings being considered is fed back and the consequent cost and profit are calculated.

- The price signal is adjusted to attempt to improve the profit and the iteration is repeated.

Several iterative methods were tried. It was surprisingly problematic to find a method which worked consistently, reliably and efficiently. A bisection method is used (requiring 12 steps to achieve reasonable accuracy). The gradient of profit against price for each proposed price (and that price plus a small increase) is used to determine whether that price represents the minimum or maximum bound for the next bisection.

4.6.3   Grid generation scenarios

In performing these functions, the grid model can use either current UK grid generation data or a dispatch model that considers the situation for a hypothetical mix of generation plant. In this study, the hypothetical grid generation mixes which were considered were those proposed by the Transition Pathways project (Foxon 2013; Foxon et al. 2010). The Transition Pathways project provides three hypothetical scenarios (based on three sets of assumptions regarding the development of the grid). Detail on the sources of generation and demand for each of the three scenarios is provided for intervals between the present and 2050 (see Table 18, page 118).

The "Seven Year Statement" (National Grid Plc 2011) provides perhaps the best indication of proposed changes to generation plant capacity (used by Hawkes (2010) to estimate future MEFs) but does not indicate how the generating companies may change their dispatch patterns

and does not suggest the generation mix which may be in operation beyond 2020 so cannot be used to investigate the effect of more radical changes to the grid.

Several scenarios are available from other projects. Some are broader and consider the electrical grid within the context of the whole energy system but do not cover the detail required for considering specifics of electrical dispatch (DECC 2009b; 2010a). Other scenarios include more detail (Ault et al. 2008; Jardine & Ault 2008) but the categories used within the Transition Pathways descriptions are more convenient for adaptation to this model. Other work considering the potential effect of DSM has used the context of the Transition Pathways scenarios so their selection also facilitated comparison with these studies (Pudjianto et al. 2013; Barton et al. 2013). Finally, the accessibility of colleagues working on the Transitions Pathways project made it easier to identify and clarify the assumptions made.

Electrical losses were applied in calculating the generation required to supply a particular demand using Equation 53.

$$\dot{W}_{G,i} = \dot{W}_{S,i}/(1 - \mathrm{k}_{GS}) \hspace{3cm} \textit{Equation 53}$$

where $\dot{W}_{G,i}$ is the generation required to supply a demand of $\dot{W}_{S,i}$. The fraction of electricity lost, k_{GS}, is taken to be 7.0% for consideration of the current grid (DECC 2011) and is given as 7.4% for the future hypothetical grid considered (Foxon 2013). Electrical losses occur primarily (74%) in the distribution system, with 22% occurring in the transmission system and non-technical losses such as meter theft accounting for the remaining 4%.

Of the electricity generated in 2010, 4.13% was used by the electricity industry (excluding the 1.28% of electricity used for pumping in pumped storage systems) (DECC, 2011 Table 5.6). This consumption is accounted for by using the "net" electricity generated for each plant type in Table 8 and Table 5.

4.6.4   Carbon emissions factors

The generation totals from each type of generating plant are used with carbon emissions factors for each plant type to calculate the total CO_2 emissions. The mass of CO_2 emissions resulting from the generation of electricity to supply the heating system, C_{GH}, (in kg) is calculated as the sum (across the types of generating plant) of the products of the generation required and the emissions factor for that generation type ($\left[\frac{\dot{c}}{\dot{W}}\right]_L$). For the average mix assumption, that is:

$$C_{GH} = \sum_L \left[\frac{\dot{C}}{\dot{W}}\right]_L W_{LH}$$

<div align="right">Equation 54</div>

For the CO_2 emissions based upon the marginal mix assumption (C_{GD}), the appropriate generation (W_{LD}) is used (instead of W_{LH}).

4.6.5 Energy and exergy requirements

Mean energy (H_{GH}) and exergy (E_{GH}) requirements are calculated in a similar way to carbon emissions, but considering the average energy requirement for energy of each plant type (Table 5) and the ratios between the enthalpy and exergy content of fuels given in Table 6, respectively. For the average mix assumption, these are calculated as:

$$H_{GH} = \sum_L W_{LH} / \eta_L$$

<div align="right">Equation 55</div>

$$E_{GH} = \sum_L \phi_L W_{LH} / \eta_L$$

<div align="right">Equation 56</div>

For the marginal mix assumption, the appropriate generation (W_{LD}) is used to calculate the energy (H_{GD}) and exergy (E_{GD}) requirements.

4.6.6 Historic UK grid generation mix

Historic data on generation in the UK is made available by Elexon (2012). This consists of generation totals (in MW) for each type of generation plant, measured every five minutes. Data for 2009, 2010 and 2011 is used; three years are used to decrease the effect of anomalies (e.g. Sizewell B was closed for 6 months in 2010). Generation data for just under 0.3% of the time-steps was either missing or discarded because of either an irregular timestamp or unreported generation data. The missing generation totals for these time-steps (typically in the order of an hour at a time) were reconstructed by linear interpolation from the nearest known generation totals. Some small generating units are omitted from the balancing mechanism reports and so are not included in these data (e.g. small scale wind) but these units are not considered dispatchable and are unlikely to affect the results.

Considering the historical case (in this case, data are for 2009), illustrated in Figure 30; as total electrical demand increases, the share of this demand being met by generation from coal power plants increases. This resulted in a higher *mean* carbon emissions factor (CEF) for electricity generated at times when demand was higher but a higher *marginal* carbon emissions factor

(MEF) when demand is mid-range (corresponding to a higher gradient for the coal generation plot at these times).
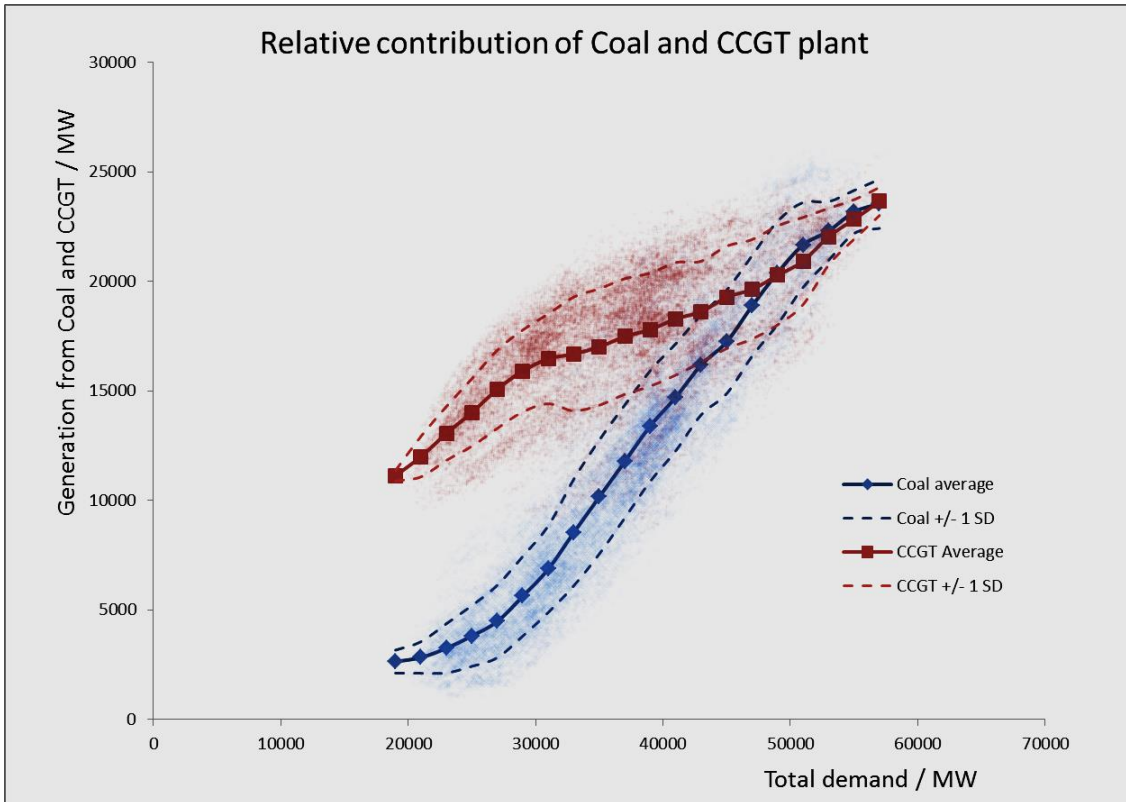

Figure 30: Relative contribution from coal and gas generating plant to meet demand, 30 minute periods through 2009. Data from Elexon 2012

4.6.6.1 Generating plant responsiveness

The gradients of the average plots in Figure 30 are the average responsivenesses of coal plant and CCGT plant. That is, the ratios between the changes in generation from each plant type and the total change in generation. Notably, the responsiveness of coal plant is higher for the middle range of total electrical demands. This may be due to a combination of factors such as the relatively slow ramp rate of coal plant, the need to maintain some flexibility and the variation in the relative costs of the fuels. However, it is clear that these responsivenesses are not constant with time and accurate calculation of the associated marginal emissions factors and primary energy requirements will therefore need to take this variation into account.

For each time period, the responsiveness of each generating plant type was calculated as the change in generation from that plant type divided by the change in total generation over the same period. Overall, these ratios will indicate the extent to which each generating plant type is used to meet changes in electrical demand. However, at times there will be uncharacteristically high or low responsiveness for particular plant types due to generating companies switching

from one plant type to another (e.g. for operational reasons). If total generation increases only very slightly but a CCGT plant is ramped up to replace a coal fired plant, the apparent responsiveness of the CCGT plant would be very high for that period. To compensate for this effect, the average responsiveness across several time periods is calculated, weighted according to the absolute value of the total change in generation in each time period, Equation 57:

$$\overline{\left(\frac{\Delta \dot{W}_L}{\Delta \dot{W}_G}\right)_S} = \sum_{i=1}^{S}\left[\left(\frac{\Delta \dot{W}_{L,i}}{\Delta \dot{W}_{G,i}}\right)\frac{|\Delta \dot{W}_{G,i}|}{\sum_{j=1}^{n}|\Delta \dot{W}_{G,j}|}\right]$$

Equation 57

where $\overline{\left(\frac{\Delta \dot{W}_L}{\Delta \dot{W}_G}\right)_S}$ is the weighted average responsiveness of plant type L for the set of time-periods i, in S. $\Delta \dot{W}_{L,i}$ is the change in power generated by generating plant type L and $\Delta \dot{W}_{G,i}$ is the change in total power generation in the same period. $\sum_{j=1}^{n}|\Delta \dot{W}_{G,j}|$ is the sum of the absolute value of all changes in total generation. For this study, the sets of time periods used were grouped according to the total generation demand at each time. The range of generation demands within each group was varied to ensure a comparable number of data points within each group. The resulting weighted average responsiveness figures are presented in Table 17 and Figure 31.
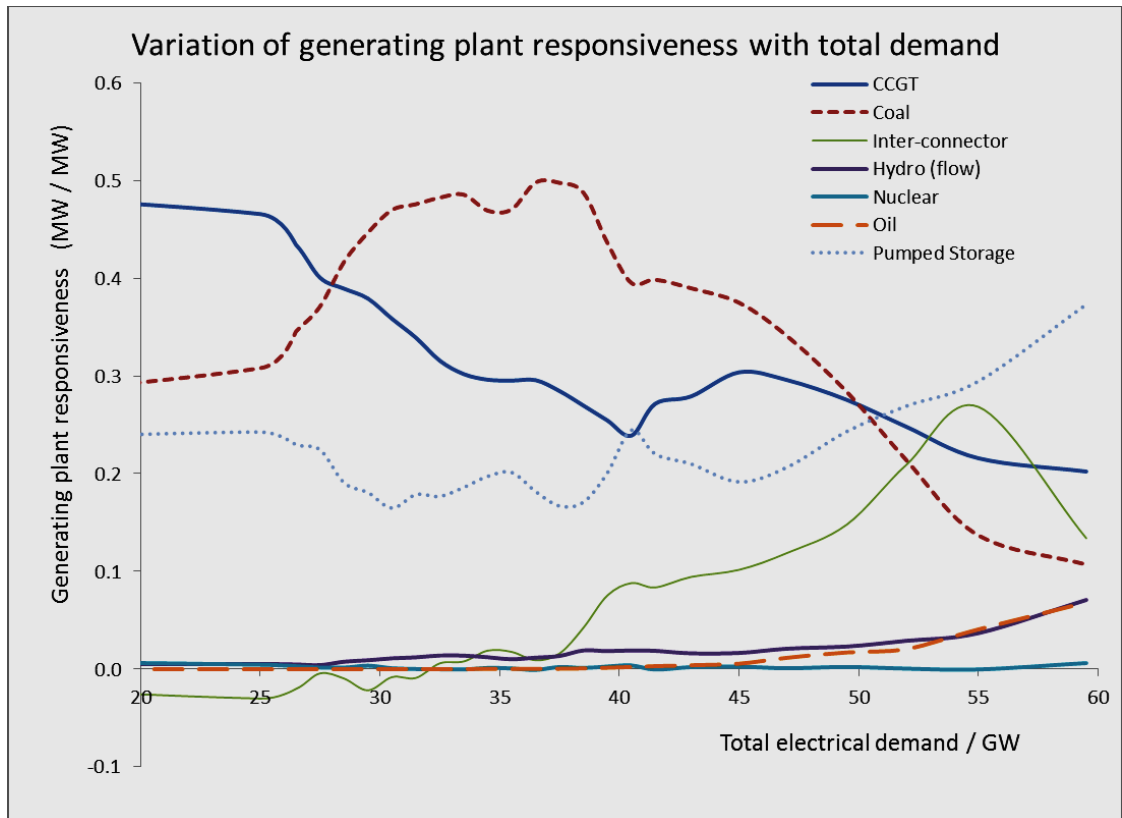

Figure 31: Variation of plant responsiveness with total demand, 5 minute periods

Table 17: Current responsiveness of different generating plant types to changes in demand (grouped by total demand)

Generation demand range / GW		Weighted average responsiveness of generating plant types (MW / MW)						
min	max	CCGT	Coal	Inter-connector	Hydro (flow)	Nuclear	Oil	Pumped storage
18.0	24.0	0.505	0.247	-0.004	0.005	0.012	0.000	0.226
24.0	26.0	0.466	0.308	-0.030	0.005	0.005	0.000	0.243
26.0	27.0	0.434	0.346	-0.020	0.005	0.003	0.000	0.230
27.0	28.0	0.400	0.371	-0.004	0.004	0.002	0.000	0.224
28.0	29.0	0.389	0.417	-0.010	0.008	0.002	0.000	0.191
29.0	30.0	0.379	0.447	-0.022	0.009	0.004	0.000	0.181
30.0	31.0	0.359	0.470	-0.008	0.011	0.001	0.000	0.165
31.0	32.0	0.339	0.476	-0.009	0.012	0.000	0.000	0.179
32.0	33.0	0.316	0.482	0.006	0.014	0.000	0.000	0.177
33.0	34.0	0.302	0.485	0.008	0.014	0.000	0.000	0.186
34.0	35.0	0.296	0.469	0.019	0.012	0.001	0.000	0.197
35.0	36.0	0.295	0.470	0.018	0.010	0.001	0.000	0.201
36.0	37.0	0.296	0.498	0.009	0.012	-0.001	0.000	0.182
37.0	38.0	0.285	0.498	0.016	0.014	0.002	0.000	0.167
38.0	39.0	0.270	0.487	0.043	0.019	0.001	0.001	0.171
39.0	40.0	0.254	0.436	0.075	0.018	0.003	0.001	0.201
40.0	41.0	0.239	0.395	0.088	0.019	0.004	0.002	0.245
41.0	42.0	0.272	0.398	0.084	0.019	0.000	0.003	0.220
42.0	44.0	0.279	0.390	0.094	0.016	0.002	0.004	0.210
44.0	46.0	0.304	0.375	0.102	0.017	0.003	0.006	0.192
46.0	48.0	0.296	0.341	0.119	0.021	0.001	0.012	0.207
48.0	51.0	0.276	0.284	0.148	0.023	0.002	0.017	0.243
51.0	53.0	0.248	0.213	0.209	0.029	0.001	0.021	0.269
53.0	57.0	0.216	0.137	0.268	0.037	0.000	0.041	0.295
57.0	62.0	0.202	0.107	0.134	0.071	0.006	0.068	0.373

This shows a general trend for the responsiveness of CCGT plant to reduce as total electrical demand increases with the responsiveness of coal-fired plant increasing to a peak at around 35 – 40GW total demand before decreasing. Pumped storage shows a reasonably high responsiveness across the range of total electrical demands. However, the overall supply from and to pumped storage is relatively low, it is likely that this responsiveness is due to the way in which the grid is balanced rather than representing a longer term response to changes in demand. Hawkes (2010) accounts for this effect by attributing the supply from pumped storage to the plant mix used to store electricity. Here, a simpler method is used; the responsiveness values are normalised such that their sum (i.e. the total responsiveness) is always one, see Figure 32.
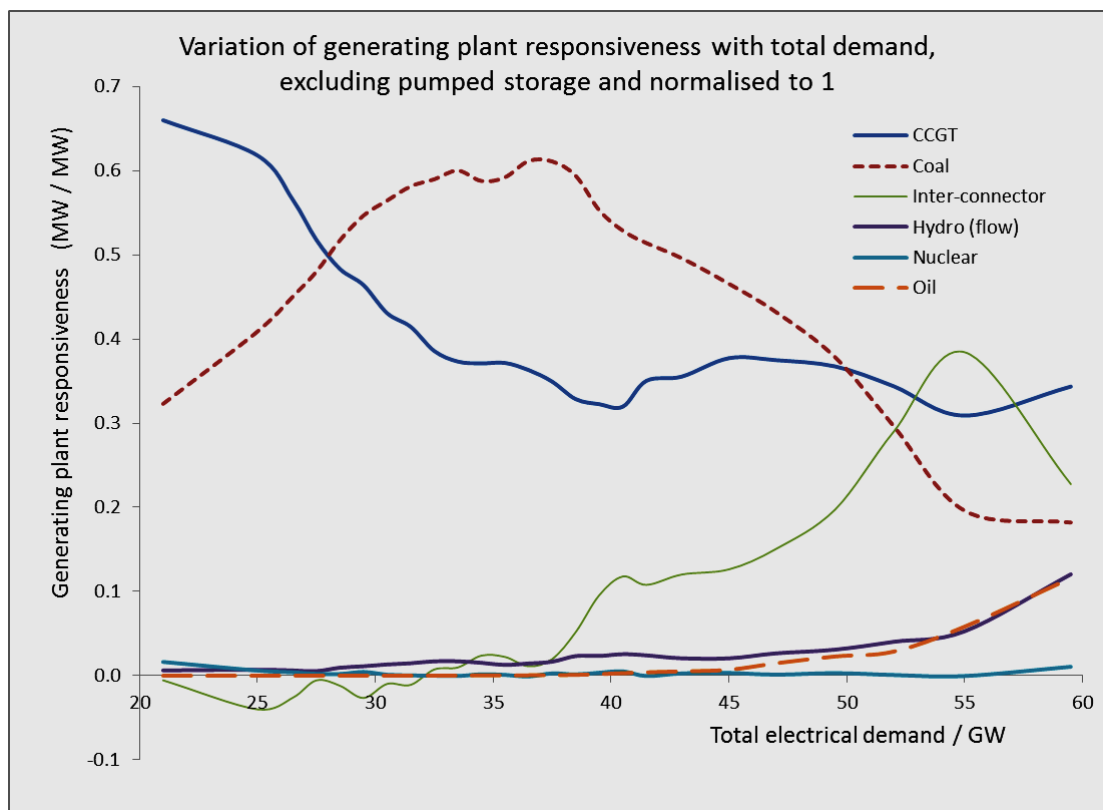

Figure 32: Variation in plant responsiveness, excluding pumped storage and normalised to unity.

4.6.7 Hypothetical dispatch model

To consider alternative grid mixes, a hypothetical dispatch model is required. The dispatch model used takes a modified merit order approach, similar to the FESA model (Barton et al. 2013; Barnacle et al. 2013).

4.6.7.1   Calculating total generation demand

Firstly, the total required generation for that time period ($\dot{W}_{G,i}$) is calculated. This is calculated as the sum of the generation required to supply the demand at that time. In this study, three demands are considered; that from electric heating ($\dot{W}_{GH,i}$), electric vehicle (EV) charging ($\dot{W}_{GV,i}$) and that other uses of electricity ($\dot{W}_{GM,i}$).

$$\dot{W}_{G,i} = \dot{W}_{GH,i} + \dot{W}_{GV,i} + \dot{W}_{GM,i} \qquad\qquad \textit{Equation 58}$$

Electric heating demand is calculated as the sum of the heating power demand across all dwellings. The associated generation requirement is calculated from demand by taking transmission and distribution (T&D) losses into account.

$$\dot{W}_{GH,i} = \left(\Sigma \dot{W}_H\right)_i / (1 - \mathrm{k}_{GS}) \qquad\qquad \textit{Equation 59}$$

where $\left(\Sigma \dot{W}_H\right)_i$ is the sum (across the population of dwellings) of heating system power demands during time period i and k_{GS} is the fraction of electricity generated which is lost during transmission and distribution.

Although it is not a focus of this study, EV charging demand is considered separately as there is clear rationale to assume that it will follow a daily profile which is different from that of historic generation demands. In this study, it is assumed to follow the daily profile which is shown in Figure 33. The peak charging level is calculated such that the total EV charging demand through the year corresponds with the scenario being considered. The real charging profile will, of course, vary dynamically but this profile is considered to provide a good compromise which takes the change in the overall shape of the demand profile into some consideration without excessive complication. Transmission and distribution losses are taken into account in the same way as for heating.
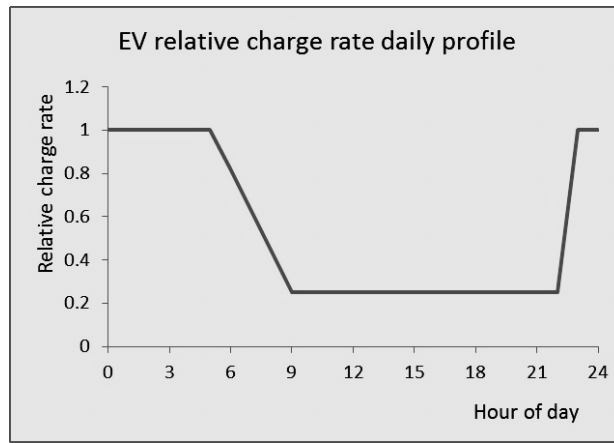
Figure 33: Assumed EV daily charging profile

The generation required to meet other demands ($\dot{W}_{GM}$) is assumed to follow the same pattern as present (i.e. 2009 - 2011) generation ($\dot{W}_{GP}$).

$$\dot{W}_{GM,i} = \mathrm{k}_{PM}\dot{W}_{GP,i}$$

Equation 60

The factor, k_{PM}, is the ratio of modelled future generation (excluding heating and EV) to current generation:

$$\mathrm{k}_{PM} = \left(\sum_{i=1}^{n} \dot{W}_{G,i} - \Sigma\dot{W}_{GH} - \sum_{i=1}^{n} \dot{W}_{GV,i}\right)/\sum_{i=1}^{n} \dot{W}_{GP}$$

Equation 61

where the yearly totals (e.g. $\sum_{i=1}^{n} \dot{W}_{G,i}$) are given in the scenario. Note that $\Sigma\dot{W}_{GH}$ is the total generation demand due to heating which is predicted in the scenario that the model uses, not the amount which is actually calculated by the model. The yearly totals for the Transition Pathways scenarios are presented in Table 18.

Table 18: Electricity generation and demand in Transition Pathways scenarios. Data from Foxon et al. 2008; Foxon 2012.

Supply / Demand	Scenario (totals given in TWh/yr)								
	MR2020	MR2035	MR2050	TF2020	TF2035	TF2050	CC2020	CC2035	CC2050
Nuclear	48.85	88.75	125.07	21.87	21.61	19.69	53.38	118.37	146.38
Hydro	5.57	5.57	5.57	5.57	5.57	5.57	5.57	5.57	5.57
Tidal & Wave	3.42	29.78	29.78	2.4	24	24	2.4	24	24
Wind	50.37	112.11	170.96	44.68	63.07	84.1	57.82	86.72	115.63
Connector	20.6	23.58	20.64	21.18	21.79	14.63	19.91	25.59	21.09
CHP	28.12	28.22	28.34	73.23	130.96	134.63	28.8	28.86	28.89
Biomass	9.93	7.37	5.73	9.04	3.8	2.37	9.04	6.08	4.66
Coal CCS	18.16	81.3	84.34	15.76	21.07	11.86	15.77	31.54	31.18
Gas CCS	0	87.3	84.34	0	24.36	12.78	0	89.35	63.3
CCGT	144.24	23.74	0.77	82.83	0	0	118.22	0	0
Coal	68.60	0.00	0.00	49.96	0	0	62.48	0	0
Generation *exc. pumped storage*	397.86	487.72	555.54	326.52	316.23	309.63	373.39	416.08	440.7
Supply (after T&D losses)	369.61	450.22	511.64	309.4	308.4	309.5	347.9	392	409.5
E heating demand	32.42	60.58	73.47	12.7	13.3	12.7	29.1	52.2	59.9
E Vehicle demand	2.33	22.58	37.78	2.1	33.9	37.4	2.2	29.4	32.8

4.6.7.2   How generation demand is satisfied

A modified merit-order dispatch model is assumed:

A. Generation from nuclear and hydro are assumed to follow the same pattern as present, scaled to match the totals in the scenario. An example of historic output from nuclear power plants (in January 2009) is given in Figure 34.
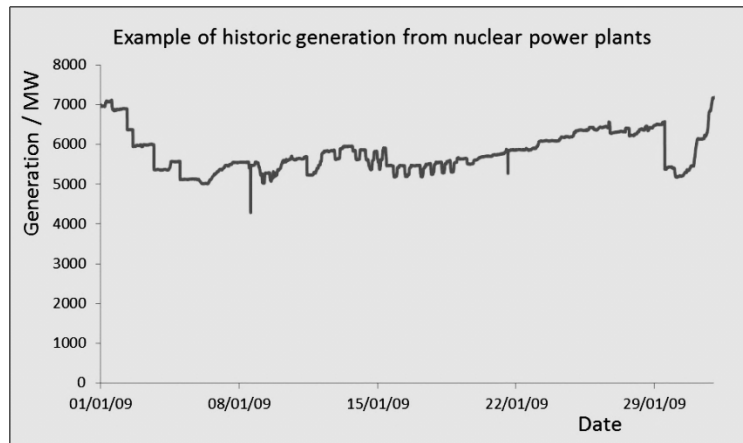
Figure 34: Example of historic generation from nuclear power plants. Data from Elexon 2012.

B. Tidal generation is assumed to follow a sinusoidal pattern, varying with an amplitude of 25% over a 28 day period and with an amplitude of 100% over a 12.4 hour period.

C. Wind generation is modelled using algorithms developed by Sturt (Sturt & Strbac 2011; Sturt 2011) for the purpose of assessing the balancing requirements that the intermittency associated with wind generation brings. The model is designed to capture both the short term transitional characteristics as well as the longer term statistical parameters of the aggregate output of wind farms across the UK. It takes into account the varied generating patterns which are likely with a mix of on-shore and off-shore wind farms. The model uses a second-order auto-regressive function with time-steps (here) of 30 minutes. Different parameters are used to calibrate the model for each season. The model produces "wind generation factors". The total output is calculated as the product of these factors and the total wind farm generation capacity. This capacity is sized to match the total wind output in the scenario. An example of the output from the model is given in Figure 35.
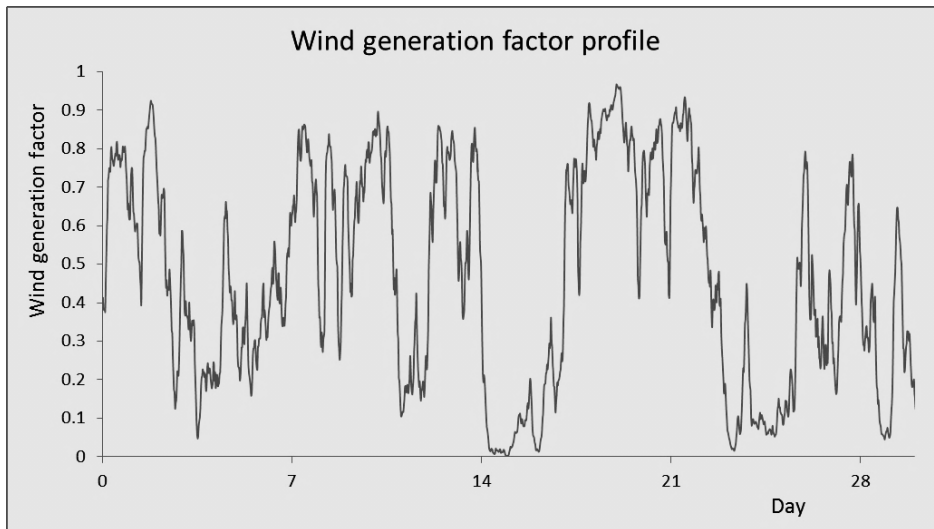
Figure 35: Example of modelled wind generation profile (model by Sturt 2011)

D. Interconnectors are assumed to export electricity when dispatchable generation (i.e. excluding nuclear, hydro, tidal and wind in this case) would otherwise be less than 3GW so that some control is maintained. If export would exceed the interconnector capacity then generation is constrained. If the required dispatchable generation is more than 3GW then the interconnector imports a fraction of this power. The fraction is fixed and selected so that the total net imports match the scenario.

E. Unless constrained, generation from CHP is assumed to be from large scale industrial applications and follows a diurnal sinusoidal output, varying by +/- 25%.

F. Generation from biomass is assumed to contribute a fraction of demand remaining after these generators, up to its maximum capacity.

G. Generation from coal plant with carbon capture and storage (CCS) is assumed to form a fraction of remaining demand (typically 50% but adjusted to fit total Coal CCS generation in the scenario). When generating at above 75% of total generating capacity, the fraction is reduced (typically to around 25%), up to the maximum plant capacity.

H. Gas CCS plant is assumed to follow a similar pattern, taking the remaining generation demand.

I. Gas CCGT plant without CCS meets the remaining demand (i.e. when the CCS plant is operating at above 75% generating capacity).

Using this hypothetical grid, the marginal contribution from each plant type to meet a particular change in demand is calculated as the difference between their generation calculated with and without the additional generation to meet that demand. However, for comparison with Figure

31, the variation in the plant responsivenesses for the hypothetical grid model is shown in Figure 36.
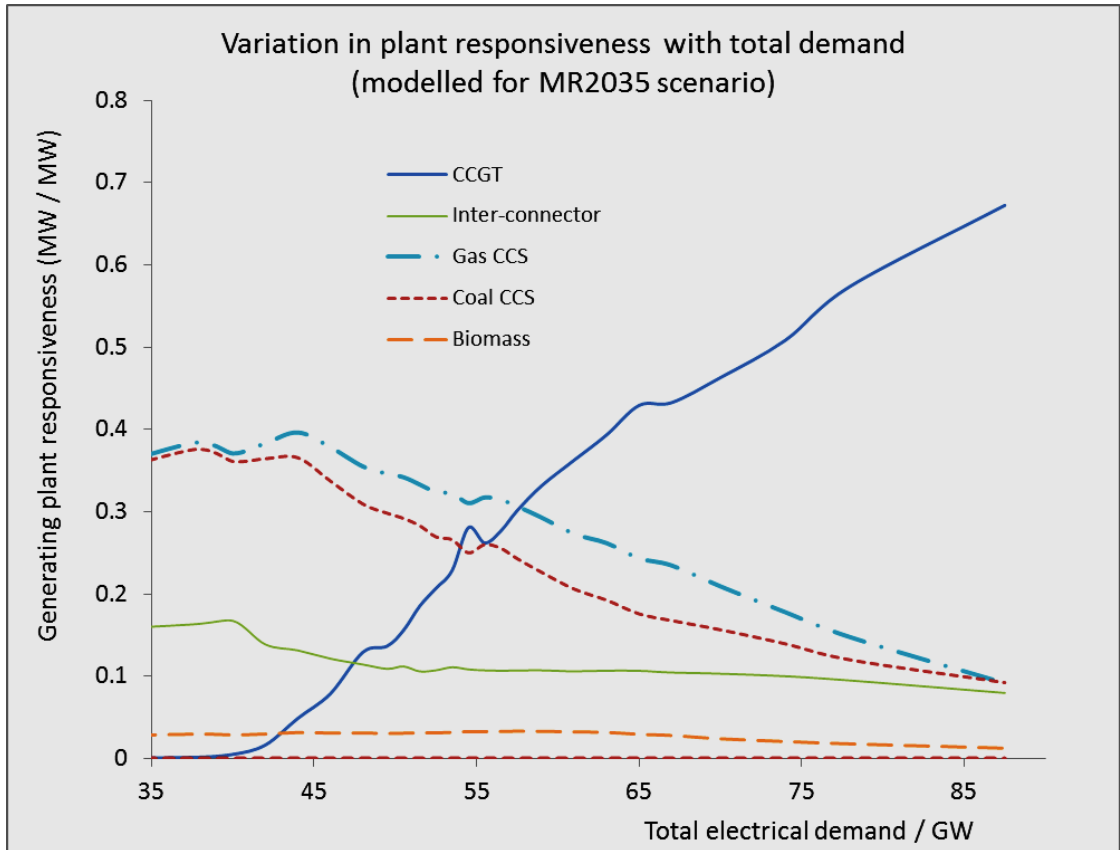

Figure 36: Variation in plant responsiveness with total demand (modelled for MR2035 scenario)

4.7 Occupancy and Appliance models

The CREST Active occupancy model has been adopted (Richardson et al. 2008). Because the implementation of the model which is available (in VBA) is for a single day and a single dwelling, it was necessary to adapt it. Rather than generating a use pattern for the whole day for each appliance in turn, the status of each appliance is modelled and then the model moves to the next time-step.

4.7.1   Active Occupancy model

This uses "Transition probability matrices". Two matrices are used for each possible number of residents in a dwelling (i.e. one to five in this case); one for days in the weekend and one for days in the week. Each matrix describes the probability, during each 10-minute period, of moving from a current number of active occupants to each of the other possible numbers of active occupants. Once every 10 minutes, for each dwelling, these probabilities are used with a random number generator to select a transition to a new number of active occupants.
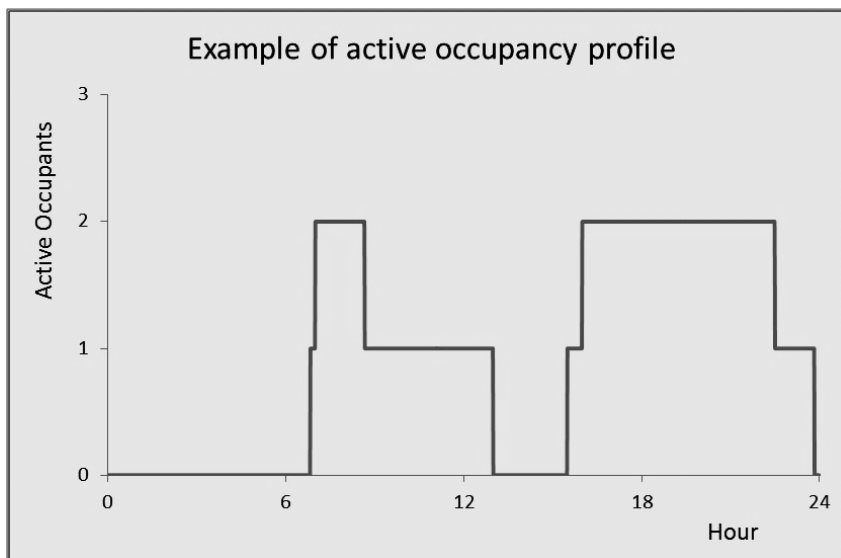

Figure 37: Example of active occupancy profile. Modelled by Richardson et al. (2008)

The heat gains from the occupants, $\dot{Q}_{RA}$, are calculated by assuming that each active occupant generates 147W of heat and that each dormant occupant generates 84W of heat (i.e. 1.4 met and 0.8 met, respectively, over an assumed body area of $1.8m^2$ (ISO 2005)). It is assumed that there are no dormant occupants between 06:00 and 21:00. Between 21:00 and 06:00, it is assumed that the number of dormant occupants is the total number of residents minus any who are active.

4.7.2   Appliance model

Appliances are assigned to each dwelling based on a probability distribution for each type of appliance. Different operating regimes are available to determine their on-off characteristics of each appliance:

- Most appliances have a probability of starting that is dependent upon the probability of an activity happening. This is in turn dependent upon the active occupancy in the dwelling and is calculated in a similar way.

- Appliances such as fridges operate on a fixed cycle of a period of operation and then a period of inactivity.

The length of time for which the appliance will operate is determined when it is turned on. If the active occupancy falls to zero while it is "on", the operation of appliances which generally involve user interaction is effectively paused. Most appliances have fixed operating and standby power consumptions, the exceptions are washing machines and tumble dryers which have a predefined cycle that determines variations in power demand.

Lighting is based on a set of bulbs for each dwelling. For each time period when a given irradiance threshold is met, there is a probability distribution for each bulb turning on which is also a function of the number of active occupants. At the time that it is turned on, the duration for which it will be illuminated is determined from another probability distribution.

Electric storage heaters and bar heaters are included as a possible appliance in the CREST model but are excluded from this model as each heating system is modelled separately in more detail. Heat gains from appliance operation are based upon the electrical consumption of the appliance scaled by a factor depending upon an estimate of the heat which remains within the building (e.g.100% for light bulbs and TVs, 20% for dish washers and washing machines).

Graphs of typical power demand profiles over a 48 hour period for a single dwelling, 12 dwellings and 140 dwellings are given in Figure 38:
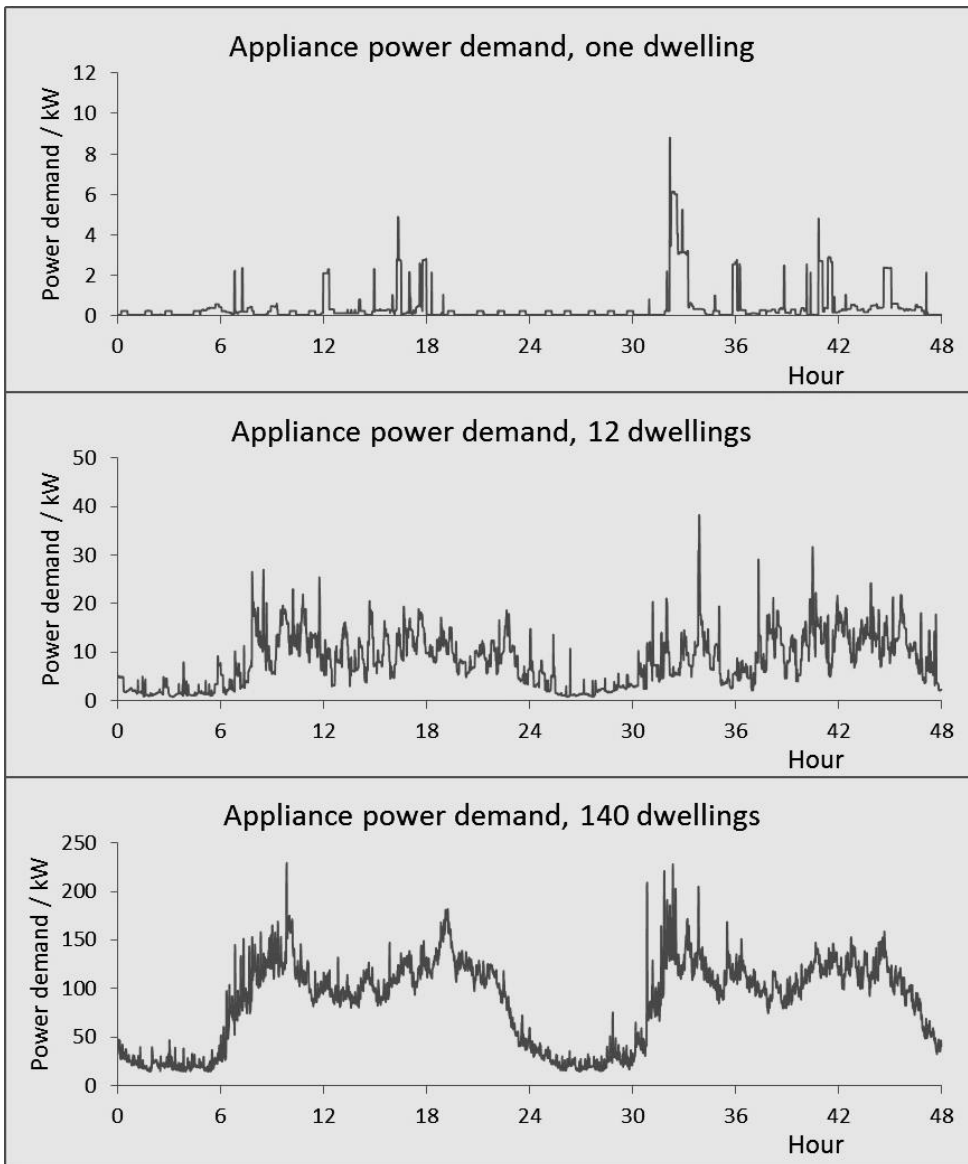
Figure 38: Example electrical demands for dwellings over 48 hour period.

4.8 Climate

4.8.1 Background to climate data for building simulation

Several sources of climate data were used during the development of the model. Initially, actual metrological recorded data was used. This is appropriate when studying the measured heat demand at a specific location but does not provide any indication of how typical that demand might be. International Weather for Energy Calculations data (ASHRAE 2001) was therefore used for earlier studies (Cooper et al. 2011b). These data were generated by selecting typical data from a set of DATSAV3 hourly weather data collected between 1982 and 1999.

More recently, probabilistic models of UK future climate have been made available; as the UK Climate Projections 2009, UKCP09, (Jones et al. 2009; DEFRA 2009). This has been used to generate Test Reference Year (TRY) climate data for various UK locations, at different levels of probability under medium and high emissions scenarios under the "PROMETHEUS" project (Eames et al. 2010). The TRY data consists of the "average" month selected from each set of 30 years. The data was selected to provide representative temperature and solar irradiation data, matching the overall means but also the hour by hour variance that is typical. This means that TRY data is suitable for assessing the average heating requirements in a building but not for assessing the extreme demands that may occur. Although the datasets contain information on other parameters such as wind speed, it is possible that these aspects of the data are not as representative.

The use of modelled future climate data to consider the effect of climate change on building and heating performance has some precedent. Kharseh et al. (2011) investigated the effect of linear temperature increases for Sweden, Syria and Saudi Arabia (i.e. considerable cooling loads) on the performance of a GSHP, plotting the conditions under which average power consumption increases and decreases. Jenkins et al. (2008) study of ASHP performance relating to an office block used TRY data, adapted using morphing algorithms to match the parameters suggested in 2002 by the UK Climate Impacts Program (Belcher et al. 2005). However, more recent work (for example, Jenkins et al. 2011) has tended to use the PROMETHEUS datasets based on the UKCP09 model.

4.8.2 Climate data used in this study

Given the potential discrepancy in results from using different datasets (Bhandari et al. 2012), these datasets are used for all of the modelling in this study, not just those relating to future conditions. Datasets for four UK locations (Cardiff, Leicester, Central London and Glasgow) were selected (see Figure 39). These have been selected as representative of inland and coastal

locations with a range of latitudes. The datasets relating to the medium emissions scenario ("a1b") and the 50% (median) probability level were selected. The air temperature variation throughout the year is shown in Figure 40 for Heathrow modelled in the period 1961 – 1990 and 2020 – 2049.
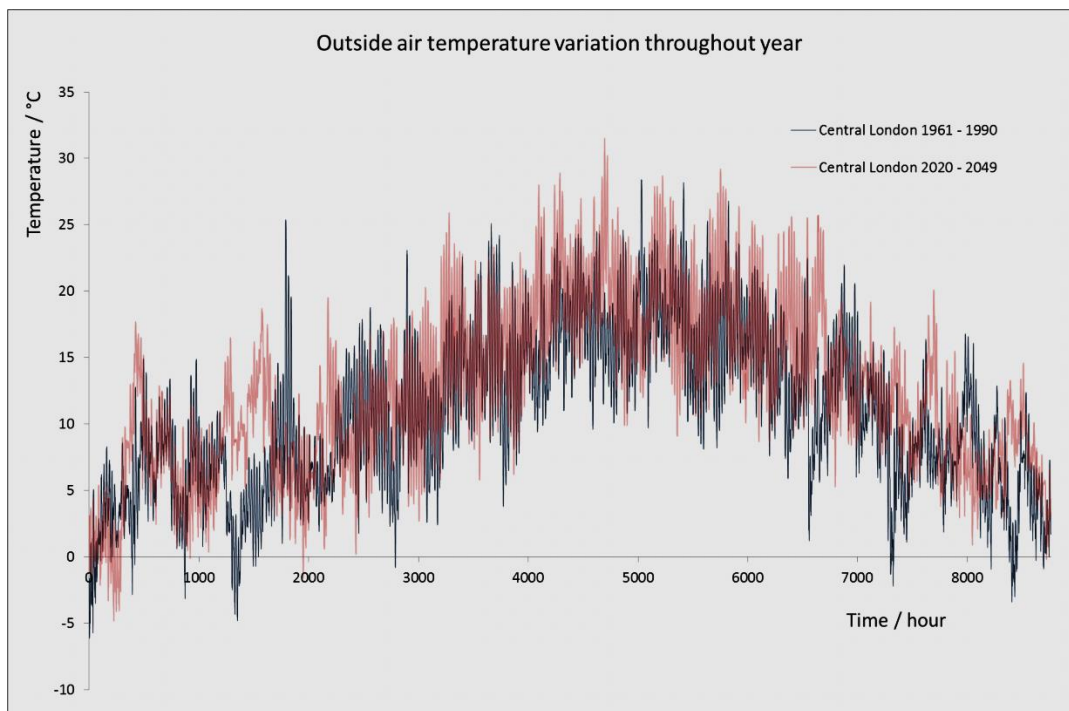

Figure 39: Climate locations selected

Figure 40: Typical outside air temperature variation throughout year for Central London

Within the model, the values for outside air temperature and solar irradiation are calculated by linear interpolation between the two adjacent hourly values. The hourly values are offset by a

random time of up to 10 minutes in order to simulate some of the variance which might occur over a neighbourhood.

If an additional solar PV system were to be added to the model, it would be necessary to add additional stochastic variation to the irradiance profile if minute by minute changes in generation are to be captured (e.g. to study net local electrical demand as per Richardson & Thomson, 2012) .

4.9 Implementation of model

4.9.1 Use of Visual Basic for Applications

The model was written using Microsoft Excel 2010 Visual Basic for Applications (VBA). VBA was selected for several reasons:

- Earlier models were created in Excel and so it was a natural progression from automating some processes using VBA through to implementing the main functions using it.

- Easy input / output streams. Keeping all data on the spreadsheet facilitated rapid development and verification that functions were operating correctly.

- Compatibility with other models. Several of the component models already used VBA (e.g. the occupancy model).

- Functional accessibility. Given the large user base for Excel, there are fewer barriers to others using or continuing development of the model.

- Sufficient support for objects to enable them to be used to represent each sub-system. This makes the structure of the code easier to read and more logical.

To facilitate any future addition of modules (for example a solar PV system), all calls to functions relating to individual dwellings are made by the dwelling class rather than directly from the main procedure or from other objects relating to that dwelling. For example, the "dwelling" object calls the "target heat generation" function from the "heating control" object and then passes this as an argument to the "heating system" object, rather than the "heating system" object calling it directly.

4.9.2   Verification of implementation

In addition to selecting appropriate models for the various components of the systems being simulated, it is necessary to confirm that they have been correctly implemented. Several sets of results are presented in this subsection to demonstrate that the outputs from the implementation of the model appear to be as they should be.

Figure 41 shows the profiles of the outside air temperature, the programme temperature, inside air temperature and building fabric temperature. In this case, the heating is disabled and there are no internal gains. Two profiles for the outside air temperature are shown, one from the input outside air temperature file and one after processing by the model; they are identical, demonstrating that the outside air temperature data is being correctly handled. Similarly, the temperature programme profile is as specified. The inside air and building fabric temperature profiles lag the outside air temperature profile as expected, with the inside air temperature remaining slightly lower and responding slightly quicker when the two are distinguishable.
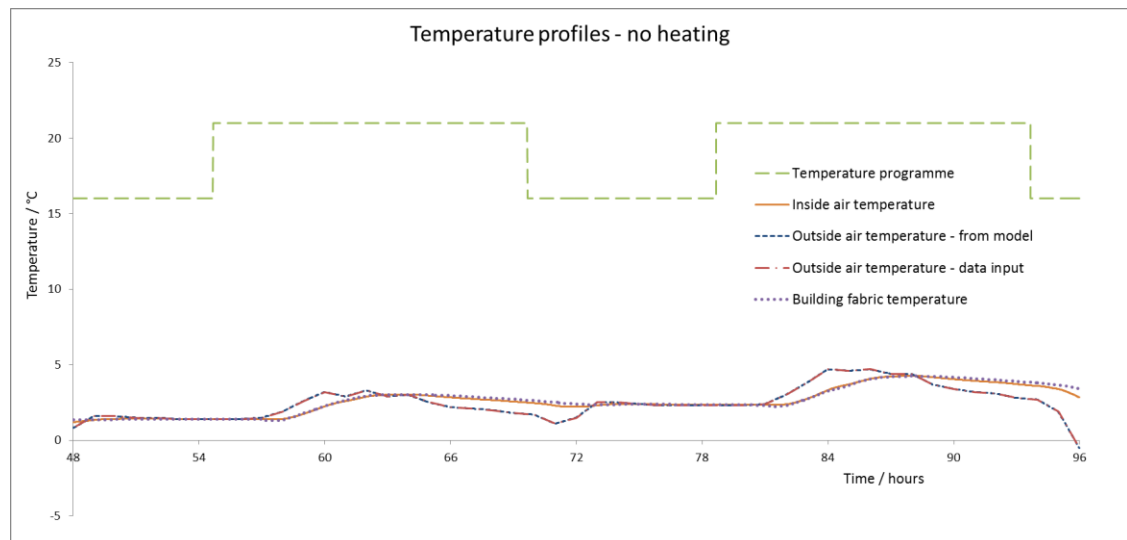

Figure 41: Temperature profiles, no heating

Figure 42 shows the temperature profiles for the inside air, the heater heat exchanger and the building fabric along with the power consumed by an ASHP ("B" in this case) and the rate of heat generated by it. In this case, the target heat generation control is replaced with a function which linearly ramps the target heat generation from 0kW to 12kW over the first 24hr (i.e. hour 48 to hour 72) and then ramps it back to 0kW over the next 24hr. DHW consumption is disabled. The minimum heat generation, eight modulation steps and maximum heat generation can be observed to match the specification of the heat pump. The electrical power consumption follows the general profile of the heat generation but increase as the heater heat exchanger temperature increases or the outside air temperature decreases. The temperature of the heat

exchanger responds rapidly to the increasing rate of heat generation but the thermal inertia of the heat emitter system is sufficient to smooth out the steps. The inside air temperature responds slightly slower and demonstrates further smoothing. The inside air achieves a maximum temperature of around 30°C just over three hours after the ASHP starts generating heat at it maximum capacity. This is around 40°C lower than the heater heat exchanger which is consistent with the steady-state heat transfer rates which should be expected.
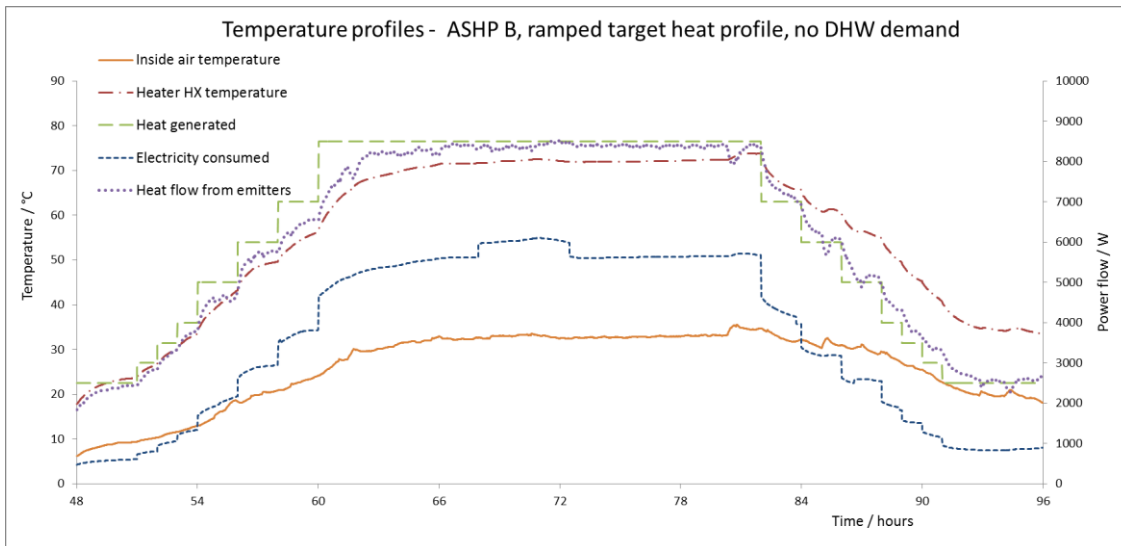
Figure 42: Temperature and energy flow profiles, ramped heat demand

Figure 43 shows similar results obtained with ASHP A with DHW demand included. The smooth ramp in heat generation can be observed (i.e. reflecting the fact that the unit is capable of continuous modulation) along with the higher (10kW) maximum thermal output of the unit, resulting in slightly higher maximum heat exchanger and inside air temperatures. Until around hour 52, DHW heating takes priority until the upper bound of its desired tank temperature is reached. The system switches to "DHW-only" heating twice more before the temperature of the heat exchanger is hot enough (around hour 60) that heat transfer to the room and to the DHW tank occur simultaneously. Whenever heat is directed entirely to heating DHW, the heat delivered by the emitters decreases and the heat exchanger temperature subsequently increases. The COP of the unit at peak power output is around 2.5, consistent with the high flow temperature which occurs during this operation.
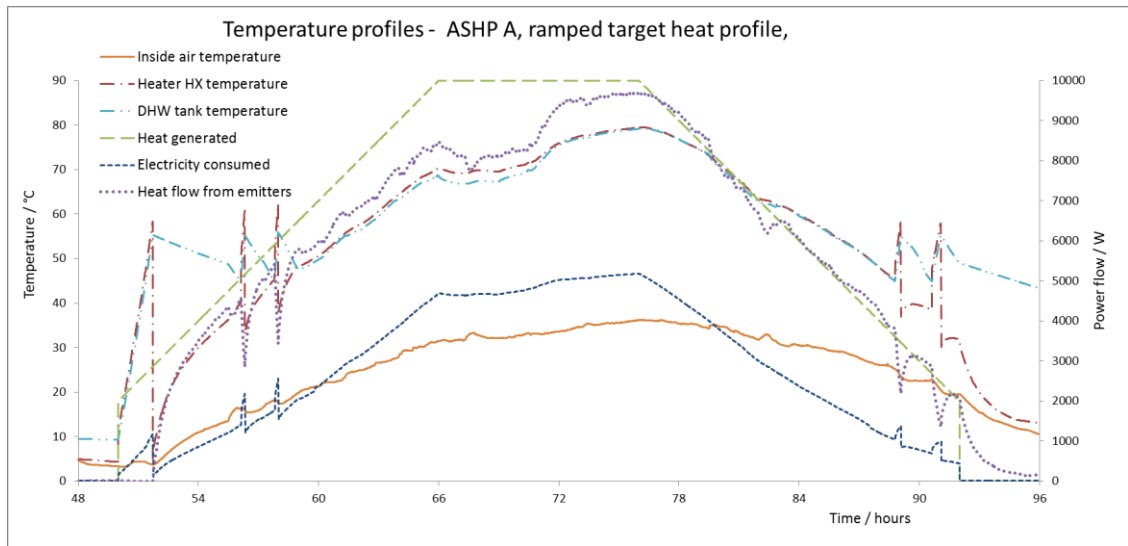
Figure 43: Temperature and energy flow profiles, ramped heat control with DHW

In Figure 44 and Figure 45, results are shown for the ASHP when it is operated in a more representative fashion, maintaining a temperature profile of 21°C during the day and 16°C at night. Under these conditions, the unit switches to heating the DHW tank several times, as expected, and reasonable air temperatures and heat exchanger temperatures are observed. The electrical demand profile is consistent with the heat generated and the known performance of the unit at these approximate conditions. The unit appears to switch to DHW heating at appropriate points, during which heat is directed away from the heat emitters. The unit achieves a typical COP of just more than 3, accurately reflecting the lower flow temperatures which it needs to supply.
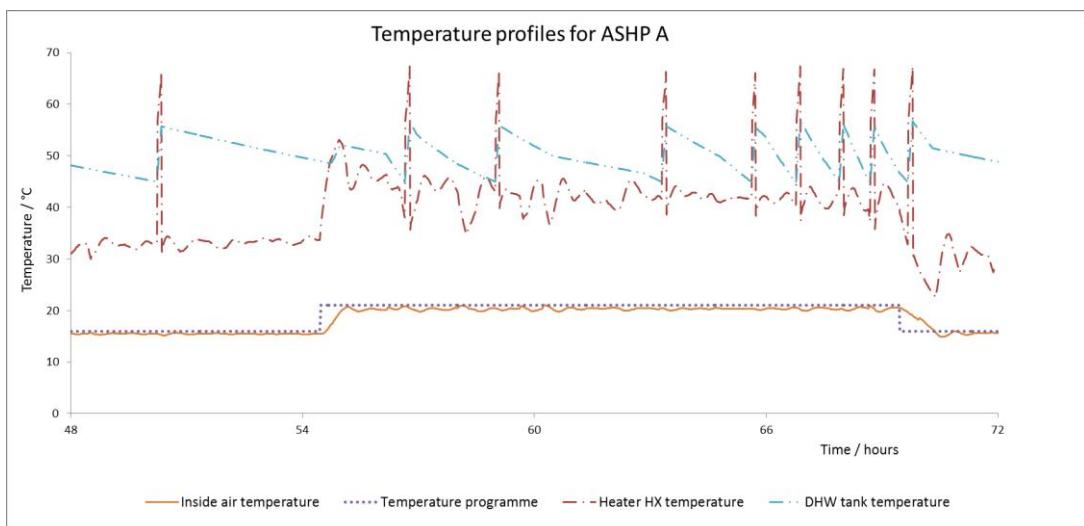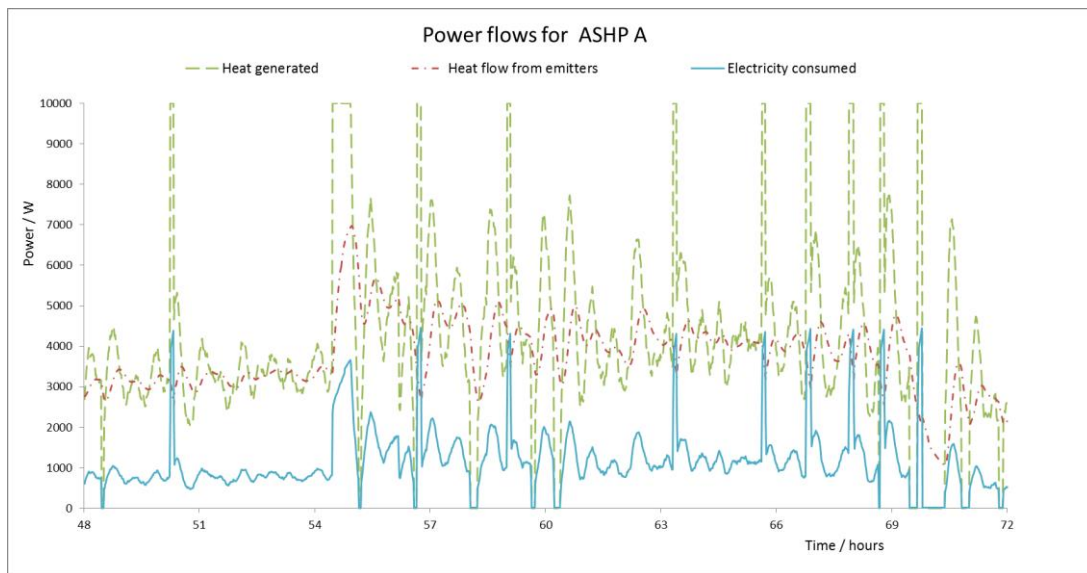

Figure 44: Example temperature profiles associated with ASHP A

Figure 45: Example heat and power flows associated with operation of ASHP

Figure 46 and Figure 47 show equivalent results for the same conditions but with a 160kg buffer tank installed. The temperature of the buffer tank is typically 3°C lower than heat exchanger when it's being heated before dropping to around the same temperature when the heat flow between them is reduced. Exponential heating and cooling curves are discernable in the buffer tank temperature profile, with the heating occurring more rapidly. Because the buffer tank is used with on-off flow control to maintain room temperature, the air temperature can be observed to cycle above and below the programme set point within the 2°C deadband specified for it. As might be expected, the buffer tank results in fewer, longer cycles in which typically the unit completely shuts off for a period. An initial "spike" in the rate of heat delivery from the buffer tank to the emitters can be seen to occur and can be attributed to the initially high temperature difference between the buffer tank and emitter system / inside air. The rate of heat delivered then decreases as the flow temperature drops before stabilising as the ASHP brings the buffer tank temperature back up.
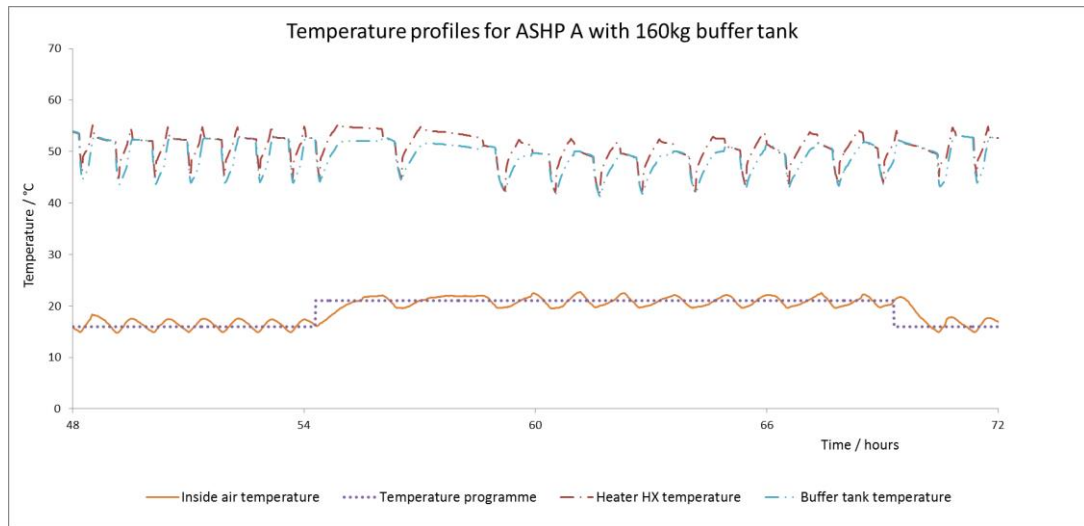
Figure 46: Example temperature profile with ASHP and buffer tank
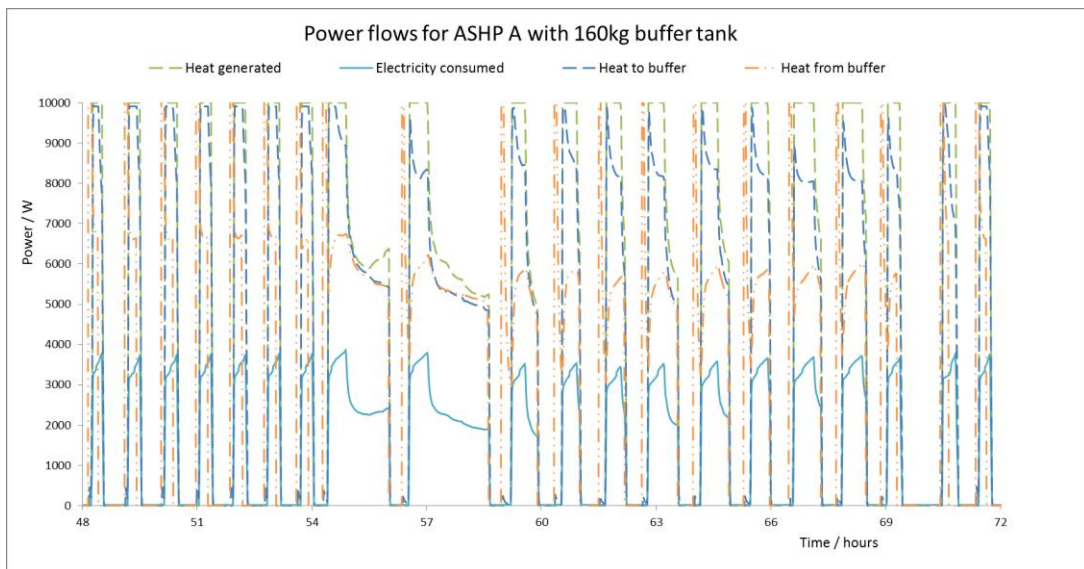

Figure 47: Example heat and power flows with ASHP and buffer tank

Equivalent profiles are shown in Figure 48, Figure 49, Figure 50 and Figure 51 for SE-mCHP B without and then with a 160kg buffer tank. Similar characteristics can be observed but with generation (i.e. negative consumption) of electricity. As with the ASHP, the introduction of the buffer tank leads to fewer, longer cycles.
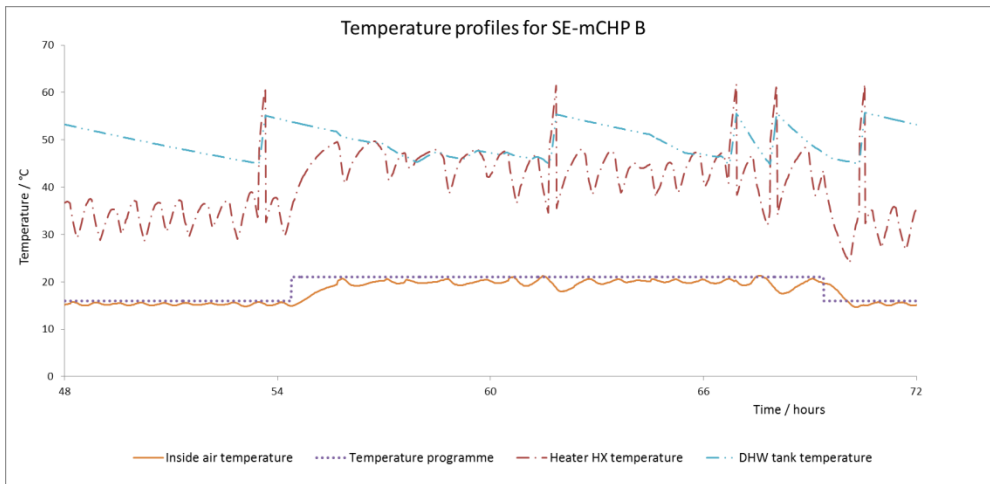
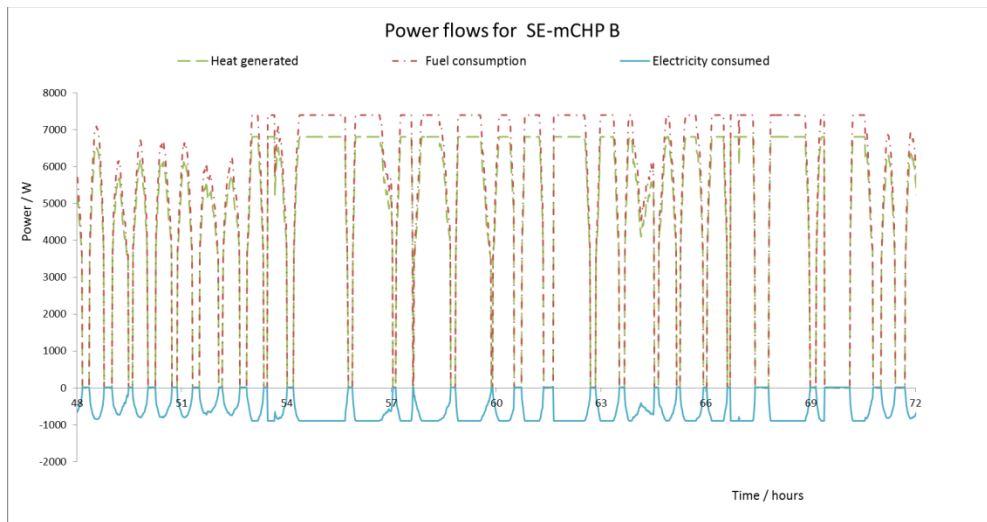*Figure 48: Example temperature profiles for SE-mCHP B*

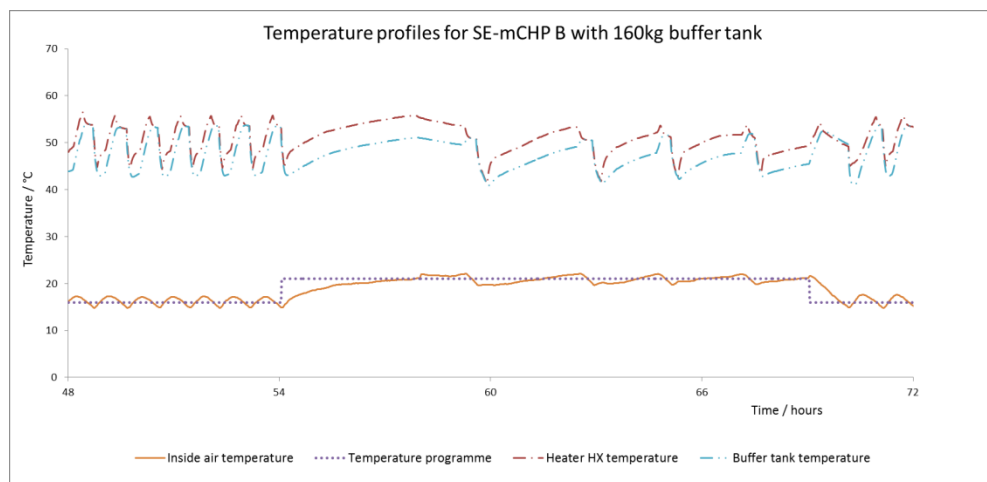*Figure 49: Example heat and power flows for SE-mCHP B*

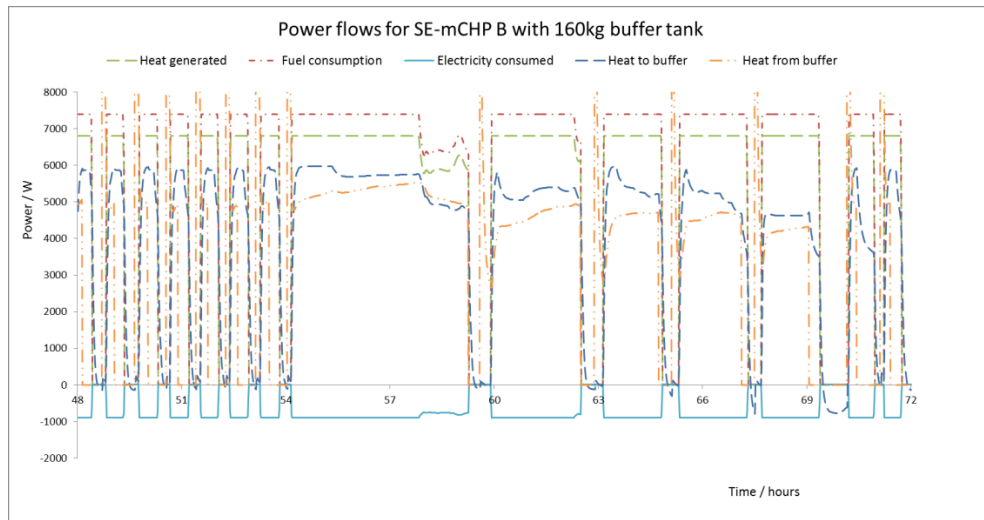*Figure 50: Example temperature profiles for SE-mCHP with buffer tank*

Figure 51: Example heat and power flows for SE-mCHP with buffer tank

Figure 52 and Figure 53 show the equivalent data for SOFC-mCHP A. This is operated continually around its peak electrical efficiency and a supplementary burner is employed to satisfy the additional heat demand. The operation of the supplementary burner and its fuel consumption are consistent.
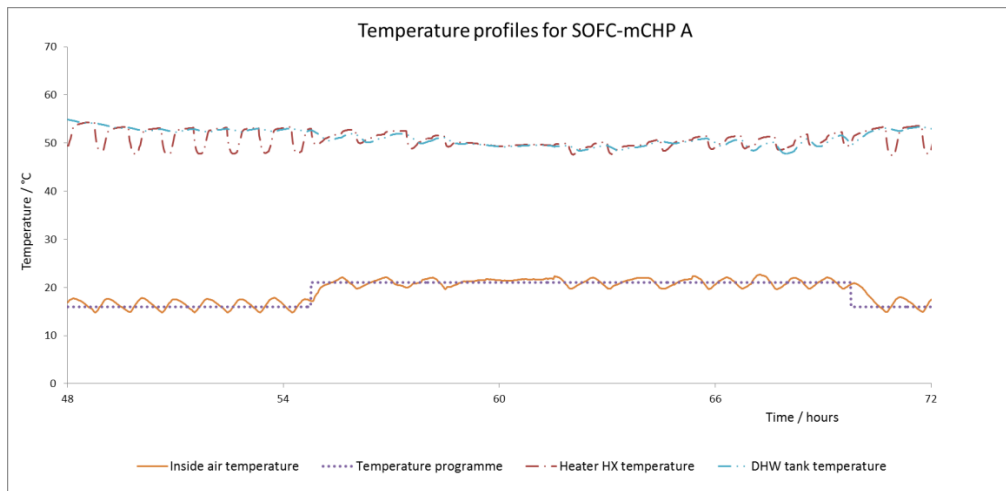

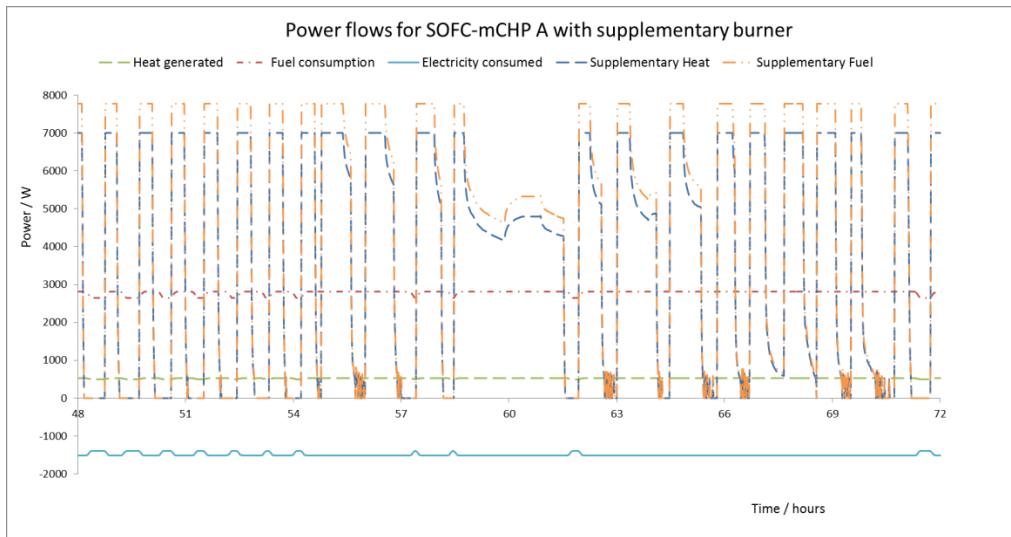*Figure 52: Example temperature profile for SOFC-mCHP A*

Figure 53: Example heat and power flows for SOFC-mCHP A

Active occupancy and appliance consumption models have been taken with relatively little modification. Typical profiles for two resident and four resident houses are given Figure 54 and Figure 55. These show the correct number of occupancy levels with transitions at times which might be expected. Baseline appliance use (i.e. fridges and freezers) can be observed with additional appliance use mainly dependent upon occupancy patterns.
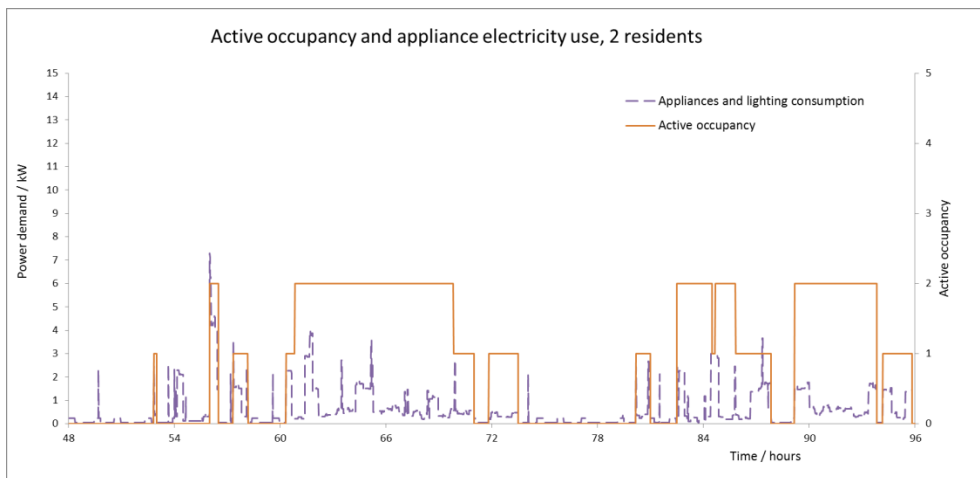

Figure 54: Example of active occupancy and appliance electrical demand for house with two residents
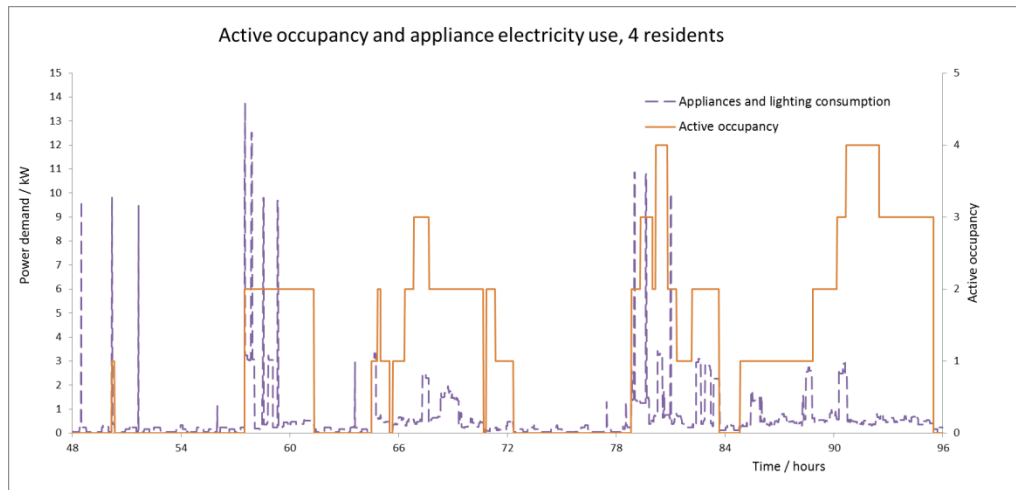
Figure 55: Example of active occupancy and appliance electrical demand for house with four residents

The sum of appliance power demand across 128 dwellings is shown in Figure 56 along with the power demands for the same period if ASHPs are fitted in all dwellings. The diversity which occurs demonstrates that the model generates separate profiles for otherwise identical dwellings and sums them correctly. Temperature profiles are shown for one house in the neighbourhood for the same time period in Figure 57. The "cost" and "price" profiles match the general shape of the electrical demand profile and can be seen to correspond directly to adjustments in the target temperature profile relative to the original programme temperature profile. In this example, this can be seen to successfully limit the total power demands of the neighbourhood. In this example, all 128 dwellings used the same default temperature programme but with a random time offset of up to an hour. The effect of this can be seen in the fact that the target temperature profile for this dwelling is initially unaffected (as the heating systems in a significant number of the other dwellings have not yet switched on) but then progressively decreases over the next 30 minutes.
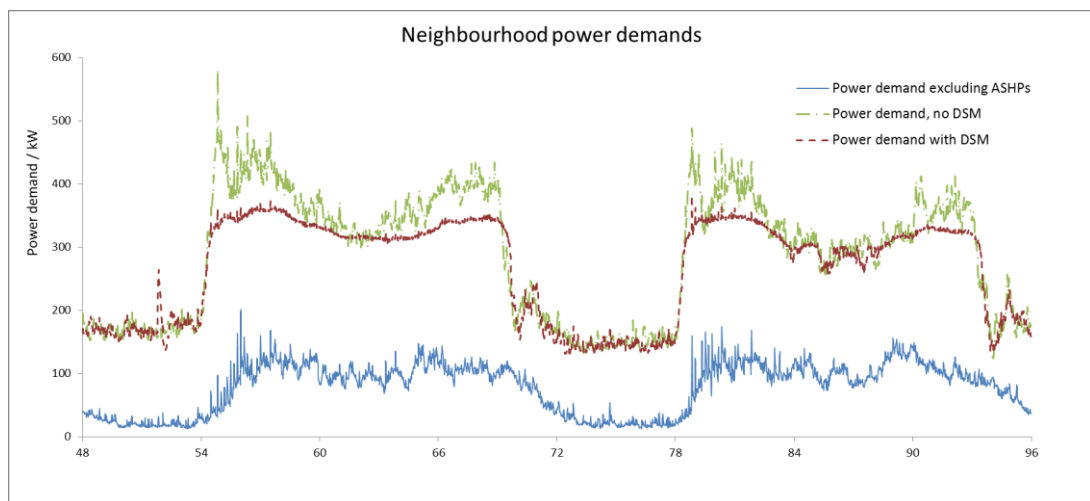
Figure 56: Example of neighbourhood power demand
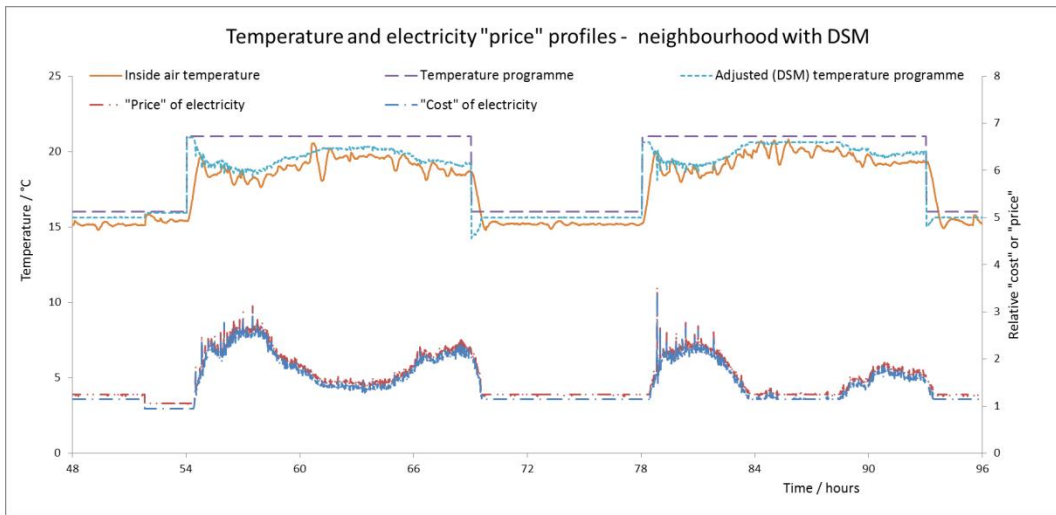
Figure 57: Example of temperature profiles and DSM control

The profile of the grid generation mix can be produced by the model as an output from the module which calculates the mix which any electrical consumption is generated by. For the present day mix, this should be identical to the input data (it is, see Figure 58) demonstrating that the data is inputted and processed correctly.
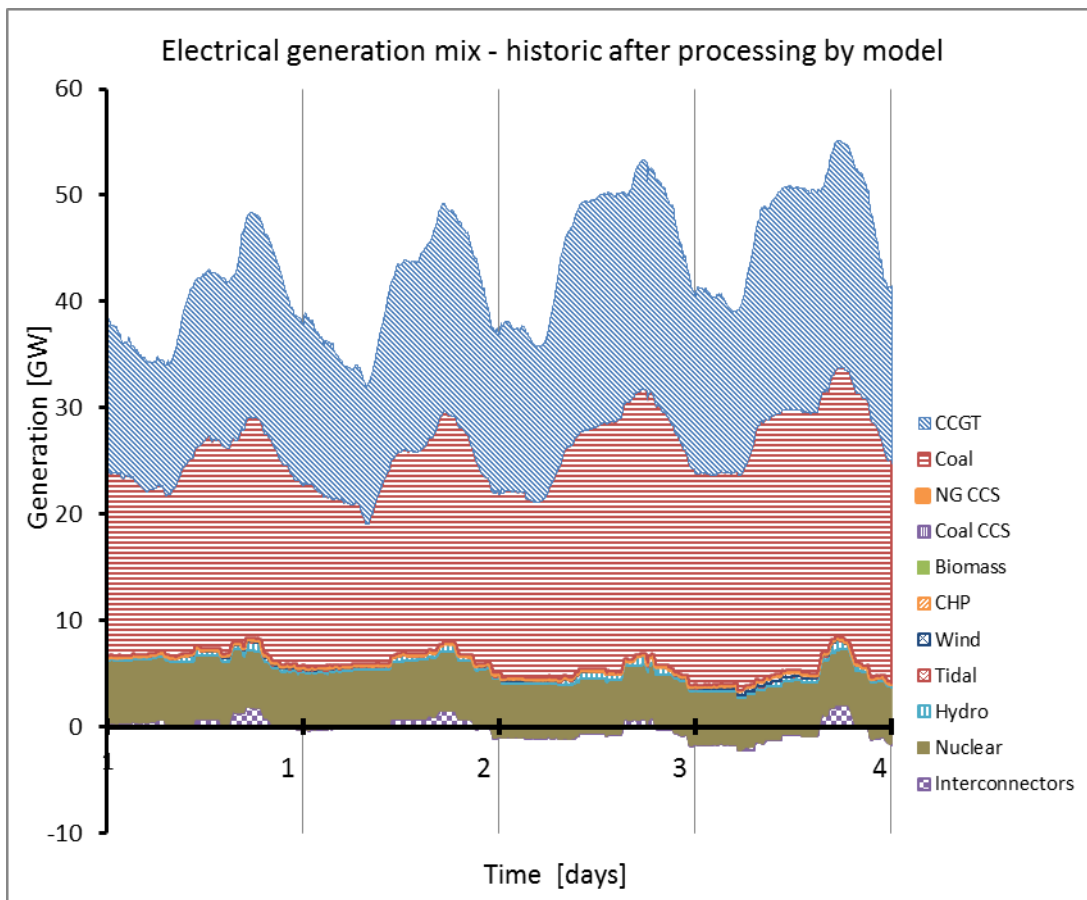
Figure 58: Example of grid generation mix, present day

Of course, there is nothing to compare the equivalent hypothetical future grid mix to but it follows the correct pattern in terms of the dispatch prioritisation and approximate magnitudes of the different generating plants (see Figure 59). The overall totals are consistent with those specified in the scenarios (see Table 18, page 118).

Figure 59: Example of grid generation mix, MR2020 scenario

5. Results and Discussion
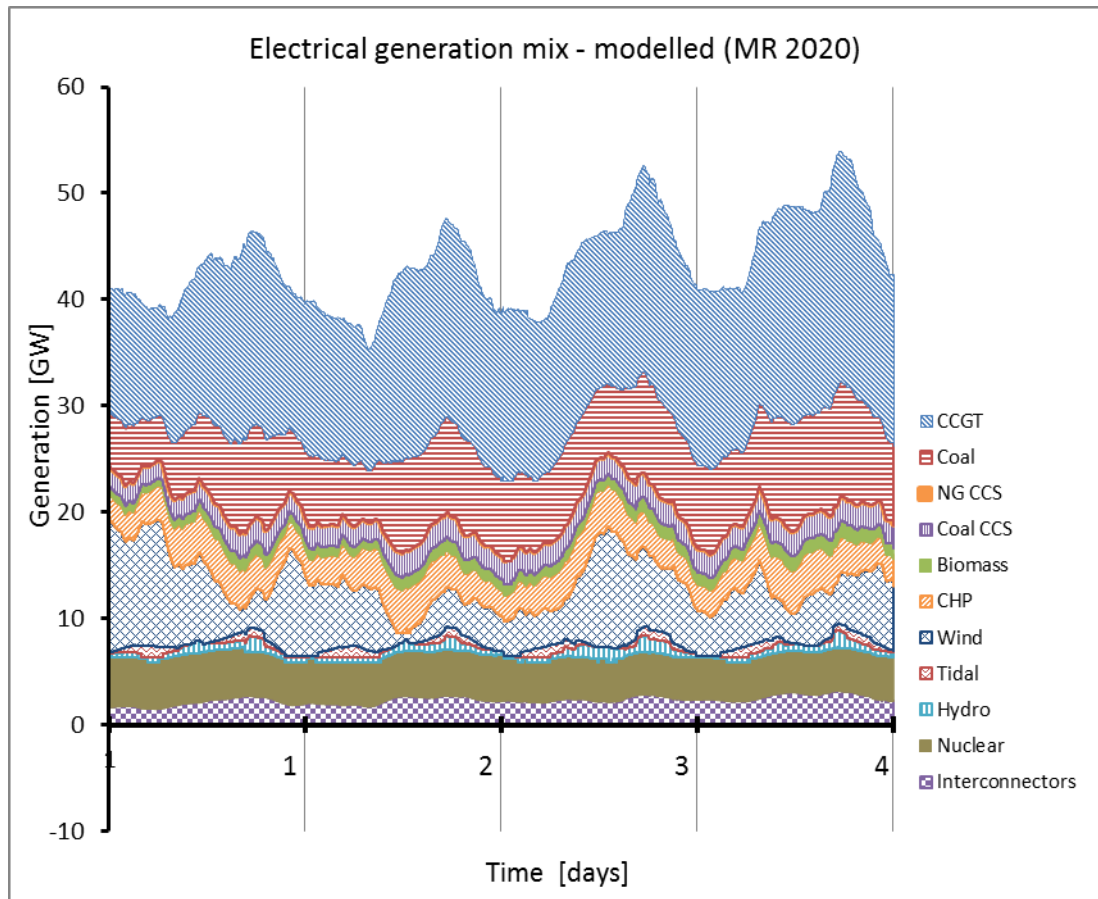
5.1 Summary of factors investigated in results

The results in section 5.2 to section 5.7 are concerned with investigating the first three sets of factors specified in the first aim of this study. The performance of the 8 ASHPs detailed in Table 3 and the 12 mCHP units detailed in Table 4 are considered before more detailed analysis is presented for selected units. The effects of varying the building type, the capacity of buffer tanks and the control methodologies listed in section 4.3.4 are discussed.

Section 5.2 presents an overview of the performance of the ASHP units before considering the effect that the building characteristics, buffer tank and control methodology has on performance. These effects are explained, primarily by relating the factors to the flow temperature which is required. The energy and exergy requirements and CO_2 emissions associated with two selected ASHPs are then compared to a condensing gas boiler in section 5.3. Section 5.4 provides an overview of the performance of the mCHP units under a similar set of operating conditions before the effect of each factor is considered in more detail in section 5.5.

The third set of factors to be considered requires additional investigation of the effect of some of the variations in the control system which are possible; this is presented in sections 5.6 and 5.7. The performance results relating to some of the mCHP units suggest alternative operating methodologies and so these are explored in section 5.6. Results in section 5.7 then finish fulfilling the third aim by discussing the effect which three alternative temperature programmes may have on the performance of the units.

Results in section 5.8 relate to the effect which changes in the climate may have on the performance of the units. Typical climate data obtained for four locations in the UK and modelled up to 2050 is used, covering the range of climate conditions which are relevant. Section 5.9 also considers future conditions but relating to the grid generation mix. The effects of generation mixes corresponding to three hypothetical scenarios in periods up to 2050 are compared to the current electrical grid. Section 5.8 and 5.9 address the requirements of the fourth and fifth aims of this study, respectively.

Sections 5.10 and 5.11 continue the theme of the effect of grid characteristics but relating to the influence of DSM on the performance of the units, fulfilling the sixth aim of this study. Section 5.10 considers DSM corresponding to network constraints in a neighbourhood of 128 dwellings heated by either a single type of heating unit or a combination of them. Section 5.11 considers the potential effect on ASHP performance of DSM signals which are influenced by MEF of electricity generation.

5.2 Effect of operating conditions on ASHP performance

This section considers the effect on the performance of the 8 ASHP units listed in Table 3 (page 23), when they supply heat to the four building types listed in Table 10 (page 78), using the three control methodologies listed in section 4.3.4 (page 86).

For the two control methodologies which are used with a buffer tank (fixed temperature and variable temperature control), three buffer tank capacities (40kg, 80kg and 160kg) are used. Figure 60 shows the total heat delivered and electrical energy consumed by the ASHP units operating for a year in the 224 permutations derived from these options. Outside air temperature data representative of present-day Glasgow has been used and in each case the control system aims for a constant indoor temperature of 21°C.
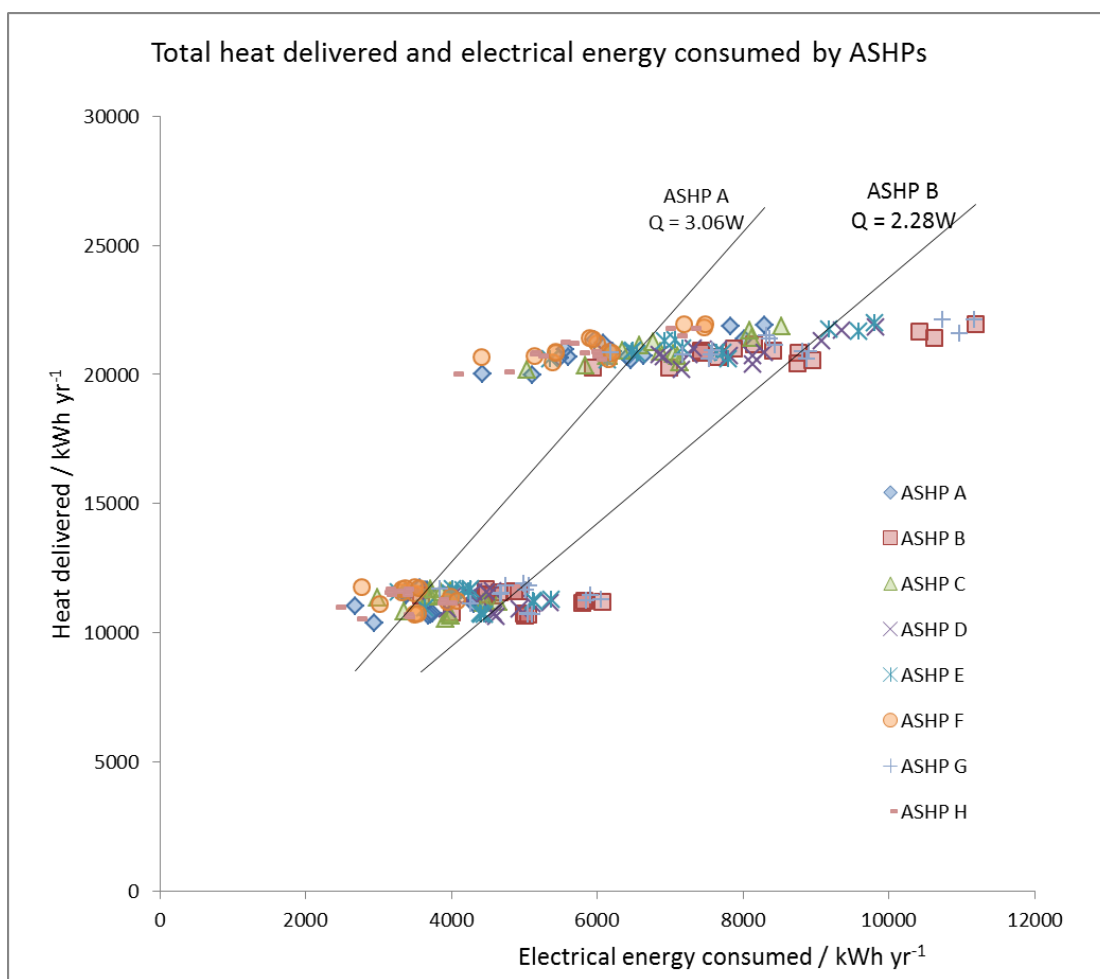
Figure 60: Heat delivered and electrical energy consumed by different ASHP units

Figure 60 provides an overview of data which will be examined in greater detail in the pages to follow. However, it can be immediately noted that there is considerable spread from the average COP (that is the gradient of a linear line of best fit in Figure 60) of a given ASHP; this is illustrated with the lines of best fit for ASHP A and ASHP B which are representative of state-

of-the-art and mid-range ASHPs which are available (Table 3, p23). When the full range of ASHPs which are available is considered, it is apparent that the range of performances which might be encountered is very wide; some installations will consume more than 150% more power than others supplying a similar quantity of heat.

The data in Figure 60 are presented again in Figure 61, but categorised by building type rather than ASHP unit. It can be seen that the heat demand associated with the flat and the semi-detached building with improved insulation are, in this case, quite similar. For each building type there is some variation in the heat delivered but large variation in the power consumption, as noted earlier. The enhanced heat emitter system slightly reduces the heat supplied to the dwellings (lower flow temperatures reduce storage losses) but considerably reduces the power consumption of the units.
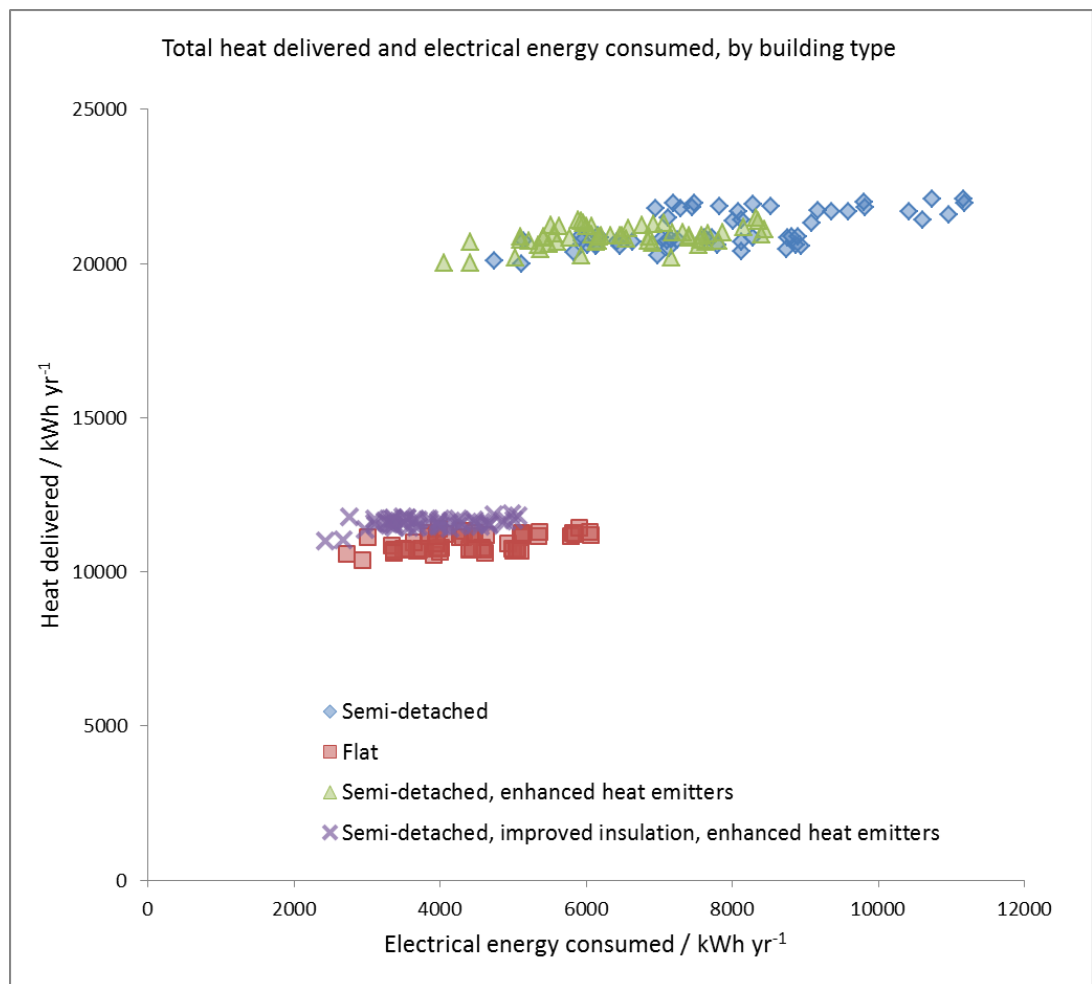

Figure 61: Heat delivered and electrical energy consumed by ASHPs in different building types

The relative thermal comfort between systems is given some consideration in Figure 62. This shows the variation in the time-integral of the pseudo-PMV (divided by an assumed heating season of 120 days) for both ASHP A and a gas boiler operating with the seven different control

system and buffer tank configurations. The four columns within each group correspond to the four buildings. There appears to be a considerable spread between dwellings and between configurations, with the boiler providing superior thermal comfort. However, this impression is largely an effect of the unfamiliar units used. A PMV of -0.1 is equivalent to an average temperature drop of just under 0.8°C in these conditions and so it is unlikely that the differences noted here would be readily discernable.
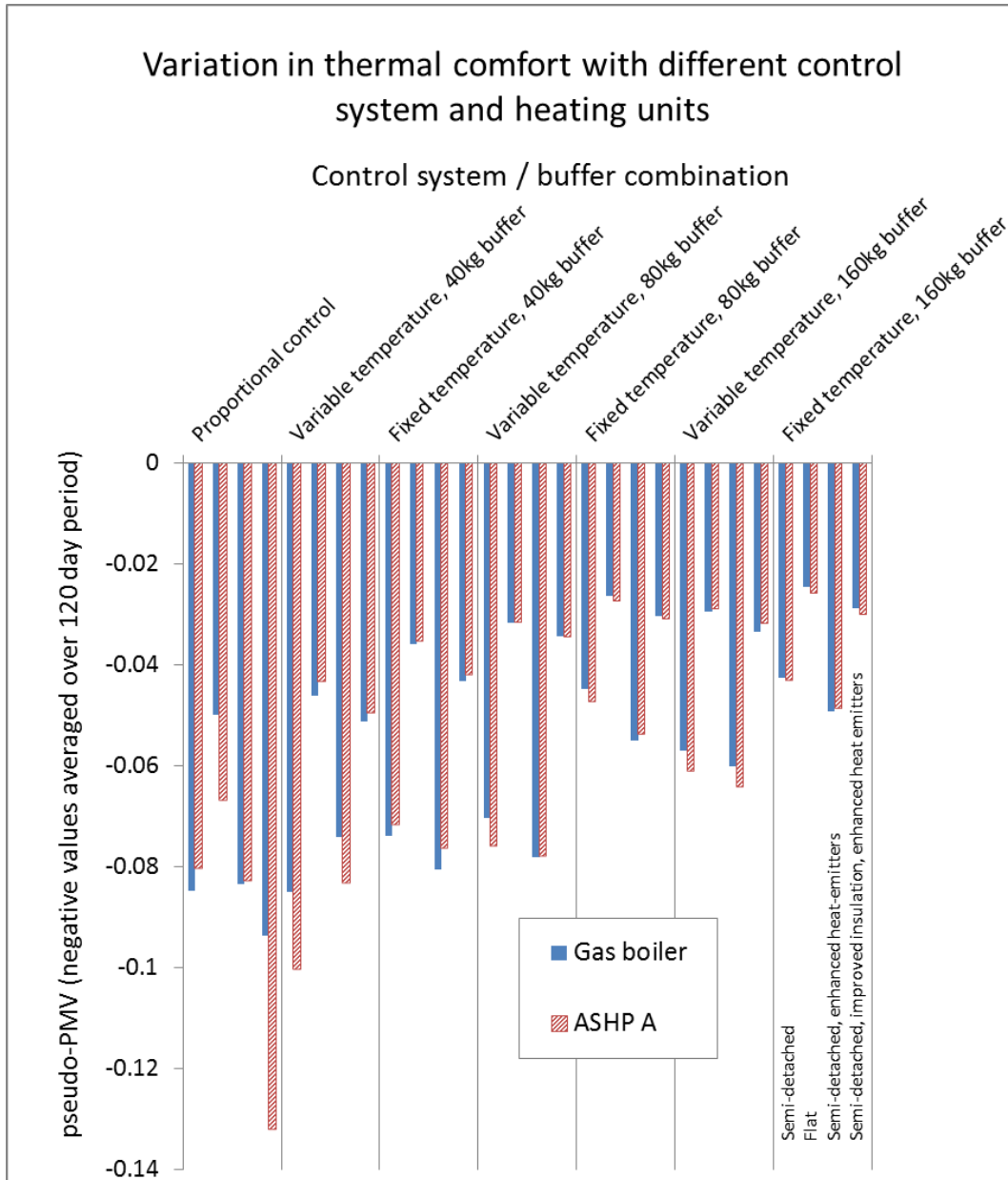
Figure 62: Variation in thermal comfort with ASHP A and a condensing gas boiler

Figure 63 illustrates the range of average seasonal COPs which the ASHPs achieved under each set of conditions. The heat delivered is used to calculate the COP (i.e. any losses from buffer tanks are taken into account). The four columns of results within each main group correspond to the four building types. Within each grouping, the relative performance difference between the

ASHP units remains fairly constant; the best units achieve COPs up to 50% higher than the lowest performing units. The performance of ASHP B generally corresponds to the higher end of the larger (lower performing) group of ASHPs in the Energy Saving Trust (2010) field trial.
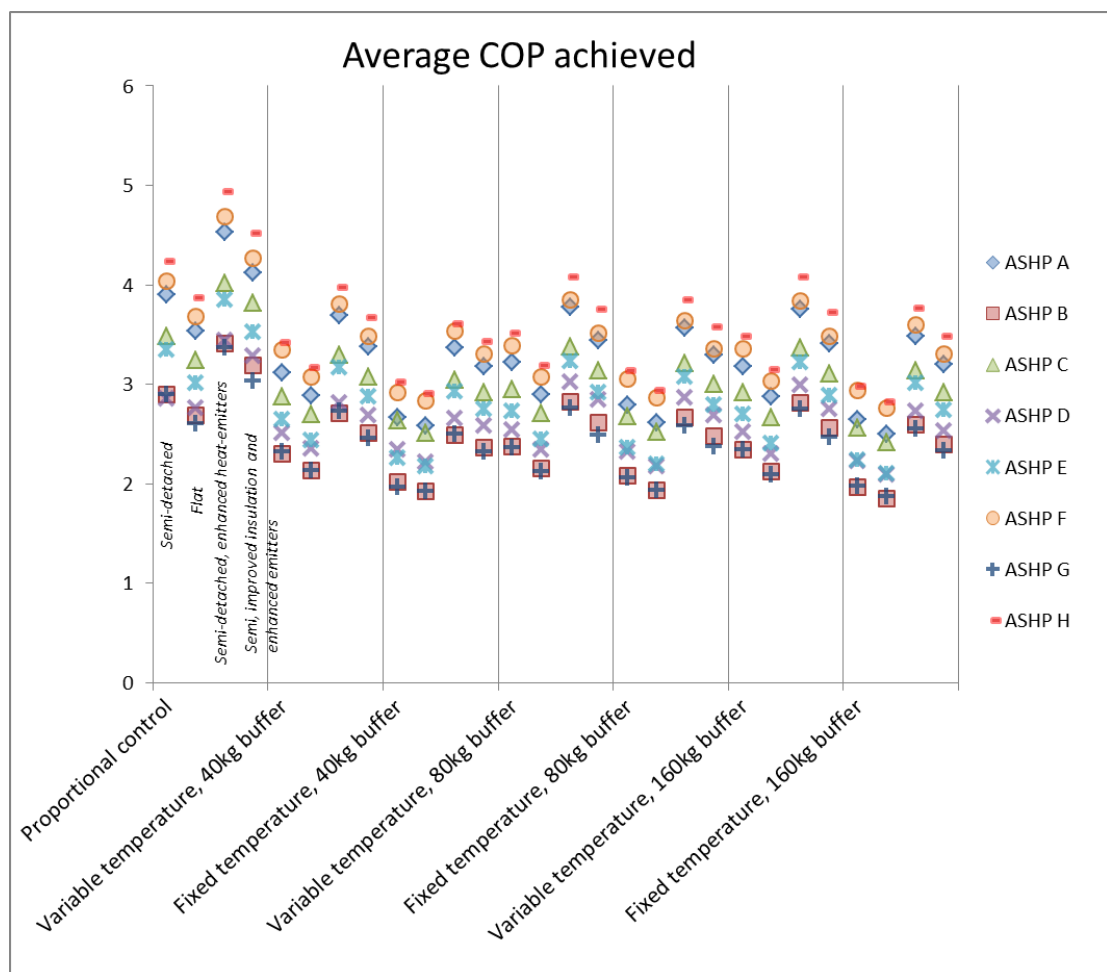
Figure 63: Average COP achieved

Although the COPs are slightly increased in some cases by larger buffer tanks, this is offset by increased demand for heat. To make the effect of the different control system and buffer tank combinations clearer, Figure 64 presents the PER for each configuration (calculated based upon mean generating plant mix and averaged across building types), relative to the PER using the proportional control system.
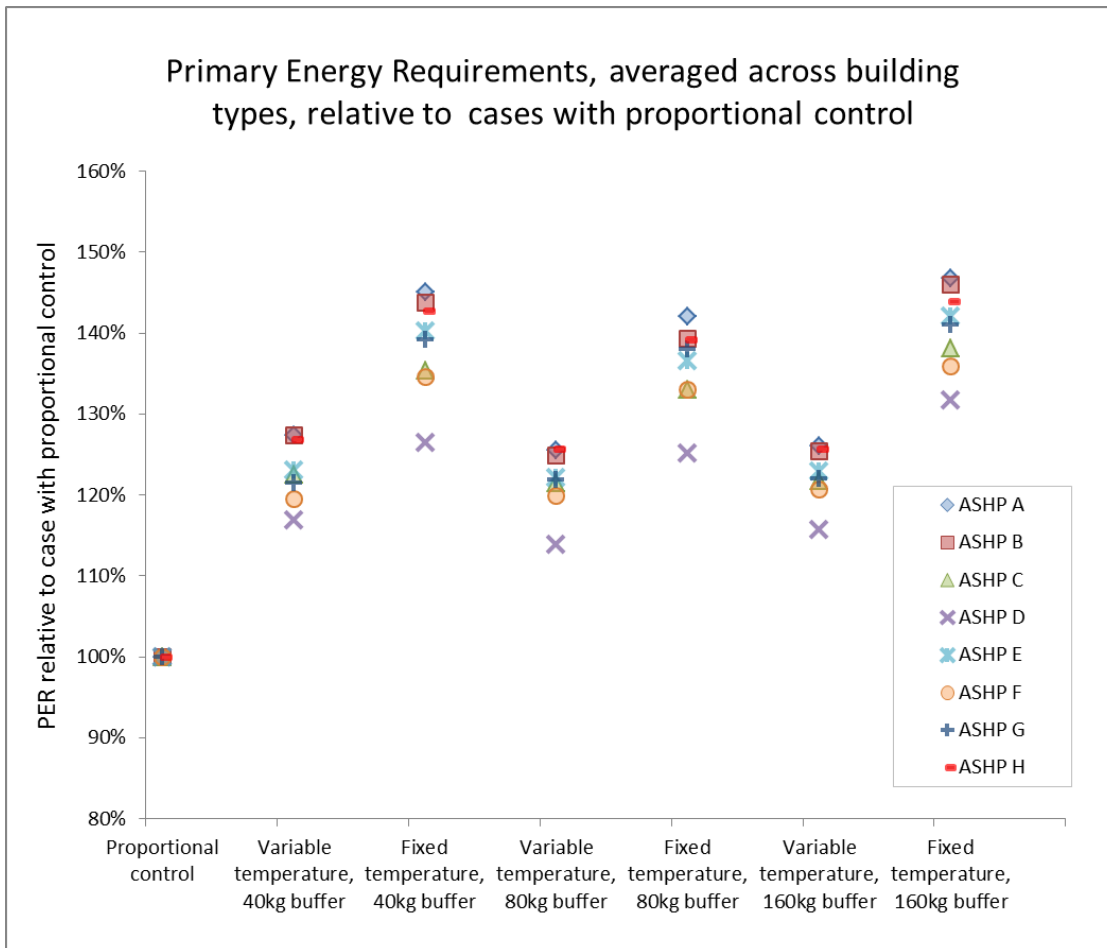
Figure 64: Primary Energy Requirements for ASHPs, relative to cases with proportional control

The ASHPs all achieve a higher COP when using the proportional control methodology compared to the alternatives. The PER is increased by 20% - 30% when using variable temperature control ("weather-compensated") rather than proportional control. The fixed temperature control system achieves the lowest performance. A similar reduction in performance associated with fixed temperature systems has been noted elsewhere (Kelly & Cockroft 2011; Dunbabin & Wickins 2012).

In apparent contrast to other studies, some small improvement is observed in the COP of the systems in the dwellings with higher heat demands (i.e. the larger and less well insulated buildings). However, this can be explained by considering that they will demand heat at times of the year that the other buildings do not require heating; that is, they have a longer heating season that allows the ASHPs to operate more efficiently at times of higher air temperature, increasing their average COP. All things being equal, the performance of the heating system at a given point in the year will still be higher if the building has a lower heat demand.

In each case, the most significant factor which can be varied by the operating conditions is the flow temperature. Some sample operating profiles for ASHP B will be discussed to illustrate

this (taken from simulations of the semi-detached building during the period from 48 hours to 96 hours from the start of the year, with outside air temperatures representative of Glasgow and averaging 2.5°C for the period shown). Figure 65 provides a winter temperature plot when proportional control is used.
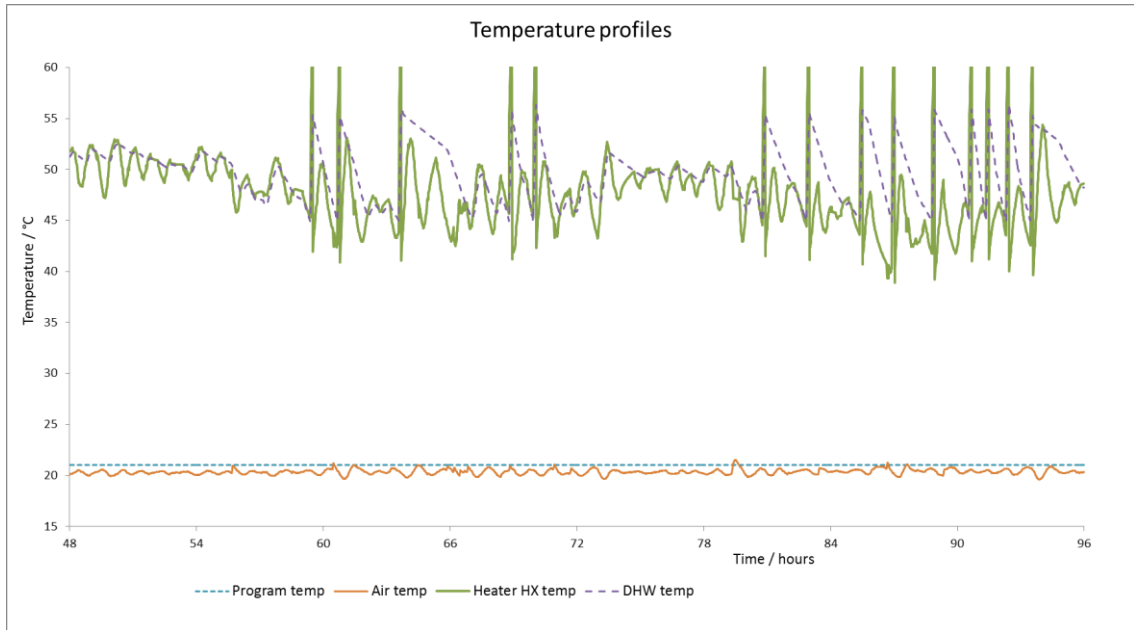
Figure 65: Temperature profile for ASHP B, proportional control

The short spikes in the temperature of the heat exchanger correspond to times at which the temperature of the domestic hot water (DHW) tank is too low and the heat pump raises its output to its full capacity in order to bring it back within tolerance (see Figure 66). Apart from these times, the temperature of the heat exchanger generally finds an equilibrium at around 50°C with small variations either side which can be attributed primarily to the stepped modulations of the unit (see Figure 66).
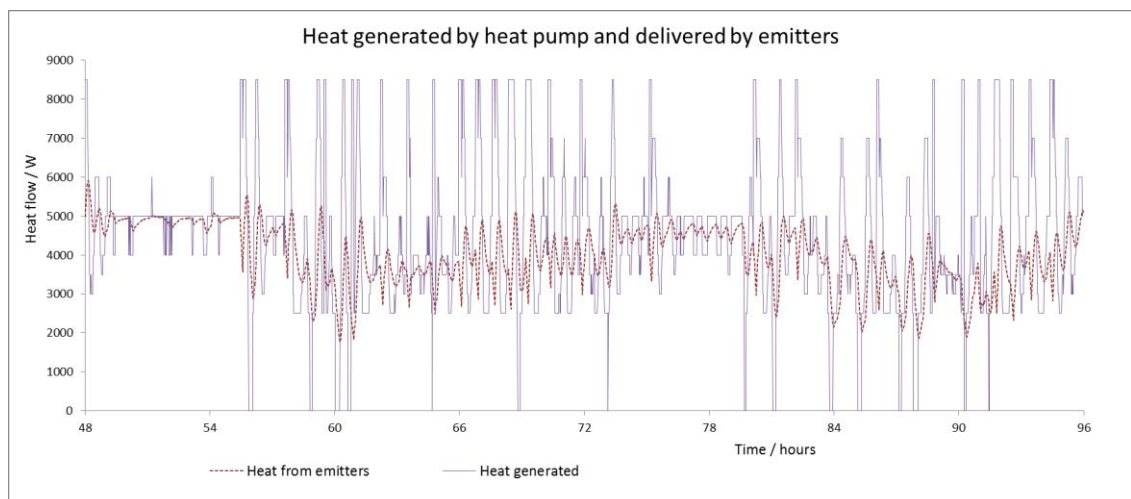
Figure 66: Heat flow profile for ASHP B, proportional control

147

The corresponding temperature profile, for the same conditions but using the variable-temperature controller is shown in Figure 67 (with an 80kg buffer tank). The DHW tank temperature is not shown; generally the heat exchanger temperature remains hot enough that it is not necessary for the heat pump to enter "DHW only" operation. The inside air temperature fluctuates slightly more due to the 2°C dead-band of the thermostatic control of the heat emitter system but is, on average, higher than that with proportional control.
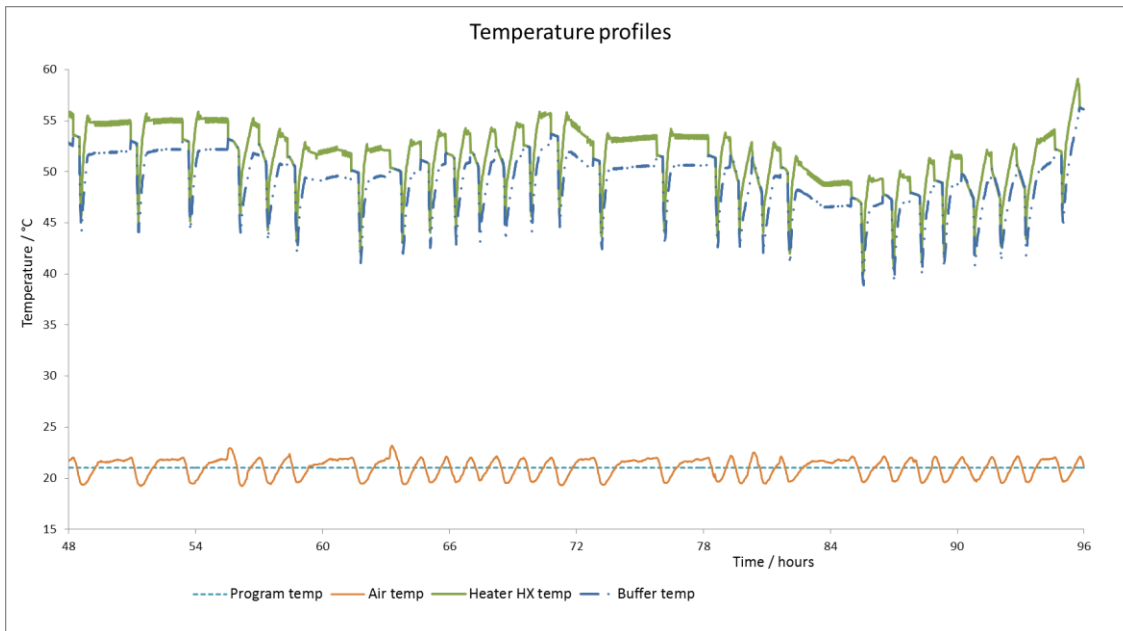
Figure 67: Temperature profile for ASHP B, variable temperature control

The on-off cycle of the heat emitters varies from around three hours on to one hour off during the night to around one hour on to one hour off during the day. Although a lower flow temperature could be used with continuous operation of the heat emitters, actually ensuring an acceptable level of thermal comfort would be problematic due to the additional gains that are not accounted for but which might not contribute during a particular period. The proportional control system can operate with the lower flow temperature primarily because it takes account of these other gains and can use a lower heat transfer rate. A significant secondary effect is the removal of the temperature losses across the buffer tank heat exchanger.

If heat emitters with a greater capacity are used then the flow temperature can be reduced. Figure 68 and Figure 69 show the temperature profile with the same conditions (proportional and variable temperature control, respectively) but using enhanced heat emitters in the building.
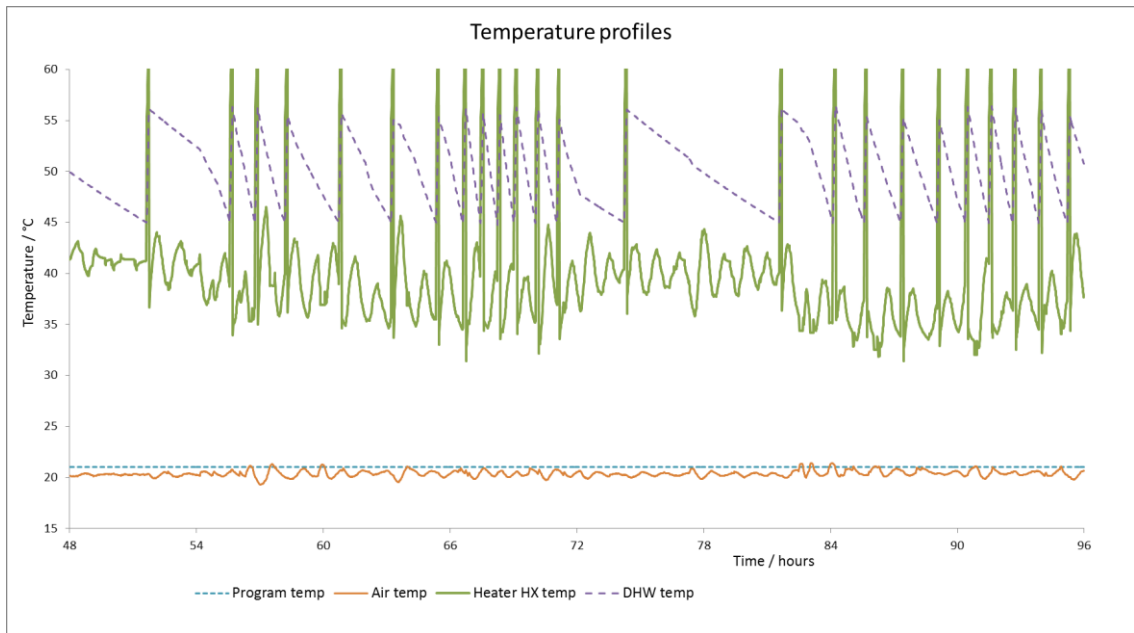
Figure 68: Temperature profile for ASHP B, proportional control with enhanced heat emitters
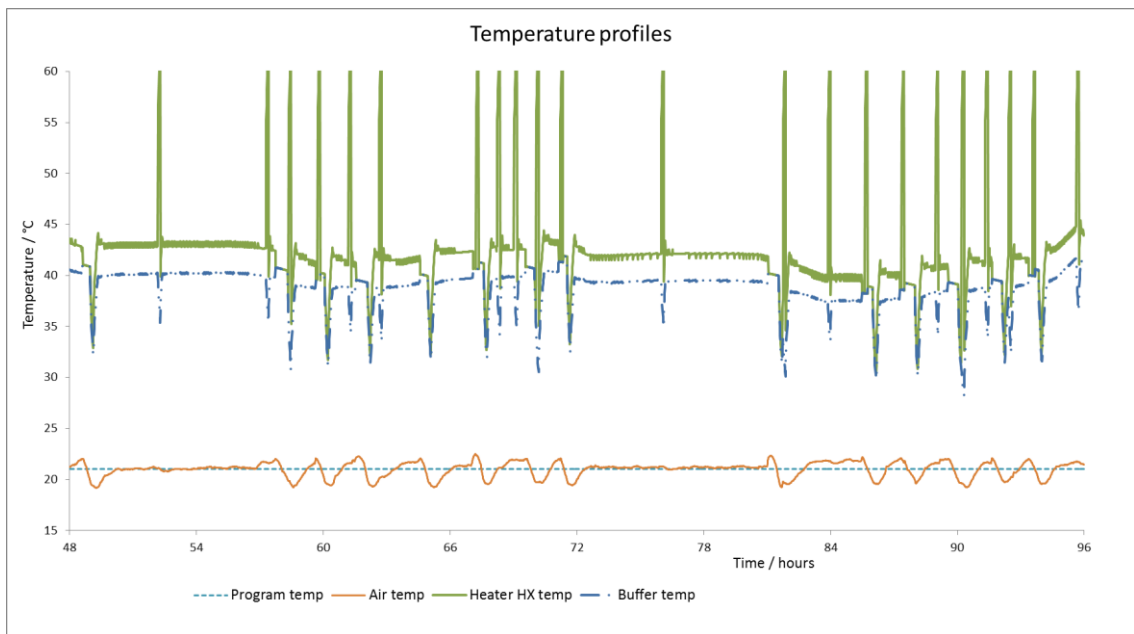
Figure 69: Temperature profile for ASHP B, variable temperature control with enhanced heat emitters

The flow temperature is significantly reduced with the resultant improvement in performance noted in Figure 63. Although an even lower flow temperature is used by the proportional control system, the improvement in the COP which is achieved is greater with the variable-temperature system. This is partly due to the DHW having a relatively larger effect with the proportional control system and partly due to the fact that the absolute reduction in flow temperature is less with the proportional control system as it was already low.

The effect of the enhanced heat emitters is shown across the range of units for both proportional and variable-temperature control in Figure 70.
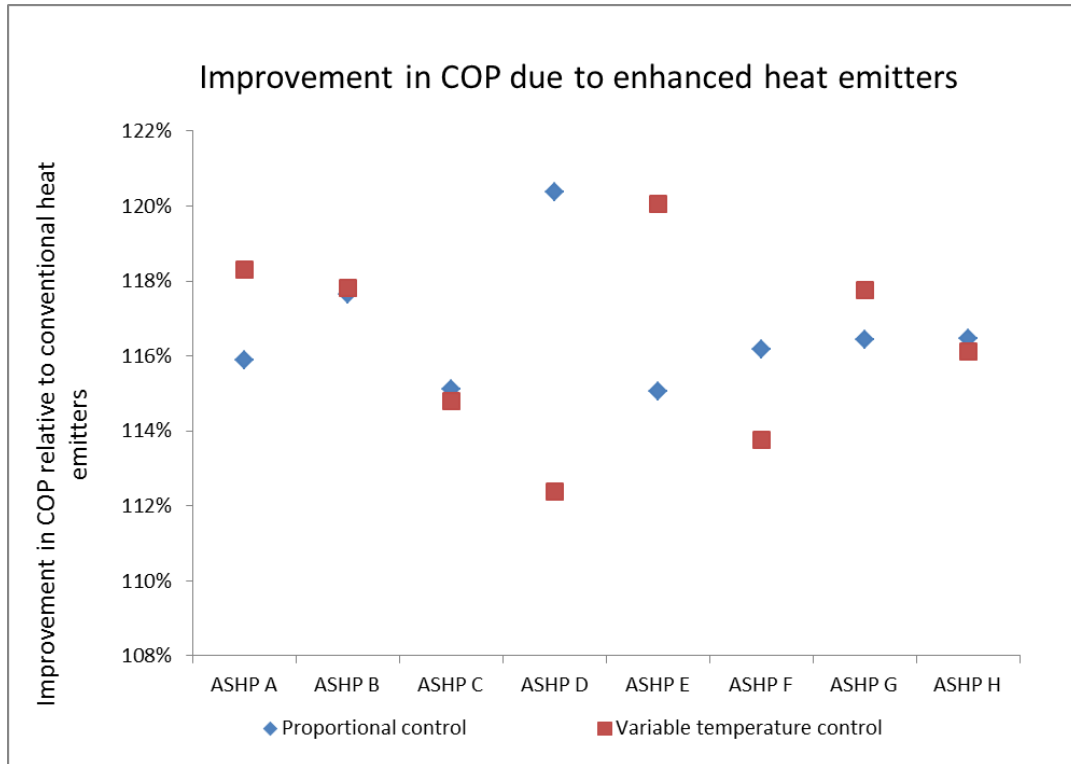
Figure 70: Improvement in COP due to enhanced heat emitters

5.3 Comparison between ASHPs and boilers

This section considers the results relating to ASHP A and ASHP B in more detail and compares them to a condensing gas boiler. PER, exergy and CO_2 emissions are considered. The effect of the buffer tank size and building properties are also noted.

The PERs associated with the operation of the three units are compared in Figure 71.
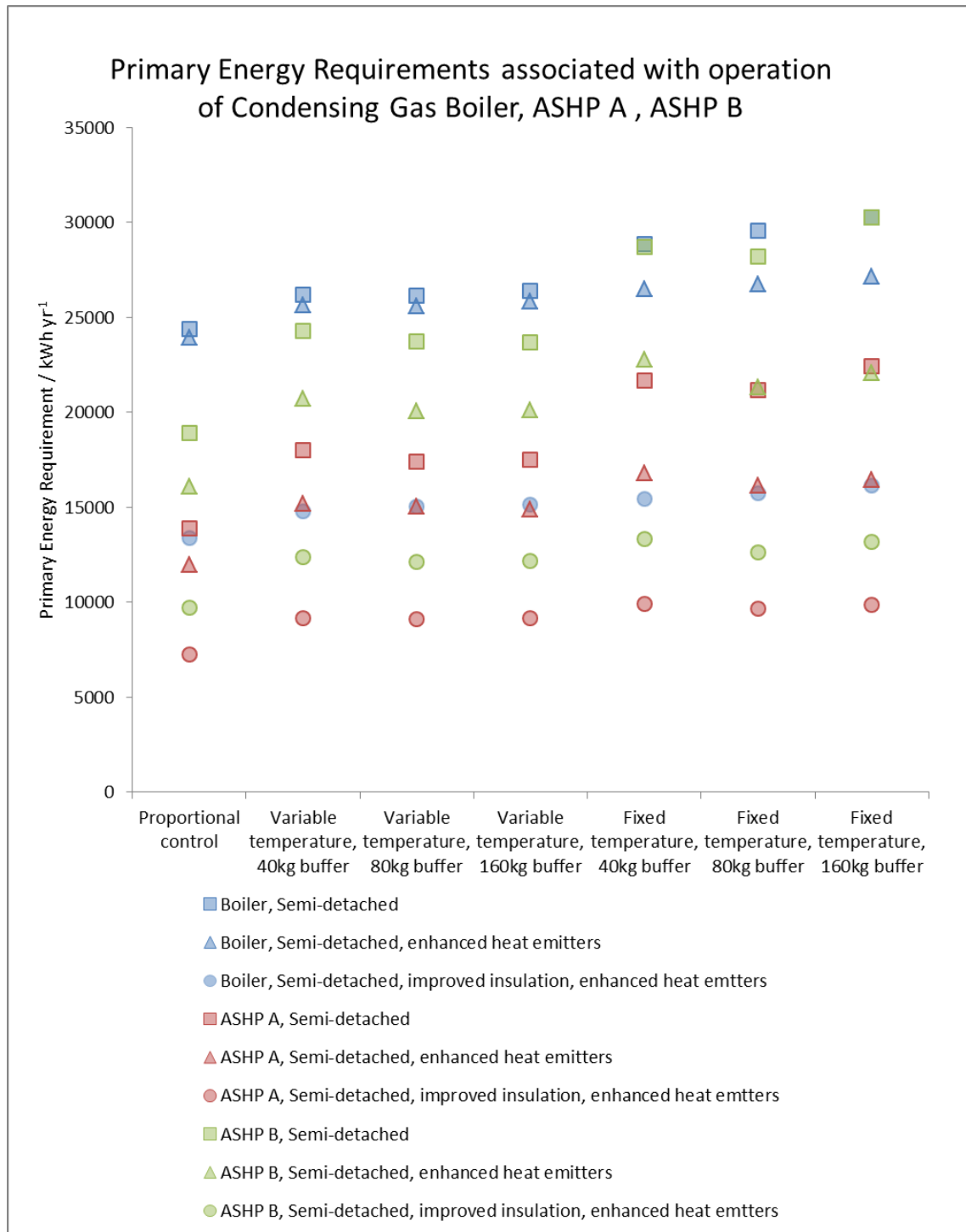
Figure 71: Primary Energy Requirements for Gas Boiler, ASHP A & ASHP B

Improving the insulation level of the building approximately halves the PER in most cases. The PER associated with each ASHP is less than that associated with the condensing gas boiler in almost every case. However, the performance of the boiler is less affected by the buffer tank and control system configuration and so the PER is approximately equal between the boiler and ASHP B in the case that fixed-temperature operation is used with the 160kg buffer tank. As noted above, using a more effective heat emitter reduces the PER associated with the operation of the ASHP units when fixed-temperature or variable-temperature control is used and to a lesser extent when proportional control is used. The PER of the ASHPs is slightly less with the 80kg buffer tank than with either the 40kg or 160kg buffer tank.

ASHP A has less than half the PER of the gas boiler if proportional control is used with enhanced heat emitters.

Because the CEF associated with energy from the grid are presently higher than those associated with natural gas, the comparison shifts in favour of the gas boiler if CO_2 emissions are considered instead (Figure 72). The emissions associated with ASHP A are still considerably lower in each case (up to 40% lower) and those associated with ASHP B are lower than those from the gas boiler in all cases which use proportional control. However, when using variable-temperature control, the emissions associated with ASHP B installed in the semi-detached house are similar to those from the gas boiler. When using fixed-temperature control, the CO_2 emissions associated with ASHP B are higher than those from the gas boiler in all three building types.
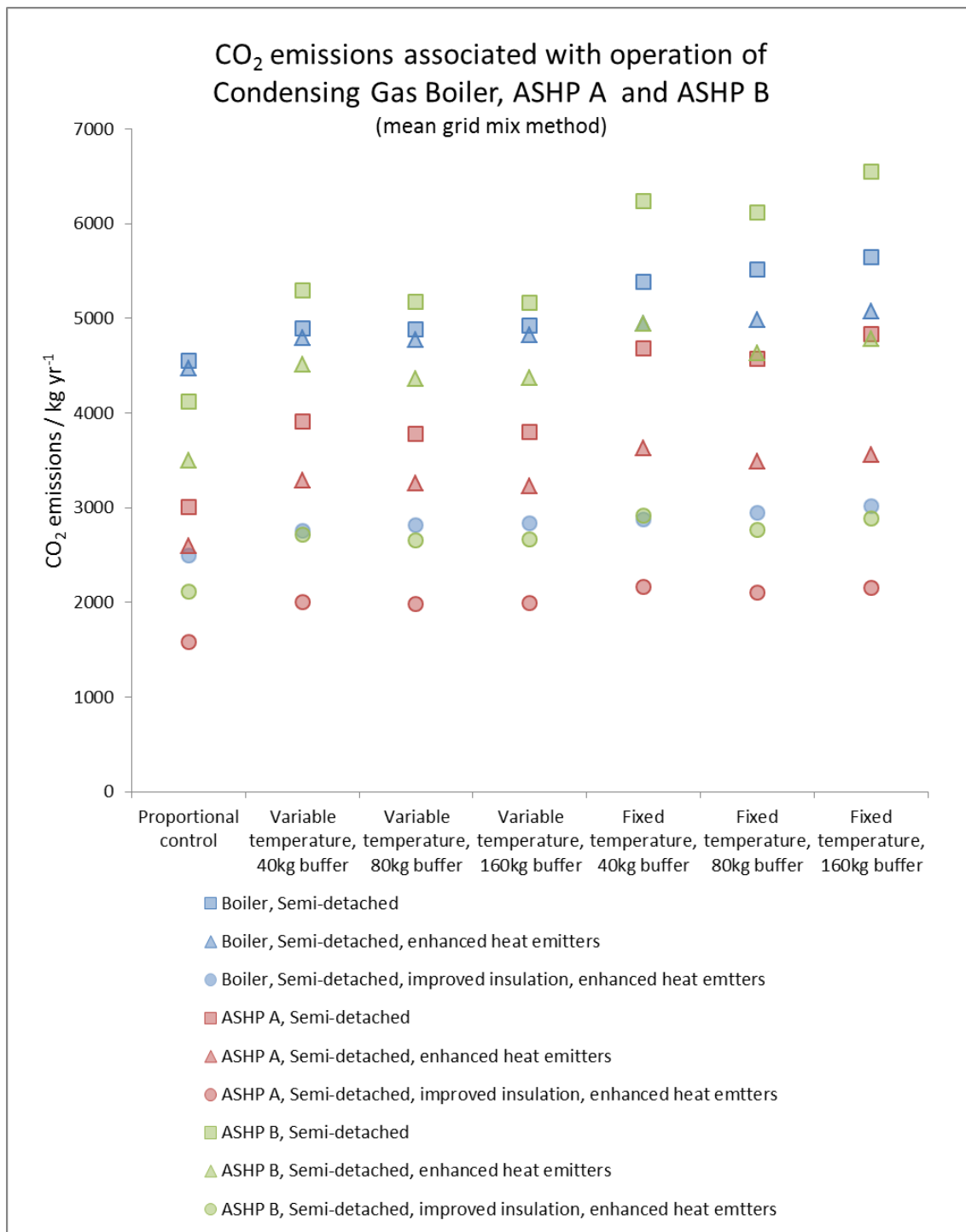
Figure 72: *CO$_2$ emissions associated with condensing gas boiler, ASHP A and ASHP B (mean grid mix method)*

The marginal emissions factor (MEF) is typically higher than the CEF. If a consequential study is being conducted to consider the effect of replacing condensing gas boilers with ASHPs then the MEF is arguably more relevant (Hawkes 2010). The emissions associated with the heating units when using this method are illustrated in Figure 73.
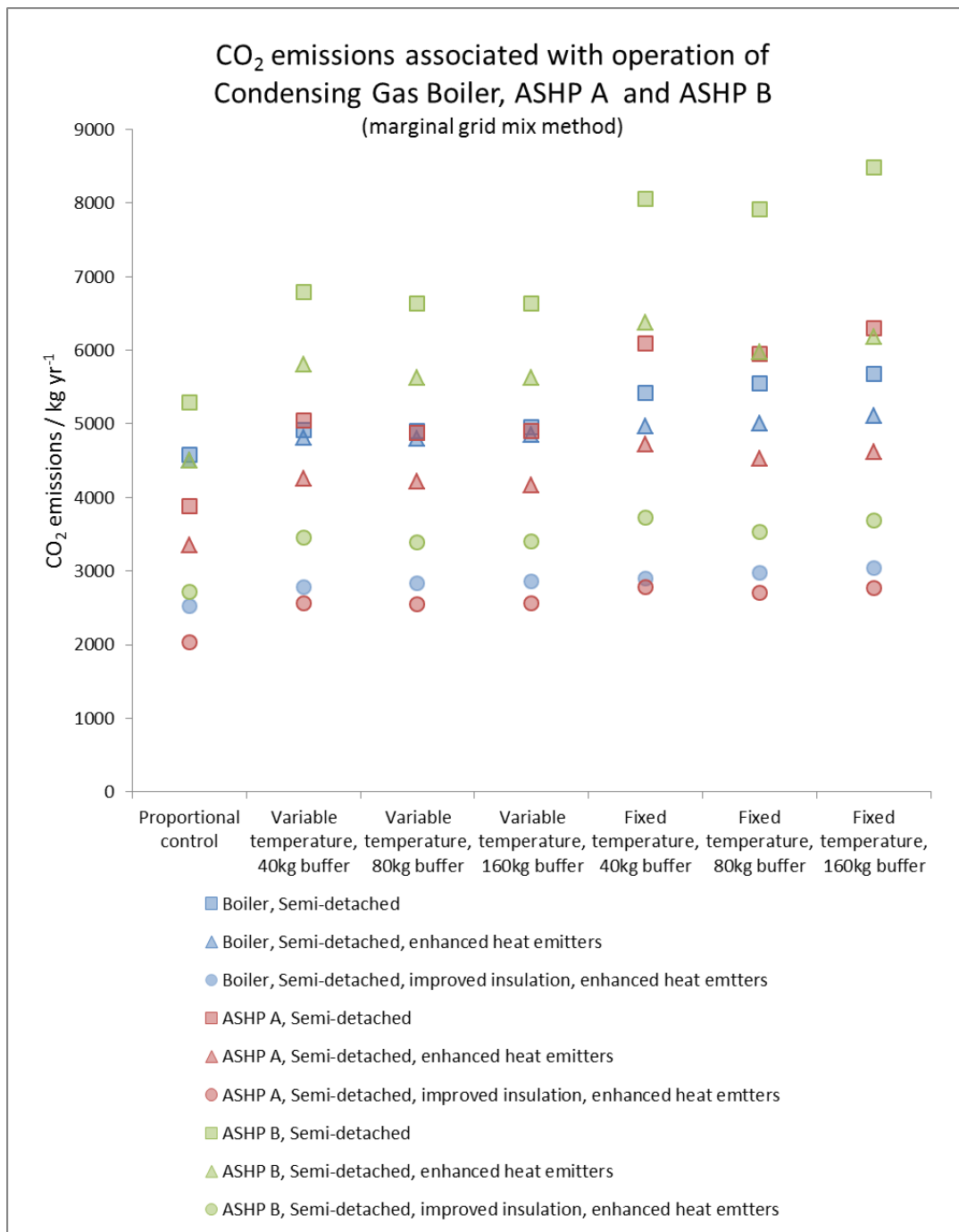
Figure 73: CO₂ emissions associated with condensing gas boiler, ASHP A and ASHP B (marginal grid mix method)

Although the emissions associated with ASHP A are still lower than those from the condensing gas boiler if a proportional control system is used, they are actually higher if fixed-temperature control is used within the semi-detached house. With the variable-temperature control system and a 40kg buffer tank, ASHP A will still result in lower emissions than the gas boiler if used with enhanced heat emitters but not if used with the conventional heat emitters in the semi-detached house. The emissions associated with ASHP B are higher in almost all cases under these assumptions.

More generally, these results show that a range of performances may be achieved. In comparing the units, single figures to summarise the performance of the technologies will often be misleading. It is also clear that the nature of the study comparing the units will have a large bearing on the results. For example, whether the study is most concerned with the efficient use of energy resources, the CO_2 emissions from a whole system perspective or the change in CO_2 emissions which would occur when replacing one type of unit with another.

The exergy content of the energy flows at each stage in Figure 11 for the condensing gas boiler, ASHP A and ASHP B are shown in Figure 74. The reduction in the exergy content of the flow across each heating unit is most notable. In the cases with the ASHPs, the drop is much lower because the unit partially compensates for the low exergy content of the heat by supplying more of it. However, there is a larger drop between the primary exergy resource and the unit itself because of losses incurred in the generation of electricity.

The final use exergy is similar in each case as the inside air temperature and DHW temperature are relatively consistent but the exergy content entering the emitter system is higher in the cases requiring higher temperature flows (e.g. those with conventional emitters). Most of the variations considered in these results so far have related to this exergy loss (i.e. the exergy destruction in the emitter system) as the exergy efficiency of each ASHP unit is quite consistent (see Figure 13). However, the losses relating to the generation of electricity are also significant.
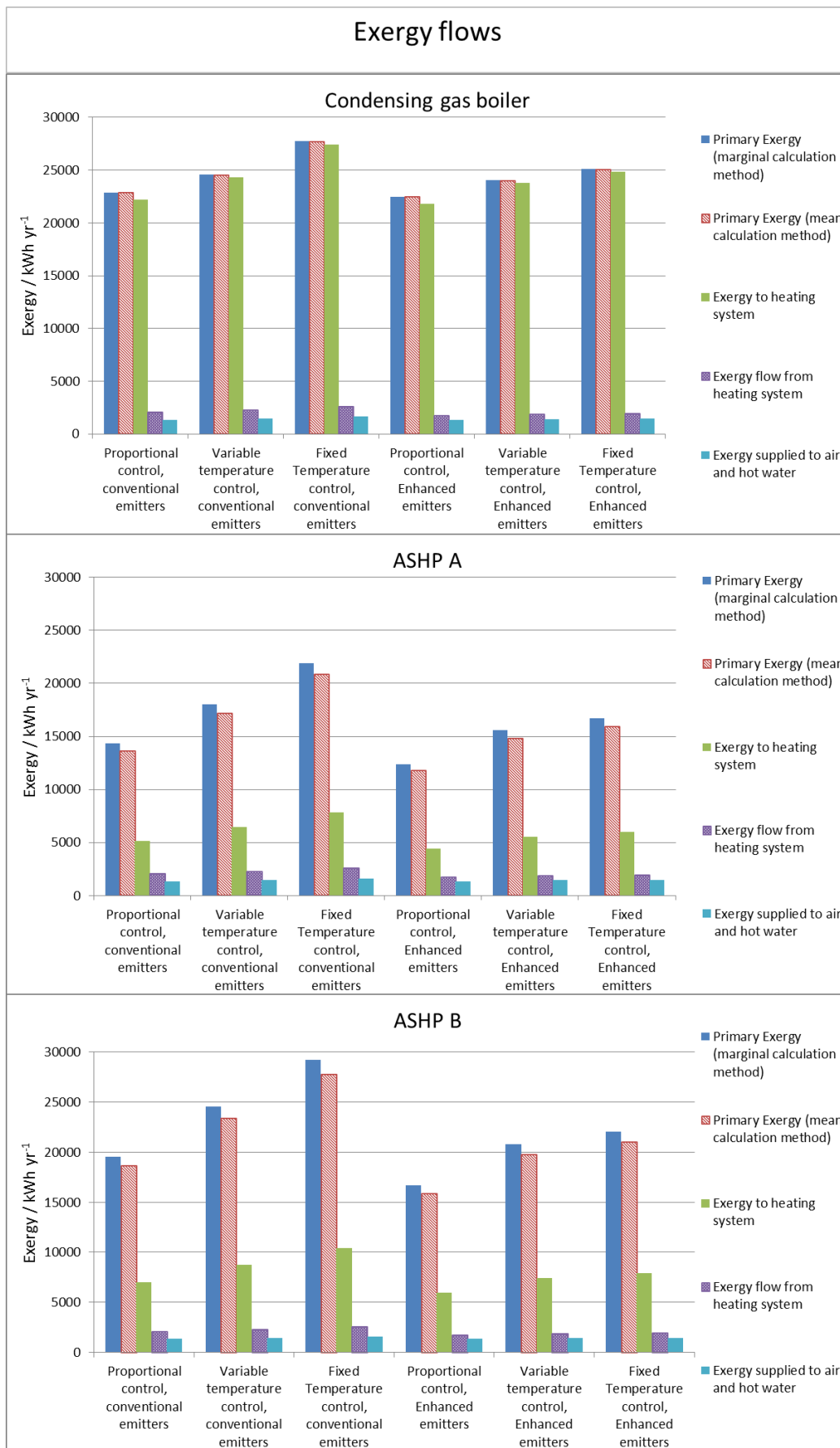
Figure 74: Exergy flows associated with condensing gas boiler, ASHP A and ASHP B

5.4 Overview of mCHP performance

This section provides an overview of the performance of the 12 mCHP units listed in Table 4 (page 38). These have been modelled with the same four building types (Table 10, page 78) and control methodologies (section 4.3.4, page 86) but with six buffer tank sizes, ranging from 40kg to 1280kg.

The average thermal and electrical efficiencies achieved by the units operating with these permutations are presented in Figure 75. The average efficiencies relate to the GCV of the fuel input to the units and the net electrical and thermal outputs from the units.
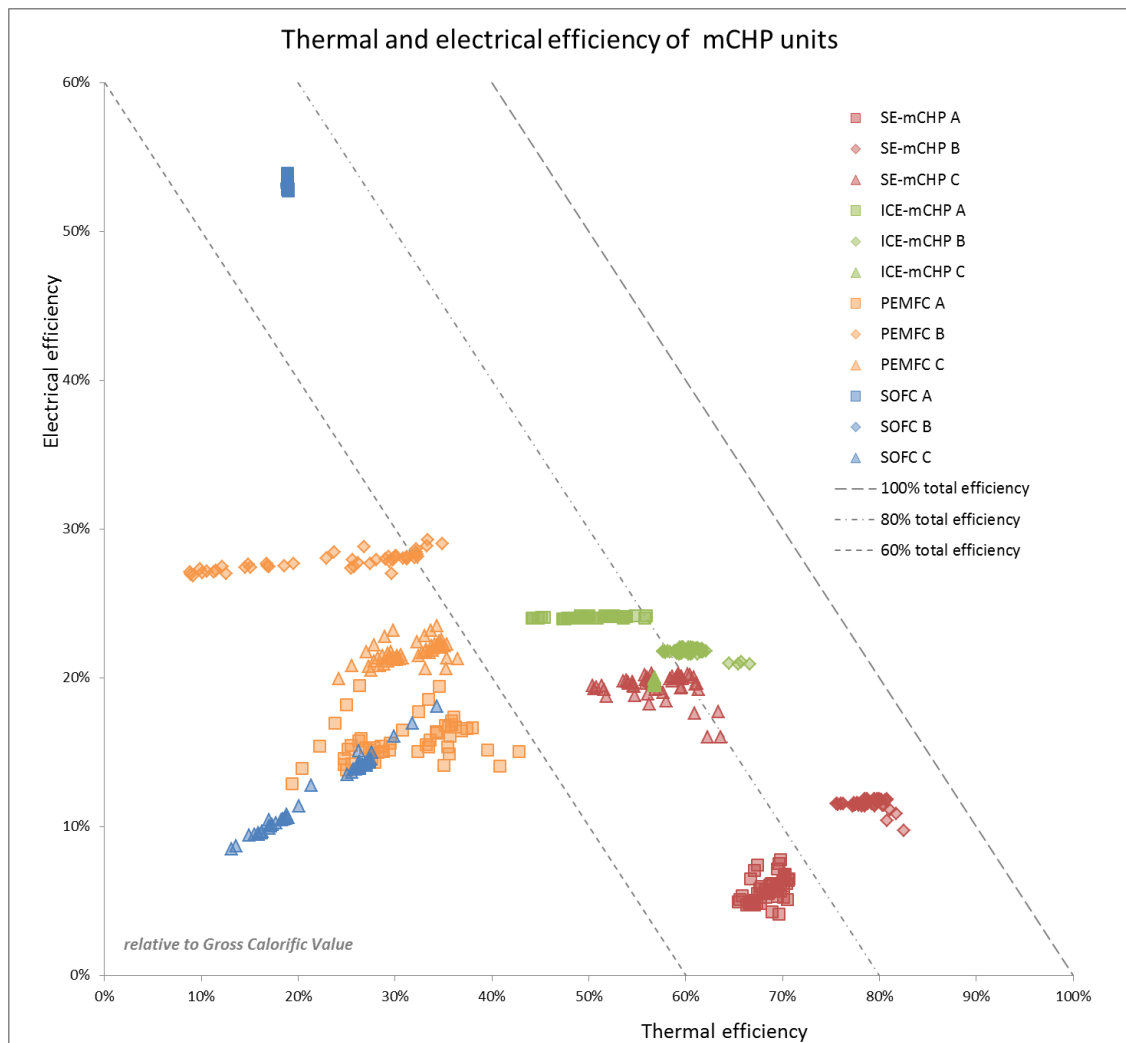
Figure 75: Average thermal and electrical efficiency achieved by mCHP units

The average total efficiency achieved by most of the units is between 60% and 80% but there are four units that do not achieve an average of 60% total efficiency. SE-mCHP B exceeds 90% total efficiency in some circumstances. In most cases, the average electrical efficiency achieved by each unit is relatively consistent but the thermal efficiency varies considerably with

operating conditions. The exceptions to this are units PEMFC A, PEMFC C and SOFC C which achieve a wider range of average electrical efficiencies. As they each have a relatively slow maximum rate-of-change of output, the nature of the loads that they supply has a large effect on the proportion of time spent ramping between different output levels (most of which are sub-optimal for electrical efficiency). This effect is explored in more detail for PEMFC C in section 5.6, below. Unit PEMFC B is smaller than the other PEMFC-mCHP units and so it operates at full capacity for a larger proportion of the time, achieving a more consistent electrical efficiency. Units SOFC A and SOFC B would demonstrate a similar range of average electrical efficiencies but in these simulations, their output has been constrained to a narrow range in order to optimise their performance; the effect of different operating regimes on their overall performance is also explored in more detail in section 5.6.

Supplementary gas boilers were assumed to supply any unmet heating demand if it exceeded 500W in the five units with thermal capacities of less than 4kW (i.e. ICE-mCHP B, PEMFC B, SOFC A, SOFC B and SOFC C). The use of this supplementary heating is shown by comparison between Figure 75 and Figure 76. Figure 76 illustrates the system thermal and electrical efficiencies, where the fuel input to both the mCHP unit and the supplementary burner are taken into account along with the heat delivered by the system (i.e. losses from buffer tanks are taken into account).

For the units which are not used with supplementary burners (for example the SE-mCHP units in these simulations), the system electrical efficiencies shown in Figure 76 are the same as the unit efficiencies shown in Figure 75 but there will be some reduction in the thermal efficiencies due to the additional losses which are taken into account. These vary depending upon operating conditions and so tend to increase the range of the system thermal efficiencies, relative to the unit thermal efficiencies, as shown in Figure 76.
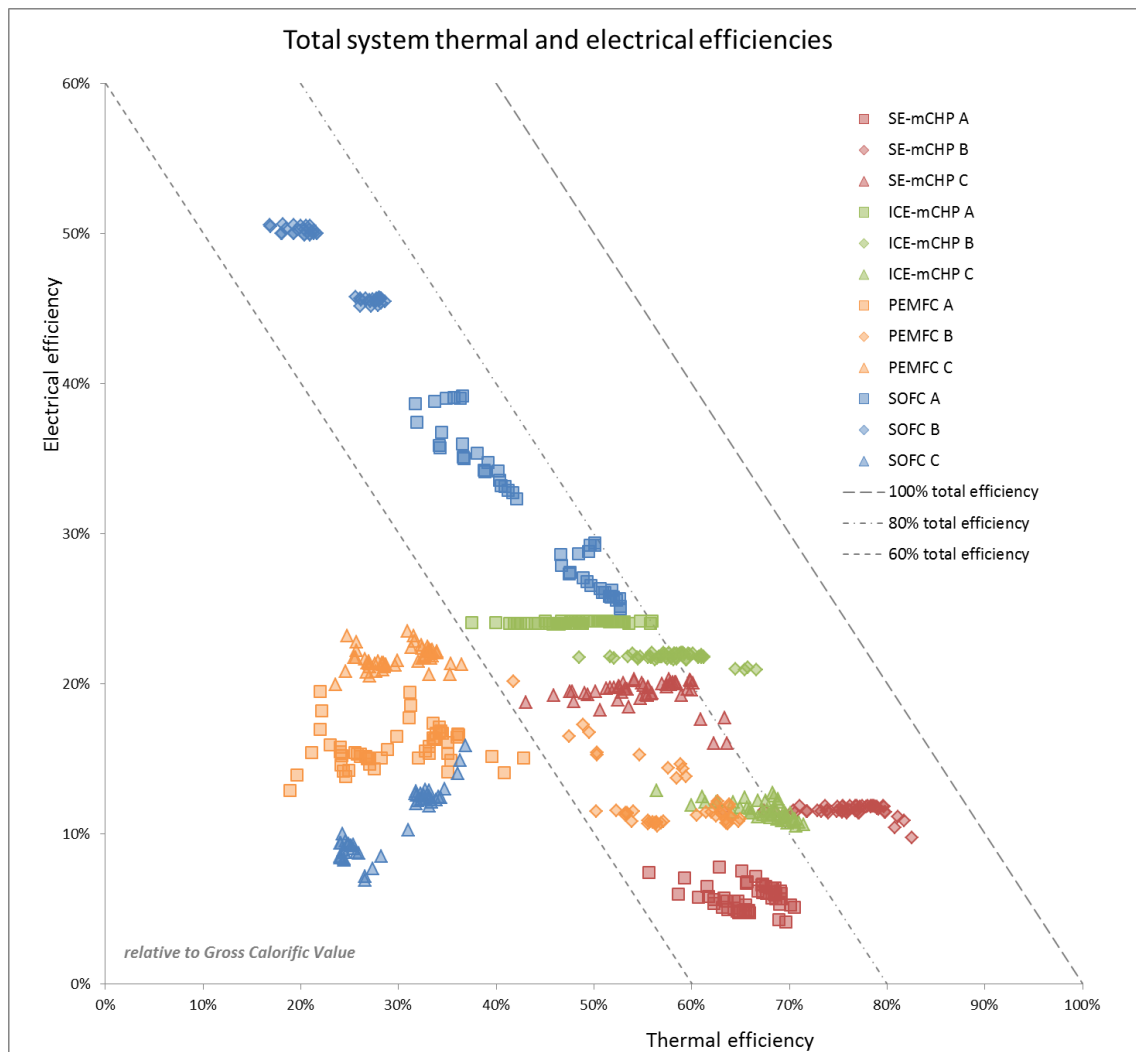
Figure 76: System efficiencies achieved with mCHP units

Given that the supplementary burner is modelled with a high thermal efficiency (90%), the effect of using it is generally to increase the thermal efficiency, slightly increase the total efficiency and decrease the electrical efficiency of the systems relative to the efficiencies of the mCHP units themselves. This effect is more significant in systems where the mCHP unit has a relatively low thermal capacity. It is most noticeable in the case of SOFC A and SOFC B which now exhibit a discernable spread of efficiencies. The two groupings which appear for each unit are due to the different thermal demands of the building types and the corresponding different proportional contribution from the supplementary burner. In the cases of ICE-mCHP C and some scenarios involving PEMFC B, the system electrical efficiencies are reduced to be approximately the same as those achieved by SE-mCHP B.

These effects can also be illustrated by comparison between the exergy efficiencies of the units and the systems. Figure 77 illustrates the exergy efficiency of four selected mCHP units and their corresponding systems under various conditions; these are plotted against the fraction of the total energy which is supplied as electrical power.
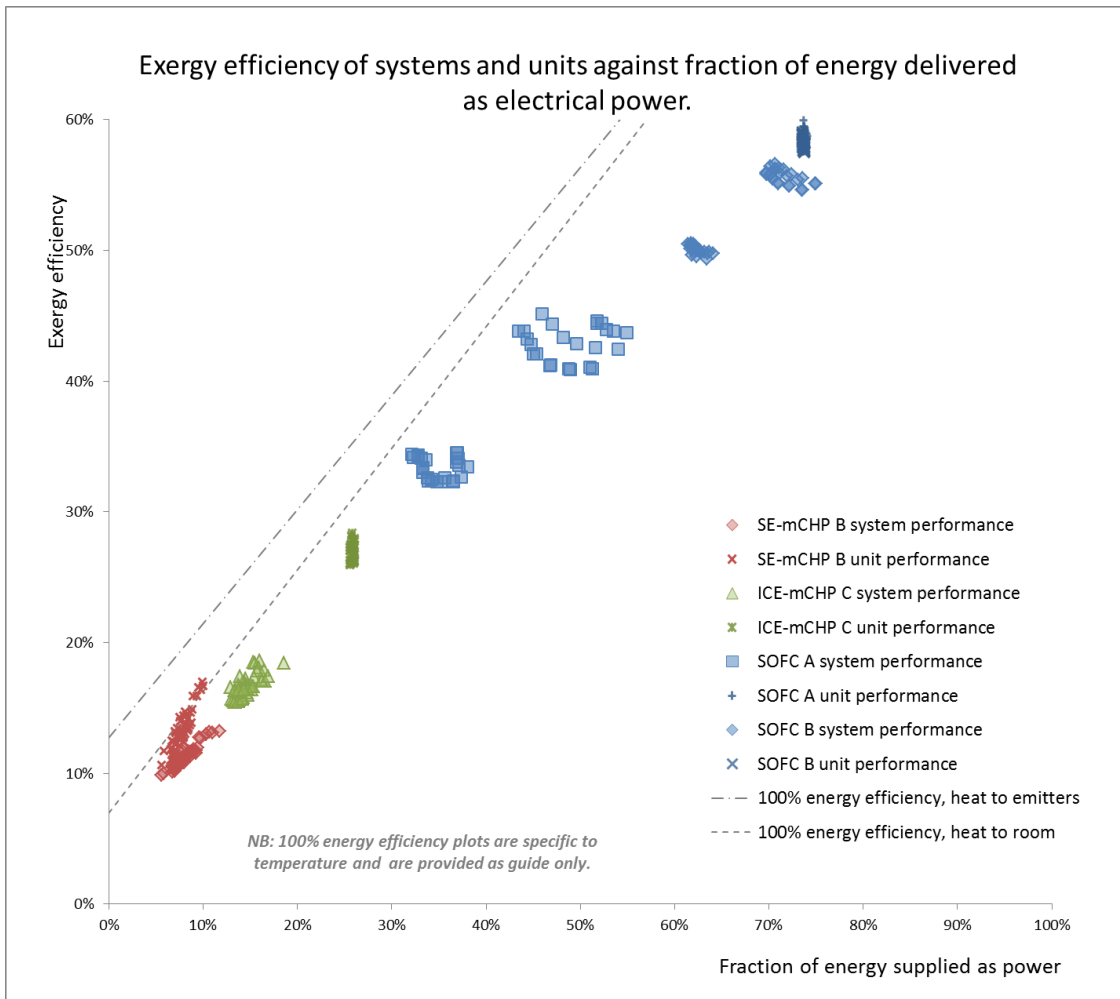
Figure 77: Exergy efficiency of selected mCHP units and systems

SE-mCHP B does not need to use the supplementary burner so only a small reduction in the exergy efficiency between the unit and the system is observed. This is primarily due to the reduction in temperature at which heat is supplied (to the inside air rather than the buffer tank). The total energy efficiency of the system based on ICE-mCHP C is similar to that of the unit itself; however, because a lower power fraction (i.e. more heat) is required, there is no way to maintain the same exergy efficiency (to do so would require more than 100% energy efficiency). The smaller SOFC unit, SOFC A is more affected than SOFC B by the inclusion of the supplementary burner energy flows as it requires proportionally more heat from it. The systems operate with a high power fraction by exporting a large proportion of the electricity generated and so exergy efficiencies of 30% to 55% are still achieved. However, if the power fraction were reduced by either a larger heat demand or by restrictions on the export of electricity then it would be impossible to maintain the same system exergy efficiency.

5.5 Comparison between mCHP units

This section uses the results from the simulations used for the overview in section 5.4 but presents more detail in terms of the CO_2 emissions and PER associated with each mCHP unit and the way in which these vary as the building properties, buffer size and control methodology are altered.

Figure 78 and Figure 79 show the range of performances of the mCHP systems, expressed in terms of the net PER associated with them.

Figure 78: PER of SE-mCHP and ICE-mCHP systems

The net PER includes a reduction corresponding to the grid electrical generation displaced by electricity generated. In these results, this is calculated using the mean generation mix method. The scale on each y-axis is the same but the different range on the SOFC graphs should be noted. The proportional control system cannot be used with a supplementary burner in this model and so results are not presented for that configuration (i.e. "configuration 1") with those units.

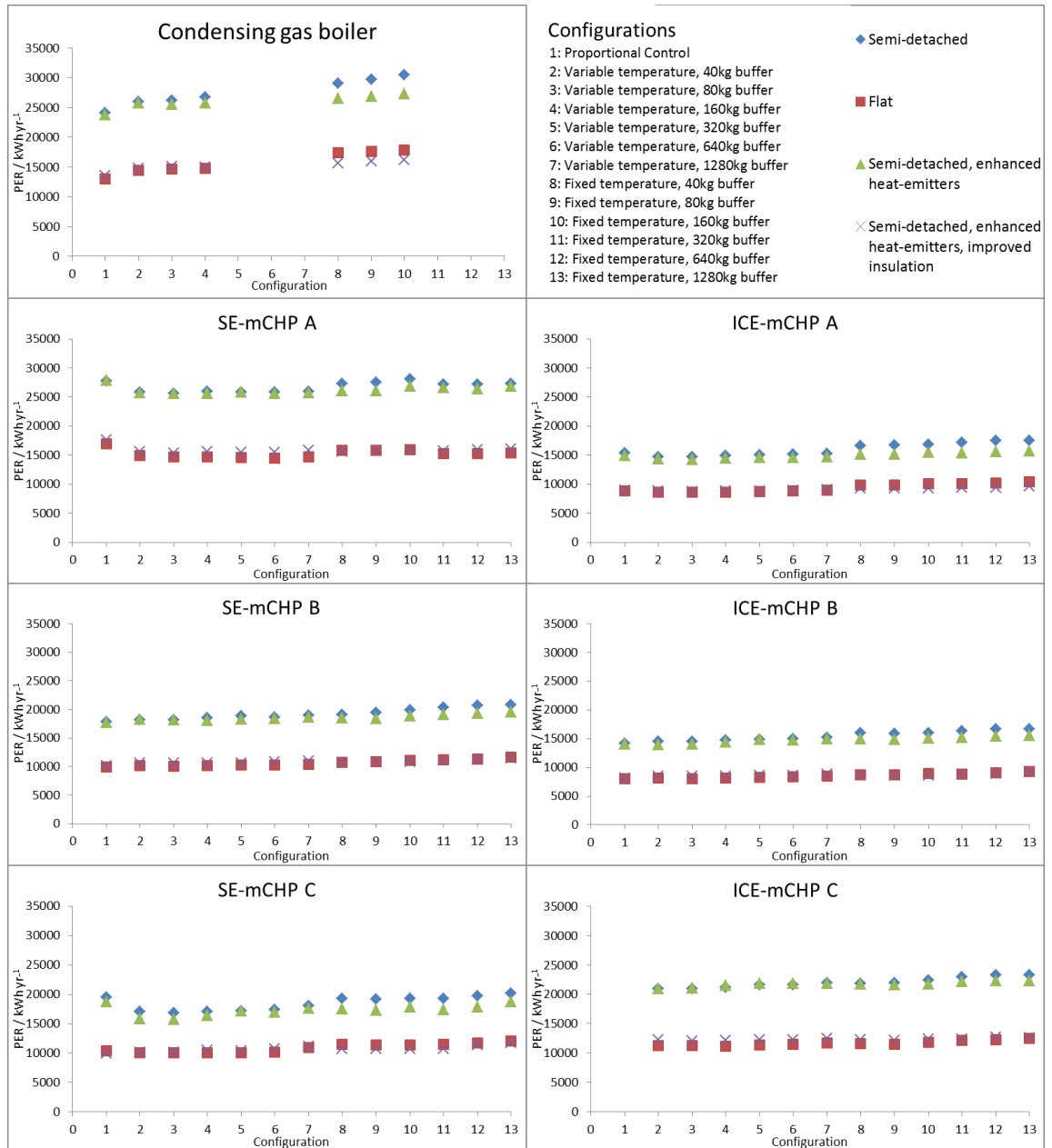Within this set of parameters, SE-mCHP A has a slightly higher PER associated with it than the gas boiler. SE-mCHP B, on the other hand, achieves a significant saving (in the order of 25%). This is surprising, given the similar nominal characteristics of SE-mCHP A and SE-mCHP B. There are four factors that contribute to the superior performance of SE-mCHP B in this modelling. Firstly, although the nominal efficiencies of the units are similar, SE-mCHP B does achieve a slightly better electrical and thermal efficiency. Secondly, SE-mCHP A requires significant power consumption (57W) for almost 30 minutes after being turned off. This is not reported for other units and so is not modelled for them; it may represent a deficiency in the model that overestimates the net electrical output from SE-mCHP B (and possibly other units) but this seems unlikely given the detailed nature of the data sources used (e.g. Lipp 2012). Another potential error is the absence of a reduced electrical efficiency during warm-up in the model of SE-mCHP B. Perhaps most significantly however, SE-mCHP B is capable of modulating its output and maintains an electrical efficiency comparable to SE-mCHP at much lower outputs. Similar explanations are appropriate to the PER associated with SE-mCHP C but this is a larger device and its relatively high electrical efficiency will be more significant.

The performance characteristics of ICE-mCHP A and ICE-mCHP B are quite similar and so the PER associated with them are also similar. ICE-mCHP B has a slightly lower PER in some cases which is largely due to its capacity to modulate. Despite having only slightly lower thermal and electrical efficiencies, the PER associated with ICE-mCHP C is generally higher, due to the use of the supplementary burner. It still achieves savings relative to the conventional boiler but these are only in the order of 10%. The PER associated with the operation of the combustion-based units is not significantly affected by the size of the buffer which they are used with, it seems that the advantage of the improved operating characteristics (for example, longer run times) is offset by larger thermal losses from the larger tanks. Unit SE-CHP A has a PER 1.2% lower when using the 640kg buffer tank compared to the 40kg buffer tank but this improvement is eliminated if a 1280kg tank is used. A similar effect is noted by Beyer & Kelly (2008).

Despite achieving high electrical efficiencies under optimum conditions, several fuel cell based mCHP units have high PERs associated with them. To understand some of the reasons for this,

the effect of alternative operating regimes on the performance of PEMFC C, SOFC A and SOFC B are explored in more detail in the next section (5.6).

The PERs associated with PEMFC A and PEMFC C can be seen to decrease (by approximately 15% and 8% respectively) when used with the enhanced heat emitters (variable temperature control with 40kg buffer configuration). This is primarily due to the improved thermal efficiency of the units when operating at lower flow temperatures. It is possible that in practice a similar efficiency improvement would be observed with PEMFC B but insufficient data was available to calibrate the effect of a lower flow temperature on the thermal efficiency of the unit. However, the proportionally large contribution to heating from the supplementary burner used with PEMFC B is likely to reduce this effect.
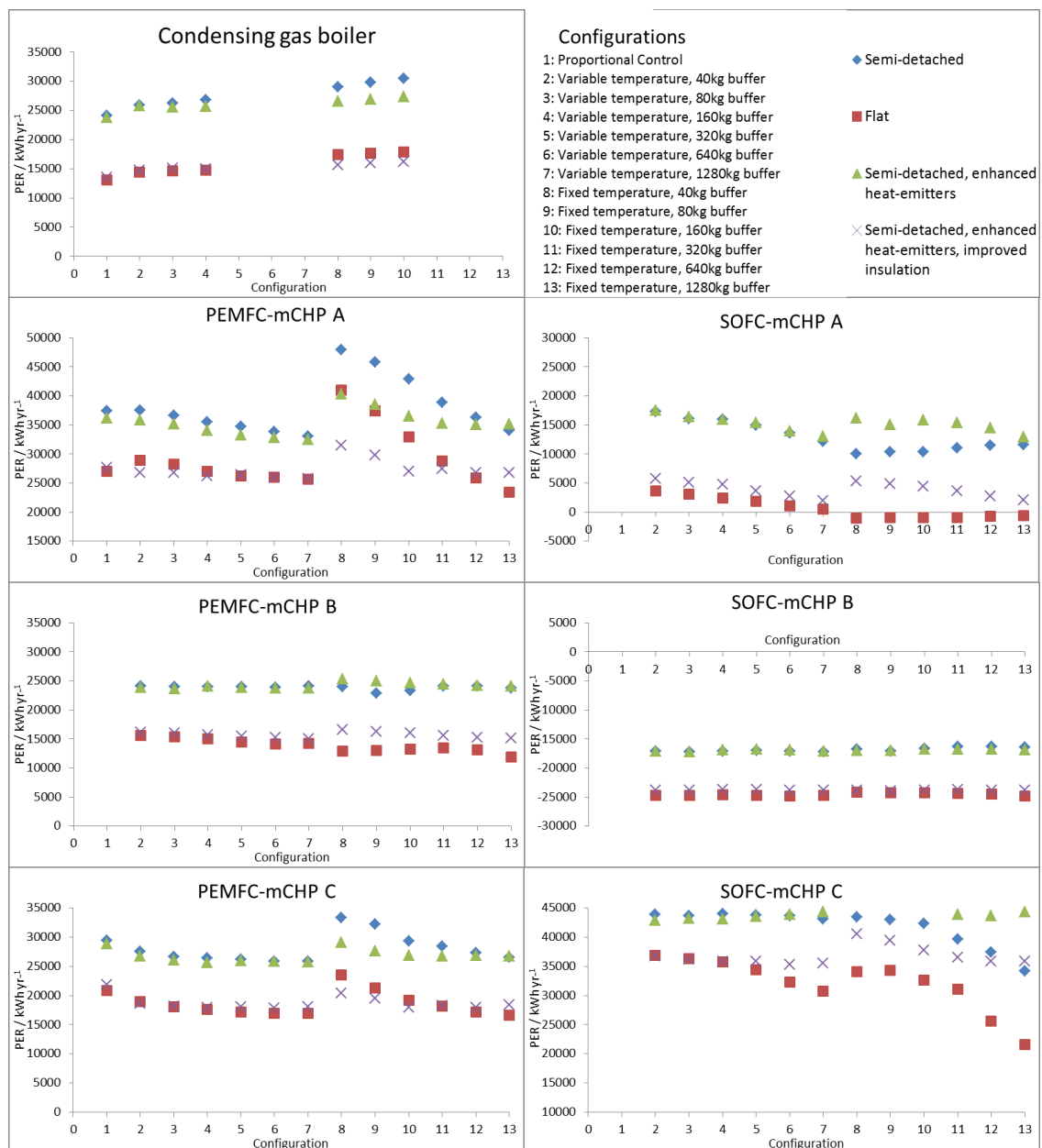
Figure 79: PER of PEMFC-mCHP and SOFC-mCHP systems

5.6 Fuel Cell mCHP alternative operating characteristics

Given the variation in the performance achieved by the fuel cell units, several alternative operating regimes for SOFC A, SOFC B and PEMFC C have been investigated and the results are presented in this section.

For SOFC A and SOFC B, five alternative operating regimes have been modelled. The resulting electrical efficiencies of the units and the systems (i.e. including supplementary burner fuel) are illustrated for SOFC A and SOFC B in Figure 80 and Figure 81, respectively.
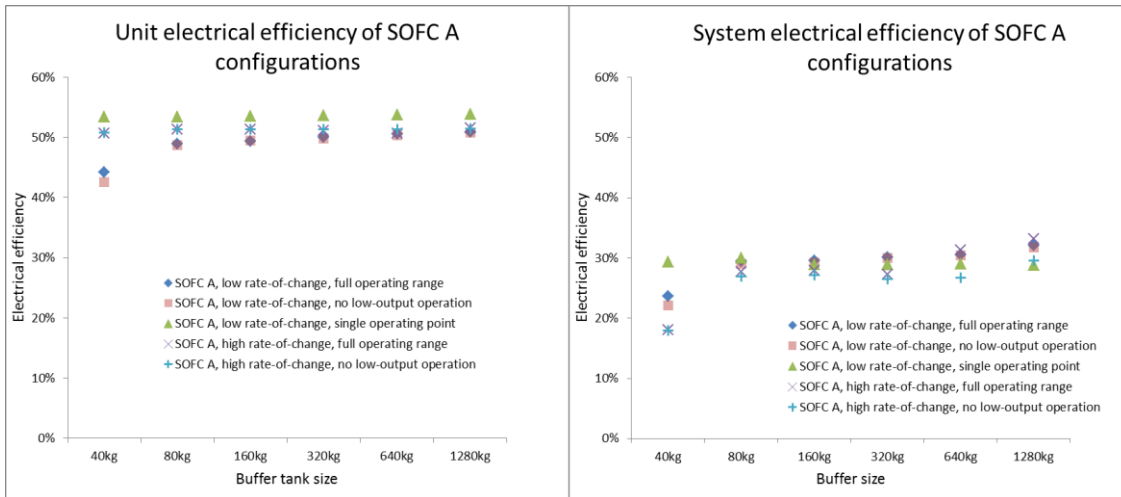
Figure 80: Electrical efficiency of SOFC A
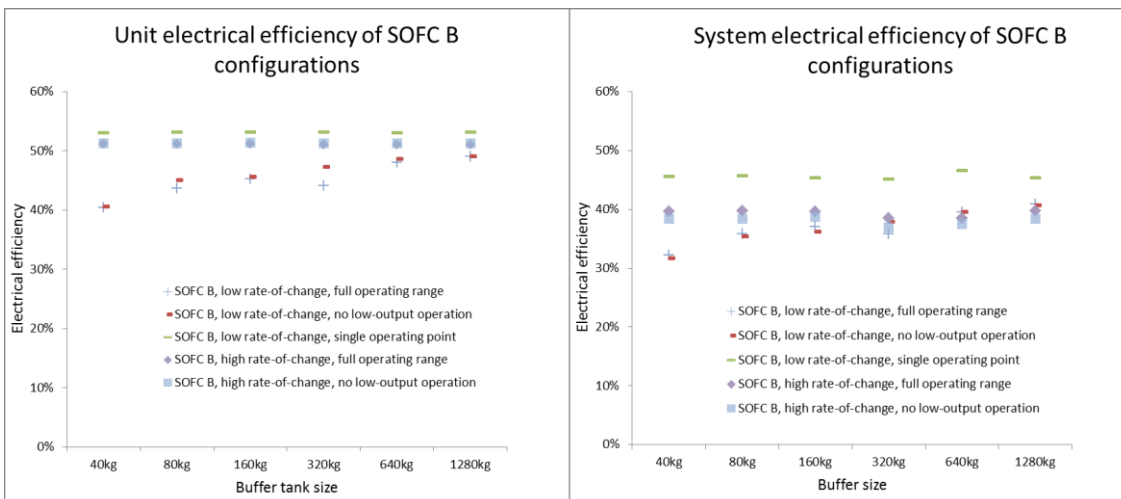
Figure 81: Electrical efficiency of SOFC B

Four of the regimes consist of the units operating either with or without restrictions on the rate-of-change of their output and either allowing them to operate across their full range or restricting their low output operation (i.e. the units are not allowed to operate with a heat output less than 50% of their capacity). The fifth modelled regime is running the units continuously at

their peak electrical efficiency. These permutations are modelled with the conventional semi-detached building and six buffer sizes from 40kg to 1280kg.

With either system, the main issue reducing the electrical efficiency of the unit is time warming up and cooling down at less than optimal electrical efficiency. This is mitigated by a large buffer tank as it requires less cycling of the unit or by hypothetically increasing the maximum rate of change that the unit can achieve as this results in less time being spent at the sub-optimal conditions. The best efficiency is, of course, achieved by running the unit consistently at its optimum efficiency. The system electrical efficiency is reduced by the additional fuel used by the supplementary burner. In the case of SOFC A, a system electrical efficiency of just over 30% can still be achieved with the smallest buffer. The system electrical efficiency of a system with a large buffer tank could feasibly exceed this as less fuel is needed by the supplementary burner; alternatively if the rate-of-change of output of the unit is unrestricted, a system electrical efficiency of around 35% might be achieved. In the case of SOFC B, the smaller supplementary heating requirement results in a higher system electrical efficiency; in the case of unit being operated continuously the system electrical efficiency just exceeds 45%. With buffer tank sizes greater than 320kg, it appears that the units with a lower maximum rate-of-change achieve a higher efficiency than those with an unrestricted rate of change. This is perhaps due to the slower units not leaving their optimal output range before a greater or lesser heat demand changes the direction in which their output is trending. It illustrates that in practice, the units may require complex operating logic that does not only consider the optimum performance of the unit but also how its output affects other systems.

The high electrical efficiency of these SOFC-mCHP units makes the overall impact of their operation sensitive to the way in which electricity is generated by the grid. Figure 82 shows the PER and CO_2 emissions associated with each of the devices in each configuration if it were operating within the current grid, and the "Transition Pathways Thousand Flowers" scenarios for 2020 (TF2020), 2035 (TF2035) and 2050 (TF2050) (see chapter 4, section 4.6.3).

The results for the current grid follow a similar pattern to the system electrical efficiency results. By operating SOFC B continuously, the net PER and CO_2 emissions are effectively negative as the PER and CO_2 emissions saved due to the avoided grid electrical generation more than offsets the impacts due to the operation of the unit. In fact, all configurations of SOFC B result in negative net CO_2 emissions and most configurations can achieve a negative net PER if the buffer tank is larger than 300kg. With SOFC A, very low net CO_2 emissions can be achieved if it is operated continuously or if a large buffer tank is used.
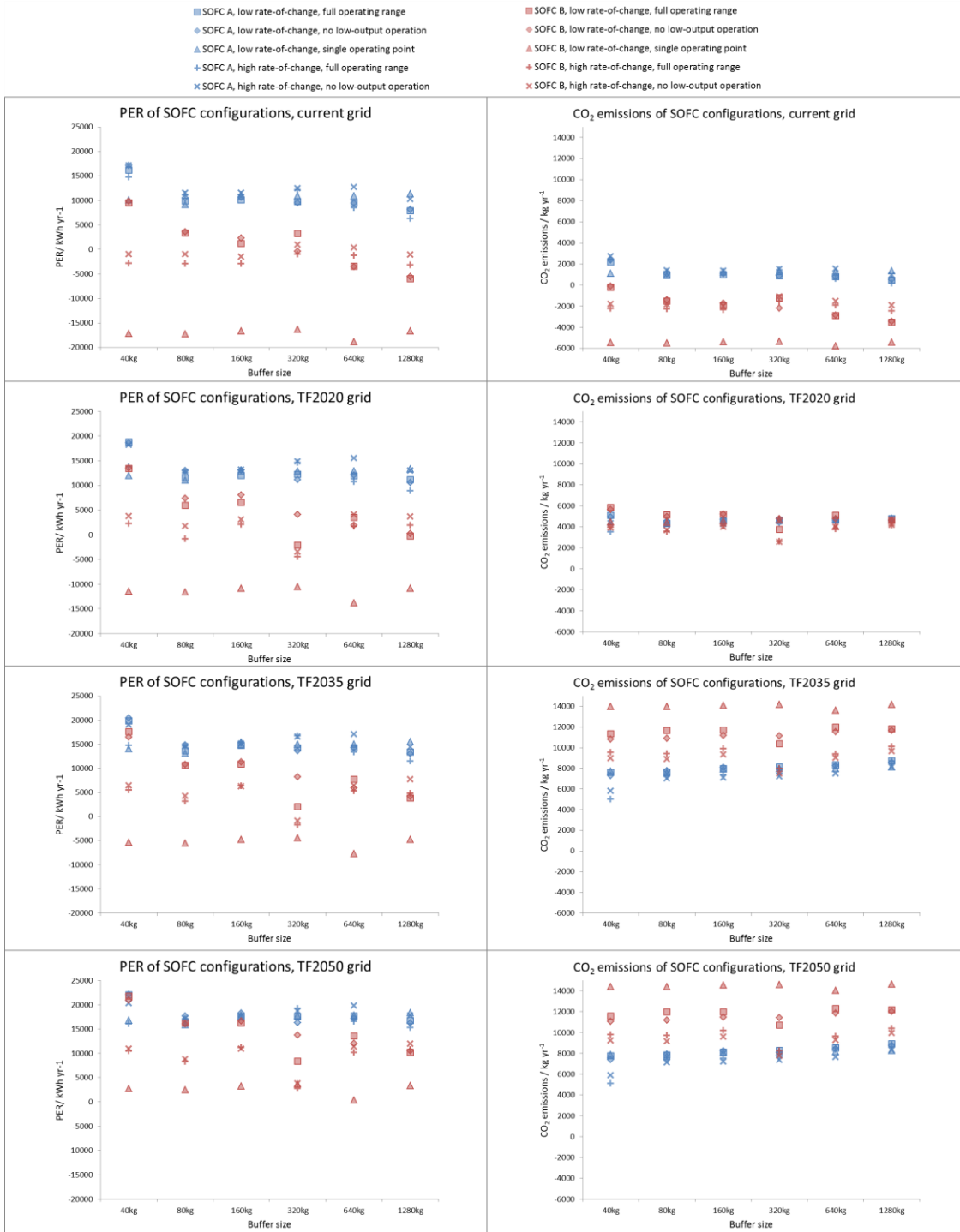
Figure 82: PER & CO₂ emissions from SOFC-mCHP systems

TF2020 has a more efficient grid generation mix with lower emissions associated with it. The savings from each SOFC are reduced, with the units which operate continuously affected the most (as they rely on the savings associated with displacing the generation of electricity by the grid). The PERs of the SOFC A configurations are all quite consistent. SOFC B still achieves a significant negative net PER if operated continuously. Because of the reduced CEF for the grid, both units have approximately the same CO_2 emissions associated with them in each configuration. These are comparable to those which would occur with a condensing gas boiler.

With the TF2035 grid, PER reductions still occur with SOFC B operating continuously but these configurations actually incur the highest CO_2 emissions (now almost three times the emissions which would occur with a condensing gas boiler). The PER in the majority of the other configurations has increased relative to TF2020 but not significantly. The CO_2 emissions from SOFC A are also significantly higher than those from a condensing boiler and are consistent across the different configurations. The grid PER and CO_2 emissions factors are only slightly improved between TF2035 and TF2050 so the results for the SOFC units are slightly worse but follow the same general patterns.

It seems that continuous operation is the best option (of those considered) for both SOFC units at the present. If operated in a context with a grid CEF lower than that in TF2020 (i.e. just under $300g_{CO2}/kWh$), then other operating regimes have the potential to result in lower CO_2 emissions but these will exceed those associated with a condensing gas boiler. The limit on the rate-of-change imposed upon the SOFC units does not appear to be a constraint on their performance in the scenarios for which it is beneficial to use the units.

PEMFC C was modelled with seven variations on its unit parameters in addition to its default properties, again supplying heat to the semi-detached building. Four increased maximum rates-of-change were simulated (twice, five times, 10 times and 20 times the default rate). As PEMFC C achieves maximum electrical efficiency with a thermal output lower than its peak heat capacity, a simulation was conducted with output limited to the point at which peak efficiency occurs in the hope that the unit would operate at this point for a greater proportion of the time. The sixth variation simulated was to operate the unit continuously at its peak electrical efficiency and the seventh option was similar, allowing the output to decrease below this level but not to turn off completely. Resultant average electrical efficiencies, PER and CO_2 emissions are shown in Figure 83, Figure 84 and Figure 85 respectively.
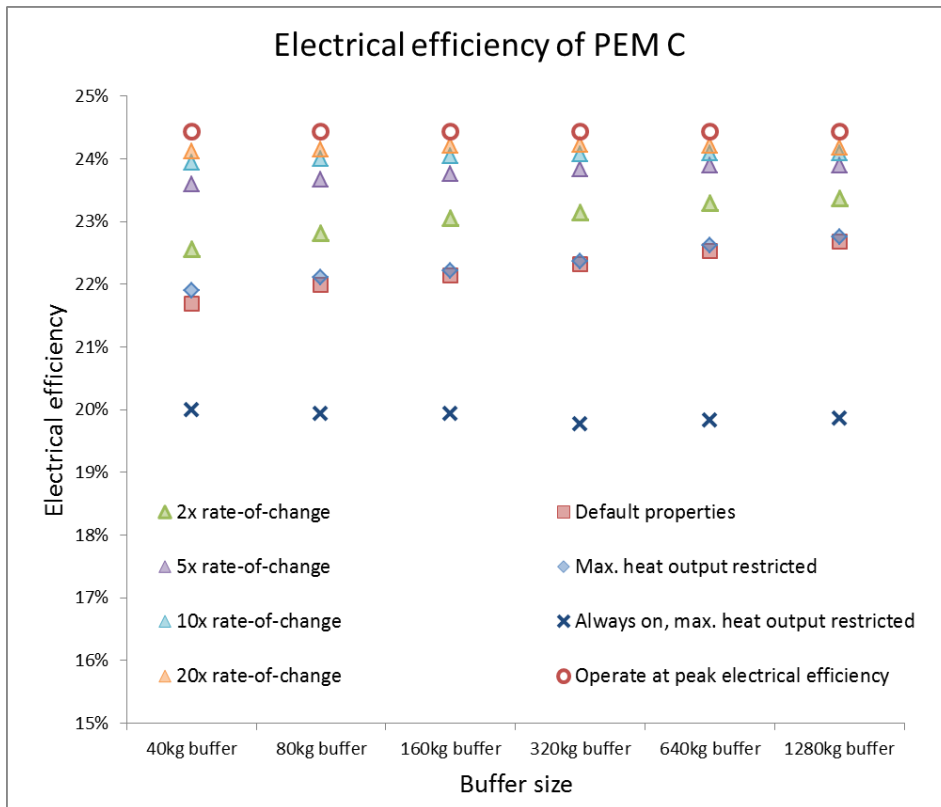
Figure 83: Electrical efficiency of PEMFC C with alternative unit parameters
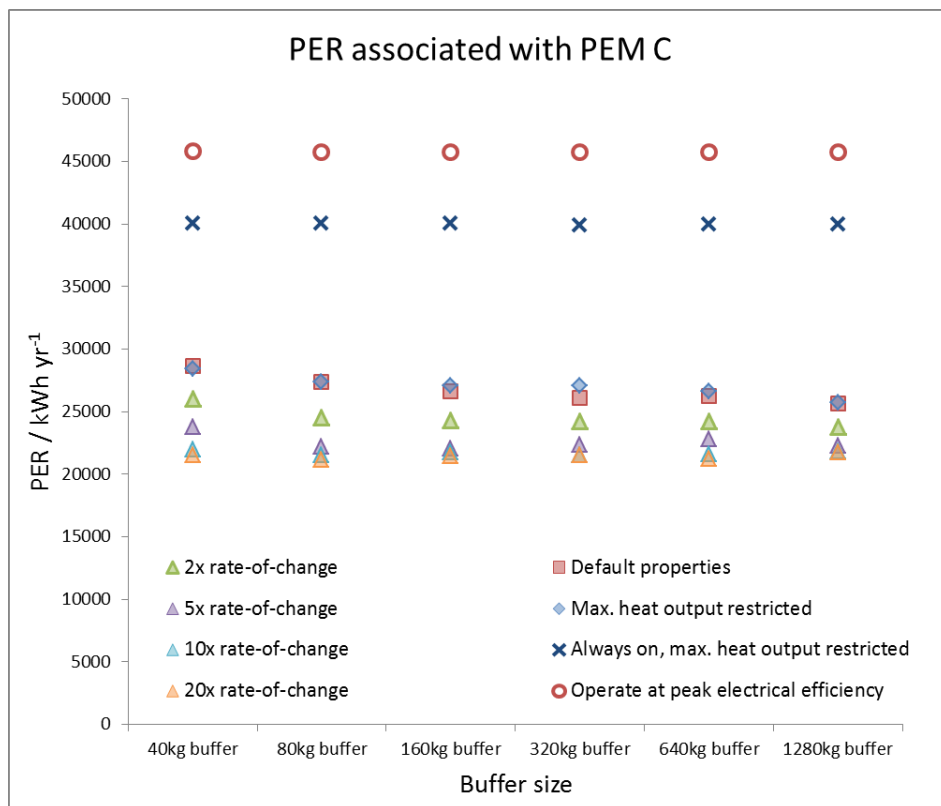
Figure 84: PER of PEMFC C with alternative unit parameters
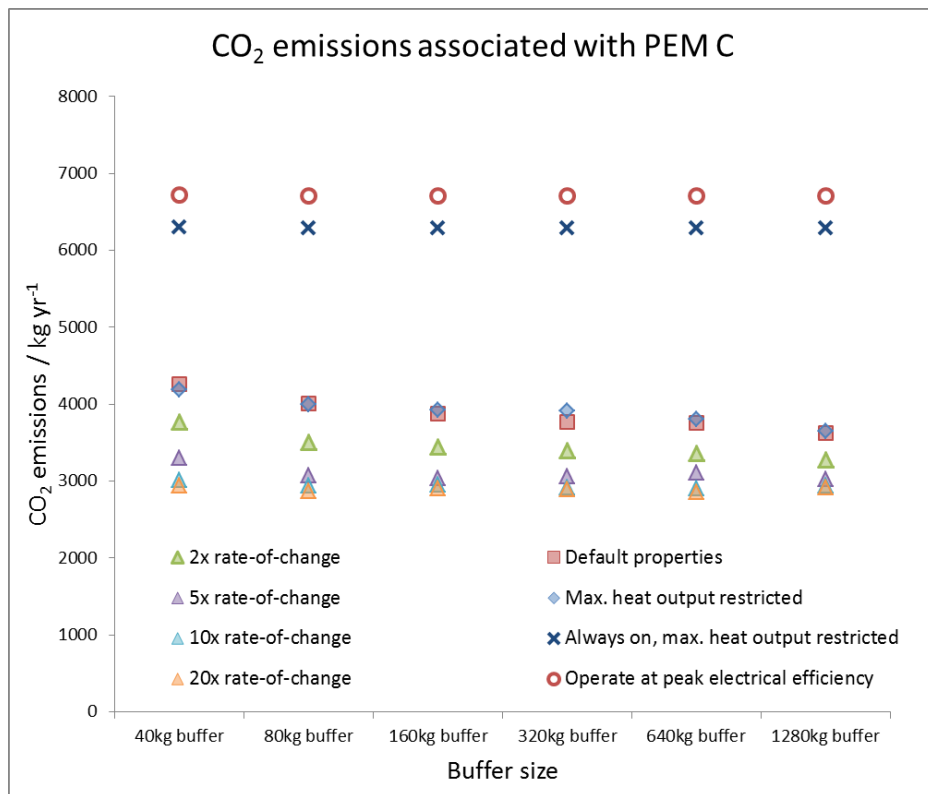
Figure 85: CO$_2$ emissions associated with PEMFC C with alternative unit parameters

The operating modes in which the PEMFC-mCHP unit is not allowed to turn off are clearly ineffective, resulting in much higher PERs and CO$_2$ emissions. The electrical efficiency of the PEMFC-mCHP units is not high enough to justify their use if the thermal energy produced cannot also be used effectively. Increasing the rate-of-change which the unit can accommodate does improve the overall performance of the system but there are relatively small returns for increasing the rate of change above 25W/s in this case (equivalent to ramping from minimum to maximum output in around four minutes) and only very small improvements above 50W/s. Using a larger buffer tank improves the performance of the system but not to the same extent as the hypothetical improvements in the rate-of-change. Using a larger buffer tank enables the PEMFC-mCHP units to operate at a reasonable output (i.e. achieving high electrical efficiency) for longer rather than cycling between high and low output levels (both of which entail lower electrical efficiencies).

5.7 Effect of alternative temperature programme profiles

It is unlikely that all occupants will wish to maintain an inside air temperature of 21°C continuously. This section will look at the effect of using the three alternative temperature profiles listed in section 4.3.1 (page 81). The first profile is the default (continuous), the second profile considers a night-time setback and the third profile is continuous at 18°C.

It may be that occupants find that a cooler air temperature with additional radiant or other local heating provides equivalent thermal comfort to air maintained at 21°C. The research to determine the parameters which might achieve this are well outside the scope of this study but it is hoped that identifying the effect of using the lower temperature programme (18°C) will indicate the scope for such a study.

The performance of two ASHP units (ASHP B and ASHP H) and four mCHP units (SE-mCHP B, ICE-mCHP B, SOFC A and SOFC B) have been simulated as these cover the range of characteristics which are of most interest. These are modelled with the semi-detached house and the semi-detached house with improved insulation and heat emitters. The units which perform well with proportional control (the ASHPs and SE-mCHP) are modelled with proportional control and variable-temperature control with a 160kg buffer tank. The other units which are less suited to proportional control are modelled with both an 80kg buffer tank and a 320kg buffer tank. The SOFC units operate continuously at their optimum electrical efficiency while ICE-mCHP B and the supplementary burners for the SOFC units use variable-temperature control.

Figure 86 shows the variation in heat supplied under each permutation. This is quite consistent between units apart from the SOFC units which generate a surplus of heat. In most cases, slightly more heat is generated when the larger buffer tank is installed. As might be expected, there is a reduction in the heating demand as the average air temperature is reduced. The houses with night-time setback have around 85% of the heat demand of the houses maintained at 21°C and the houses maintained at 18°C have around 75% of the heat demand. The saving is slightly less in the better insulated houses as DHW demand (which is unaffected) forms a larger proportion of demand.
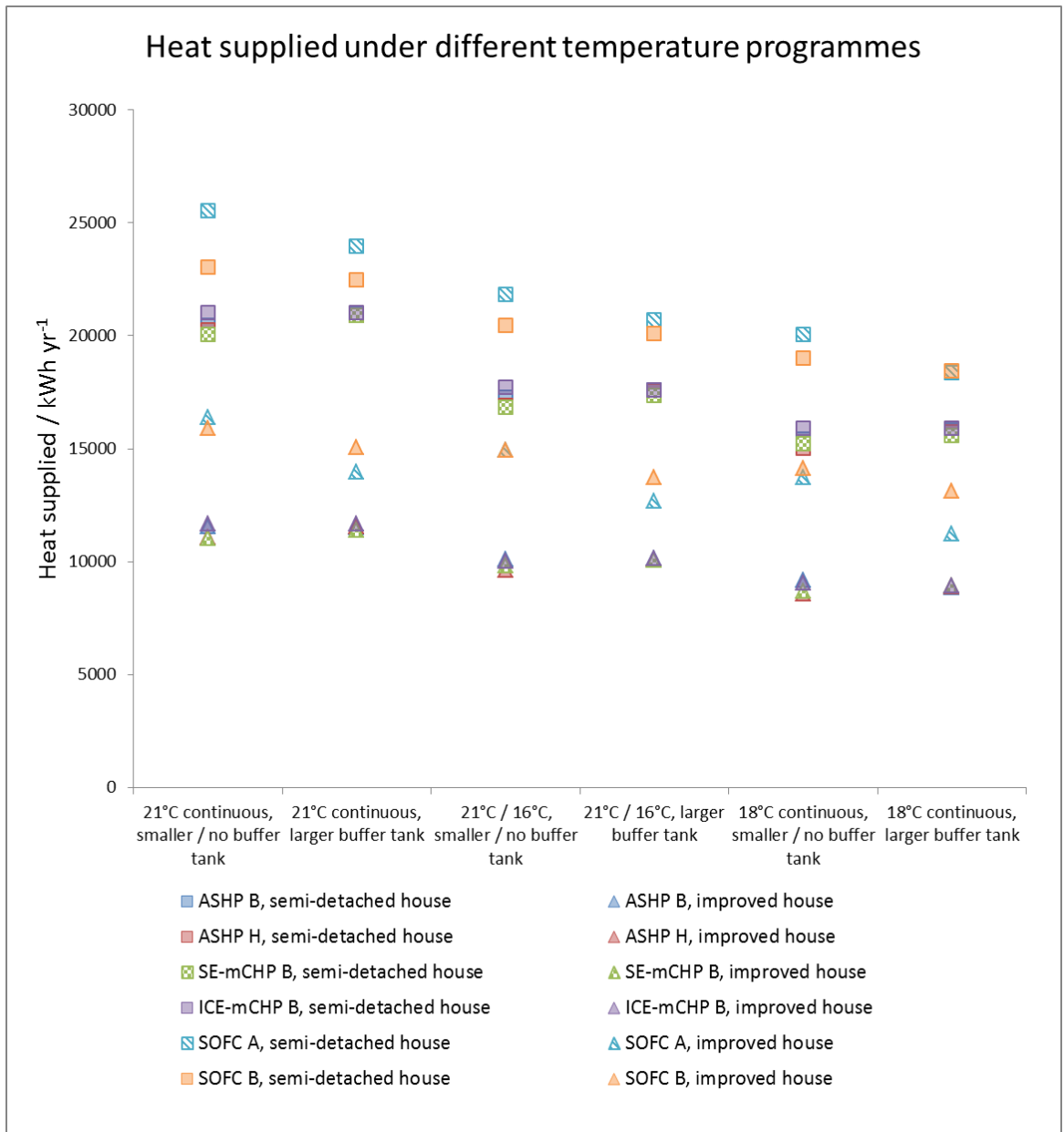
Figure 86: Heat supplied under different temperature programmes

The net PER and CO_2 emissions associated with SOFC B are strongly negative (Figure 87). They both decrease (i.e. become more negative) as the average inside air temperature and associated heat demand decrease as this reduces the demand for the supplementary burner to operate.

The PER and CO_2 emissions associated with the other systems are shown in Figure 88 and Figure 89 respectively.
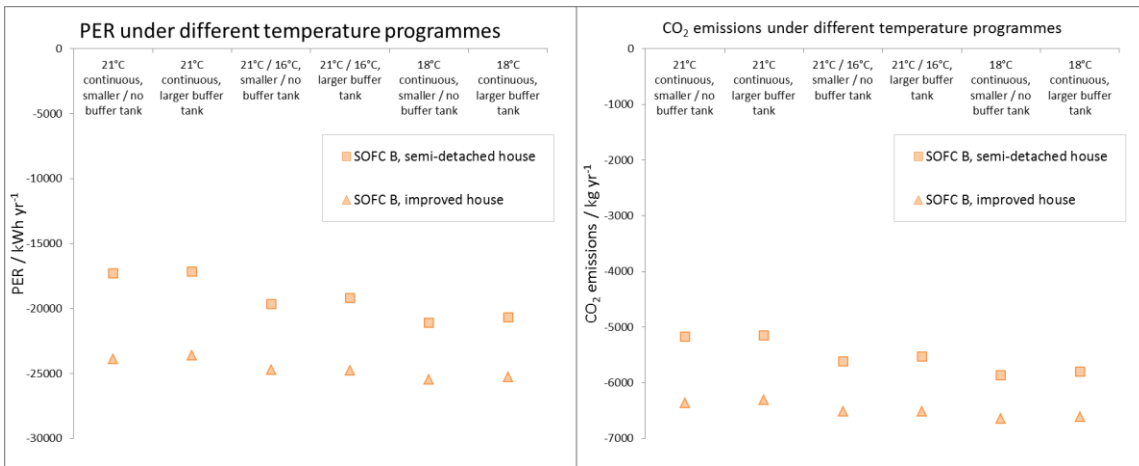
Figure 87: Effect of temperature programme on SOFC B performance
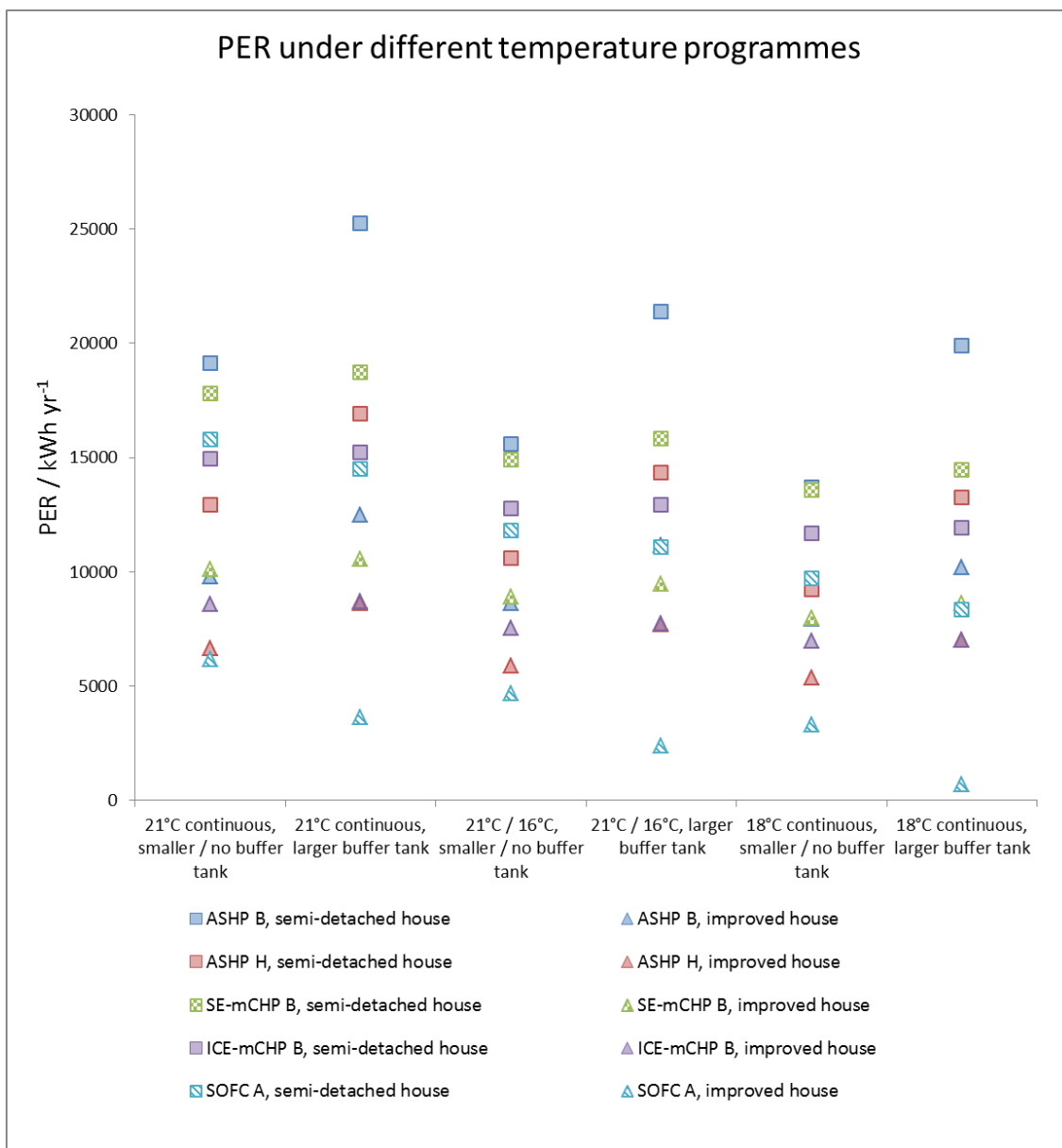
Figure 88: Effect of temperature programme on PER of selected units
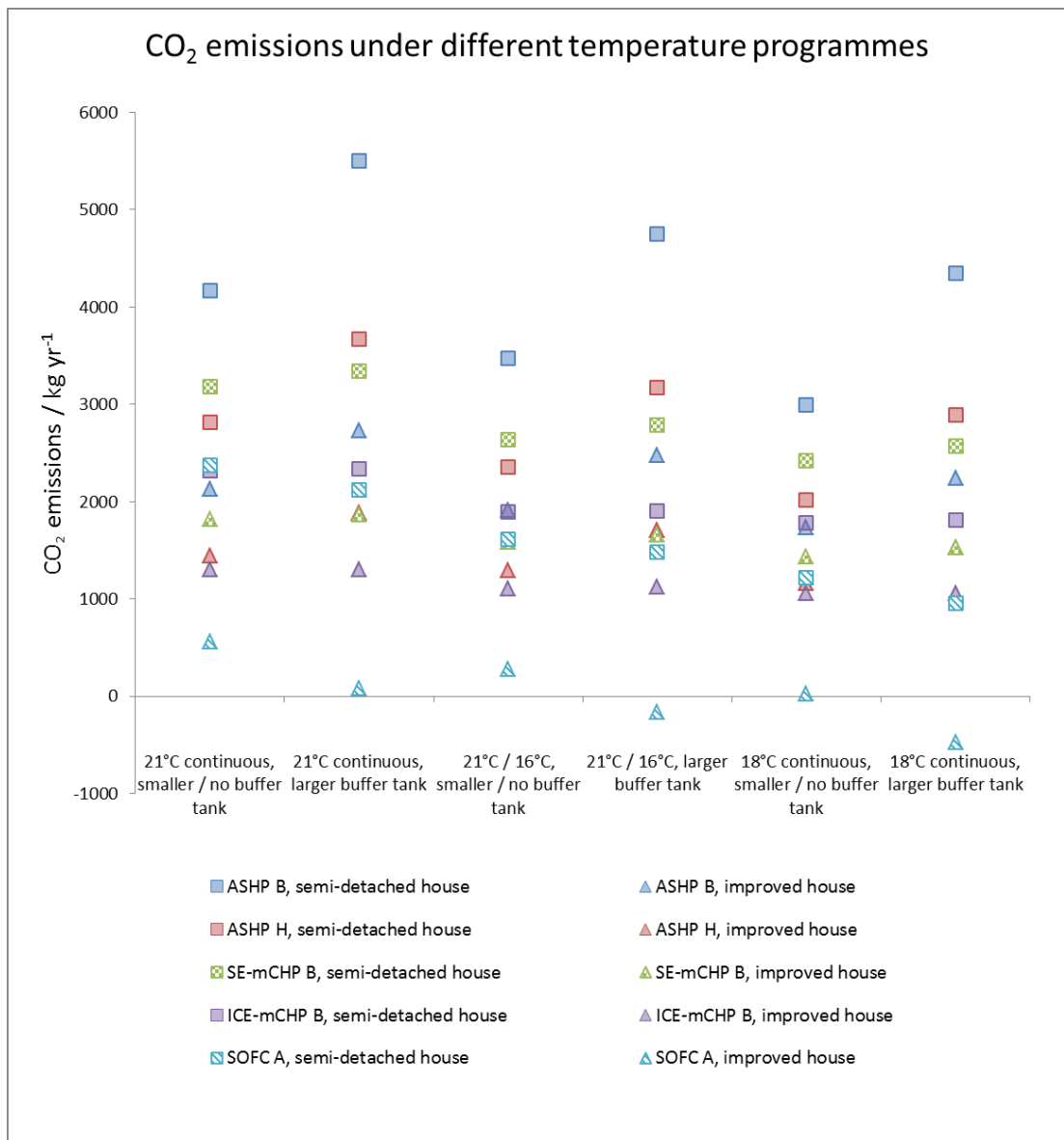
Figure 89: Effect of temperature programme on CO_2 emissions from selected units

The performance of SOFC A largely reflects that of SOFC B but with a proportionally greater effect from the supplementary burner which decreases in the better insulated house and in the scenarios with the lower average internal air temperatures.

The CO_2 emissions from the two combustion-based mCHP units also reduces as heat demand decreases but the effect is slightly less marked for the temperature profile with the night-time set-back compared to the other heating units. This may be due to additional heat losses as the temperature profile transitions to the cooler period. However, the effect is small and does not affect the overall trend.

The power demand of the ASHPs decreases with the reduced heat demand. It is worth noting that even with the default, continuous warmer temperature programme, the ASHPs with the

proportional control system have lower PER and CO_2 emissions than those with the cooler temperature programmes using variable-temperature control. Interestingly, the COP of the ASHPs operating in the improved buildings (i.e. improved insulation and heat emitters) decreases as the average inside air temperature decreases while the COP of the ASHPs operating in the standard buildings increases as the average inside air temperature decreases (see Figure 90). A lower internal air temperature will tend to improve the COP of ASHPs by decreasing the flow temperature which is required (as less heat is required and the flow temperature to achieve a reasonable temperature differential is reduced). However, the heating season will be shorter, covering a period in which the average outside air temperature is cooler, decreasing the COP of ASHPs. Another factor affecting the performance of an ASHP when night-time setback is used, is the period of typically an hour in which the heat delivery rate (and therefore flow temperature) is increased in order to achieve the increase in inside air temperature at 07:00.
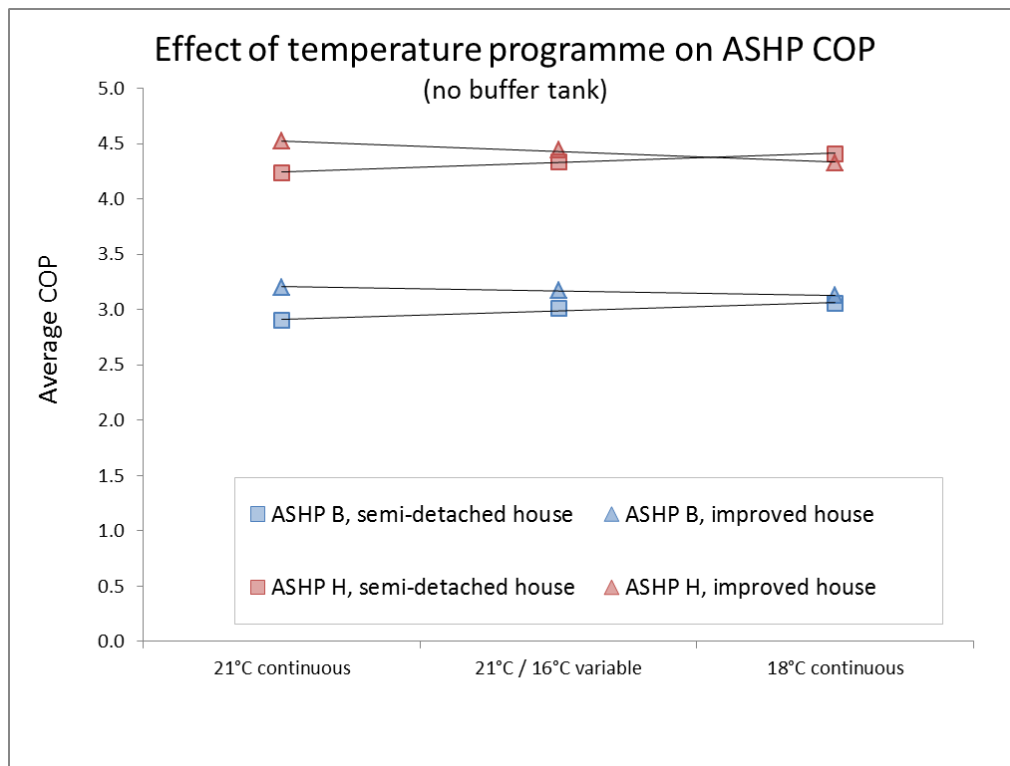
Figure 90: Effect of temperature programme on ASHP COPs

5.8 Effect of climate

This section considers the effect that climate has on the performance of heating units by simulating them with Test Reference Year (TRY) data typical for Glasgow, London, Cardiff and Loughborough. TRY data representative of the present has been used along with data obtained which is modelled to be representative of median estimates of the climate in those locations in the 2030's and the 2050's. Eight units are considered: ASHP A, ASHP B, ASHP H, SE-mCHP B, ICE-mCHP B, SOFC A and SOFC B. Each simulation was repeated with the model of the conventional semi-detached house and the semi-detached house with improved insulation and enhanced heat emitters. The PERs calculated in this section do not include the effect of changes to the grid generation mix between the present and 2050.

The annual heat supplied by the units to the conventional semi-detached house is plotted in Figure 91 against the corresponding mean ambient air temperature.
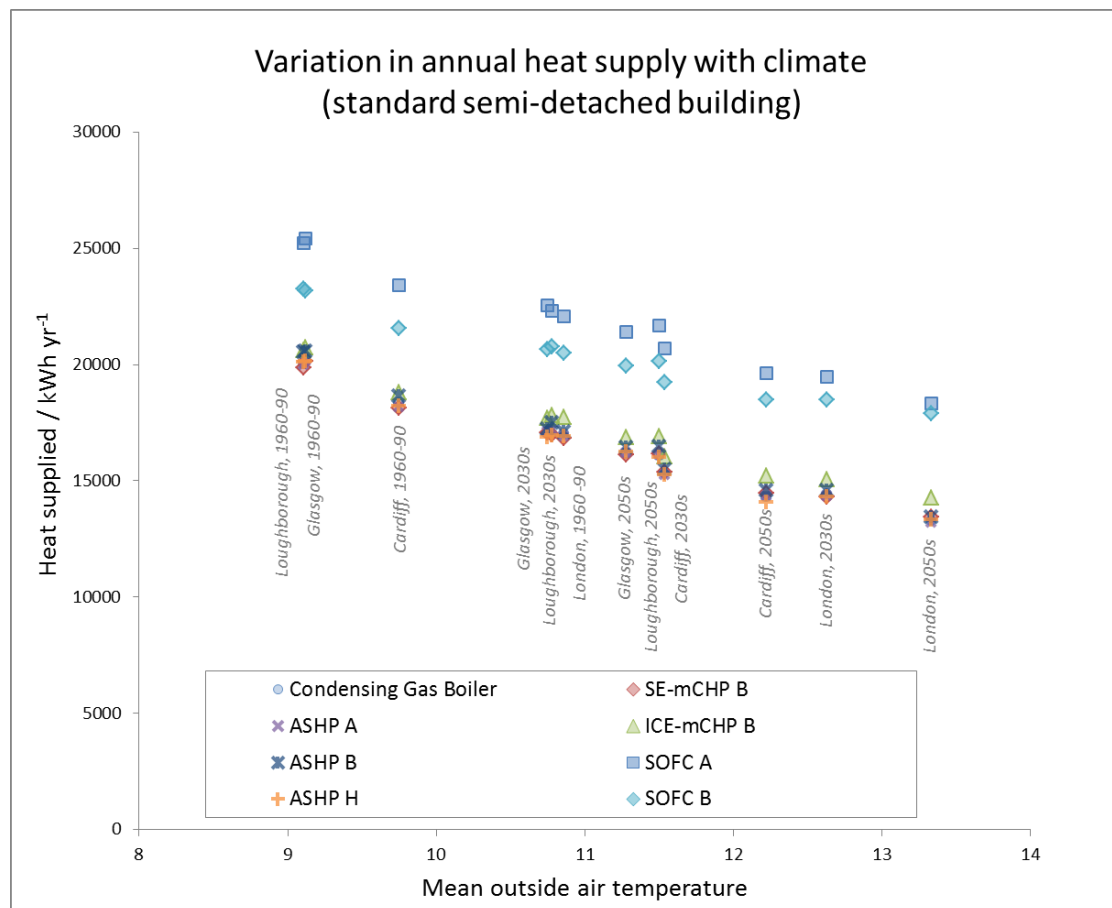
Figure 91: Effect of climate on heat delivered to semi-detached house

As with previous results, the SOFC units generate surplus heat but there is a clear trend of warmer outside air temperatures leading to a decrease in the heat supplied. There are a few minor anomalies to this trend; the heat demand in Loughborough slightly exceeds that in

Glasgow despite a slightly warmer average air temperature. This is probably due to the distribution of temperatures being more even in Glasgow (a coastal city, see Figure 39, with a temperature standard deviation of 5.7°C to 5.9°C) than in Loughborough (temperature standard deviation of 6.2°C to 6.4°C). A location which experiences a greater range of temperatures will have more cold days and hot days for a given average temperature. This effect increases if the heat supplied to the semi-detached house with improved insulation is considered as its heating demand is proportionally more weighted to the coldest days, Figure 92:
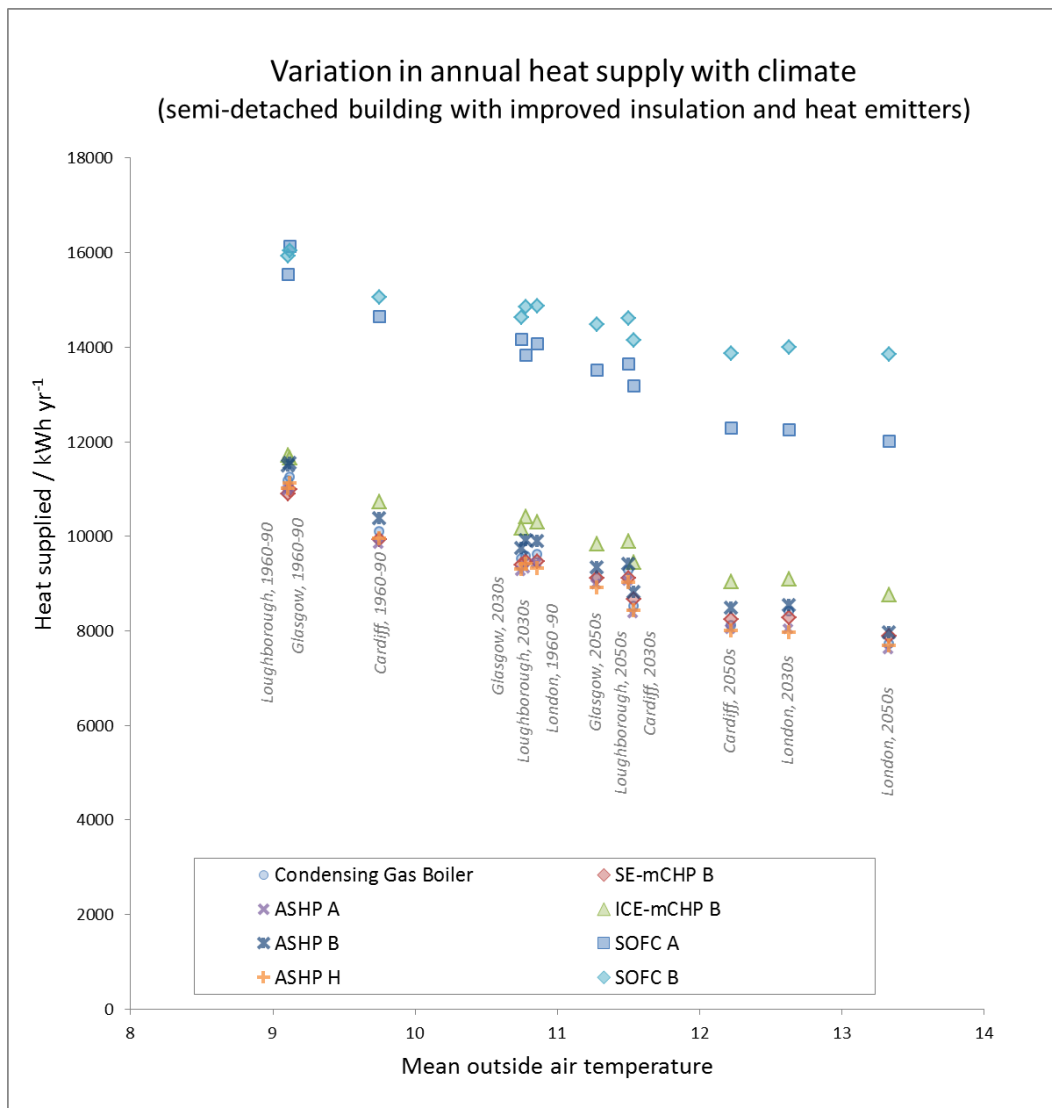
Figure 92: Effect of climate on heat delivered to improved house

When considering the PER of SOFC B, this tendency for more consistent climates to have lower heating demands is amplified by the fact that the unit supplies constant baseload heat (Figure 93). The PER (in the conventional house) is 10% to 15% higher in Loughborough than Glasgow despite the average air temperature being typically slightly lower in Glasgow. Similarly, the PER in Cardiff (temperature standard deviation 5.6°C to 5.9°C) is consistently

lower than that in central London (temperature standard deviation 6.0°C to 6.4°C) despite lower average air temperatures in Cardiff.
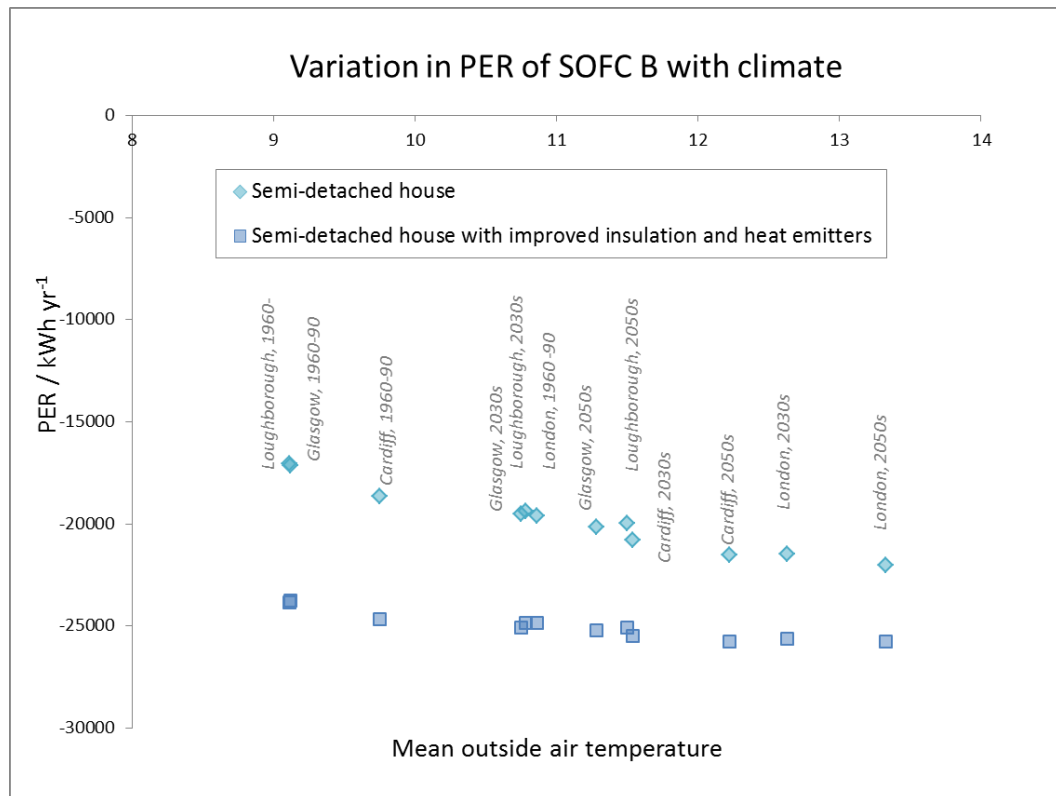
Figure 93: PER of SOFC B in different climates

The same trend (but less pronounced) can be seen in the COP of ASHPs in conventional semi-detached houses (Figure 94) but is not significant in ASHPs installed in houses with improved insulation and heat emitters (Figure 95).

Interestingly, the average COP of the highest performing ASHP (the hypothetical ASHP H) actually decreases very slightly with increased ambient air temperatures. This is possibly due to the combination of little potential for reduction of the ASHP flow temperature along with the larger range of temperatures anticipated for the future climates.

The PER of SE-mCHP B, ICE-mCHP B and SOFC A follows the same pattern as the heating demand for each location when used in the standard semi-detached house; there is no clear pattern regarding the actual performance of each unit (Figure 96). When used in the house with improved insulation, the increased variability of the heat demand is reflected in the PERs of the units (Figure 97).
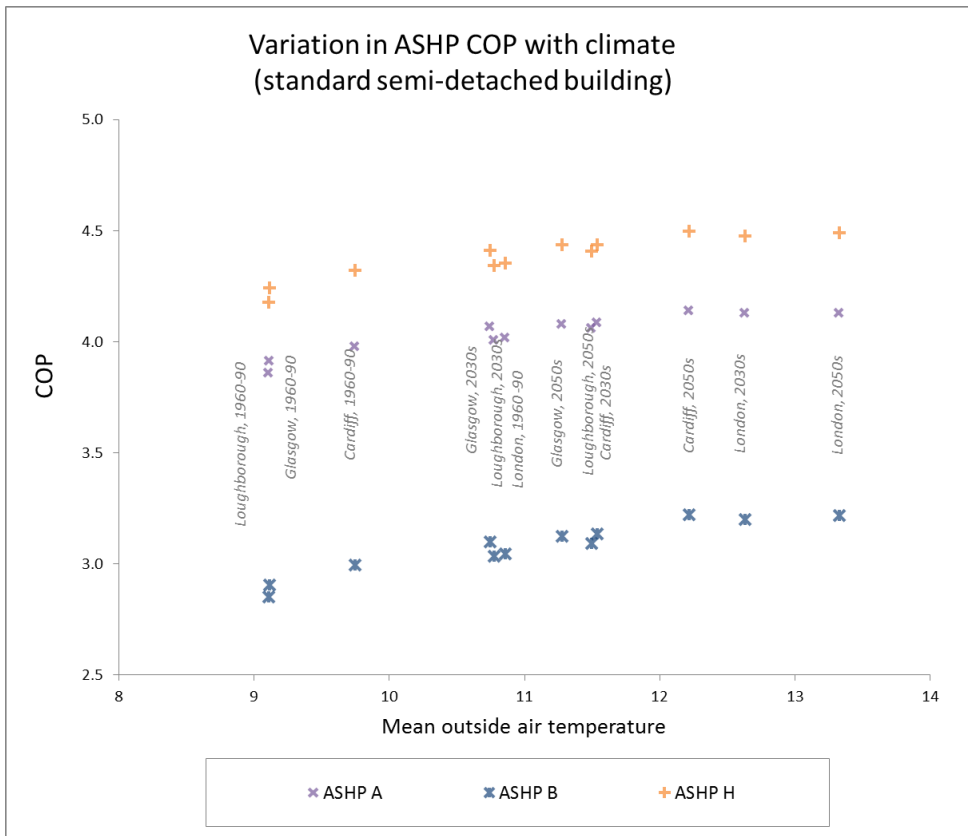
Figure 94: Effect of climate on ASHP average COPs (standard house)
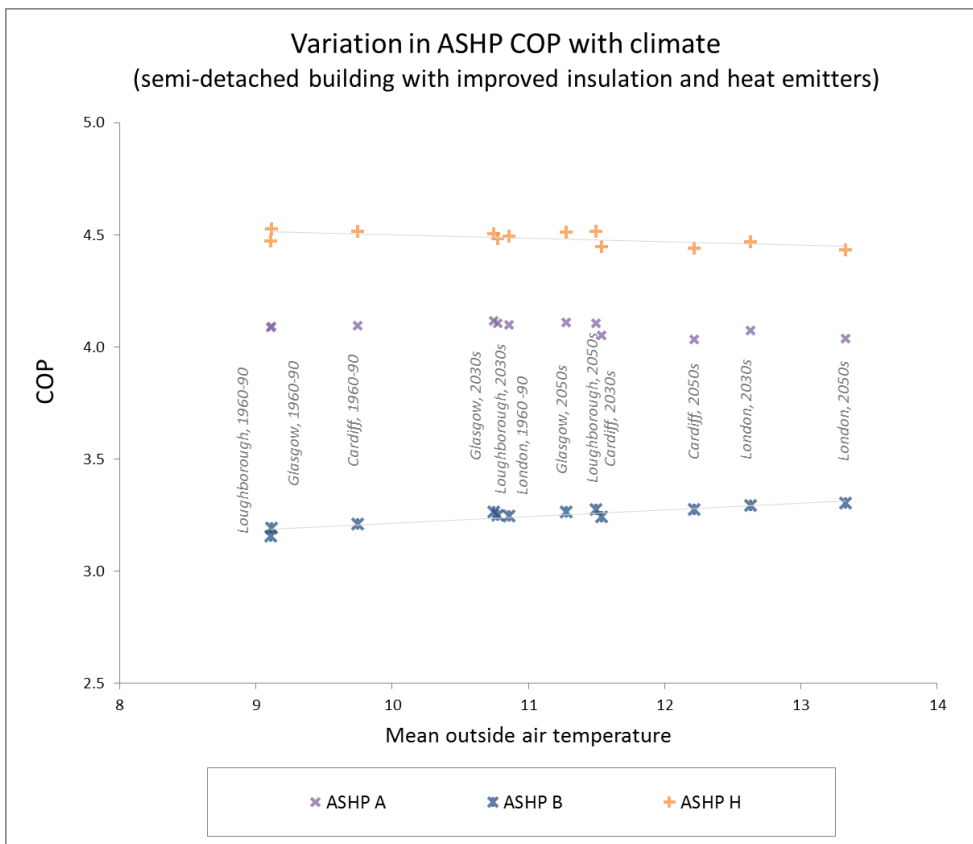
Figure 95: Effect of climate on ASHP average COPs (improved house)
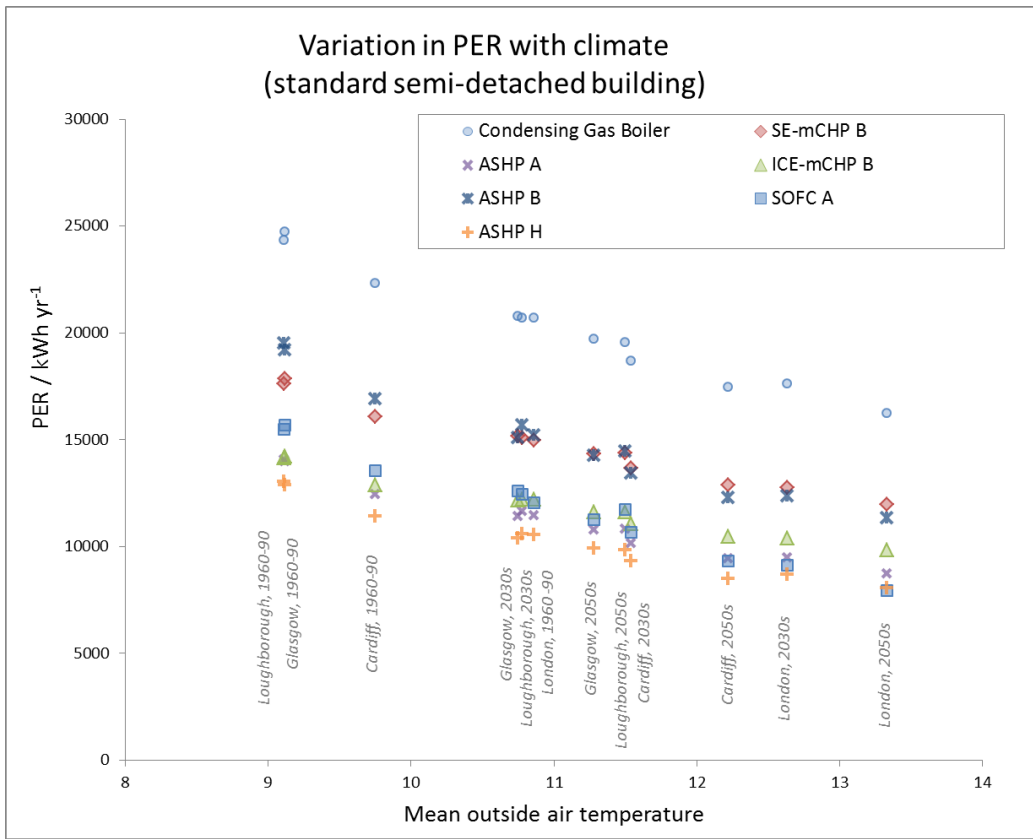
Figure 96: Effect of climate on PER of selected units (semi-detached house)
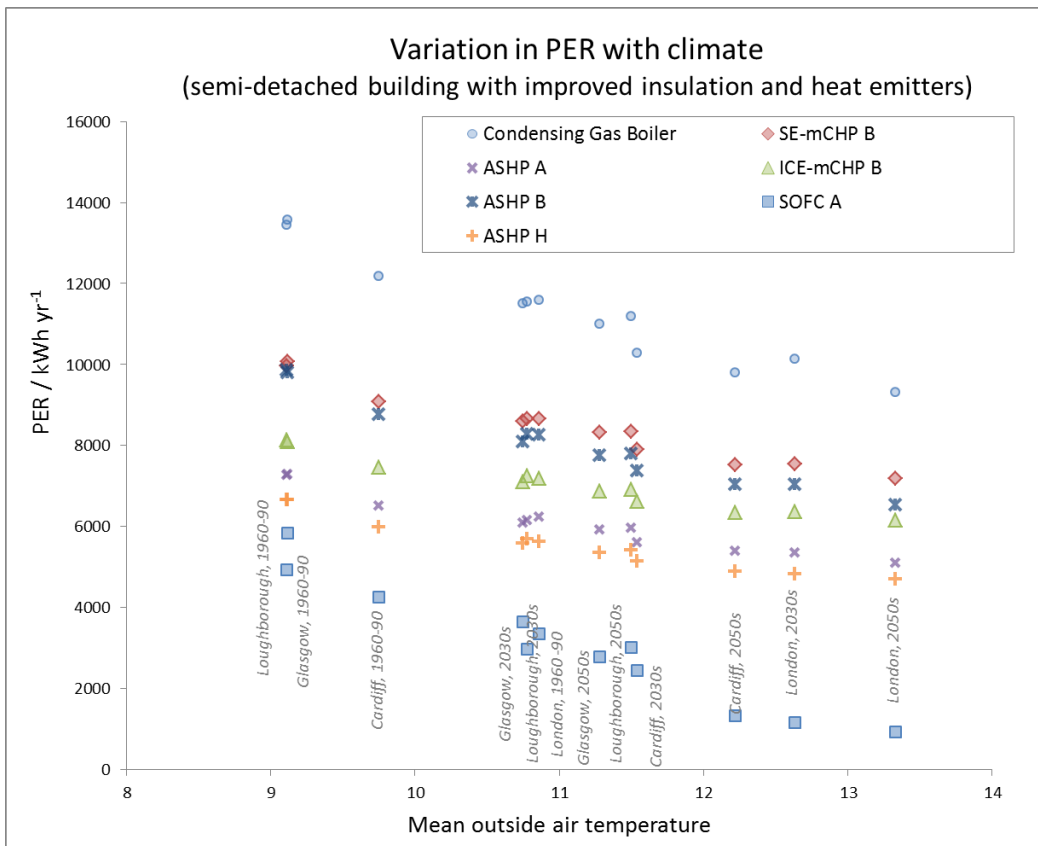
Figure 97: Effect of climate on PER of selected units (improved house)

5.9 Effect of grid generation mix

This section considers the effect of the electrical grid generation mix on the relative performance of the units. Six units have been simulated within the context of the grid generation mixes suggested by the Transition Pathways project's "Central Co-ordination" (CC), "Market Rules" (MR) and "Thousand Flowers"(TF) scenarios for 2020, 2035 and 2050 (see Table 18, page 118). The systems are ASHP B, ASHP H, SE-mCHP B, ICE-mCHP B, SOFC A and SOFC B. Each simulation was repeated with the model of the conventional semi-detached house and the semi-detached house with improved insulation and enhanced heat emitters.

Figure 98 and Figure 99 show the different CO_2 emissions associated with the units in the conventional semi-detached house and the improved building, respectively. If a comparison between the units is to be based upon the CO_2 emissions which could be attributed to them, treating all electrical demands equally, then the "mean" methodology is appropriate for calculating the CO_2 emissions. In this case, although the SOFC-mCHP units would provide the lowest CO_2 emissions when operated with the current grid conditions and operation of ASHP B would be responsible for the highest emissions, the situation rapidly changes in all three scenarios. By 2020, the ASHPs provide the lowest carbon solution except in the case of the MR scenario where SOFC B still does. By 2035 it is likely that using a SOFC-mCHP unit continuously would result in much higher CO_2 emissions than other solutions unless the gas used to fuel them is decarbonised. The CO_2 emissions associated with SE-mCHP B and ICE-mCHP B would remain comparable to those from a condensing gas boiler but would not provide the savings which are required.

If the comparison between the units is intended to investigate the consequences of selecting one unit over another then it is more appropriate to use the "marginal" methodology for calculating the emissions. In this case, the mCHP units have more favourable performance. The option with the lowest CO_2 emissions at the moment is the SOFC units, by a considerable margin (see Figure 100 and Figure 101). Selecting an ASHP would result in the highest CO_2 emissions of these alternatives; ASHP B is actually likely to cause more CO_2 emissions than a condensing gas boiler. The difference between the options is decreased in the 2020 scenarios but the SOFC units still offer the lowest CO_2 emissions of the options considered with SOFC B still achieving significant negative net CO_2 emissions. However, significant decarbonisation of the marginal plant between 2020 and 2035 (primarily CCS-equipped plant in these scenarios) reverses the situation in each 2035 scenario. The SE-mCHP B and ICE-mCHP units have emissions associated with them that are slightly lower than a condensing gas boiler in these cases.
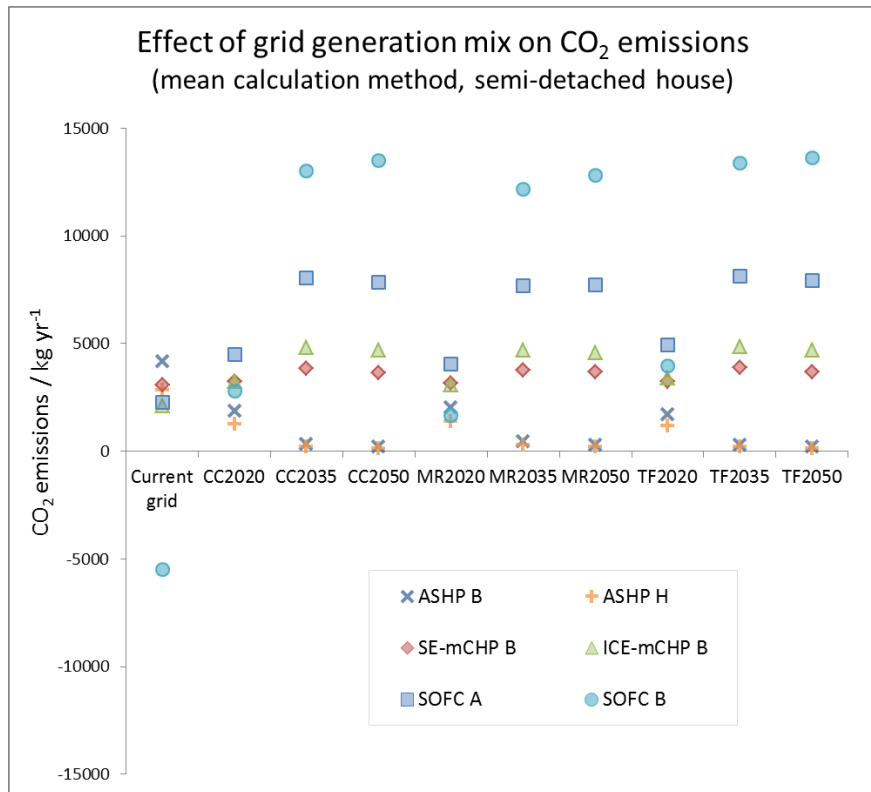
Figure 98: Effect of grid mix on CO_2 emissions, mean calculation method with semi-detached house

Figure 99: Effect of grid mix on CO_2 emissions, mean calculation method with improved house

181

Figure 100: Effect of grid mix on CO$_2$ emissions, marginal calculation method with semi-detached house

Figure 101: Effect of grid mix on CO$_2$ emissions, marginal calculation method with improved house

The effect on the PER of the units is less dramatic as the use of nuclear and CCS-equipped power plants in the scenarios tends to reduce the CO_2 emissions associated with them more than the PERs (see Figure 102 and Figure 103). After decreasing relative to the current situation, the PER of the ASHPs is consistently low but remains significant (in contrast to the CO_2 emissions associated with them). The PER of SOFC B remains low throughout each scenario and is negative even in 2050 in the TF scenario due to the (on average) less efficient generating plant used in it. However, the PER of SOFC A increases with time and is amongst the highest in most of the scenarios. The PERs of the two combustion-based mCHP units tend to increase slightly with time as the electricity which they displace is generated with a lower PER but the effect is relatively small given the dominance of their heat output over electrical output.

Although measures which reduce energy will generally cause a corresponding reduction in CO_2 emissions at present, this correlation will almost certainly weaken as the grid is decarbonised.

The PER associated with the units in each scenario, calculated relative to the marginal PER of electrical generation (i.e. the change in PER caused by selecting one technology over another) is more interesting and is illustrated in Figure 104 and Figure 105. The PER calculated using this methodology is relatively consistent across the technologies across the scenarios. This is because despite the average efficiency (in terms of primary energy) improving across each scenario, the marginal plant in each case is invariably dominated by some form of combustion-based plant (e.g. CCS-equipped plant or biomass CHP). These have relatively low efficiencies.

In each scenario, the mean primary energy efficiency of the marginal generating plant slightly increases by 2020 relative to the present which has the effect of reducing the PER for the ASHP units and increasing the net PER for the mCHP units. However, between 2020 and 2035, this trend is reversed as more CCS-equipped plant is used, increasing the PER associated with the ASHPs and decreasing the PER associated with the mCHP units.

In the CC and MR scenarios, the trend is reversed again between 2035 and 2050, with marginal PERs returning to similar values to those observed at present. However, in the case of the TF scenario, an increase in the use of low-efficiency biomass CHP units causes the average marginal efficiency to drop further, favouring the units with high electrical exports such as SOFC B. This finding is highly sensitive to the efficiency which is assumed for the biomass CHP in this scenario which is, in turn, sensitive to the way in which it is assumed that the fuel input is distributed between the generation of heat and electricity and also assumptions regarding the allocation of energy inputs for biomass. However, it does illustrate that despite decarbonisation of the grid making the SOFC-mCHP units almost inevitably unfavourable from an emissions perspective in the future, there are feasible scenarios in which they are arguably favourable from an energy perspective.
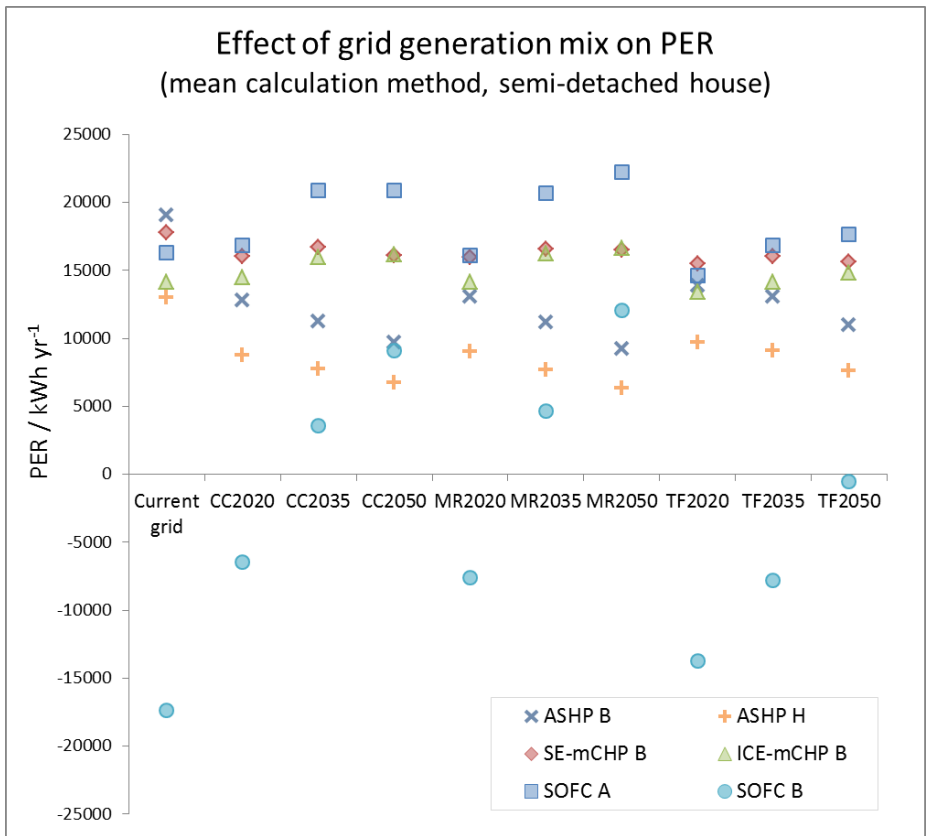
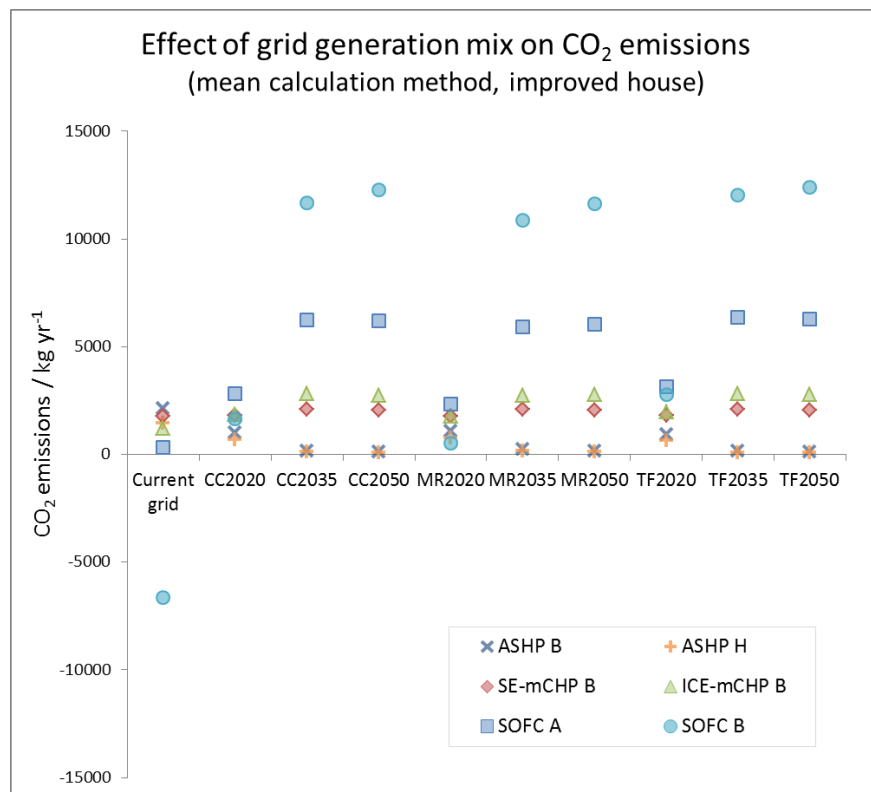*Figure 102: Effect of grid mix on unit PER, mean calculation method with semi-detached house*
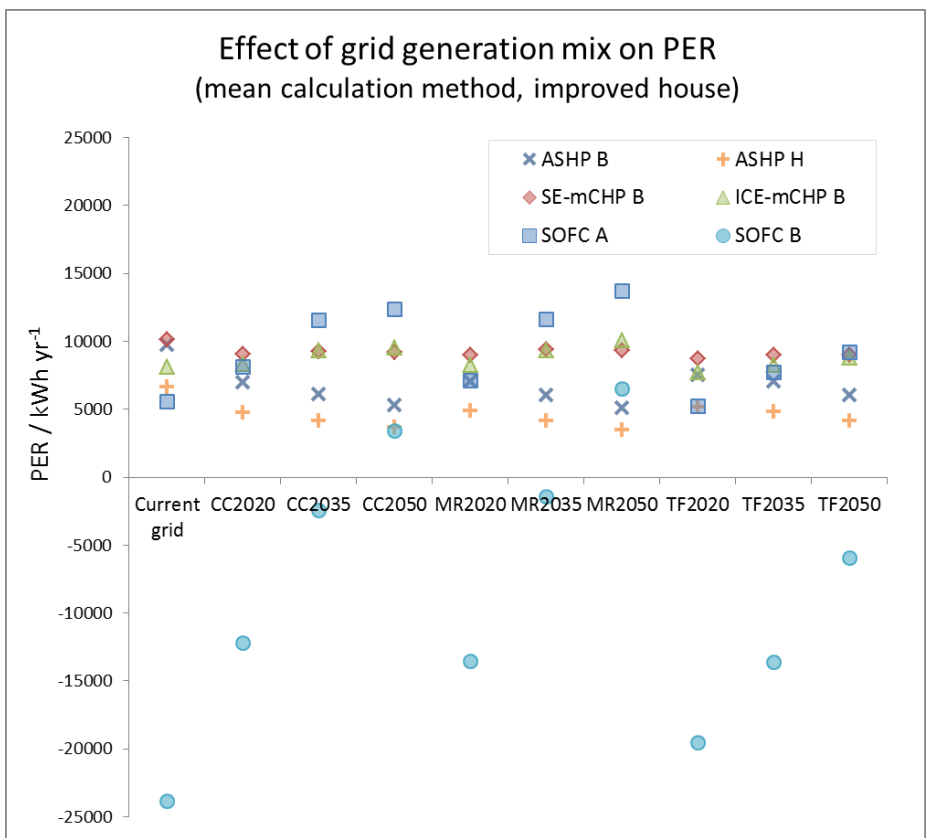
Figure 103: Effect of grid mix on unit PER, mean calculation method with improved house

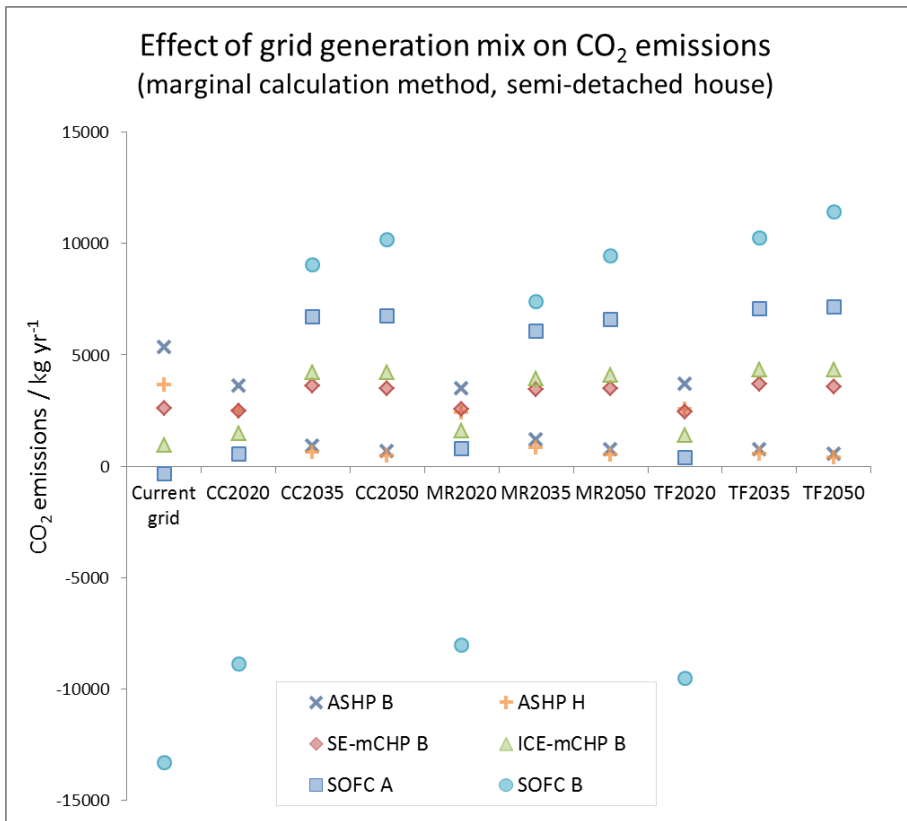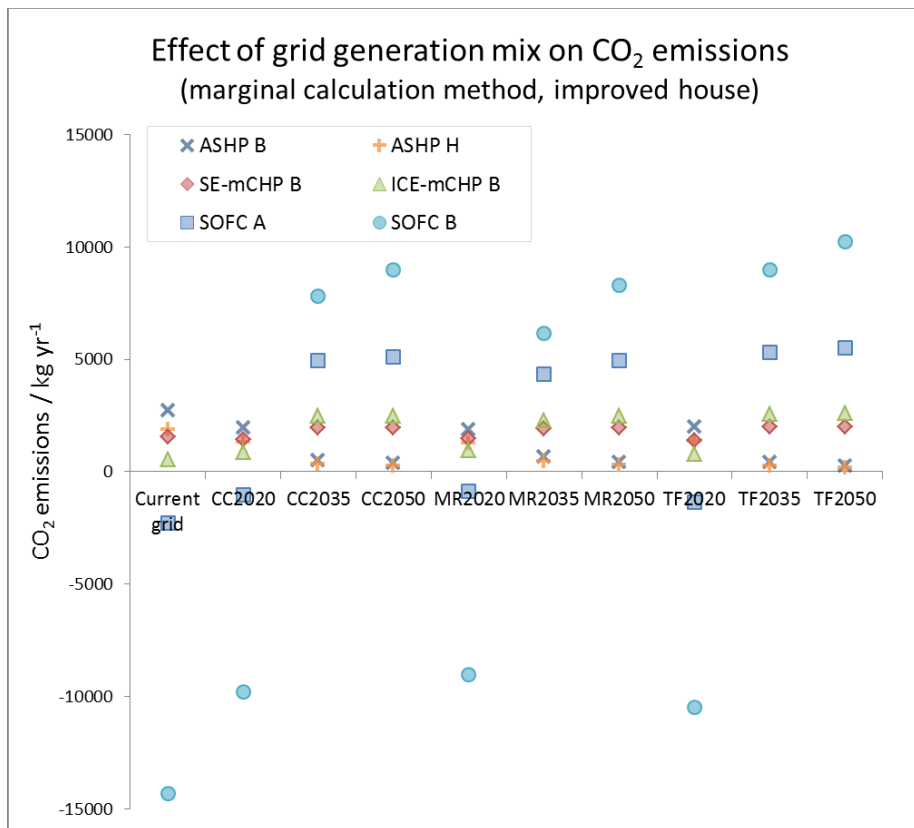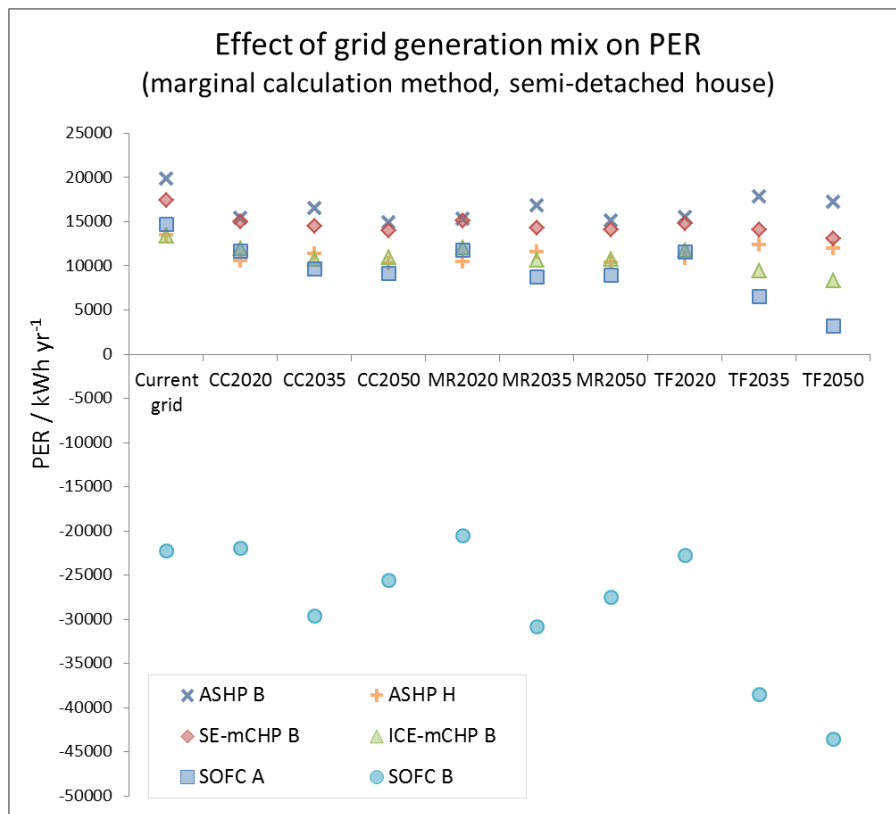*Figure 104: Effect of grid mix on PER, marginal calculation method with semi-detached house*
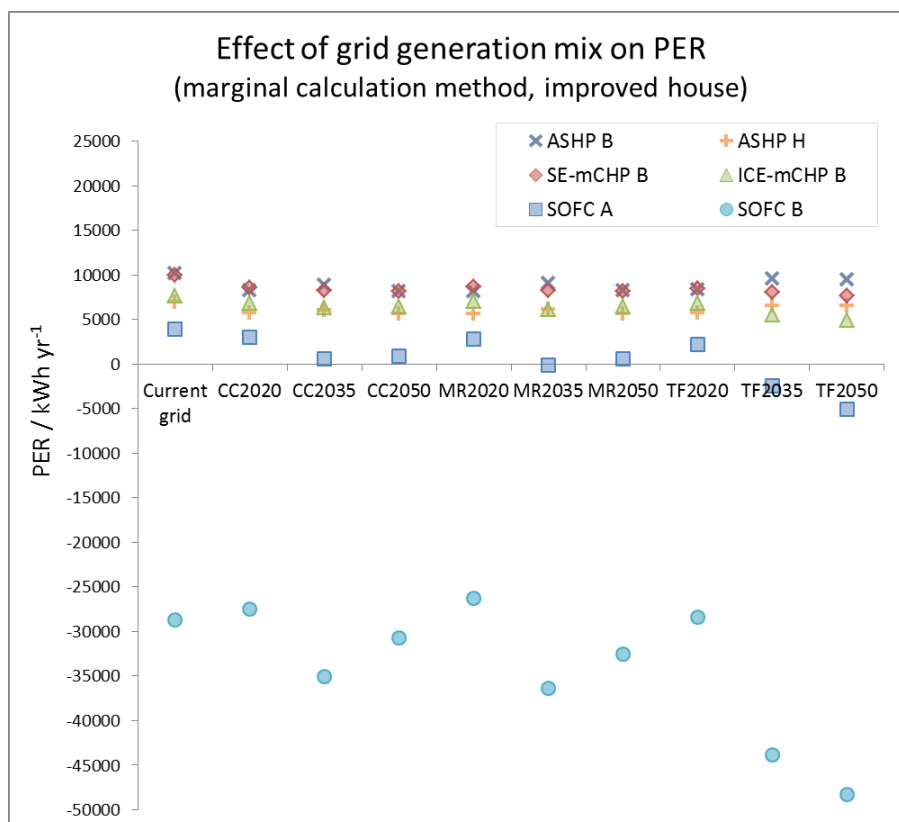
Figure 105: Effect of grid mix on PER, marginal calculation method with improved house

5.10   Demand Side Management based upon local grid constraints

This section considers the effect of DSM control based upon local grid constraints on the performance of some of the units. A neighbourhood of 128 dwellings is modelled in each case. The dwellings are based upon the standard semi-detached house for the first set of results, illustrating the demand patterns which might currently occur. Subsequent results relate to the "improved house" (i.e. the semi-detached building with improved insulation and heat emitters) and grid electricity generation based upon the MR2035 scenario (see Table 18, page 118). Each simulation is run for a period of one month (representative of January) as the most extreme power flows are expected then; it is likely that the strength of any DSM signal based on local network constraints would be less in other months and that their effect on system performance would be correspondingly lower. Figure 106 illustrates the distribution of power flows which might reasonably be expected if all 128 semi-detached houses are fitted with the same heating unit. In the case with condensing gas boilers, the power demands range from a minimum of just under 15kW (i.e. each dwelling drawing around 100W for appliances such as refrigerators) to about 190kW with modal values of around 20kW for the night-time and around 90kW to 125kW for the day-time. This is consistent with the capacity of the Low Voltage transformer which would be probably be specified for such a neighbourhood (200kVA, Haggis 2006).
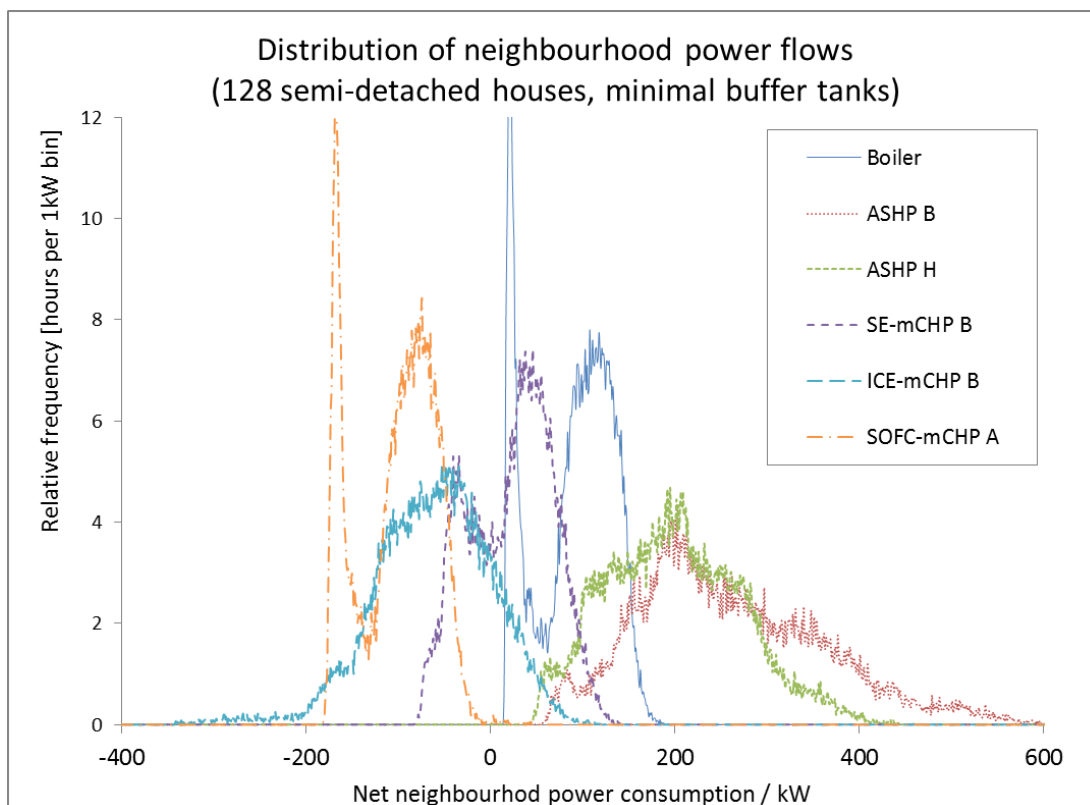
Figure 106: Distribution of local network power flows with different units.

SOFC A is operated continuously to achieve maximum efficiency (see section 5.6) and so the electrical demand distribution is almost identical to that with the gas boiler but translated to the left by 190kW (i.e. 1.5kW per unit) resulting in significant net exports for most of the time. The ASHP units increase the power consumption with a modal value of around 200kW for both units but also a much wider range; up to 600kW in the case of ASHP B or 400kW in the case of ASHP H. A large range of power flows are also observed with ICE-mCHP B but are mostly exports from the network. In some cases these would approach 400kW. The power flows associated with SE-mCHP share the characteristics seen with the boiler and the ICE-mCHP unit; power exports do occur but have a lower magnitude (around 100kW) and, although less pronounced, two modes occur again. These power flows can alternatively be illustrated as the power flow during each time period, ordered according to the size of the power demand rather than chronologically. This is shown in Figure 107 for the same data presented in Figure 106. Plotted in each way, the net electrical energy consumed by the neighbourhood is given as the net area above the x-axis.
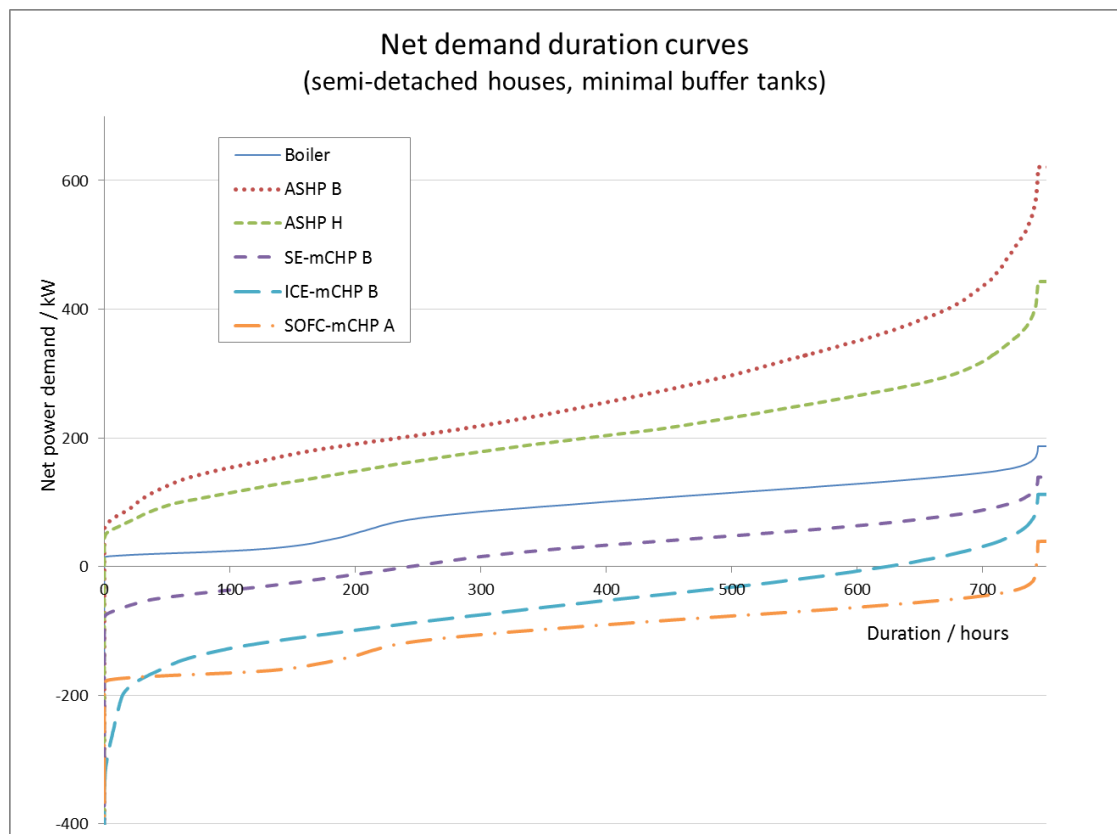
Figure 107: Net demand duration curves for neighbourhoods with standard semi-detached houses

By improving the level of insulation and heat emitters within each building, the power flows are reduced in the majority of cases (Figure 108). The power flows associated with the systems using gas boilers and SOFC-A are unaffected. However, the additional power consumption associated with the ASHP units is still significant and would cause a 200kVA transformer

supplying the neighbourhood to be overloaded for around 20% to 35% of the time (during January). Although the power exports associated with ICE-mCHP B are reduced, they still exceed 200kW for around 2% of the month.
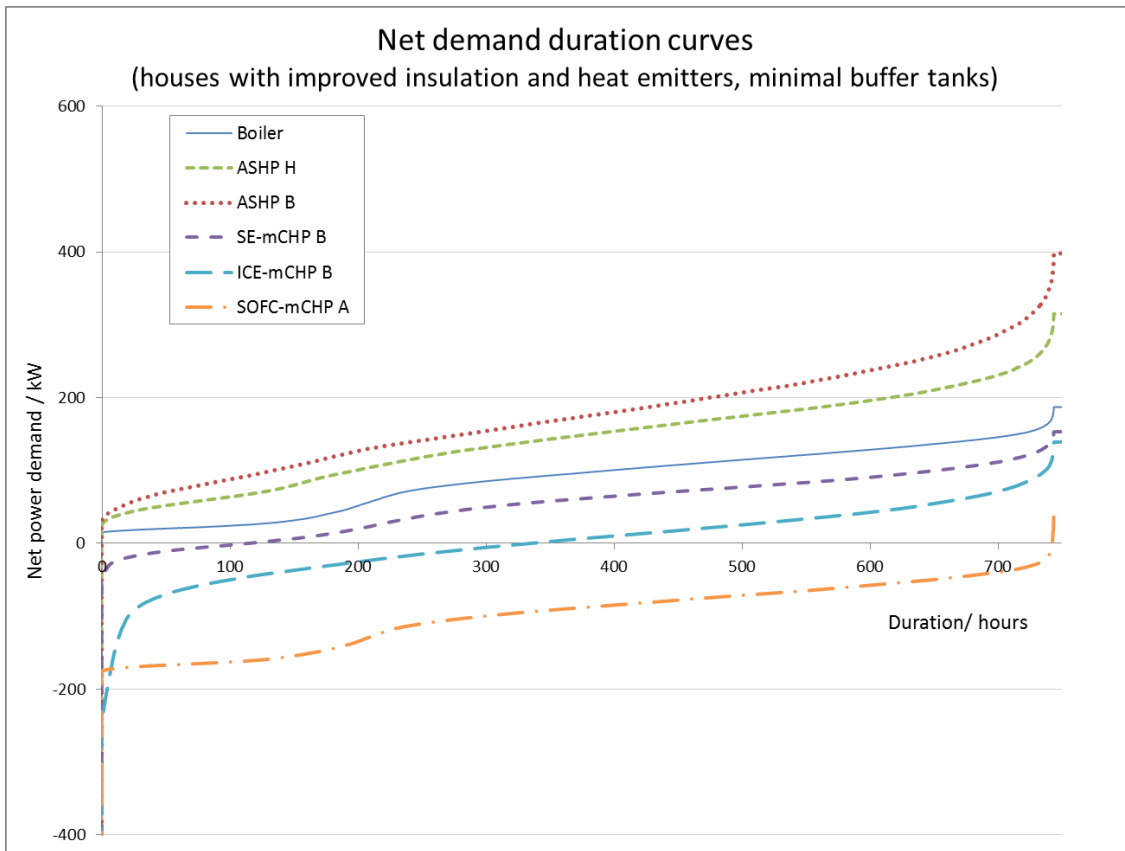
Figure 108: Net demand duration curves for neighbourhoods with improved buildings

Figure 109 illustrates the effect of including medium (160kg) buffer tanks in the systems. The power flows associated with ASHP B are shown for the case with the conventional semi-detached house to illustrate the extent to which local power infrastructure would be overloaded under typical present day conditions if all houses were heated using a mid-range ASHP. The other three cases are shown for the case with the improved houses. The two combustion-based mCHP units demonstrate characteristics which are more favourable to the electrical grid infrastructure. Although total power exports from ICE-mCHP B are increased, the largest power flows are decreased, with exports which exceed 200kW occurring only half as often. The ICE-mCHP B units are relatively large and so it is the longer, more diverse operation of the units which occurs with buffer tanks which causes this. However, diversification alone is not enough to smooth the peaks in generation from the units.
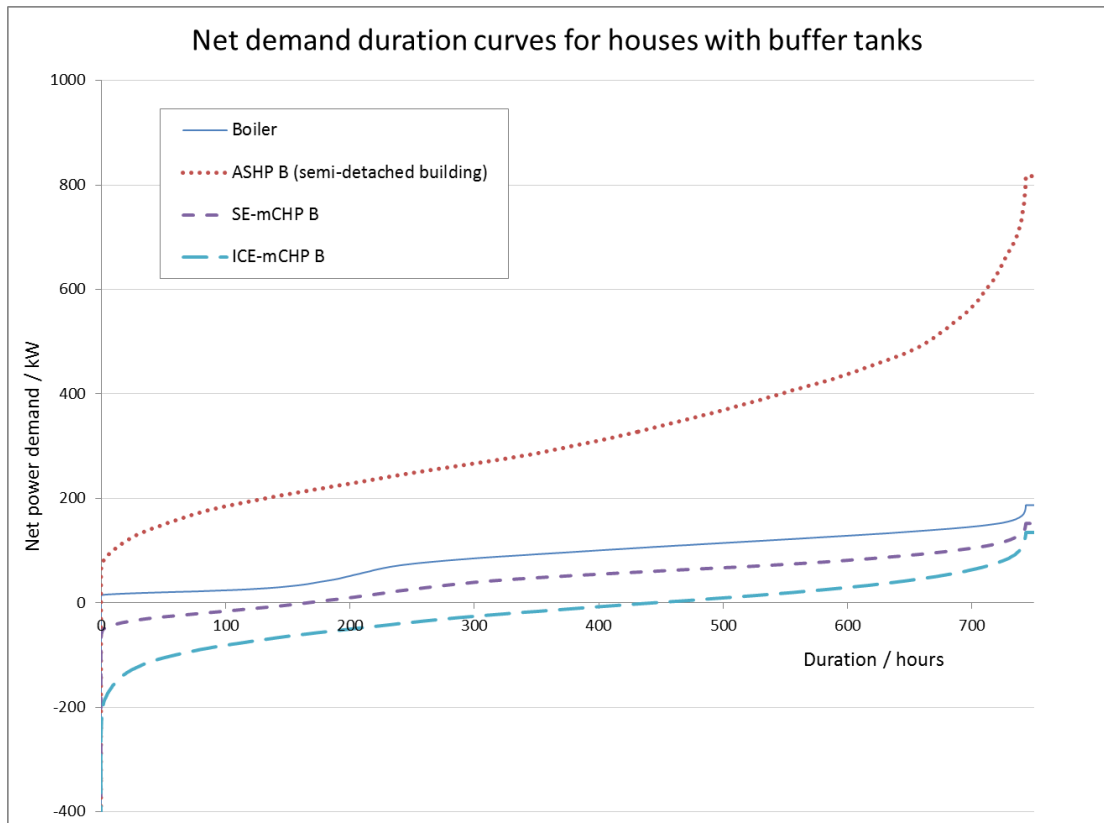
Figure 109: Net demand duration curves for neighbourhoods, houses with buffer tanks.

In order to supply a neighbourhood with sufficient electricity to provide heating using ASHPs, it would be necessary to reinforce the local network infrastructure, initially by upgrading the local distribution transformer. However, it is possible that the use of DSM could reduce the extent to which this is necessary. Figure 110 (and detail in Figure 111) show the power flow distributions which might be expected if all residents in the neighbourhood are prepared to accept a given deviation in inside air temperature at times of peak demand.

Reinforcement would be required in each case. However, if residents accept temperature deviations of +1°C to -3°C then the total supply capacity required could be reduced from around 320kW to around 260kW. This is an illustration which is specific to the conditions assumed but demonstrates the order of the effect which might reasonably be achieved. Although using a buffer tank (160kg in this case) increases the power demand at most times (see section 5.2), it doesn't affect the peak demand as significantly. However, it does not appear to offer the potential for reductions in the peak (under these constraints), either.

Using this DSM system will reduce the inside air temperature of the dwellings at times. Figure 112 illustrates the CO_2 emissions which would occur due to the operation of ASHP H under these conditions, plotted against the average pseudo-PMV in each dwelling. Note that for this

189

set of results, CO_2 emissions relate to one month only and were calculated using the mean emissions methodology.
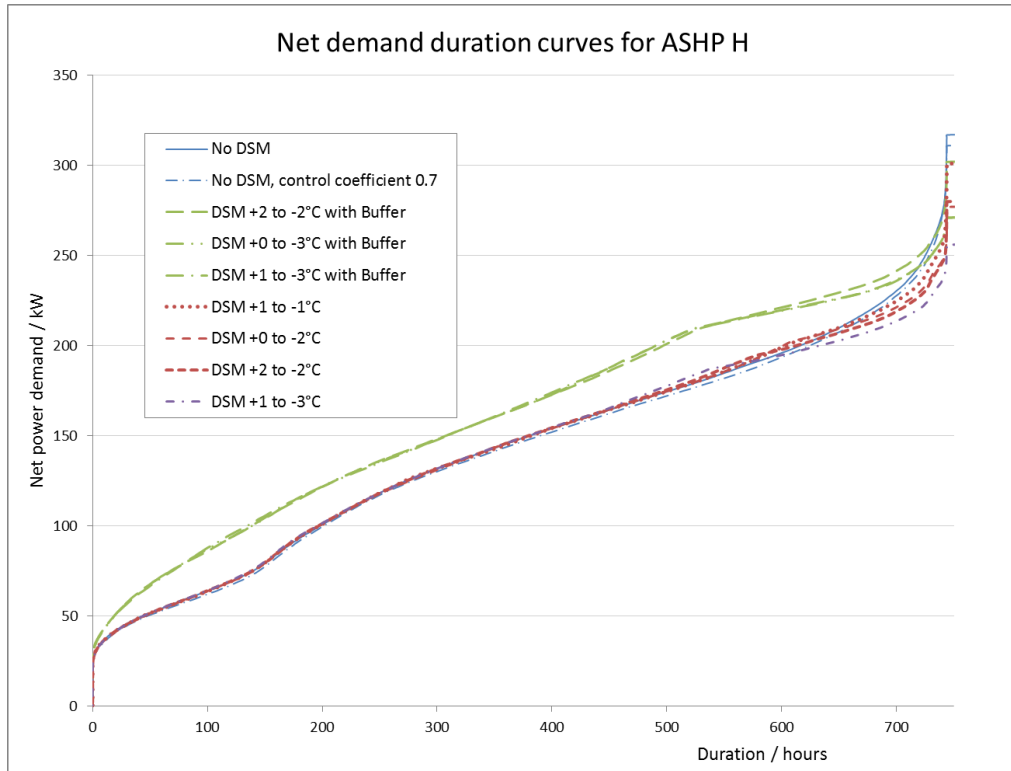
Figure 110: Net demand duration curves for neighbourhoods using ASHP H with DSM.
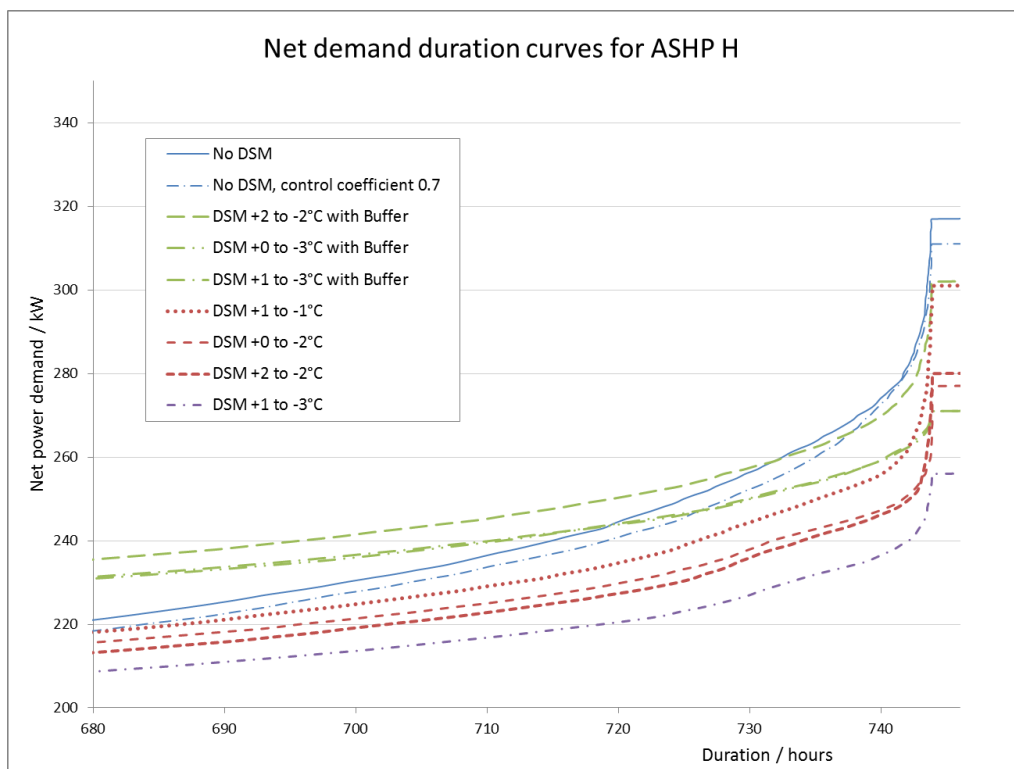
Figure 111: Detail of demand duration curves for ASHP H with DSM

190
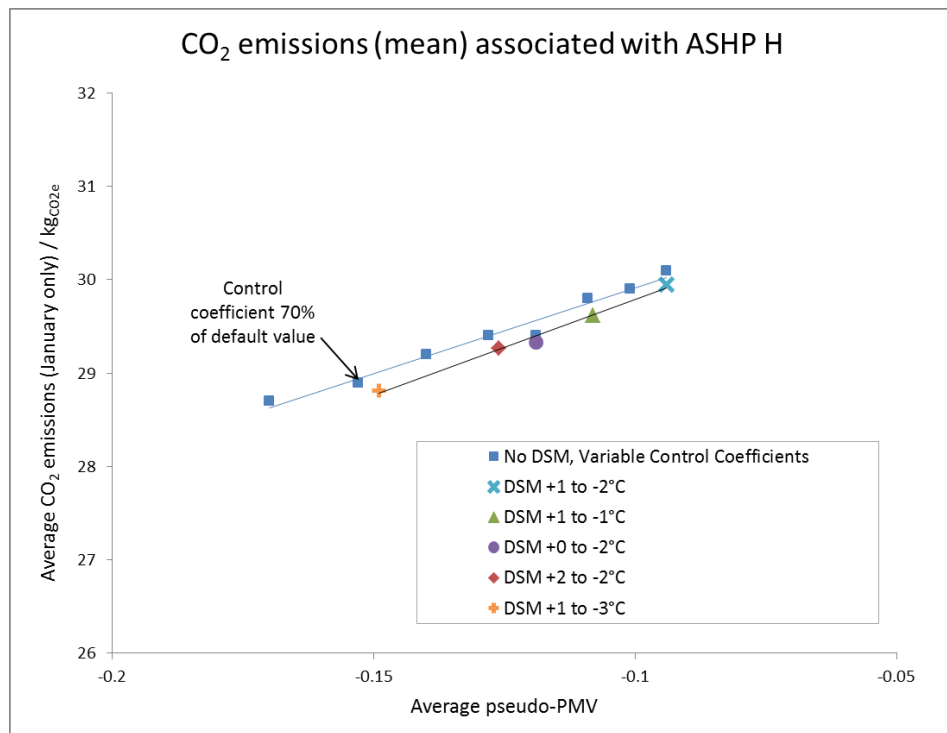
Figure 112: Average CO$_2$ emissions associated with ASHP H with and without DSM

In addition to the emissions and pseudo-PMV associated with the different levels of DSM intervention, results are plotted in Figure 112 for dwelling without any DSM intervention but with the control coefficient relaxed (in increments of 5%) in order that comparable thermal comfort is achieved. In each case, an approximately linear relationship is observed between the pseudo-PMV and CO$_2$ emissions. This is primarily due to the reduction in heating required if a lower air temperature is accepted and, secondarily, a slight improvement in ASHP COP in some cases due to a lower requisite flow temperature. It is also interesting to note that the units operating with DSM are generally associated with slightly lower CO$_2$ emissions for a given pseudo-PMV. This may be due to the coincidence of the peak demands (which are discouraged) and higher grid CEFs. Section 5.11 will explore the potential to take advantage of this effect in more detail. Although less electricity is required by the ASHPs when operating with a relaxed control coefficient, it does not appear to significantly reduce the peak power demand associated with them. Figure 110 and Figure 111 include the power demands of a unit operated without DSM but with a control coefficient relaxed by 30% (achieving a similar pseudo-PMV to that when DSM can alter the target temperature by +1°C to -3°C, Figure 112).

Another approach to potentially reduce the need for local network reinforcement is to encourage the use of a mix of ASHP and mCHP units within the neighbourhood. Figure 113 and Figure 114 illustrate the power flows which might occur with various mixtures of SOFC A and ASHP H.
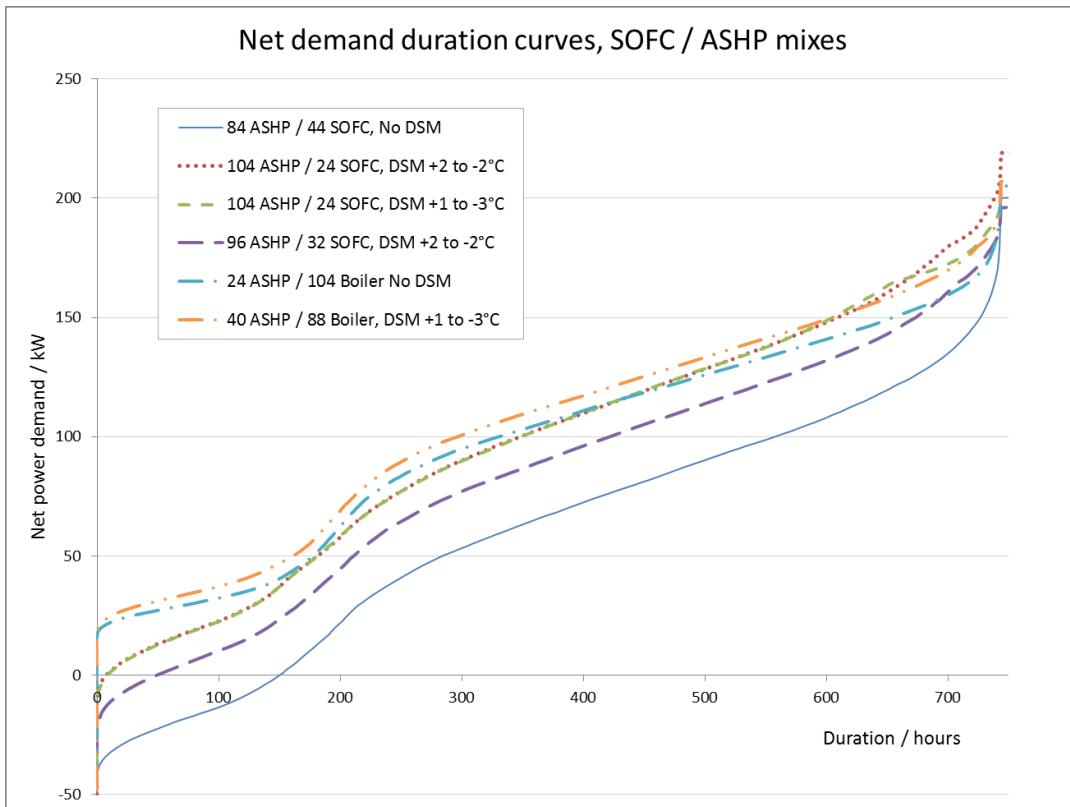
Figure 113: Net demand duration curves for neighbourhoods with mixes of SOFC & ASHP units
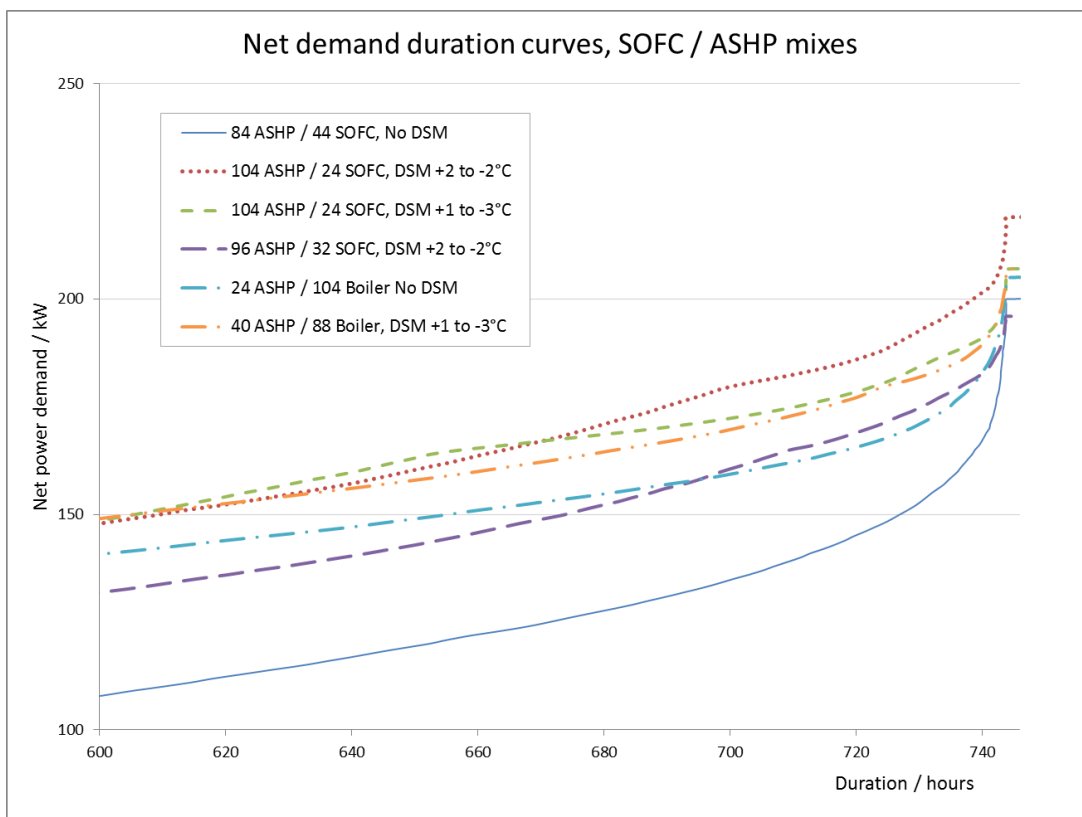
Figure 114: Detail of demand duration curves for mixes of SOFC & ASHP units.

192

In the circumstances modelled here, it is possible to support around 24 ASHP H units if DSM is not used and heat is supplied to the other dwellings using gas boilers. This increases to around 40 ASHP H units is DSM (+1°C to -3°C) is used. However, if a mixture of SOFC A units are used with ASHP H units then 84 ASHP units can be supported without overloading the Low Voltage transformer. If DSM is used with the ASHP units then up to 104 ASHP H units could be supported. This reduces to around 96 ASHP H units if the temperature range available to the DSM system is changed to +2°C to -2°C. The average CO_2 emissions (in the context of the MR2035 scenario) and the pseudo-PMV associated with these arrangements are given in Figure 115.
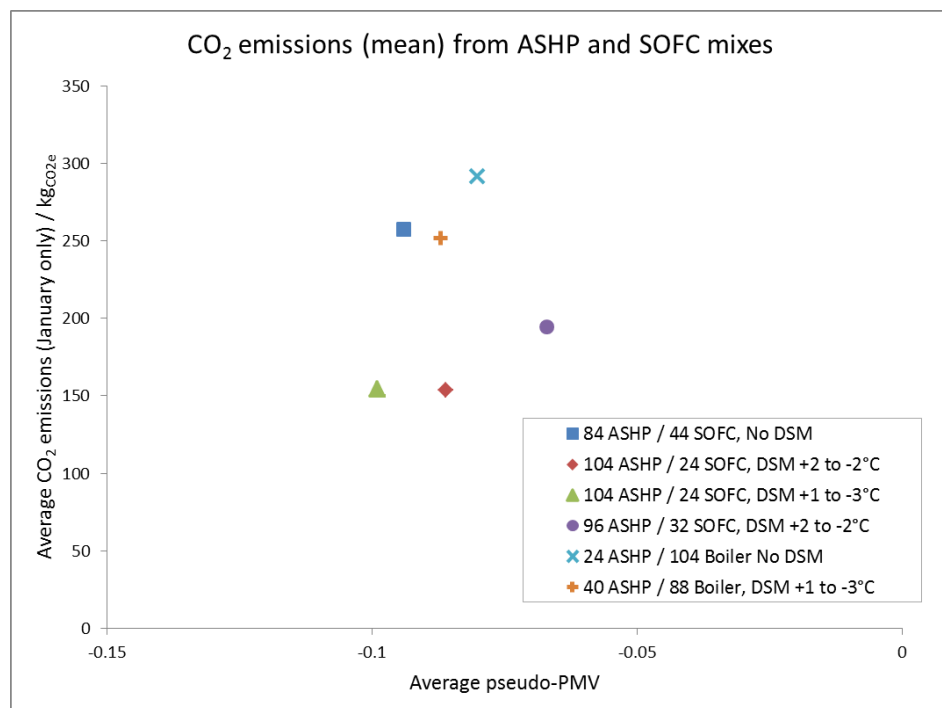
Figure 115: Average CO_2 emissions associated with mixture of SOFC and ASHP units

As noted earlier (section 5.9), in this grid generation context, the low CEF favours ASHPs while disadvantaging SOFC units with their relatively large gas consumption. This means that the scenarios in which there are more ASHP units tend to generate fewer CO_2 emissions. Even though a dwelling with SOFC A would be associated with higher CO_2 emissions than a dwelling with a gas boiler in this context, if the grid infrastructure cannot be reinforced then the combination of SOFC mCHP units with ASHPs offers the potential for greater overall emissions reductions than just the ASHPs with gas boilers. The emissions associated with the two scenarios in which there are 104 ASHP units and 24 SOFC-mCHP units are, unsurprisingly, similar. The difference in the temperature range available to the DSM systems (+2°C to -2°C compared to +1°C to -3°C) effectively trades a reduction in thermal comfort in order to limit maximum net power demand to 200kW.

A similar arrangement could be constructed from ASHPs and combustion-based mCHP units. Figure 116 and Figure 117 show the power flows, CO_2 emissions and pseudo-PMVs associated with combinations of ASHP H and SE-mCHP B.
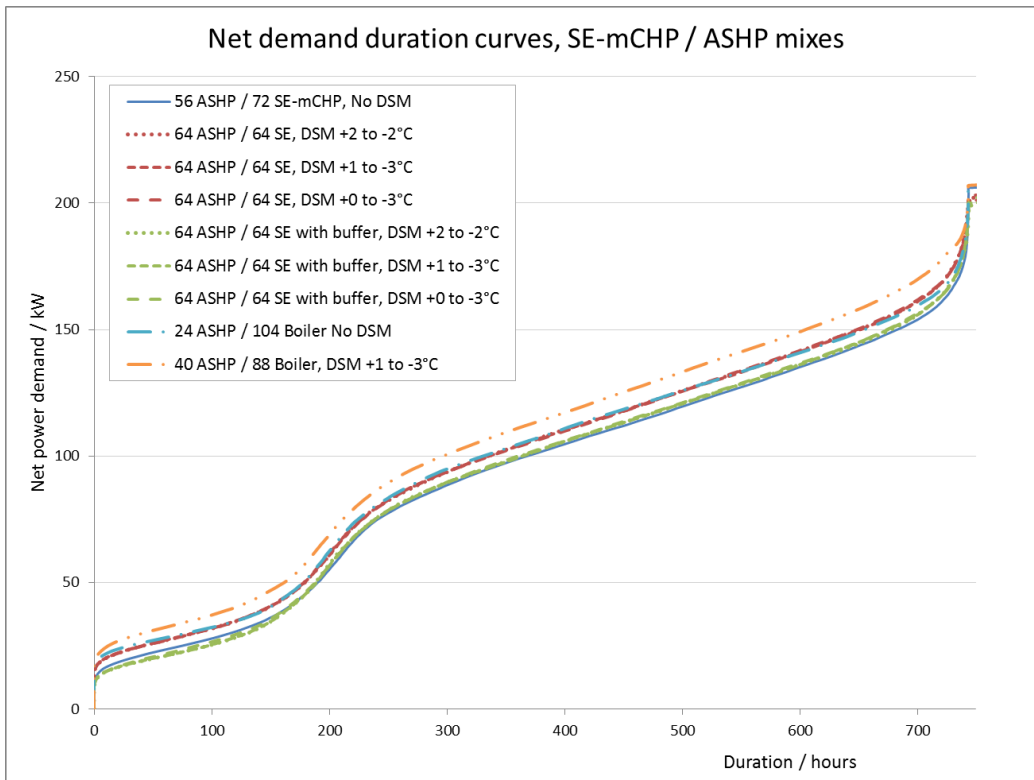
Figure 116:Net demand duration curves for neighbourhoods with mixes of ASHP & SE-mCHP B units
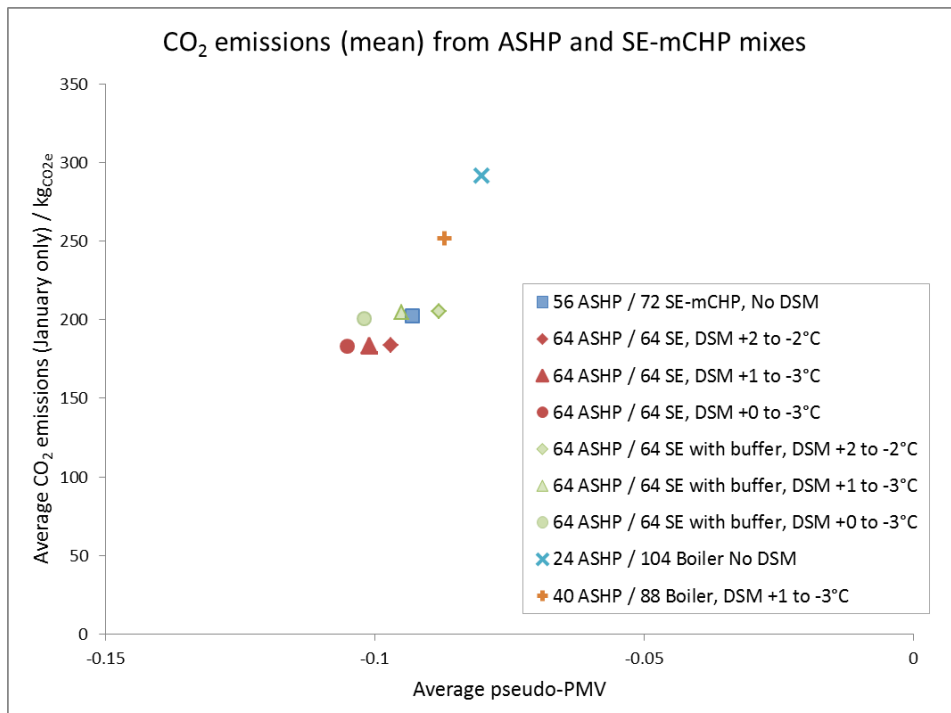
Figure 117: Average CO_2 emissions associated with mixture of SE-mCHP and ASHP units

A reduction in emissions can be achieved by using the SE-mCHP unit in combination with ASHPs (relative to using the ASHPs with boilers with a fixed grid power constraint), but it is not quite as large as the improvement which can be achieved with the SOFC-mCHP units. Additionally, the lower number of ASHP units which can be supported decreases the usefulness of the DSM approach in this case.

Of the three mCHP units considered in this section, only the ICE-mCHP B unit has the potential to create export power flows which exceed 200kW. The relatively large size of the unit means that it is more likely to operate for shorter periods and sometimes the diversity across the local network will smooth out these peaks. However, the diversity across 128 dwellings is insufficient to cover all of them and so some short periods of high power export are very hard to avoid without some form of active central coordination, even with a relatively low number of ICE-mCHP B units installed in the neighbourhood.

Figure 118, Figure 119 and Figure 120 show the power flows associated with a neighbourhood in which an ICE-mCHP B unit is installed in each dwelling, along with the pseudo-PMV and CO_2 emissions. Using the ICE-mCHP units without buffer tanks, it appears that it would be possible to limit export power flows to less than 200kW in the conditions of the scenario modelled.

Although the use of the buffer tank has some benefit when DSM is not used, it seems that in some of the circumstances here, the combination results in higher power generation with exports exceeding 200kW for about twice as long as they do when DSM is not used. This is partly due to a combination of the additional generation which occurs when buffer tanks are installed but is also due to the DSM algorithm tending to discourage generation too early and then having reduced scope to influence demand when the power export is even higher. It would, no doubt, be possible to develop a more sophisticated algorithm which could mitigate this effect but this demonstrates that it would not be trivial.
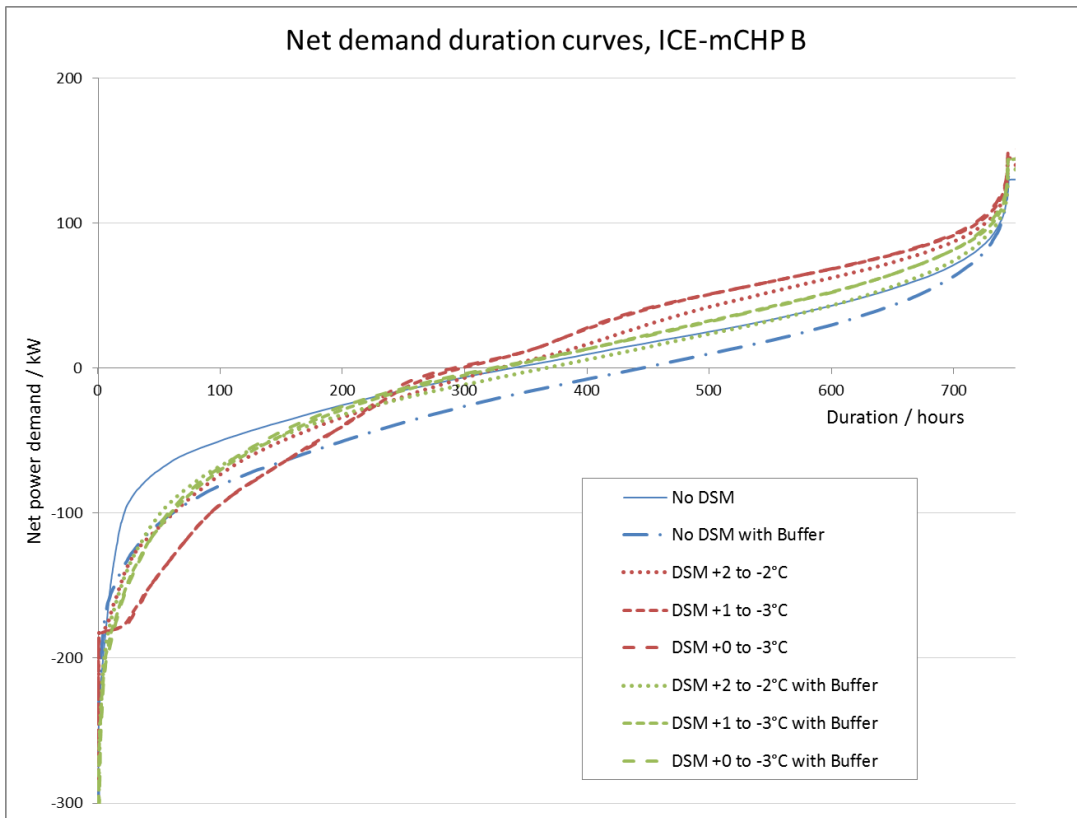
Figure 118: Net demand duration curves for neighbourhoods with ICE-mCHP B.
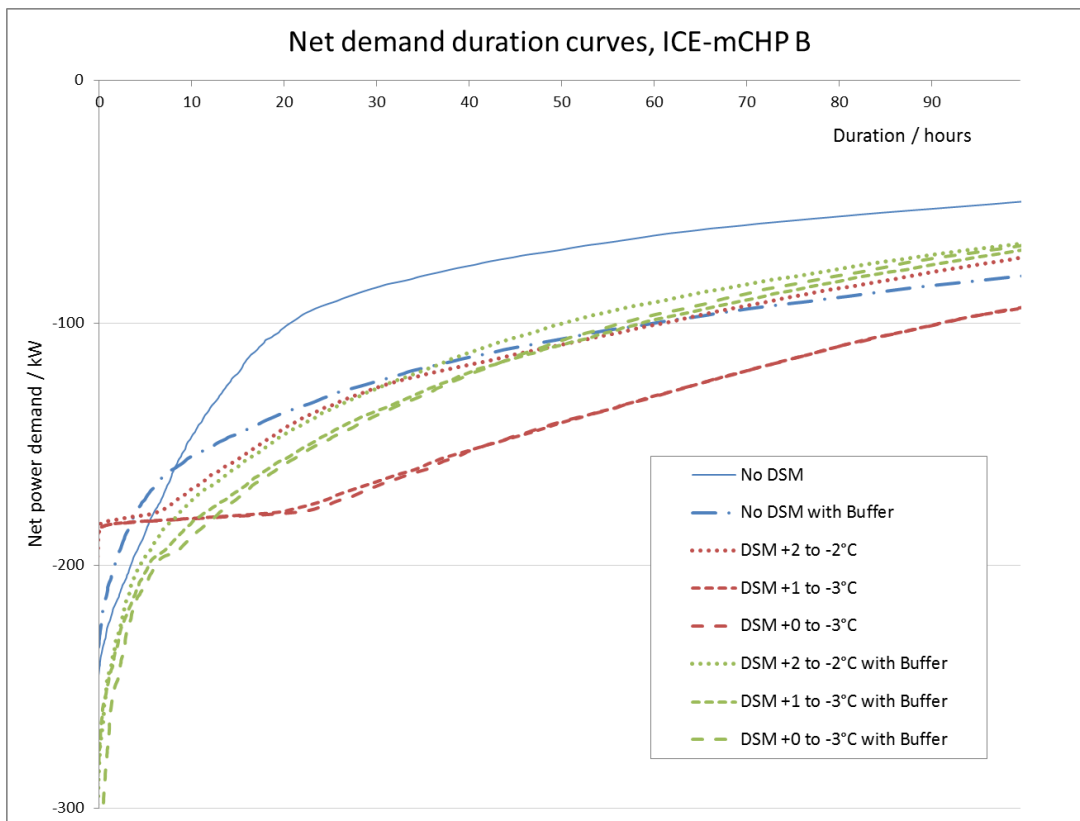
Figure 119: Detail of demand duration curves for neighbourhoods with ICE-mCHP B.

196
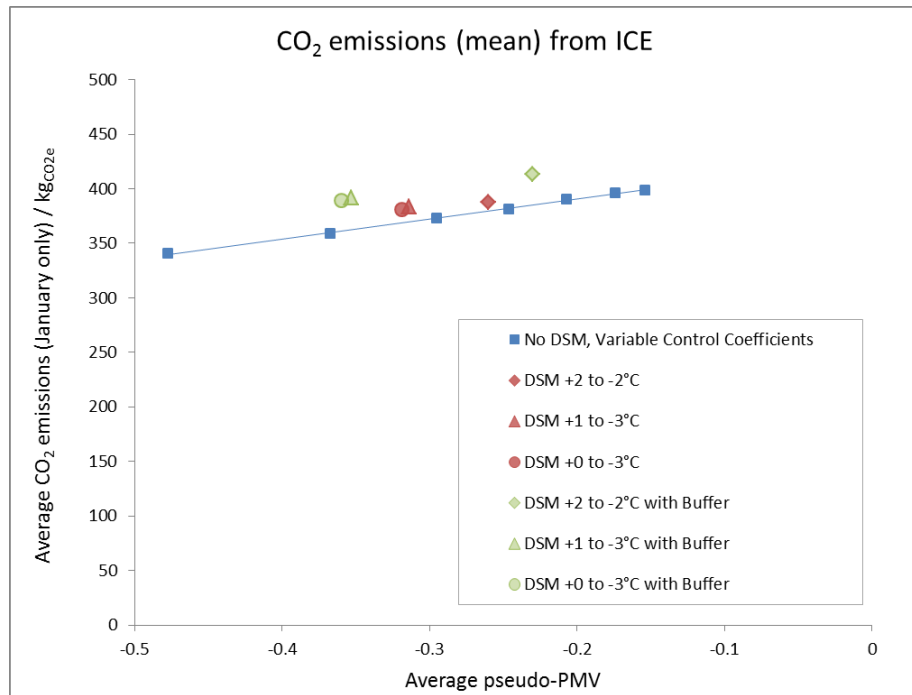
Figure 120: Average CO2 emissions associated with neighbourhood with ICE-mCHP B units

In contrast to the case with the ASHP (Figure 112), the CO_2 emissions associated with the ICE-mCHP with a relaxed control coefficient are slightly lower than those with equivalent thermal comfort but subject to DSM. Again, however, the difference is not large and the overall trend is for a reduction in CO_2 emissions as the psuedo-PMV is reduced. There is relatively little effect associated with changes in the upper bound of the temperature range available to the DSM (i.e. little difference between the +1°C to -3°C and the +0°C to -3°C results). This is to be expected as the local network is exporting for almost half of the time and net imports rarely exceed 120kW and so there is no reason for the DSM system to discourage generation within the parameters set for it.

5.11 Demand Side Management based upon marginal carbon emissions factors

The effect of using a DSM signal to encourage the operation of ASHPs when the marginal carbon emissions factor (MEF) of the grid is low and to discourage it when the MEF is high is considered in this section. This was modelled with the current grid, the three "Market Rules" (MR) scenarios (see Table 18, page 118) and the MR2050 scenario but with the number of ASHPs increased (see Table 19). The DSM signal was based upon a DSM weighting factor for the cost of CO_2 emissions and the MEF calculated during each iteration of each time-step. Each DSM weighting factor is selected such that a value of one is generated for the "price of electricity" (i.e. the signal is neutral) when the MEF is at its average (modal) value.

Table 19: Grid scenarios used to investigate the effect of DSM based upon marginal emissions factors

Scenario:	2010	2020	2035	2050	2050 +ASHP*
Number of dwellings with ASHPs:	50,000	2.56M	5.12M	6.14M	15.4M
DSM weighting factor:	1.7	1.8	5	5	5
* i.e. with additional ASHPs. Note that each of these scenarios is repeated with and without DSM. These figures (especially for last scenario) are indicative as the exact totals vary depending upon the dynamic nature of the simulation.					

Each of the simulations was run for a period of 120 days.

Each of these five scenarios was repeated with and without the DSM signal applied. A network of 512 permutations of dwellings was modelled to achieve an acceptable level of diversity. These permutations were constructed using four building types (the three main types and the improved semi-detached house), four climates (Cardiff, Glasgow, London and Loughborough adjusted as before for the future scenarios), four temperature programmes and eight temperature-range options for the cases with DSM (given in Table 13) or eight variations on the proportional controller coefficient in the cases without DSM. The power demands from the network of 512 dwellings were multiplied by factors corresponding to the total number of dwellings in each scenario (Table 19) to give the total power demand.

An overview of the CO_2 emissions associated with each of the ASHPs is given in Figure 121. Clearly, there is a considerable range of results with both the thermal comfort and CO_2 emissions varying widely. The broadly left to right, linear groups within each scenario relate to the groups of scenarios differentiated by the building specification and climate. The variation within each of these groups of results (i.e. with wide variation in thermal comfort but relatively

limited variation in CO_2 emissions) relates to the different temperature profiles, control system responsiveness and level of DSM participation in each permutation.
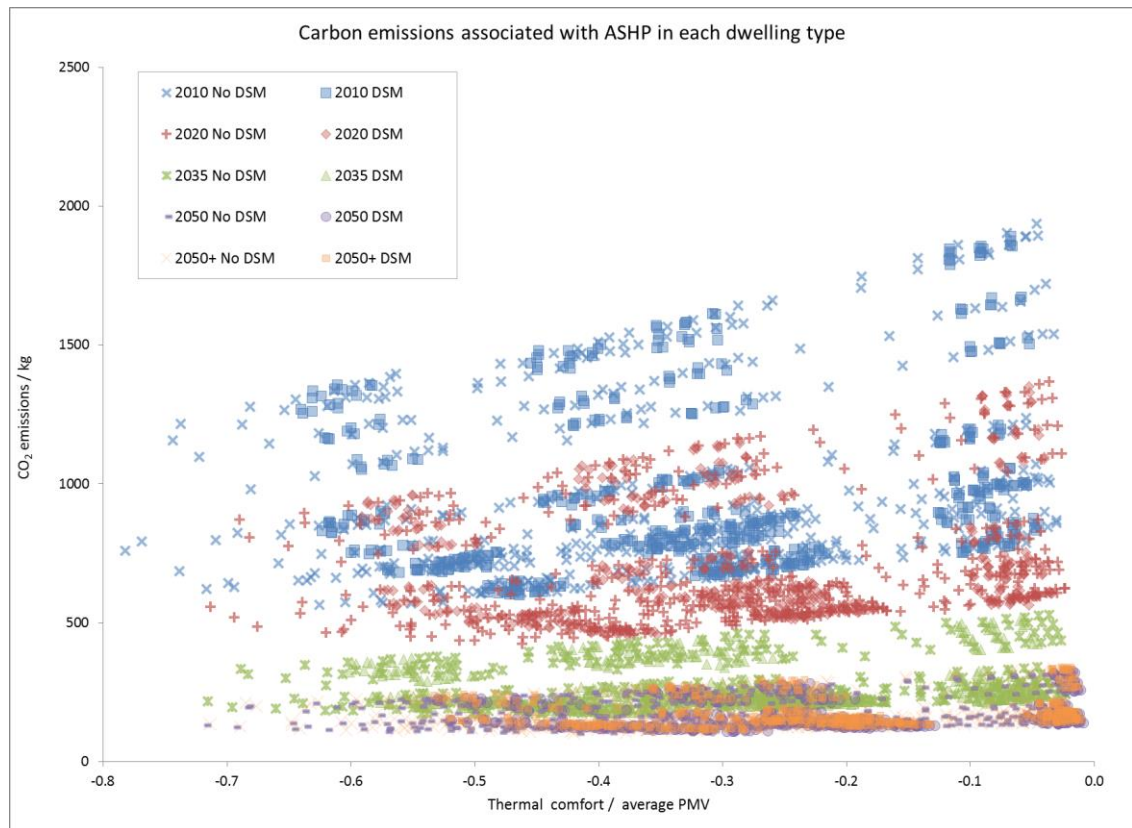
Figure 121: CO$_2$ emissions with grid carbon emissions factor based DSM

The effect of the different control systems on the performance of the ASHPs can be more clearly observed by taking the mean results across the four climates and by considering the grid scenarios separately. This is shown in Figure 122 to Figure 125 for the 2035 and 2050 (with additional ASHPs) scenarios. The results for the scenarios in which DSM is not used are presented as plots rather than individual data as their range reflects a continuous set of possibilities which is only dependent upon the control system coefficient which is used. In each scenario, the different building types have a large effect on the CO_2 emissions associated with them but a similar trend in emissions with thermal comfort.
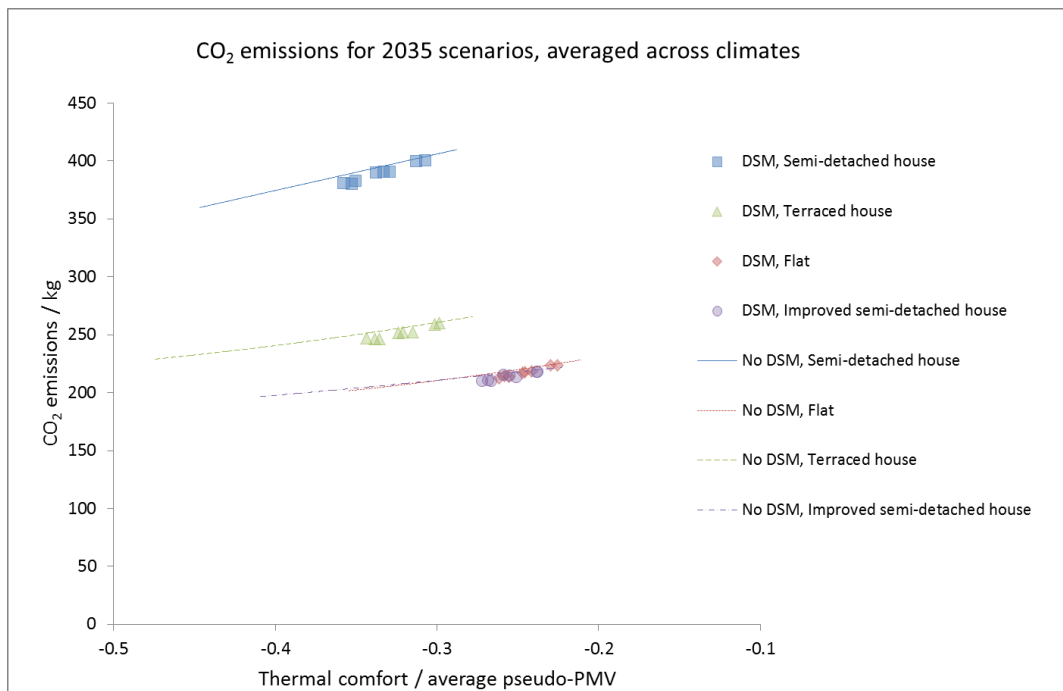
Figure 122: ASHP CO$_2$ emissions in 2035 scenarios
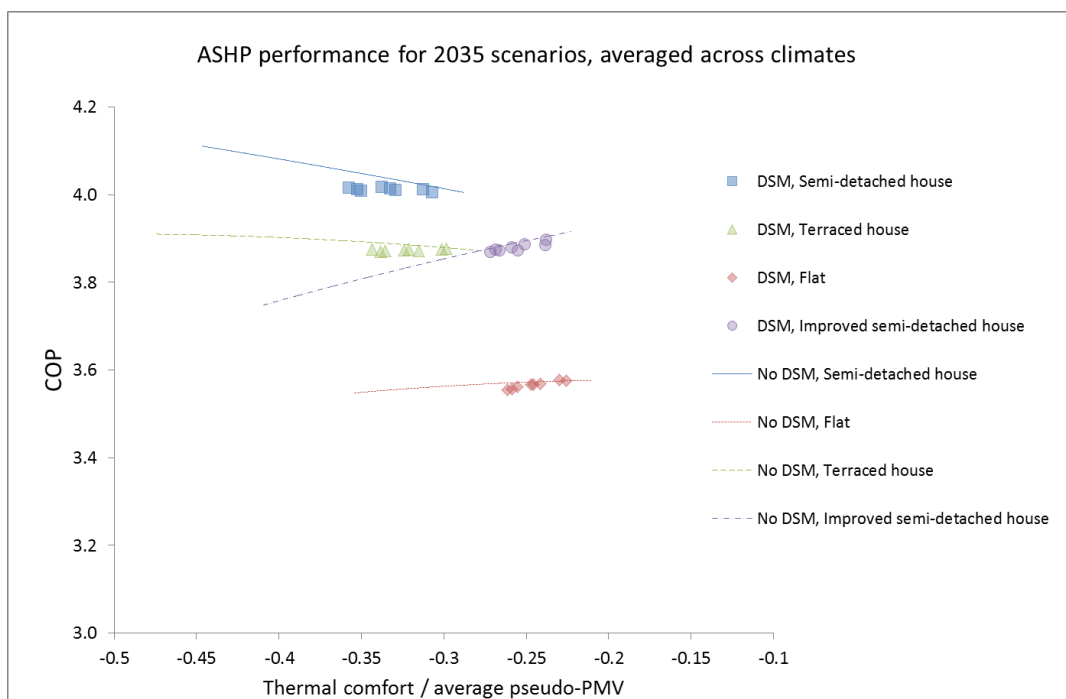
Figure 123: ASHP performance in 2035 scenarios.
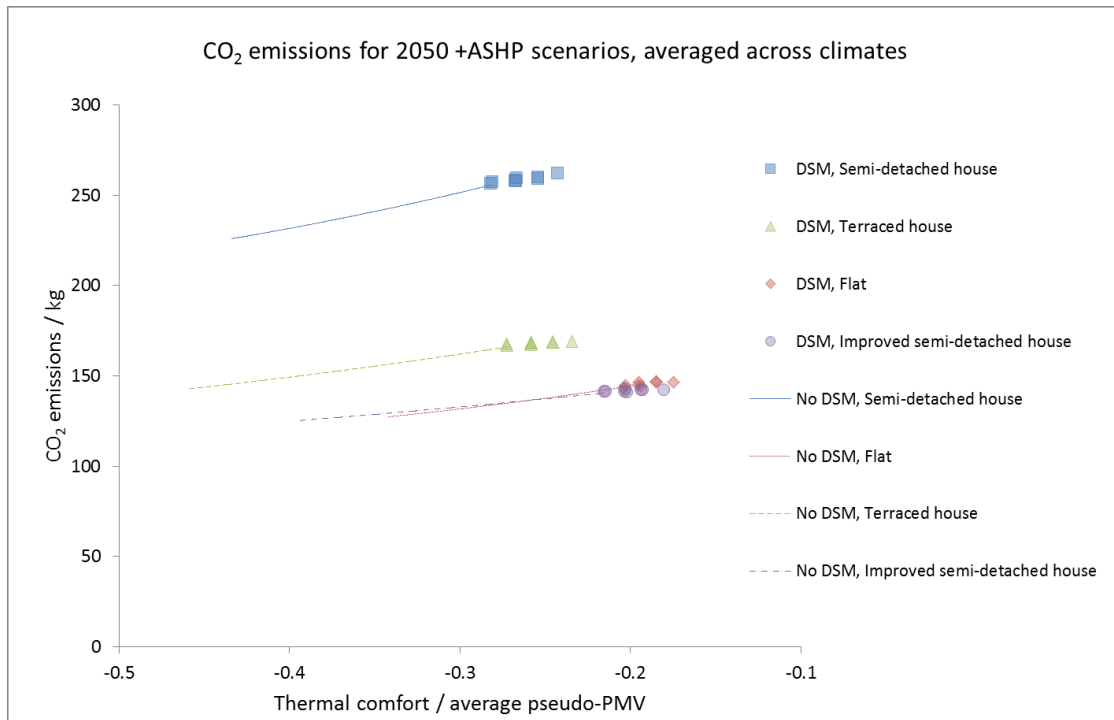
Figure 124: ASHP CO$_2$ emissions in 2050 +ASHP scenarios
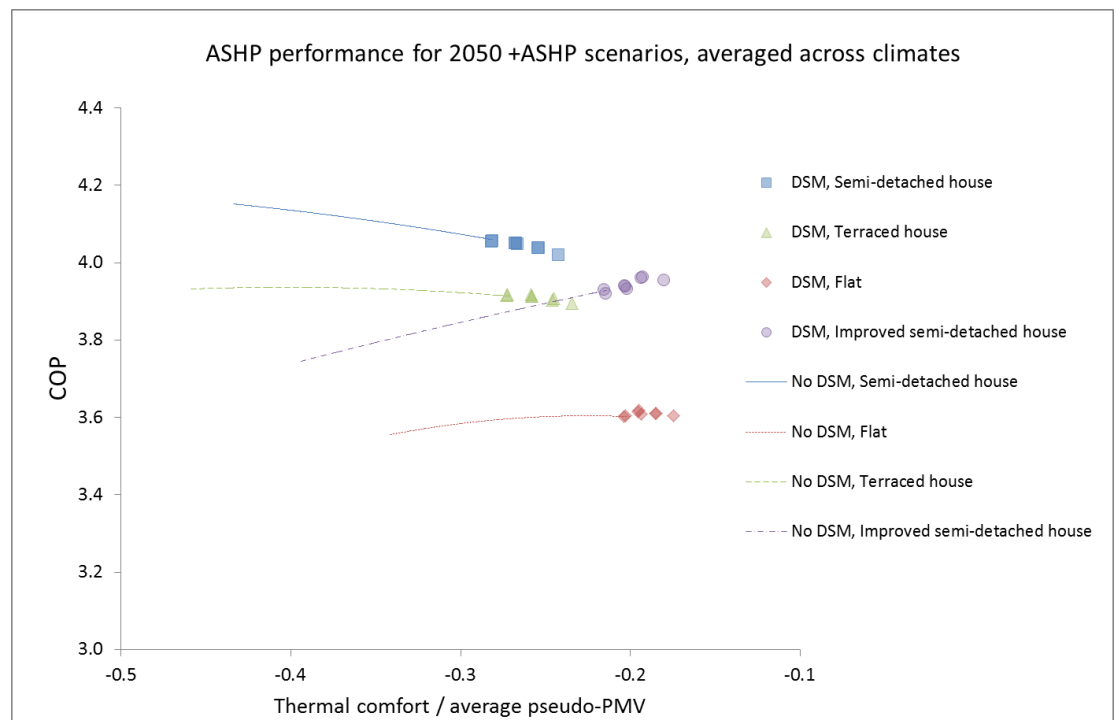
Figure 125: ASHP performance in 2050 +ASHP scenarios

In the 2035 scenarios, a slight reduction in CO$_2$ emissions is observed (approximately 3%) with the cases in which DSM is used compared to the cases in which it isn't (at the same level of thermal comfort). This underwhelming result can be partially explained by reference to the COP achieved by the ASHP in each scenario. In the cases in which DSM is used, a slight reduction in

COP occurs which partially offsets the advantage of preferentially operating at times when the marginal CO_2 emissions factor is lower. The reduction in COP is due to the increase in average flow temperature which is required in order to deliver heat more rapidly at certain times in scenarios which involved DSM.

The effect of the DSM is different in the 2050 (with additional ASHPs) scenario. Rather than decreasing the thermal comfort, the DSM signal actually increases it. The CO_2 emissions slightly increase with this increase of thermal comfort but not at the same rate as they do with the non-DSM control system.

Referring to the demand profiles illustrated in Figure 126 and Figure 127 helps to demonstrate why this is. These show the profile of net dispatchable demand after wind, nuclear and other non-dispatchable generation have been accounted for.
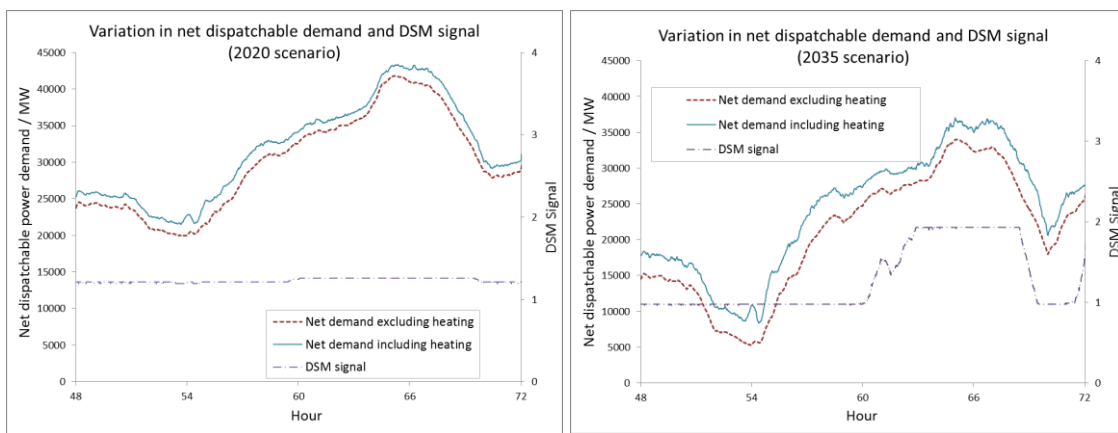
Figure 126: Demand profile for 24 hours in 2020 (left) and 2035 (right)

In the 2020 scenario, the DSM signal shows little fluctuation as the MEF remains fairly constant across the 24 hour period, most dispatchable generation is from CCGTs without CCS.

In the 2035 scenario there is significantly more CCS equipped plant and so the main effect on the DSM signal is to increase (i.e. discouraging ASHP use) when dispatchable demand is high and a greater proportion of additional demand would come from CCGTs without CCS (e.g. hours 60 to 69). In the plots for both 2020 and 2035, there is no point at which the MEF drops below the level of CCS plant (i.e. dispatchable plant is always required) and so the DSM does not encourage higher temperatures (resulting in the three sets of data in each grouping observed in Figure 128, corresponding to the three lower temperature deviations, -1°C, -2°C or -3°C). The 2035 scenarios show the greatest variation in the MEF of electricity and is subsequently the only scenario in which some reduction in emissions is achieved by the DSM (Figure 122 and Figure 128).
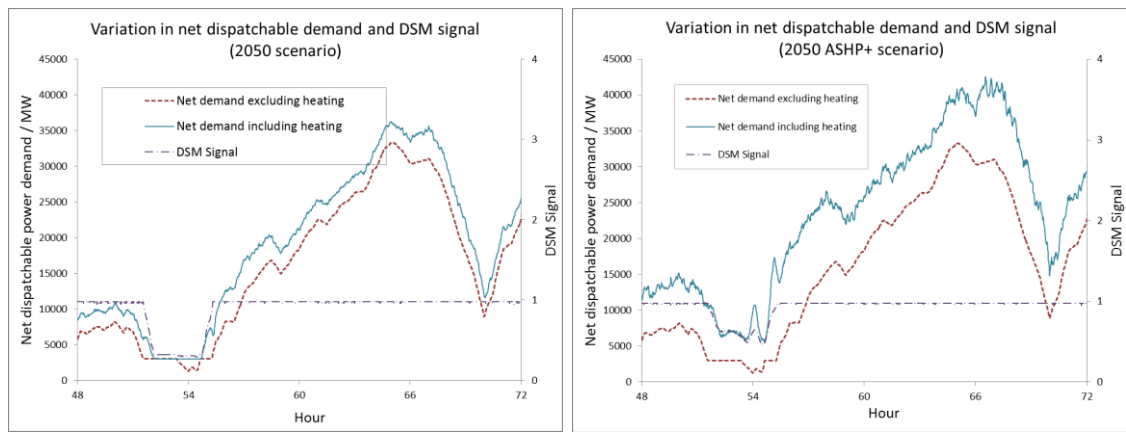
Figure 127: Demand profile for 24 hours in 2050 (left) and in 2050 with additional ASHPs (right)

Conversely, almost all dispatchable generation is met by CCS equipped plant in the 2050 scenarios. The DSM signal therefore rarely discourages consumption. However, there are periods (e.g. hours 52 to 56) when there is no dispatchable generation demand (and so renewable generation will be constrained) and so the DSM signal encourages consumption with higher temperatures. This explains the relatively higher (i.e. less negative) groupings of pseudo-PMV values relating to these scenarios in Figure 125 and Figure 128; the DSM rarely causes a decrease in the temperature within dwellings in these scenarios. Although the temperatures within the dwellings are increased at times using the low MEF electricity, this does not lead to a net reduction in electricity demand at other times and so the CO_2 emissions are not reduced but neither are they significantly increased. This finding suggests that alternative storage methods such as phase change materials or thermal storage which can be bypassed during warmer periods may decrease the CO_2 emissions resulting in these scenarios.

By averaging across buildings as well as climate, all of the results can be compared (Figure 128). The four groupings of data which can be observed for each scenario relate to the four temperature programmes used. In the 2010 to 2035 scenarios, the three sets of indistinguishable data points within each of these groups relate to the three values of maximum temperature decrease which the occupants of a dwelling will tolerate (-1°C, -2°C or -3°C). In the 2050 scenarios, the sets relate to the four values of the maximum temperature increase which are available to the DSM system (+0°C, +1°C, +2°C or 3°C).

Although the DSM signal had a limited net effect on emissions in these scenarios, in most cases it slightly decreased the COP of the ASHP relative to the equivalent conditions without DSM, (see Figure 129). This suggests that other types of DSM which might use a stronger signal without giving consideration to the MEF of the electricity might increase the CO_2 emissions associated with the use of the ASHPs. This potential effect should be considered when evaluating the relative merits of such systems.
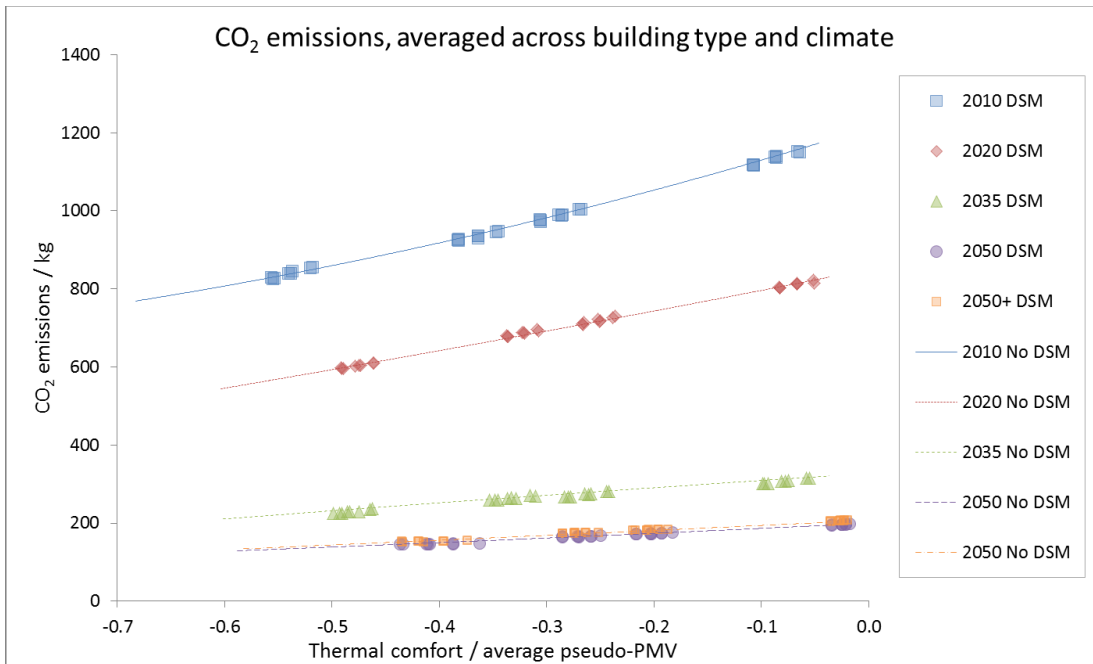
Figure 128: CO₂ emissions averaged across building type and climate
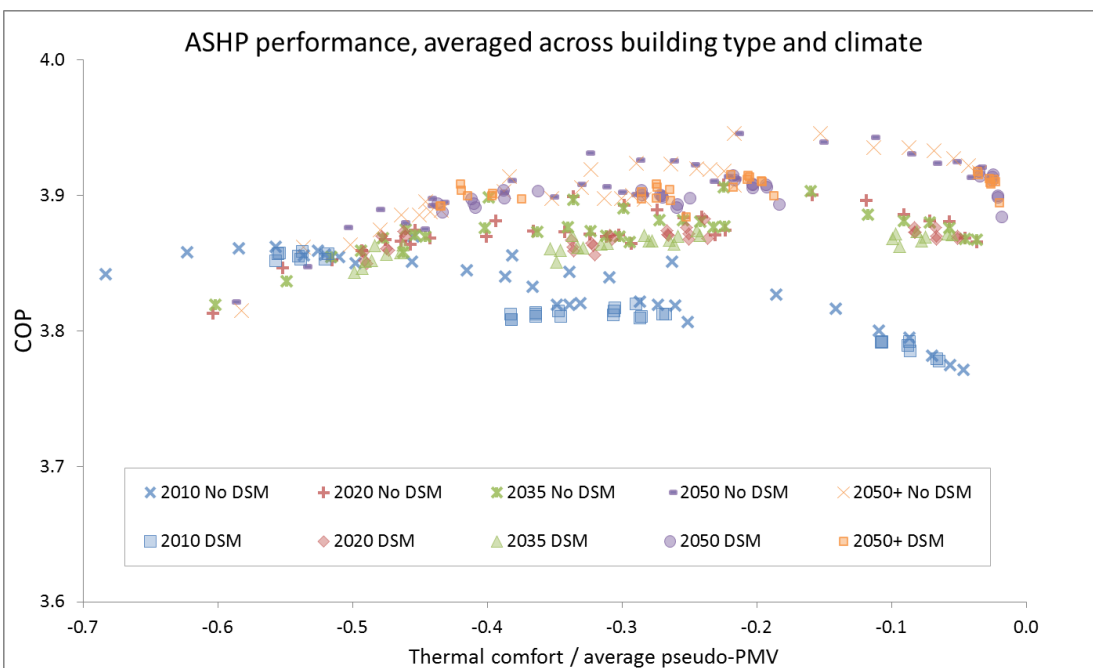
Figure 129: Effect of DSM signal on COP of ASHP

6.   Conclusions

6.1 Fulfilling the aims of this study

A new model has been developed and applied successfully to fulfil the aims of this study (section 3.2). This model is described in chapter 4 and has been used to generate results which consider the effect of the six factors listed under the first aim (relating to results, section 3.1). An overview of these results is given in section 5.1 before they are detailed in sections 5.2 to 5.11. The key findings are summarised in section 6.2, below.

6.2 Key findings

Several key findings have been made and are summarised below. Each of these findings is either more comprehensively covered than elsewhere in the literature or completely novel. Results relating to this research have been published in conference proceedings and a journal paper, as noted in Appendix C.

For a given heat demand, a state-of-the-art ASHP could consume less than 40% of the power of a mid-range unit installed with sub-optimal control.

The performance of the ASHP unit itself is responsible for around half of this range. Typically the state-of-the-art ASHP will require 65% to 75% as much power as a mid-range unit operating in the same conditions.

If the proportional control methodology is used, it typically reduces the power demands of the ASHP to around 77% to 84% of the demand if variable-temperature control is used. Using fixed-temperature control is likely to increase power demands to around 108% to 115% of that when variable-temperature control is used. A 30% reduction in power consumption can be achieved simply by changing fixed-temperature control to proportional control in some cases!

Enhancing the heat emitter system in a dwelling could improve the COP achieved by ASHPs by 10% to 20% if variable-temperature control is used but offers less of an improvement (up to 10%) if proportional control is used.

Although improving the level of insulation in a building has the potential to drastically reduce the heating demand (and therefore the power consumed by an ASHP), it is likely to slightly *decrease* the average COP of an ASHP (contrary to conventional advice). The lower heating demands (which would improve the COP) are balanced against the shorter (and therefore relatively colder) heating season.

A suitably installed ASHP can reduce CO_2 emissions by 40% relative to a good condensing gas boiler (if the mean grid carbon emissions factor is used). However, a mid-range ASHP will typically achieve very modest emissions savings relative to a condensing gas boiler and may cause an increase in CO_2 emissions if the installation conditions are unfavourable. If the marginal carbon emissions factor is considered more relevant then although it is possible to reduce CO_2 emissions with an ASHP, it is unlikely at present and mid-range ASHPs will typically increase emissions (by around 35% in the examples simulated here).

Although mCHP with high electrical efficiencies are available, the use of supplementary gas boilers with them will significantly reduce their system electrical efficiency. Although over-sizing is identified as a potential issue in the literature, it seems that under-sizing could have just as great a detrimental effect.

The results support the finding found elsewhere that large heat loads which allow more consistent operation will improve the performance of the SE-mCHP units. However, it seems that this improvement can also be achieved by units which maintain reasonable efficiency at part-load. For most of the combustion-based units, there will be an optimum buffer tank capacity. This is typically between 160kg and 640kg depending upon the unit and circumstances.

The unit electrical efficiency of SOFC A exceeds that of the electrical grid and has significantly lower CO_2 emissions associated with it. If a large SOFC unit with the same characteristics (e.g. the hypothetical SOFC B) were used without any restriction on electrical exports, the displacement of electrical generation would result in a net reduction in CO_2 emissions ("negative emissions"), even if none of the heat is used. This effect is amplified if marginal emissions are considered in place of mean emissions but it is not clear that this would be appropriate for larger penetrations of the technology.

SOFC A and SOFC B can operate with lower PER and CO_2 emissions if they are run continuously at the power output corresponding to their peak electrical output (compared to heat-led operation). The effect of electrical exports more than makes up for any wasted thermal output. This finding makes the restrictions on the rate-of-change exhibited by the units largely irrelevant.

It is relatively hard to achieve the PER or CO_2 emissions savings which might otherwise be assumed for the PEMFC-mCHP units. The control strategy for these units will need to be more advanced than that used here. In contrast to the SOFC units, a higher limit on the maximum rate-of-change which they can achieve would improve their overall performance. A large

capacity buffer tank is also likely to improve their performance but the CO_2 emissions savings achieved were less than 20% in the circumstances simulated in this study.

The savings associated with using different temperature programmes are largely correlated to the reduction in heat demand. Reducing the programme air temperature from 21°C to 18°C tends to reduce total heat demand (and associated impacts) by around 25%.

When considering the effect of the climate, an additional complication is the effect of the variability of the outside air temperature. If the air temperature is more variable (for example inland locations or the modelled future climates) then the heating demand tends to be higher relative to a more consistent climate with the same mean air temperature. This effect is amplified in the case of the SOFC units which provide a baseload of heat. The average COP of ASHPs is likely to remain consistent despite increases in the average air temperature as the times at which they operate are, necessarily, when it is cooler.

The marginal CO_2 emissions factors do not decrease as rapidly as the mean CO_2 emissions factors in the scenarios considered. If mean emissions are considered then the ASHP units tend to be favourable in most cases by 2020. However, if marginal CO_2 emissions are considered more appropriate then the window in which mCHP units can offer emissions reductions is extended by several years after this time. Additionally, the marginal PER of electricity in the scenarios does not significantly reduce. It is possible that some of the mCHP units will be able to offer PER savings in some circumstances even in the later scenarios.

Even with the use of DSM and optimistic assumptions regarding the installation of the units, local grid power infrastructure will need to be reinforced if the majority of dwellings within a neighbourhood are to have heat supplied by ASHPs. It is possible that the use of DSM could reduce and delay the level of reinforcement required but only a limited reduction in the required capacity is possible (e.g. from 320kW down to 260kW in these scenarios).

If reinforcement of the local infrastructure is not possible and the alternative would be a lower number of ASHP units, then the use of a mixture of SOFC-mCHP units in combination with ASHPs and DSM can reduce CO_2 emissions, even in the context of a relatively decarbonised grid in which the SOFC-mCHP units are unfavourable on their own.

Attempts to use DSM to discourage operation of ASHPs when the MEF of electricity is high and encourage it when the MEF is low had little success; the emissions reduction was similar to that achieved with the DSM signal which considered only local network constraints and had a minimal effect in both cases.

Innovative steps have been used during the development of the model for this research. These include the use of exergy interpolation for the calculation of the momentary performance of the ASHPs, the use of different levels of detail in the model with different time-steps in order to perform efficient simulations which are sufficiently accurate, plotting exergy performance against power-fractions, and devising new control methodologies which simulate the potential nature of a DSM signal.

6.3 Conclusions

Efficient Air Source Heat Pumps units have the potential to make PER and CO_2 emissions savings at present but, more significantly, as a contribution to a future low-carbon society. However, their performance is sensitive to the conditions studied. In particular, appropriate control of the units can yield energy savings of around 25%. Additionally, the carbon emissions intensity of the grid is an important consideration. These factors should be understood when assessing their relative merits.

Similarly, mCHP units demonstrate a wide range of performances which should be understood but also have the potential to contribute to reducing PERs and CO_2 emissions. Different approaches will be appropriate to the control of fuel cell based units compared to combustion-based units. SOFC units with high electrical outputs offer the greatest potential savings during the next 10 to 15 years. If the grid is significantly decarbonised then their potential to reduce CO_2 emissions is reduced but in most cases, they can still offer PER savings.

7. Recommendations

This study suggests several avenues of additional research which are likely to be productive.

7.1 Additional studies involving model

A more complete picture of the environmental performance of the technologies could be achieved by applying a full Life Cycle Assessment methodology. The model provides data of energy flows and generation in disaggregated form in order to facilitate the calculation of other environmental impacts associated with the consumption of fuel and generation of electricity. However, a complete assessment should include the other life stages of the technologies.

The optimum frequency at which DSM signals to dwellings could be updated in order to achieve certain aims could be readily investigated using the model if clear criteria for the objectives of the DSM system were established.

7.2 Development of modelling

The model could be expanded to include GSHPs and similar analysis performed to investigate the effect of the factors considered here on their performance. The main additional complexity involved in this would be the construction of a thermal model for soil which has already been achieved elsewhere.

Given the potential fit observed between the properties of transcritical heat pumps and the heat demands of a well-insulated dwelling, equivalent analysis including one would be valuable. Achieving acceptable fidelity would require an alternative heat exchanger model that can accurately represent the temperature glide which occurs as well as the mean flow temperature.

The ability to store more thermal energy at a lower temperature could reduce the energy penalty of using buffer tanks, increasing the flexibility which they could provide. Additional development of the model could include the option for phase-change materials in the buffer tanks or in the fabric of the buildings.

The model currently uses the heat generation from the heating units to describe their status which is then used with other parameters (e.g. temperatures) in order to calculate other energy flows (e.g. fuel and power). Using the power or fuel flow to describe the status of the units may lead to models which more closely reflect real units. This could be weighed against the additional complexity which would be involved.

Clustering of micro-generation technologies has been shown to have some advantages but there are other potential synergies which could be explored. Solar thermal units could be used to reduce summer time operation of mCHP units (when either excessive cycling or dumping of heat might otherwise occur). Biomass burners could be used in series with the output of an ASHP (reducing the flow temperature which the ASHP needs to supply but still generating the majority of heat from it). Solar PV units could balance the reduction in output from mCHP units during the summer (when their potential generation is higher but that from heat-led mCHP is lower). Electricity generated by intermittent renewables which is surplus to requirements could be used to supply high temperature heat storage which may have synergies with an absorption heat pump.

7.3 Larger studies

The large performance improvement which can apparently be achieved through the use of the proportional control methodology with ASHPs should be investigated in more detail. This could include more detailed modelling but ideally experimental verification of the result should be pursued.

Similarly, a cross-disciplinary study into the implications of achieving thermal comfort with lower air temperatures and the ways in which this could be achieved could result in the potential to reduce energy demands.

8. Appendix A: Bibliography

AEA Consulting, 2009. *Environmental Product Declaration of Electricity from Torness Nuclear Power Station*, London: British Energy Group Plc.

AEA Consulting, Oxford Economics, Biomass Energy Centre & Forest Research, 2011. *UK and Global Bioenergy Resource – Final report*, London: DECC.

AEA Energy & Environment, 2008. *Environmental Product Declaration of Electricity from Sizewell B Nuclear Power Station Technical Report*, London: British Energy Group Plc.

AirconWarehouse Ltd, 2012. Heat Pumps. Available at: http://www.airconwarehouse.com/acatalog/Heat_Pump_Boiler_Water_Heaters.html [Accessed January 18, 2013].

Aliabadi, A., Thomson, M.J. & Wallace, J.S., 2010. Efficiency Analysis of Natural Gas Residential Micro-cogeneration Systems. *Energy & Fuels*, 24(3), pp.1704–1710. Available at: http://pubs.acs.org/doi/abs/10.1021/ef901212n [Accessed January 11, 2011].

Allen, S.R., 2009. *Micro-generation for UK households. Thermodynamic and related analyses*, Thesis (PhD): University of Bath.

Allen, S.R. & Hammond, G.P., 2010. Thermodynamic and carbon analyses of micro-generators for UK households. *Energy*, 35(5), pp.2223–2234. Available at: http://linkinghub.elsevier.com/retrieve/pii/S0360544210000605 [Accessed November 14, 2010].

Anandarajah, G., Strachan, N., Ekins, P., Kannan, R. & Hughes, N., 2009. *Pathways to a Low Carbon Economy: Energy Systems Modelling*, London: UKERC. Available at: http://www.inference.phy.cam.ac.uk/sustainable/refs/ukerc/PathwaysLowCarbonEconomy.pdf [Accessed August 24, 2011].

ASHRAE, 2001. *International Weather for Energy Calculations (IWEC Weather Files) Users manual and CD-ROM*, Atlanta: American Society of Heating Refrigerating and Air-Conditioning Engineers Inc.

Ault, G., Frame, D., Hughes, N., Strachan, N., Watson, J. & Pollitt, M.G., 2008. *Electricity Network Scenarios for Great Britain in 2050 Final Report for Ofgem's LENS Project*, London: Ofgem.

Austin, B.T. & Sumathy, K., 2011. Transcritical carbon dioxide heat pump systems: A review. *Renewable and Sustainable Energy Reviews*, 15(8), pp.4013–4029. Available at: http://dx.doi.org/10.1016/j.rser.2011.07.021 [Accessed July 26, 2012].

Bakalis, D.P. & Stamatis, A.G., 2013. Incorporating available micro gas turbines and fuel cell: Matching considerations and performance evaluation. *Applied Energy*, 103, pp.607–617. Available at: http://linkinghub.elsevier.com/retrieve/pii/S0306261912007325 [Accessed May 17, 2013].

Banfill, P.F.G. & Peacock, A.D., 2007. Energy-efficient new housing - the UK reaches for sustainability. *Building Research & Information*, 35(4), pp.426–436. Available at: http://www.informaworld.com/openurl?genre=article&doi=10.1080/09613210701339454&magic=crossref||D404A21C5BB053405B1A640AFFD44AE3 [Accessed June 29, 2010].

Barbieri, E.S., Spina, P.R. & Venturini, M., 2012. Analysis of innovative micro-CHP systems to meet household energy demands. *Applied Energy*, 97, pp.723–733. Available at: http://linkinghub.elsevier.com/retrieve/pii/S0306261911007872 [Accessed March 9, 2013].

Barelli, L., Bidini, G., Gallorini, F. & Ottaviano, A., 2011. An energetic–exergetic analysis of a residential CHP system based on PEM fuel cell. *Applied Energy*, 88(12), pp.4334–4342. Available at: http://linkinghub.elsevier.com/retrieve/pii/S0306261911003126 [Accessed July 24, 2011].

Barnacle, M., Robertson, E., Galloway, S., Barton, J. & Ault, G., 2013. Modelling generation and infrastructure requirements for transition pathways. *Energy Policy*, 52, pp.60–75. Available at: http://linkinghub.elsevier.com/retrieve/pii/S030142151200331X [Accessed June 13, 2013].

Barton, J., Huang, S., Infield, D., Leach, M., Ogunkunle, D., Torriti, J. & Thomson, M., 2013. The evolution of electricity demand and the role for demand side participation, in buildings and transport. *Energy Policy*, 52, pp.85–102. Available at: http://linkinghub.elsevier.com/retrieve/pii/S0301421512007227 [Accessed June 13, 2013].

Beausoleil-Morrison, I., Arndt, U., et al., 2007. *Experimental Investigation of Residential Cogeneration Devices and Calibration of Annex 42 Models. A Report of Subtask B of FC+COGEN-SIM The Simulation of Building-Integrated Fuel Cell and Other Cogeneration Sys- tems. Annex 42 of the International Energy* I. Beausoleil-Morrison, ed., Annex 42 of the International Energy Agency Energy Conservation in Buildings and Community Systems Programme. Available at: www.ecbcs.org.

Beausoleil-Morrison, I., Weber, A., Maréchal, F., Griffith, B., Ferguson, A., Kelly, N.J. & Marechal, F., 2007. *Specifications for Modelling Fuel Cell and Combustion-Based Residential Cogeneration Devices within Whole-Building Simulation Programs. A Report of Subtask B of FC+COGEN-SIM The Simulation of Building-Integrated Fuel Cell and Other Cogeneration Systems. A* N. Kelly & I. Beausoleil-Morrison, eds., Annex 42 of the International Energy Agency Energy Conservation in Buildings and Community Systems Programme. Available at: www.cogen-sim.net.

Belcher, S., Hacker, J. & Powell, D., 2005. Constructing design weather data for future climates. *Building Services Engineering Research and Technology*, 26(1), pp.49–61. Available at: http://bse.sagepub.com/cgi/doi/10.1191/0143624405bt112oa.

Berntsson, T., 2002. Heat sources — technology , economy and environment. *International Journal of Refrigeration*, 25, pp.428–438.

Bettanini, E., Gastaldello, A. & Schibuola, L., 2003. Simplified models to simulate part load performances of air conditioning equipments. In *Eighth International IBPSA Conference, 11 - 14 August 2003*. Eindhoven, pp. 107–114.

Beyer, D. & Kelly, N.J., 2008. Modelling the behaviour of domestic micro-cogeneration under different operating regimes and with variable thermal buffering. In *In: Micro-Cogen 2008, 1st International Conference on Micro-Cogeneration Technologies and Applications, 29 April - 1 May 2008*. Ottawa.

Bhandari, M., Shrestha, S. & New, J., 2012. Evaluation of weather datasets for building energy simulation. *Energy and Buildings*, 49, pp.109–118. Available at: http://linkinghub.elsevier.com/retrieve/pii/S0378778812000503 [Accessed April 1, 2013].

Bi, Y., Wang, X., Liu, Y., Zhang, H. & Chen, L., 2009. Comprehensive exergy analysis of a ground-source heat pump system for both building heating and cooling modes. *Applied Energy*, 86(12), pp.2560–2565. Available at: http://linkinghub.elsevier.com/retrieve/pii/S0306261909001342.

Bianchi, M., De Pascale, A. & Spina, P.R., 2012. Guidelines for residential micro-CHP systems design. *Applied Energy*, 97, pp.673–685. Available at: http://linkinghub.elsevier.com/retrieve/pii/S0306261911007203 [Accessed May 17, 2013].

Biaou, A.L. & Bernier, M.A., 2008. Achieving total domestic hot water production with renewable energy. *Building and Environment*, 43(4), pp.651–660. Available at: http://linkinghub.elsevier.com/retrieve/pii/S0360132306003222 [Accessed December 16, 2010].

Blom, I., Itard, L. & Meijer, A., 2010. LCA-based environmental assessment of the use and maintenance of heating and ventilation systems in Dutch dwellings. *Building and Environment*, 45(11), pp.2362–2372. Available at: http://linkinghub.elsevier.com/retrieve/pii/S0360132310001198 [Accessed May 5, 2011].

Boait, P.J., Fan, D. & Stafford, A., 2011. Performance and control of domestic ground-source heat pumps in retrofit installations. *Energy and Buildings*, 43(8), pp.1968–1976. Available at: http://linkinghub.elsevier.com/retrieve/pii/S037877881100154X [Accessed May 5, 2011].

Boardman, B., 2007a. Examining the carbon agenda via the 40% House scenario. *Building Research & Information*, 35(4), pp.363–378. Available at: http://www.informaworld.com/openurl?genre=article&doi=10.1080/09613210701238276&magic=crossref||D404A21C5BB053405B1A640AFFD44AE3 [Accessed January 10, 2011].

Boardman, B., 2007b. *Home Truths: A low-carbon strategy to reduce UK housing emissions by 80% by 2050*, Oxford: Environmental Change Institute, University of Oxford.

Boardman, B., Darby, S., Killip, G., Hinnells, M., Jardine, C.N., Palmer, J. & Sinden, G., 2005. *40% house*, Oxford: Environmental Change Institute, University of Oxford.

Borg, S., Hong, J., Jardine, C.N., Johnstone, C.M., Kelly, N.J. & Tuohy, P., 2010. The Energy Characteristics of Low and Zero-Carbon Dwellings and the Implications for Future Energy Systems The Highly Distributed Energy Future Consortium (HiDEF). , pp.1–20.

Borgeson, S. & Brager, G., 2011. Comfort standards and variations in exceedance for mixed-mode buildings. *Building Research & Information*, 39(2), pp.118–133. Available at: http://www.informaworld.com/openurl?genre=article&doi=10.1080/09613218.2011.556345&magic=crossref%7c%7cD404A21C5BB053405B1A640AFFD44AE3 [Accessed March 30, 2011].

Bourke, G. & Bansal, P., 2010. Energy consumption modeling of air source electric heat pump water heaters. *Applied Thermal Engineering*, 30(13), pp.1769–1774. Available at: http://linkinghub.elsevier.com/retrieve/pii/S1359431110001626 [Accessed July 23, 2012].

Bove, R., 2007. 11. Solid Oxide Fuel Cells : Principles , Designs and State-of-the-Art in Industries. In S. Basu, ed. *Recent Trends in Fuel Cell Science and Technology*. New Dehli: Anamaya Publishers, pp. 267 – 285.

BRE, 2010. *SAP 2009 - The Government's Standard Assessment Procedure for Energy Rating of Dwellings*, Garston: Building Research Establishment Ltd.

BSI, 2007a. *BS EN14511-2 Air conditioners , liquid chilling packages and heat pumps with electrically driven compressors for space heating and cooling - Part2: Test conditions*, London: BSI.

BSI, 2007b. *BS EN14511-3 Air conditioners , liquid chilling packages and heat pumps with electrically driven compressors for space heating and cooling - Part 3: Test methods*, London: BSI.

BSI, 2008. *BS EN15316-4-2 Heating systems in buildings — Method for calculation of system energy requirements and system efficiencies — Part 4-2:Space heating generation systems, heat pump systems*, London: BSI.

BSI, 1997. *BS EN255-3:1997 Air conditioners , liquid chilling packages and heat pumps with electrically driven compressors - Heating mode Part 3 . Testing and requirements for sanitary hot water units*, London: BSI.

Burt, G.M., Elders, I.M., Galloway, S.J., Kelly, N.J. & Tumilty, R.M., 2008. Assessment of highly distributed power systems using an integrated simulation approach. *Proceedings of the Institution of Mechanical Engineers, Part A: Journal of Power and Energy*, 222(7), pp.657–668. Available at: http://journals.pepublishing.com/openurl.asp?genre=article&id=doi:10.1243/09576509JPE535.

Butler, D. & Hyde, K., 2007. *Ecodan PUHZ-W90VHA air to water heat pump tests*, Garston: Building Research Establishment Ltd.

Carbon Trust, 2010a. *Conversion factors*, London: The Carbon Trust.

Carbon Trust, 2010b. *Degree days for energy management*, London: HMSO.

Carbon Trust, 2011. *Micro-CHP Accelerator*, London: Carbon Trust.

Carbon Trust, 2007. *Micro-CHP Accelerator Interim report*, London: The Carbon Trust.

CFCL, 2008. *BlueGEN Modular Generator - Power + Heat*, Victoria: Ceramic Fuel Cells Ltd. Available at: www.cfcl.com.au.

Chandrashekar, M., Le, N.T., Sullivan, H.F. & Hollands, K.G.T., 1982. A comparative study of solar assisted heat pump systems for Canadian locations. *Solar Energy*, 28(3), pp.217–226.

Choi, H.-J., Kim, B.-S., Kang, D. & Kim, K.C., 2011. Defrosting method adopting dual hot gas bypass for an air-to-air heat pump. *Applied Energy*, 88(12), pp.4544–4555. Available at: http://linkinghub.elsevier.com/retrieve/pii/S0306261911003345 [Accessed September 21, 2011].

Choudhury, A., Chandra, H. & Arora, a., 2013. Application of solid oxide fuel cell technology for power generation—A review. *Renewable and Sustainable Energy Reviews*, 20, pp.430–442. Available at: http://linkinghub.elsevier.com/retrieve/pii/S1364032112006430 [Accessed January 23, 2013].

Chow, T.T., Fong, K.F., Pei, G., Ji, J. & He, M., 2010. Potential use of photovoltaic-integrated solar heat pump system in Hong Kong. *Applied Thermal Engineering*, 30(8-9), pp.1066–1072. Available at: http://linkinghub.elsevier.com/retrieve/pii/S1359431110000268 [Accessed October 11, 2010].

Chua, K.J., Chou, S.K. & Yang, W.M., 2010. Advances in heat pump systems: A review. *Applied Energy*, 87(12), pp.3611–3624. Available at: http://linkinghub.elsevier.com/retrieve/pii/S030626191000228X [Accessed August 20, 2010].

Clarke, J.A., Johnstone, C.M., Kelly, N.J., Strachan, P.A. & Tuohy, P., 2008. The role of built environment energy efficiency in a sustainable UK energy economy. *Energy Policy*, 36(12), pp.4605–4609. Available at: http://linkinghub.elsevier.com/retrieve/pii/S0301421508004904 [Accessed November 26, 2012].

Clay, A. & Tansley, G.D., 2010. A micro gas turbine for UK domestic combined heat and power. *Proceedings of the Institution of Mechanical Engineers, Part A: Journal of Power and Energy*, 224(6), pp.839–849. Available at: http://journals.pepublishing.com/openurl.asp?genre=article&id=doi:10.1243/09576509JPE 996 [Accessed January 4, 2011].

Cockroft, J. & Kelly, N.J., 2006. A comparative assessment of future heat and power sources for the UK domestic sector. *Energy Conversion and Management*, 47(15-16), pp.2349–2360. Available at: http://linkinghub.elsevier.com/retrieve/pii/S0196890405003195 [Accessed November 11, 2010].

Comakli, O., Kaygusuz, K. & Ayhan, T., 1993. Solar-assisted heat pump and energy storage for residential heating. *Solar Energy*, 51(5), pp.357–366. Available at: http://linkinghub.elsevier.com/retrieve/pii/0038092X9390148H.

Cooper, S., Hammond, G.P. & McManus, M.C., 2012. Thermodynamic efficiency of low-carbon domestic heating systems: heat pumps and micro-cogeneration. *Proceedings of the Institution of Mechanical Engineers, Part A: Journal of Power and Energy*, 227(1), pp.18–29. Available at: http://pia.sagepub.com/lookup/doi/10.1177/0957650912466011 [Accessed February 27, 2013].

Cooper, S.J.G., Dowsett, J., Hammond, G.P., Mcmanus, M.C. & Rogers, J.G., 2012. Performance implications of heat pumps participating in demand side management. In *Proceedings of SDEWES 2012, 1 - 7 July 2012*. Ohrid, Macedonia.

Cooper, S.J.G., Hammond, G.P. & McManus, M.C., 2011a. Heat pump performance and factors affecting it. In *Buildings Don't Use Energy, People Do? - Domestic Energy Use and CO2 Emissions in Existing Dwellings, 28 June 2011*. Bath, UK.

Cooper, S.J.G., Hammond, G.P. & McManus, M.C., 2011b. Thermodynamic analysis of efficient domestic heating systems. In *Proceedings of 2nd International Conference in Microgeneration and Related Technologies in Buildings: Microgen 2, 4 - 6th April 2011*. Glasgow.

Critoph, R.E. & Metcalf, S.J., 2012. Development of a gas-fired domestic heat pump. In *Proceedings of WREF 2012, 13 - 17 May 2012*. Denver, pp. 1–5. Available at: http://ases.conference-services.net/resources/252/2859/pdf/SOLAR2012_0547_full paper.pdf.

Cruden, A., Houghton, T., Gair, S., Duerr, M., Agnew, G.D., Stewart, E.M. & Lutz, A., 2008. Fuel cells as distributed generation. *Proceedings of the Institution of Mechanical Engineers, Part A: Journal of Power and Energy*, 222(7), pp.707–720. Available at: http://journals.pepublishing.com/openurl.asp?genre=article&id=doi:10.1243/09576509JPE 609 [Accessed December 2, 2010].

Daikin, *Altherma Outdoor Units, ERHQ006-016BAV3*, Daikin Industries Ltd.

Danfoss, 2012. *DHP-A air source heat pump*, Sheffield: Danfoss Heat Pumps UK.

Danov, S., Carbonell, J., Cipriano, J. & Martí-Herrero, J., 2013. Approaches to evaluate building energy performance from daily consumption data considering dynamic and solar gain effects. *Energy and Buildings*, 57(2010), pp.110–118. Available at: http://linkinghub.elsevier.com/retrieve/pii/S0378778812005841 [Accessed March 3, 2013].

Davies, G. & Woods, P., 2009. *The potential and costs of district heating networks*, Oxford: Poyry Energy (Oxford) Ltd.

DCLG, 2007a. *Building Regulations - Energy efficiency requirements for new dwellings*, London: Department For Communities And Local Government.

DCLG, 2009. *Code for Sustainable Homes*, London: Department For Communities And Local Government.

DCLG, 2007b. *English House Condition Survey*, London: Department For Communities And Local Government.

DCLG, 2007c. *Homes for the future: more affordable, more sustainable*, London: TSO.

De Dear, R., 2011. Revisiting an old hypothesis of human thermal perception: alliesthesia. *Building Research & Information*, 39(2), pp.108–117. Available at: http://www.informaworld.com/openurl?genre=article&doi=10.1080/09613218.2011.5522 69&magic=crossref%7c%7cD404A21C5BB053405B1A640AFFD44AE3 [Accessed March 30, 2011].

DECC, 2010a. *2050 Pathways Analysis*, London: HM Government.

DECC, 2011. *Digest of United Kingdom Energy Statistics 2011*, London: TSO.

DECC, 2009a. *Smarter Grids : The Opportunity*, London: Department for Energy and Climate Change.

DECC, 2012. *The Future of Heating: A strategic framework for low carbon heat in the UK*, London: Department for Energy and Climate Change.

DECC, 2009b. *The UK Low Carbon Transition Plan*, London: TSO.

DECC, 2007. *The UK Renewable Energy Strategy*, London: TSO.

DECC, 2010b. *Warm Homes , Greener Homes: A Strategy for Household Energy Management Supporting Paper VIII An Enabling Framework for District Heating and Cooling*, London: Department for Energy and Climate Change.

DEFRA, 2011. *2011 Guidelines to Defra / DECC's GHG Conversion Factors for Company Reporting: Methodology Paper for Emission Factors*, London: Department for Environment, Food and Rural Affairs.

DEFRA, 2009. *Adapting to climate change - UK Climate Projections*, London: Department For Communities And Local Government.

Degner, T., Schmid, J. & Strauss, P. eds., 2006. *Distributed Generation with High Penetration of Renewable Energy Sources*, Kassel: Institut fur Solare Energieversorgungstechnik e.V.

DeLonghi, *BRAN M Climaventa Heat Pump Performance*,

Demir, H., Mobedi, M. & Ülkü, S., 2008. A review on adsorption heat pump: Problems and solutions. *Renewable and Sustainable Energy Reviews*, 12(9), pp.2381–2403. Available at: http://linkinghub.elsevier.com/retrieve/pii/S1364032107000998 [Accessed July 24, 2011].

Dong, L., Liu, H. & Riffat, S., 2009. Development of small-scale and micro-scale biomass-fuelled CHP systems – A literature review. *Applied Thermal Engineering*, 29(11-12), pp.2119–2126. Available at: http://linkinghub.elsevier.com/retrieve/pii/S1359431108004766 [Accessed August 30, 2010].

Dorer, V. & Weber, A., 2009. Energy and CO2 emissions performance assessment of residential micro-cogeneration systems with dynamic whole-building simulation programs. *Energy Conversion and Management*, 50(3), pp.648–657. Available at: http://linkinghub.elsevier.com/retrieve/pii/S0196890408004123 [Accessed October 4, 2010].

Dorer, V., Weber, R. & Weber, A., 2005. Performance assessment of fuel cell micro-cogeneration systems for residential buildings. *Energy and Buildings*, 37(11), pp.1132–1146. Available at: http://linkinghub.elsevier.com/retrieve/pii/S0378778805001076 [Accessed December 9, 2010].

Douglas, C. a, Harrison, G.P. & Chick, J.P., 2008. Life cycle assessment of the Seagen marine current turbine. *Proceedings of the Institution of Mechanical Engineers, Part M: Journal of Engineering for the Maritime Environment*, 222(1), pp.1–12. Available at: http://pim.sagepub.com/lookup/doi/10.1243/14750902JEME94 [Accessed November 4, 2012].

Dowson, M., Poole, A., Harrison, D. & Susman, G., 2012. Domestic UK retrofit challenge: Barriers, incentives and current performance leading into the Green Deal. *Energy Policy*, 50, pp.294–305. Available at: http://dx.doi.org/10.1016/j.enpol.2012.07.019 [Accessed March 3, 2013].

Dunbabin, P. & Wickins, C., 2012. *Detailed analysis from the first phase of the Energy Saving Trust's heat pump field trial*, London: Department for Energy and Climate Change.

E4Tech, 2009. *Biomass supply curves for the UK*, London: Department for Energy and Climate Change.

Eames, M., Kershaw, T. & Coley, D., 2010. On the creation of future probabilistic design weather years from UKCP09. *Building Services Engineering Research and Technology*, 32(2), pp.127–142. Available at: http://bse.sagepub.com/cgi/doi/10.1177/0143624410379934 [Accessed November 8, 2012].

EC, 2001. Directive 2001/80/EC on the limitation of emissions of certain pollutants into the air from large combustion plants. *Official Journal of the European Communities*.

EC, 2002. Directive 2002/91/EC on the Energy Performance of Buildings. *Official Journal of the European Communities*, pp.65–71.

EC, 2004. Directive 2004/8/EC on the promotion of cogeneration based on a useful heat demand in the internal energy market and amending Directive 92/42/EEC. *Official Journal of the European Communities*.

EC, 2009. Directive 2009/28/EC on the Promotion of the use of energy from renewable sources and amending and subsequently repealing Directives 2001/77/EC and 2003/30/EC. *Official Journal of the European Communities*, pp.16–62.

Ecoinvent, 2010. *Ecoinvent Database v2.2*, Zurich: Swiss Centre for Life Cycle Inventories.

Electricity Networks Strategy Group, 2009. A Smart Grid Vision. In ENSG, pp. 1–27.

Elexon, 2012. Balancing Mechanism Reports. Available at: http://www.bmreports.com/ [Accessed June 10, 2012].

Energimyndigheten, 2012. Air Water Heat Pumps - Comparison. Available at: http://www.energimyndigheten.se/sv/Hushall/Testerresultat/Testresultat/Luftvattenvarmep umpar1/?tab=1 [Accessed January 24, 2013].

Energy Saving Trust, 2012. *A buyer's guide to heat pumps*, London: Energy Saving Trust.

Energy Saving Trust, 2007. *Domestic Ground Source Heat Pumps: Design and installation of closed-loop systems – A guide for specifiers, their advisors and potential users*, London: Energy Saving Trust.

Energy Saving Trust, 2010. *Getting warmer: a field trial of heat pumps*, London: Energy Saving Trust.

Energy Saving Trust, 2008. *Measurement of Domestic Hot Water Consumption in Dwellings*, London: Energy Saving Trust.

Ertesvåg, I.S., 2011. Uncertainties in heat-pump coefficient of performance (COP) and exergy efficiency based on standardized testing. *Energy and Buildings*, 43(8), pp.1937–1946. Available at: http://linkinghub.elsevier.com/retrieve/pii/S0378778811001484 [Accessed May 17, 2013].

European Heat Pump Association, 2009. *EHPA Testing Regulation Testing of Air / Water Heat Pumps. Terms , Test Conditions and Test Method based on EN14511-1 through 4*,

Fanger, P.O., 1973. Assessment of man's thermal comfort in practice. *British journal of industrial medicine*, 30(4), pp.313–24. Available at: http://www.pubmedcentral.nih.gov/articlerender.fcgi?artid=1069471&tool=pmcentrez&re ndertype=abstract.

Fantazzini, D., Höök, M. & Angelantoni, A., 2011. Global oil risks in the early 21st century. *Energy Policy*, 39(12), pp.7865–7873. Available at: http://linkinghub.elsevier.com/retrieve/pii/S0301421511007245 [Accessed March 29, 2013].

Fardoun, F., Ibrahim, O. & Zoughaib, A., 2011. Quasi-Steady State Modeling of an Air Source Heat Pump Water Heater. *Energy Procedia*, 6, pp.325–330. Available at: http://linkinghub.elsevier.com/retrieve/pii/S1876610211014482 [Accessed April 11, 2013].

Fernandez, N., Hwang, Y. & Radermacher, R., 2010. Comparison of CO2 heat pump water heater performance with baseline cycle and two high COP cycles. *International Journal of Refrigeration*, 33(3), pp.635–644. Available at: http://linkinghub.elsevier.com/retrieve/pii/S0140700709002850 [Accessed September 13, 2012].

Forsen, M., 2005. *Heat Pumps, Technology and Environmental Impact*, Swedish Heat Pump Association.

Foxon, T.J., 2013. Transition pathways for a UK low carbon electricity future. *Energy Policy*, 52, pp.10–24. Available at: http://linkinghub.elsevier.com/retrieve/pii/S0301421512002868 [Accessed March 19, 2013].

Foxon, T.J., Hammond, G.P. & Pearson, P.J.G., 2010. Developing transition pathways for a low carbon electricity system in the UK. *Technological Forecasting and Social Change*, 77(8), pp.1203–1213. Available at: http://linkinghub.elsevier.com/retrieve/pii/S0040162510000697 [Accessed March 20, 2013].

Freeman, T., Mitchell, J.W. & Audit, T.E., 1979. Performance of combined solar-heat pump systems. *Solar Energy*, 22(2), pp.125–135. Available at: http://linkinghub.elsevier.com/retrieve/pii/0038092X79900963.

Fuel Cell Today, 2012. BlueGen Domestic Fuel Cell Available for Under £20,000 in the UK. Available at: http://www.fuelcelltoday.com/news-events/news-archive/2012/august/bluegen-domestic-fuel-cell-available-for-under-£20,000-in-the-uk [Accessed January 21, 2012].

Van Gool, W., 1998. Thermodynamics of chemical references for exergy analysis. *Energy Conversion and Management*, 39(16-18), pp.1719–1728. Available at: http://linkinghub.elsevier.com/retrieve/pii/S0196890498000892.

Greenhouse Gas Technology Centre Southern Research Institute, 2004. *Environmental Technology Verification Report Electric Power and Heat Generation Using UTC Fuel Cells ' PC25C Power Plant and Anaerobic Digester Gas*, Durham, NC.

Haggis, T., 2006. *Network Design Manual*, Nottingham: E.On Central Networks.

Hammond, G.P., 2004a. Engineering sustainability: thermodynamics, energy systems, and the environment. *International Journal of Energy Research*, 28(7), pp.613–639. Available at: http://doi.wiley.com/10.1002/er.988 [Accessed January 4, 2011].

Hammond, G.P., 2004b. Towards sustainability: energy efficiency, thermodynamic analysis, and the "two cultures". *Energy Policy*, 32(16), pp.1789–1798. Available at: http://linkinghub.elsevier.com/retrieve/pii/S030142150300301X [Accessed January 4, 2011].

Hammond, G.P. & Ondo Akwe, S.S., 2007. Thermodynamic and related analysis of natural gas combined cycle power plants with and without carbon sequestration. *International Journal*

of *Energy Research*, 31(12), pp.1180–1201. Available at: http://doi.wiley.com/10.1002/er.1328 [Accessed January 6, 2011].

Hammond, G.P. & Stapleton, A.J., 2001. Exergy analysis of the United Kingdom energy system. *Proceedings of the Institution of Mechanical Engineers, Part A: Journal of Power and Energy*, 215(2), pp.141–162. Available at: http://journals.pepublishing.com/openurl.asp?genre=article&id=doi:10.1243/09576500115 38424.

Hawkes, A., 2010. Estimating marginal CO2 emissions rates for national electricity systems. *Energy Policy*, 38(10), pp.5977–5987. Available at: http://linkinghub.elsevier.com/retrieve/pii/S0301421510004246 [Accessed February 24, 2011].

Hawkes, A., Brett, D.J.L. & Brandon, N.P., 2011. Role of fuel cell based micro-cogeneration in low carbon heating. *Proceedings of the Institution of Mechanical Engineers, Part A: Journal of Power and Energy*, 225(2), pp.198–207. Available at: http://journals.pepublishing.com/openurl.asp?genre=article&id=doi:10.1177/20412967103 94268 [Accessed March 21, 2011].

Hawkes, A. & Leach, M., 2005. Impacts of temporal precision in optimisation modelling of micro-Combined Heat and Power. *Energy*, 30(10), pp.1759–1779. Available at: http://linkinghub.elsevier.com/retrieve/pii/S036054420400475X [Accessed September 7, 2010].

Hawkes, A., Staffell, I., Brett, D.J.L. & Brandon, N.P., 2009. Fuel cells for micro-combined heat and power generation. *Energy & Environmental Science*, 2(7), p.729. Available at: http://xlink.rsc.org/?DOI=b902222h [Accessed January 4, 2011].

Hayton, J., 2010. *Calculation procedure for the SAP Appendix Q process for electrically driven heat pumps*, Garston: Building Research Establishment Ltd.

Healy, D.P., 2012. Influence of the carbon intensity of electricity on carbon savings from CHP. *Building Research & Information*, 40(3), pp.317–326.

Heliotherm, *Stepless modulating*, Langkampfen, Austria: Heliotherm Wärmepumpentechnik GmbH.

Hepbasli, A., 2008. A key review on exergetic analysis and assessment of renewable energy resources for a sustainable future. *Renewable and Sustainable Energy Reviews*, 12(3), pp.593–661. Available at: http://linkinghub.elsevier.com/retrieve/pii/S1364032106001225 [Accessed September 27, 2010].

Hepbasli, A. & Akdemir, O., 2004. Energy and exergy analysis of a ground source (geothermal) heat pump system. *Energy Conversion and Management*, 45(5), pp.737–753. Available at: http://linkinghub.elsevier.com/retrieve/pii/S0196890403001857 [Accessed November 24, 2010].

Hepbasli, A., Erbay, Z., Icier, F., Colak, N. & Hancioglu, E., 2009. A review of gas engine driven heat pumps (GEHPs) for residential and industrial applications. *Renewable and Sustainable Energy Reviews*, 13(1), pp.85–99. Available at: http://linkinghub.elsevier.com/retrieve/pii/S1364032107001268 [Accessed January 4, 2013].

Hepbasli, A. & Kalinci, Y., 2009. A review of heat pump water heating systems. *Renewable and Sustainable Energy Reviews*, 13(6-7), pp.1211–1229. Available at: http://linkinghub.elsevier.com/retrieve/pii/S1364032108001032 [Accessed July 14, 2012].

Hiller, C., 2012. Influence of residents on energy use in 57 Swedish houses measured during four winter days. *Energy and Buildings*, 54, pp.376–385. Available at: http://linkinghub.elsevier.com/retrieve/pii/S0378778812003520 [Accessed April 11, 2013].

HM Government, 2008. *Climate Change Act 2008*, London: HMSO.

Honda Motor Co. Ltd., 2007. Honda's Compact Household Cogeneration Unit Achieves Cumulative Sales of 50,000 units in Japan. Available at: http://world.honda.com/news/2007/c070717Compact-Household-Cogeneration-Unit/ [Accessed January 17, 2012].

Hong, J., Johnstone, C.M., Kelly, N.J., McManus, M.C. & Jardine, C.N., 2010. Identifying characteristic building types for use in the modelling of highly distributed power systems performance.

Hong, J., Kelly, N.J., Richardson, I. & Thomson, M., 2012. Assessing heat pumps as flexible load. *Proceedings of the Institution of Mechanical Engineers, Part A: Journal of Power and Energy*, 227(1), pp.30–42. Available at: http://pia.sagepub.com/lookup/doi/10.1177/0957650912454830 [Accessed May 16, 2013].

Hot Water Association, 2010. *Performance Specification for Thermal Stores*, London: Hot Water Association Ltd.

IEA Heat Pump Programme Annex28, 2006. *Test procedure and seasonal performance calculation for residential heat pumps with combined space and domestic hot water heating*, Boras, Sweden: IEA Heat Pump Centre.

Incropera, F.P. & DeWitt, D., 1985. *Fundamentals of heat and mass transfer; 2nd Edition*, New York: John Wiley & Sons, Inc.

IPCC, 2007. *Climate Change 2007: The Physical Science Basis. Contribution of Working Group 1 to the Fourth Assessment Report on the Intergovernmental Panel on Climate Change* S. Solomon, D. Qin, M. Manning, Z. Chen, M. Marquis, K. B. Averyt, M. Tignor, & H. L. Miller, eds., Cambridge: Cambridge University Press.

ISO, 2005. *ISO 7730 Ergonomics of the thermal environment — Analytical determination and interpretation of thermal comfort using calculation of the PMV and PPD indices and local thermal comfort criteria*, Geneva: International Standards Organisation.

Ito, S., Miura, N. & Wang, K., 1999. Performance of a Heat Pump Using Direct Expansion Solar Collectors. *Solar Energy*, 65(3), pp.189–196. Available at: http://linkinghub.elsevier.com/retrieve/pii/S0038092X98001248.

Iwata, S., 2004. Study on efficient operation control of gas engine residential co-generation system. In *Proceedings of International Gas Research Conference (IGRC 2004), 2–4 November 2004*. Vancouver, pp. 1–15.

Jardine, C.N. & Ault, G., 2008. Scenarios for examination of highly distributed power systems. *Proceedings of the Institution of Mechanical Engineers, Part A: Journal of Power and Energy*, 222(7), pp.643–655. Available at:

http://journals.pepublishing.com/openurl.asp?genre=article&id=doi:10.1243/09576509JPE 517.

Jelle, B.P., 2011. Traditional, State-of-the-Art and Future Thermal Building Insulation Materials and Solutions - Properties, Requirements and Possibilities. *Energy and Buildings*, 43(7465), pp.2549–2563. Available at: http://linkinghub.elsevier.com/retrieve/pii/S0378778811002295 [Accessed June 30, 2011].

Jenkins, D.P., Peacock, A.D., Banfill, P.F.G., Kane, D., Ingram, V. & Kilpatrick, R., 2012. Modelling carbon emissions of UK dwellings – The Tarbase Domestic Model. *Applied Energy*, 93, pp.596–605. Available at: http://linkinghub.elsevier.com/retrieve/pii/S0306261911007902 [Accessed May 17, 2013].

Jenkins, D.P., Tucker, R., Ahadzi, M. & Rawlings, R., 2008. The performance of air-source heat pumps in current and future offices. *Energy and Buildings*, 40(10), pp.1901–1910. Available at: http://linkinghub.elsevier.com/retrieve/pii/S0378778808000947 [Accessed January 4, 2011].

Jenkins, D.P., Tucker, R. & Rawlings, R., 2009. Modelling the carbon-saving performance of domestic ground-source heat pumps. *Energy and Buildings*, 41(6), pp.587–595. Available at: http://linkinghub.elsevier.com/retrieve/pii/S0378778808002703 [Accessed January 4, 2011].

Jingying, H., Yuanyang, Z., Liansheng, L., Zhizhong, W. & Pengcheng, S., 2010. Theoretical and experimental study on the performance of CO2 hermetic scroll compressor. *Proceedings of the Institution of Mechanical Engineers, Part A: Journal of Power and Energy*, 224(7), pp.1019–1028. Available at: http://journals.pepublishing.com/openurl.asp?genre=article&id=doi:10.1243/09576509JPE 952 [Accessed April 27, 2011].

Johansson, L.S., Leckner, B., Gustavsson, L., Cooper, D., Tullin, C. & Potter, A., 2004. Emission characteristics of modern and old-type residential boilers fired with wood logs and wood pellets. *Atmospheric Environment*, 38(25), pp.4183–4195. Available at: http://linkinghub.elsevier.com/retrieve/pii/S1352231004004212 [Accessed November 26, 2012].

Johnson, E.P., 2010. Air-source heat pump carbon footprints: HFC impacts and comparison to other heat sources. *Energy Policy*, 39(3), pp.1369–1381. Available at: http://linkinghub.elsevier.com/retrieve/pii/S0301421510008906 [Accessed January 5, 2011].

Johnston, D., Lowe, R. & Bell, M., 2005. An exploration of the technical feasibility of achieving CO2 emission reductions in excess of 60% within the UK housing stock by the year 2050. *Energy Policy*, 33(13), pp.1643–1659. Available at: http://linkinghub.elsevier.com/retrieve/pii/S0301421504000370.

Jones, P.D., Kilsby, C.G., Harpham, C., Glenis, V. & Burton, A., 2009. *UK Climate Projections science report: Projections of future daily climate for the UK from the Weather Generator*, University of Newcastle, UK.

Karakoussis, V., Brandon, N.P., Leach, M. & Van der Vorst, R., 2001. The environmental impact of manufacturing planar and tubular solid oxide fuel cells. *Journal of Power Sources*, 101(1), pp.10–26. Available at: http://linkinghub.elsevier.com/retrieve/pii/S0378775301004827.

Kelly, N.J., Clarke, J.A., Ferguson, A. & Burt, G.M., 2008. Developing and testing a generic micro-combined heat and power model for simulations of dwellings and highly distributed power systems. *Proceedings of the Institution of Mechanical Engineers, Part A: Journal of Power and Energy*, 222(7), pp.685–695. Available at: http://journals.pepublishing.com/openurl.asp?genre=article&id=doi:10.1243/09576509JPE 532.

Kelly, N.J. & Cockroft, J., 2011. Analysis of retrofit air source heat pump performance: Results from detailed simulations and comparison to field trial data. *Energy and Buildings*, 43(1), pp.239–245. Available at: http://linkinghub.elsevier.com/retrieve/pii/S0378778810003385 [Accessed January 10, 2011].

Kelly, S., Crawford-Brown, D. & Pollitt, M.G., 2012. Building performance evaluation and certification in the UK: Is SAP fit for purpose? *Renewable and Sustainable Energy Reviews*, 16(9), pp.6861–6878. Available at: http://linkinghub.elsevier.com/retrieve/pii/S1364032112004595 [Accessed November 7, 2012].

Kharseh, M., Altorkmany, L. & Nordell, B., 2011. Global warming's impact on the performance of GSHP. *Renewable Energy*, 36(5), pp.1485–1491. Available at: http://linkinghub.elsevier.com/retrieve/pii/S096014811000529X [Accessed March 15, 2011].

Kim, M., Kim, M.S. & Chung, J.D., 2004. Transient thermal behavior of a water heater system driven by a heat pump. *International Journal of Refrigeration*, 27(4), pp.415–421. Available at: http://linkinghub.elsevier.com/retrieve/pii/S0140700703001804 [Accessed August 24, 2012].

Kinoshita, H., 2011. Microgeneration activities in Japan, Europe and North America. In *Proceedings of 2nd International Conference in Microgeneration and Related Technologies in Buildings: Microgen 2, 4 - 6th April 2011*. Glasgow.

Kokogiannakis, G., Strachan, P.A. & Clarke, J.A., 2008. Comparison of the simplified methods of the ISO 13790 Standard and detailed modelling programs in a regulatory context. *Journal of Building Performance Simulation*, 1(4), pp.209–219.

Koroneos, C., Spachos, T. & Moussiopoulos, N., 2003. Exergy analysis of renewable energy sources. *Renewable Energy*, 28(2), pp.295–310. Available at: http://linkinghub.elsevier.com/retrieve/pii/S0960148101001252.

Kotas, T.J., 1980. Exergy concepts for thermal plant. First of two papers on exergy techniques in thermal plant analysis. *International Journal of Heat and Fluid Flow*, 2(3), pp.105–114. Available at: http://linkinghub.elsevier.com/retrieve/pii/0142727X80900284.

Kotas, T.J., 1986. Exergy method of thermal and chemical plant analysis. *Chemical Engineering Research and Design*, 64, pp.212–229.

Kotas, T.J., Mayhew, Y.R. & Raichura, R.C., 1995. Nomenclature for exergy analysis. *Proceedings of the Institution of Mechanical Engineers, Part A: Journal of Power and Energy*, 209(41), pp.275–280. Available at: http://archive.pepublishing.com/openurl.asp?genre=article&id=doi:10.1243/PIME_PROC _1995_209_006_01.

Larminie, J. & Dicks, A., 2003. *Fuel Cell Systems Explained*, Chichester, UK: John Wiley & Sons Ltd.

Layberry, R., 2009. Analysis of errors in degree days for building energy analysis using Meteorological Office weather station data. *Building Services Engineering Research and Technology*, 30(1), pp.79–86. Available at: http://bse.sagepub.com/cgi/doi/10.1177/0143624408098221 [Accessed September 6, 2010].

Layberry, R., 2008. Degree days for building energy management - presentation of a new data set. *Building Services Engineering Research and Technology*, 29(3), pp.273–282. Available at: http://bse.sagepub.com/cgi/doi/10.1177/0143624408093886.

Li, M., Rao, A.D., Brouwer, J. & Samuelsen, G.S., 2011. Effects of carbon capture on the performance of an advanced coal-based integrated gasification fuel cell system. *Proceedings of the Institution of Mechanical Engineers, Part A: Journal of Power and Energy*, 225(2), pp.208–218. Available at: http://journals.pepublishing.com/openurl.asp?genre=article&id=doi:10.1177/20412967103 94261 [Accessed March 21, 2011].

Lian, Z., Park, S., Huang, W., Baik, Y. & Yao, Y., 2005. Conception of combination of gas-engine-driven heat pump and water-loop heat pump system. *International Journal of Refrigeration*, 28(6), pp.810–819. Available at: http://linkinghub.elsevier.com/retrieve/pii/S0140700705000551.

Lipp, J., 2012. Field test with Stirling engine micro-combined heat and power units in residential buildings. *Proceedings of the Institution of Mechanical Engineers, Part A: Journal of Power and Energy*, 227(1), pp.43–52. Available at: http://pia.sagepub.com/lookup/doi/10.1177/0957650912458755 [Accessed May 17, 2013].

Liu, H., Shao, Y. & Li, J., 2011. A biomass-fired micro-scale CHP system with organic Rankine cycle (ORC) – Thermodynamic modelling studies. *Biomass and Bioenergy*, 35(9), pp.3985–3994. Available at: http://linkinghub.elsevier.com/retrieve/pii/S0961953411003497 [Accessed September 21, 2011].

Lohani, S.P. & Schmidt, D., 2010. Comparison of energy and exergy analysis of fossil plant, ground and air source heat pump building heating system. *Renewable Energy*, 35(6), pp.1275–1282. Available at: http://linkinghub.elsevier.com/retrieve/pii/S0960148109004285 [Accessed November 22, 2010].

Love, J., Amarasinghe, S., Selvey, D., Zheng, X. & Christiansen, L., 2009. Development of SOFC Stacks at Ceramic Fuel Cells Limited. In *ECS Transactions*. ECS, pp. 115–124. Available at: http://link.aip.org/link/ECSTF8/v25/i2/p115/s1&Agg=doi [Accessed May 17, 2013].

Lowe, R., 2007. Technical options and strategies for decarbonizing UK housing. *Building Research & Information*, 35(4), pp.412–425. Available at: http://www.informaworld.com/openurl?genre=article&doi=10.1080/09613210701238268 &magic=crossref||D404A21C5BB053405B1A640AFFD44AE3 [Accessed September 8, 2010].

Maeda, K., Masumoto, K. & Hayano, A., 2010. A study on energy saving in residential PEFC cogeneration systems. *Journal of Power Sources*, 195(12), pp.3779–3784. Available at: http://linkinghub.elsevier.com/retrieve/pii/S0378775309023374 [Accessed January 10, 2011].

Magri, G., Di Perna, C. & Serenelli, G., 2012. Analysis of electric and thermal seasonal performances of a residential microCHP unit. *Applied Thermal Engineering*, 36, pp.193–201. Available at: http://linkinghub.elsevier.com/retrieve/pii/S1359431111006533 [Accessed January 15, 2012].

Marsh, G., 2002. Zero energy buildings Key role for RE at UK housing development. *Refocus*, 3(3), pp.58–61. Available at: http://linkinghub.elsevier.com/retrieve/pii/S1471084602800452 [Accessed January 8, 2011].

McKenna, E., McManus, M.C., Cooper, S.J.G. & Thomson, M.J., 2013. Economic and environmental impact of lead-acid batteries in grid-connected domestic PV systems. *Applied Energy*, 104, pp.239–249. Available at: http://linkinghub.elsevier.com/retrieve/pii/S0306261912008094 [Accessed January 7, 2013].

Miara, M., 2008. Two large field-tests of new heat pumps in Germany. In *9th IEA Heat Pump Conference, 20 - 22 May 2008*. Zurich.

Milewski, J. & Miller, A., 2006. Influences of The Type and Thickness of Electrolyte on Solid Oxide Fuel Cell Hybrid System Performance. *Journal of Fuel Cell Science and Technology*, 3(4), p.396. Available at: http://link.aip.org/link/JFCSAU/v3/i4/p396/s1&Agg=doi [Accessed May 17, 2013].

Mitchell, C., Sweet, J. & Jackson, T., 1990. A study of leakage from the UK natural gas distribution system. *Energy Policy*, 18(9), pp.809–818. Available at: http://linkinghub.elsevier.com/retrieve/pii/030142159090060H [Accessed May 17, 2013].

Mitsubishi Electric Europe, 2008. *Service manual No. OCH439 Air to water heat pump*, Mitsubishi.

Monahan, J. & Powell, J.C., 2010. A comparison of the energy and carbon implications of new systems of energy provision in new build housing in the UK. *Energy Policy*, 39(1), pp.290–298. Available at: http://linkinghub.elsevier.com/retrieve/pii/S0301421510007275 [Accessed December 14, 2010].

Moreau, A., 2011. Control Strategy for Domestic Water Heaters during Peak Periods and its Impact on the Demand for Electricity. In *ICSGCE 2011: 27–30 September 2011*. Chengdu: Energy Procedia, pp. 1074–1082. Available at: http://linkinghub.elsevier.com/retrieve/pii/S1876610211019667 [Accessed September 3, 2012].

MTT, 2013. MTT micro turbine technology. Available at: http://www.mtt-eu.com/en/technology [Accessed January 17, 2013].

National Grid Plc, 2011. *National Electricity Transmission System Seven Year Statement*, London: National Grid Plc.

Nichi Gas, 2012. ENE-FARM. Available at: http://www.nichigas.co.jp/en/appliances/enefarm.html [Accessed January 21, 2013].

O'Grady, A., 2012. Personal communication.

Odeh, N.A. & Cockerill, T.T., 2008. Life cycle GHG assessment of fossil fuel power plants with carbon capture and storage. *Energy Policy*, 36(1), pp.367–380. Available at:

http://linkinghub.elsevier.com/retrieve/pii/S0301421507004120 [Accessed April 11, 2012].

Ozgener, O. & Hepbasli, A., 2007. A review on the energy and exergy analysis of solar assisted heat pump systems. *Renewable and Sustainable Energy Reviews*, 11(3), pp.482–496. Available at: http://linkinghub.elsevier.com/retrieve/pii/S136403210500050X [Accessed November 3, 2010].

Ozgener, O. & Hepbasli, A., 2005. Exergoeconomic analysis of a solar assisted ground-source heat pump greenhouse heating system. *Applied Thermal Engineering*, 25(10), pp.1459–1471. Available at: http://linkinghub.elsevier.com/retrieve/pii/S1359431104002790 [Accessed September 6, 2010].

De Paepe, M., D'Herdt, P. & Mertens, D., 2006. Micro-CHP systems for residential applications. *Energy Conversion and Management*, 47(18-19), pp.3435–3446. Available at: http://linkinghub.elsevier.com/retrieve/pii/S0196890406000124 [Accessed July 22, 2010].

Palmer, J. & Cooper, I., 2011. *Great Britain's housing energy fact file*, London: DECC.

Parker, J., 2009. *It looks ordinary. But just how low can we go ?* Delta T Ma., London: BSRIA.

Payne, R., Love, J. & Kah, M., 2009. Generating Electricity at 60% Electrical Efficiency from 1 - 2 kWe SOFC Products. In *ECS Transactions*. ECS, pp. 231–239. Available at: http://link.aip.org/link/ECSTF8/v25/i2/p231/s1&Agg=doi [Accessed May 17, 2013].

Peacock, A.D. & Newborough, M., 2007. Controlling micro-CHP systems to modulate electrical load profiles. *Energy*, 32(7), pp.1093–1103. Available at: http://linkinghub.elsevier.com/retrieve/pii/S0360544206002131 [Accessed January 4, 2011].

Peacock, A.D. & Newborough, M., 2008. Effect of heat-saving measures on the CO2 savings attributable to micro-combined heat and power (μCHP) systems in UK dwellings. *Energy*, 33(4), pp.601–612. Available at: http://linkinghub.elsevier.com/retrieve/pii/S0360544207001971 [Accessed July 22, 2010].

Peacock, A.D. & Newborough, M., 2005. Impact of micro-CHP systems on domestic sector CO2 emissions. *Applied Thermal Engineering*, 25(17-18), pp.2653–2676. Available at: http://linkinghub.elsevier.com/retrieve/pii/S1359431105001018 [Accessed November 11, 2010].

Peacock, A.D. & Newborough, M., 2006. Impact of micro-combined heat-and-power systems on energy flows in the UK electricity supply industry. *Energy*, 31(12), pp.1804–1818. Available at: http://linkinghub.elsevier.com/retrieve/pii/S036054420500215X [Accessed November 14, 2010].

Pehnt, M., 2008. Environmental impacts of distributed energy systems—The case of micro cogeneration. *Environmental Science & Policy*, 11(1), pp.25–37. Available at: http://linkinghub.elsevier.com/retrieve/pii/S1462901107000779 [Accessed July 24, 2011].

Pihl, E., Heyne, S., Thunman, H. & Johnsson, F., 2010. Highly efficient electricity generation from biomass by integration and hybridization with combined cycle gas turbine (CCGT) plants for natural gas. *Energy*, 35(10), pp.4042–4052. Available at: http://linkinghub.elsevier.com/retrieve/pii/S0360544210003221 [Accessed November 8, 2012].

Pudjianto, D., Djapic, P., Aunedi, M., Gan, C.K., Strbac, G., Huang, S. & Infield, D., 2013. Smart control for minimizing distribution network reinforcement cost due to electrification. *Energy Policy*, 52, pp.76–84. Available at: http://linkinghub.elsevier.com/retrieve/pii/S0301421512004338 [Accessed March 20, 2013].

Pudjianto, D., Ramsay, C. & Strbac, G., 2008. Microgrids and virtual power plants: concepts to support the integration of distributed energy resources. *Proceedings of the Institution of Mechanical Engineers, Part A: Journal of Power and Energy*, 222(7), pp.731–741. Available at: http://journals.pepublishing.com/openurl.asp?genre=article&id=doi:10.1243/09576509JPE556.

Pudjianto, D. & Strbac, G., 2012. Maximising the utilisation of micro-generation using a multi-state optimal power flow. *Proceedings of the Institution of Mechanical Engineers, Part A: Journal of Power and Energy*, 227(1), pp.94–104. Available at: http://pia.sagepub.com/lookup/doi/10.1177/0957650912466647 [Accessed April 16, 2013].

Rabaçal, M., Fernandes, U. & Costa, M., 2013. Combustion and emission characteristics of a domestic boiler fired with pellets of pine, industrial wood wastes and peach stones. *Renewable Energy*, 51, pp.220–226. Available at: http://linkinghub.elsevier.com/retrieve/pii/S0960148112005915 [Accessed November 26, 2012].

Radov, D., Klevnas, P., Hanif, A., Abu-ebid, M., Barker, N. & Stambaugh, J., 2009. *The UK Supply Curve for Renewable Heat Study*, London: NERA Economic Consulting.

Ramallo-González, A.P., Eames, M.E. & Coley, D. a., 2013. Lumped parameter models for building thermal modelling: An analytic approach to simplifying complex multi-layered constructions. *Energy and Buildings*, 60, pp.174–184. Available at: http://linkinghub.elsevier.com/retrieve/pii/S0378778813000315 [Accessed February 27, 2013].

Rawlings, R. & Sykulski, J.R., 1999. Ground source heat pumps: A technology review. *Proceedings CIBSE A: Building Services Research & Technology*, 20(3), pp.119 – 129.

Rey Martínez, F.J., Velasco Gómez, E., Martín García, C., Sanz Requena, J.F., Navas Gracia, L.M., Hernández Navarro, S., Correa Guimaraes, a. & Martin-Gil, J., 2011. Life cycle assessment of a semi-indirect ceramic evaporative cooler vs. a heat pump in two climate areas of Spain. *Applied Energy*, 88(3), pp.914–921. Available at: http://linkinghub.elsevier.com/retrieve/pii/S0306261910003429 [Accessed August 19, 2011].

Richardson, I. & Thomson, M., 2012. Integrated simulation of photovoltaic micro-generation and domestic electricity demand: a one-minute resolution open-source model. *Proceedings of the Institution of Mechanical Engineers, Part A: Journal of Power and Energy*, 227(1), pp.73–81. Available at: http://pia.sagepub.com/lookup/doi/10.1177/0957650912454989 [Accessed May 16, 2013].

Richardson, I., Thomson, M.J. & Infield, D.G., 2008. A high-resolution domestic building occupancy model for energy demand simulations. *Energy and Buildings*, 40(8), pp.1560–1566. Available at: http://linkinghub.elsevier.com/retrieve/pii/S0378778808000467 [Accessed July 16, 2010].

Ristic, M., Brujic, D. & Thoma, K., 2008. Economic dispatch of distributed combined heat and power systems participating in electricity spot markets. *Proceedings of the Institution of Mechanical Engineers, Part A: Journal of Power and Energy*, 222(7), pp.743–752. Available at: http://journals.pepublishing.com/openurl.asp?genre=article&id=doi:10.1243/09576509JPE522 [Accessed January 4, 2011].

Rivera-Tinoco, R., Schoots, K. & Van der Zwaan, B., 2012. Learning curves for solid oxide fuel cells. *Energy Conversion and Management*, 57, pp.86–96. Available at: http://linkinghub.elsevier.com/retrieve/pii/S0196890411003360 [Accessed February 21, 2012].

Rogers, J.G., Cooper, S.J.G., McManus, M.C. & Hammond, G.P., 2013. Use of micro CHP plants to support the local operation of electric heat pumps. In *Proceedings of 3rd International Conference in Microgeneration and Related Technologies in Buildings: Microgen 3, 15 - 17th April 2013*. Naples.

Roossien, B., Hommelberg, M.P.F., Warmer, C., Kok, K. & Turkstra, J.-W., 2008. Virtual power plant field experiment using 10 micro-CHP units at consumer premises. In *CIRED Seminar 2008: SmartGrids for Distribution, 23 - 24 June 2008*. Frankfurt. Available at: http://link.aip.org/link/IEESEM/v2008/i12380/p5/s1&Agg=doi.

Roselli, C., Sasso, M., Sibilio, S. & Tzscheutschler, P., 2011. Experimental analysis of microcogenerators based on different prime movers. *Energy and Buildings*, 43(4), pp.796–804. Available at: http://linkinghub.elsevier.com/retrieve/pii/S0378778810004184 [Accessed November 6, 2012].

Rosen, M.A. & Dincer, I., 2001. Exergy as the confluence of energy, environment and sustainable development. *Exergy, An International Journal*, 1(1), pp.3–13. Available at: http://linkinghub.elsevier.com/retrieve/pii/S1164023501000048.

Royal Academy of Engineering, 2012. *Heat: degrees of comfort?*, London: Royal Academy of Engineering.

Sarkar, J., 2012. Ejector enhanced vapor compression refrigeration and heat pump systems—A review. *Renewable and Sustainable Energy Reviews*, 16(9), pp.6647–6659. Available at: http://linkinghub.elsevier.com/retrieve/pii/S1364032112004765 [Accessed November 26, 2012].

Sarkar, J., Bhattacharyya, S. & Ram Gopal, M., 2005. Transcritical CO2 heat pump systems: exergy analysis including heat transfer and fluid flow effects. *Energy Conversion and Management*, 46(13-14), pp.2053–2067. Available at: http://linkinghub.elsevier.com/retrieve/pii/S0196890404002699 [Accessed September 13, 2012].

Schmidt, D., 2009. Low exergy systems for high-performance buildings and communities. *Energy and Buildings*, 41(3), pp.331–336. Available at: http://linkinghub.elsevier.com/retrieve/pii/S0378778808002223 [Accessed December 9, 2010].

Secretary of State, 2010. *Statutory Instruments 2009 No. 785 The Renewables Obligation Order 2009*,

Shorrock, L.D., Henderson, J. & Utley, J.I., 2005. *Reducing carbon emissions from the UK housing stock*, Garston: Building Research Establishment Ltd.

Siemens AG, 2010. *SGT5-8000H datasheet*, Erlangen: Siemens Energy Inc.

Simader, G.R., Krawinkler, R. & Trnka, G., 2006. *Micro CHP systems: state-of-the-art* F. Unterpertinger, ed., Vienna: Österreichische Energieagentur – Austrian Energy Agency. Available at: http://www.energyagency.at.

Singhal, S., 2000. Advances in solid oxide fuel cell technology. *Solid State Ionics*, 135(1-4), pp.305–313. Available at: http://linkinghub.elsevier.com/retrieve/pii/S0167273800004525.

Sorrell, S., Speirs, J., Bentley, R., Brandt, A.R. & Miller, R., 2010. Global oil depletion: A review of the evidence. *Energy Policy*, 38(9), p.228. Available at: http://linkinghub.elsevier.com/retrieve/pii/S0301421510003204 [Accessed January 4, 2011].

Spath, P.L. & Mann, M.K., 2000. *Life Cycle Assessment of a Natural Gas Combined-Cycle Power Generation System NREL/TP-570-27715*, Golden, US: National Renewable Energy Laboratory.

Speirs, J., Gross, R., Deshmukh, S., Heptonstall, P., Manuera, L., Leach, M. & Torriti, J., 2010. *Building a roadmap for heat 2050 scenarios and heat delivery in the UK*, London: Combined Heat and Power Association.

Staffell, I., 2009. *Fuel Cells for domestic heat and power: Are they worth it?*, Thesis (PhD): University of Birmingham.

Staffell, I. et al., 2010. UK microgeneration. Part II: technology overviews. *Proceedings of the ICE - Energy*, 163(4), pp.143–165. Available at: http://www.icevirtuallibrary.com/content/article/10.1680/ener.2010.163.4.143 [Accessed March 2, 2011].

Stene, J., 2007. Integrated CO2 heat pump systems for space heating and hot water heating in low-energy houses and passive houses. In *IEA HPP Annex 32 - Workshop, 6 December 2007*. Kyoto, pp. 1–14.

Stern, N., 2006. *The Economics of Climate Change: The Stern Review*, London: HMSO.

Strbac, G., 2008. Demand side management: Benefits and challenges. *Energy Policy*, 36(12), pp.4419–4426. Available at: http://linkinghub.elsevier.com/retrieve/pii/S0301421508004606 [Accessed June 21, 2011].

Sturt, A., 2011. *Stochastic Scheduling of Wind-Integrated Power Systems*, Thesis (PhD): Imperial College.

Sturt, A. & Strbac, G., 2011. Time series modelling of power output for large-scale wind fleets. *Wind energy*, 14(8), pp.953 – 966.

Sulka, T. & Jenkins, N., 2008. Modelling of a housing estate with micro-combined heat and power for power flow studies. *Proceedings of the Institution of Mechanical Engineers, Part A: Journal of Power and Energy*, 222(7), pp.721–729. Available at: http://journals.pepublishing.com/openurl.asp?genre=article&id=doi:10.1243/09576509JPE 516 [Accessed January 4, 2011].

Supergen HDPS, 2006. *SUPERGEN HDPS Scenarios*, ECI, University of Oxford.

Sustainable Development Commission, 2006. *Stock Take: Delivering improvements in existing housing*, London: Sustainable Development Commission.

Szargut, J., 2007. Local and System Exergy Losses in Cogeneration Processes. *International Journal of Thermodynamics*, 10(4), pp.135–142.

Thomas, B., 2008. Benchmark testing of Micro-CHP units. *Applied Thermal Engineering*, 28(16), pp.2049–2054. Available at: http://linkinghub.elsevier.com/retrieve/pii/S1359431108001282 [Accessed January 4, 2011].

Thomson, M.J. & Infield, D.G., 2008. Modelling the impact of micro-combined heat and power generators on electricity distribution networks. *Proceedings of the Institution of Mechanical Engineers, Part A: Journal of Power and Energy*, 222(7), pp.697–706. Available at: http://journals.pepublishing.com/openurl.asp?genre=article&id=doi:10.1243/09576509JPE 574.

Thorsteinson, E., Strathearn, B., Mackenzie, G. & Amow, G., 2011. Performance Testing of a 1kWe PEM Fuel Cell Cogeneration system. In *Proceedings of 2nd International Conference in Microgeneration and Related Technologies in Buildings: Microgen 2, 4 - 6th April 2011*. Glasgow.

Tian, H., Yang, Z., Li, M. & Ma, Y., 2009. Research and application of CO2 refrigeration and heat pump cycle. *Science in China Series E: Technological Sciences*, 52(6), pp.1563–1575. Available at: http://www.springerlink.com/index/10.1007/s11431-009-0175-4 [Accessed May 17, 2013].

Utley, J.I. & Shorrock, L.D., 2008. *Domestic energy fact file 2008*, Garston: Building Research Establishment Ltd.

Viessmann, 2011. Innovative solutions for tomorrow: Use energy more efficiently with Viessmann technology. Available at: http://www.viessmann.com/com/en/press/press_releases/innovative_solutions_for_tomorrow/shk-107017.html [Accessed January 8, 2013].

Viessmann, 2009. *Technical guide Vitocal 300-A*, Allendorf: Viessmand Werke GmBH.

Vijay, P., Samantaray, A.K. & Mukherjee, A., 2010. Constant Fuel Utilization Operation of a SOFC System: An Efficiency Viewpoint. *Journal of Fuel Cell Science and Technology*, 7(4). Available at: http://link.aip.org/link/JFCSAU/v7/i4/p041011/s1&Agg=doi [Accessed May 17, 2013].

Visser, W.P.J., Shakariyants, S.A. & Oostveen, M., 2011. Development of a 3 kW Microturbine for CHP Applications. *Journal of Engineering for Gas Turbines and Power*, 133(4).

Voorspools, K.R. & D'haeseleer, W., 2002. The evaluation of small cogeneration for residential heating. *International Journal of Energy Research*, 26(13), pp.1175–1190. Available at: http://doi.wiley.com/10.1002/er.843 [Accessed August 10, 2011].

Wang, W., Xiao, J., Guo, Q.C., Lu, W.P. & Feng, Y.C., 2011. Field test investigation of the characteristics for the air source heat pump under two typical mal-defrost phenomena. *Applied Energy*, 88(12), pp.4470–4480. Available at: http://linkinghub.elsevier.com/retrieve/pii/S0306261911003424 [Accessed September 21, 2011].

Warmepumpen-Testzentrum, 2010. *Test results of air to water heat pumps based on EN 14511*, Buchs, Switzerland: Institut fur Energiesysteme, Interstaatliche Hochschule für Technik.

Warmepumpen-Testzentrum, 2013. *Test results of air to water heat pumps based on EN 14511:2011*, Buchs, Switzerland: Institut fur Energiesysteme, Interstaatliche Hochschule für Technik.

Warmer, C., Hommelberg, M.P.F., Kamphuis, I.G., Derzsi, Z. & Kok, K., 2007. Wind Turbine and Heat Pumps – Balancing wind power fluctuations using flexible demand. In *Sixth International Workshop on Large-Scale Integration of Wind Power and Transmission Networks from Offshore Wind Farms*. pp. 1–9.

Wemhoener, C., Afjei, T. & Dott, R., 2008. IEA HPP Annex 28 – standardised testing and seasonal performance calculation for multifunctional heat pump systems. *Applied Thermal Engineering*, 28(16), pp.2062–2069. Available at: http://linkinghub.elsevier.com/retrieve/pii/S135943110700405X [Accessed October 11, 2010].

Whispergen Ltd, 2006. *Whispergen MkVb microCHP System Design Manual*, Christchurch, NZ: Whisper Tech Ltd.

Wood, S.R. & Rowley, P.N., 2011. A techno-economic analysis of small-scale, biomass-fuelled combined heat and power for community housing. *Biomass and Bioenergy*, 35(9), pp.3849–3858. Available at: http://linkinghub.elsevier.com/retrieve/pii/S096195341100242X [Accessed July 6, 2011].

Wu, J., Yang, Z., Wu, Q. & Zhu, Y., 2012. Transient behavior and dynamic performance of cascade heat pump water heater with thermal storage system. *Applied Energy*, 91(1), pp.187–196. Available at: http://linkinghub.elsevier.com/retrieve/pii/S0306261911005927 [Accessed September 13, 2012].

Yagoub, W., Doherty, P. & Riffat, S., 2006. Solar energy-gas driven micro-CHP system for an office building. *Applied Thermal Engineering*, 26(14-15), pp.1604–1610. Available at: http://linkinghub.elsevier.com/retrieve/pii/S135943110500414X [Accessed August 3, 2011].

Yamada, Y. & Nishizaki, K., 2009. Next generation model of the world's first residential PEMFC cogeneration system goes on sale. In *Proceedings of the 24th World Gas Conference 5 - 9 October 2009*. Buenos Aires, pp. 1–7.

Yang, Z., Wang, W. & Wu, X., 2013. Thermal modeling and operating tests for a gas-engine driven heat pump working as a water heater in winter. *Energy and Buildings*, 58(2010), pp.219–226. Available at: http://linkinghub.elsevier.com/retrieve/pii/S037877881200583X [Accessed May 17, 2013].

Yari, M. & Sirousazar, M., 2007. Performance analysis of the ejector-vapour compression refrigeration cycle. *Proceedings of the Institution of Mechanical Engineers, Part A: Journal of Power and Energy*, 221(8), pp.1089–1098. Available at: http://pia.sagepub.com/lookup/doi/10.1243/09576509JPE484 [Accessed January 9, 2013].

Young, B. & Henderson, J., 2008. *Domestic heating systems ranked by carbon emissions*, Garston: Building Research Establishment Ltd.

Yun, K.T., Cho, H., Luck, R. & Mago, P.J., 2013. Modeling of reciprocating internal combustion engines for power generation and heat recovery. *Applied Energy*, 102, pp.327–

335. Available at: http://linkinghub.elsevier.com/retrieve/pii/S0306261912005326 [Accessed March 26, 2013].

Zhang, H., Arens, E. & Pasut, W., 2011. Air temperature thresholds for indoor comfort and perceived air quality. *Building Research & Information*, 39(2), pp.134–144. Available at: http://www.informaworld.com/openurl?genre=article&doi=10.1080/09613218.2011.5527 03&magic=crossref%7c%7cD404A21C5BB053405B1A640AFFD44AE3 [Accessed March 30, 2011].

9. Appendix B: Nomenclature

Note that although SI units are used wherever possible in equations, values are occasionally expressed in alternative units (e.g. °C or kWh) in the text when these units make the values clearer to the reader. These occurrences are clearly indicated in the text.

Units used:

- J   Joules
- kg   kilogram
- K   degrees Kelvin
- m   metres
- Pa   Pascals (N/m^2)
- W   Watts

A_R Predicted mean vote – measure of thermal comfort

c_B Building fabric mean specific heat capacity (J/kgK)

c_E Heat emitter system mean specific heat capacity (J/kgK)

c_H Heater block mean specific heat capacity (J/kgK)

c_p Specific heat capacity of air at constant pressure (J/kgK)

c_W Specific heat capacity of water (J/kgK)

c_X Heater heat exchanger mean specific heat capacity (J/kgK)

C CO_2 emissions (kg)

C_{GH} CO_2 emissions from electricity for heating (average mix assumption) (kg)

C_{GD} CO_2 emissions from electricity for heating (marginal mix assumption) (kg)

E Exergy (J)

$\dot{E}_{EA}$ Exergy flow rate entering inside air from emitter system (W)

E_F Exergy content of fuel entering heating system (J)

E_{GD} Exergy requirement for electricity generated to supply heating (marginal mix assumption) (J)

E_{GH} Exergy requirement for electricity generated to supply heating (average mix assumption) (J)

$\dot{E}_{XE}$ Exergy flow rate entering heat emitter system (W)

F Primary energy requirement (J)

G Gibbs energy of reaction (J)

H Enthalpy (J)

h_F	Specific enthalpy of combustion of fuel (J/kg)
H_F	Enthalpy content of fuel entering heating system (J)
H_{GD}	Energy requirement for electricity generated to supply heating (marginal mix assumption) (J)
H_{GH}	Energy requirement for electricity generated to supply heating (average mix assumption) (J)
H_S	Enthalpy content of fuel entering supplementary (gas boiler) heating system (J)
i	Time step index
I	Irradiation intensity (W/m^2)
k_{AB}	Inside air to building fabric, heat transfer coefficient (W/K)
k_{B0}	Building fabric to outside air, heat transfer coefficient (W/K)
k_C	Heating control coefficient (W/K)
k_{EA}	Heat emitters to inside air, heat transfer coefficient when temperature difference is T_{DE} (W/K)
k_F	SE-mCHP fuel consumption adjustment coefficient
k_{GS}	Fraction of electricity lost during transmission and distribution
k_{H0}	Heater block heat loss coefficient (W/K)
k_{HH}	Thermal efficiency coefficient, i.e. effectively gross thermal efficiency before thermal losses from engine block are taken into account
k_{HX}	Heater block to heater heat exchanger, heat transfer coefficient (W/K)
k_{IB}	Effective solar area ("windows area") (m^2)
k_{PM}	Ratio of modelled future demand to current generation (excluding heating and EV)
k_{UA}	Buffer tank heat loss coefficient (W/K)
k_{UE}	Buffer tank to heat emitter system heat transfer coefficient (W/K)
k_{WA}	DHW tank heat loss coefficient (W/K)
k_{WQ}	Heat pump coefficient of performance
k_{XE}	Heater heat exchanger to heat emitter system, heat transfer coefficient (W/K)
k_{XU}	Heater heat exchanger to buffer tank, heat transfer coefficient (W/K)
k_{XW}	Heater heat exchanger to DHW tank, heat transfer coefficient (W/K)
k_P	Heating control coefficient adjustment factor
L	used to denote different generating power plant types
m_A	Inside air mass (kg)
$\dot{m}_A$	Air infiltration rate (kg/s)
m_B	Building fabric effective thermal mass (kg)

m_E	Heat emitter system effective thermal mass (kg)
$\dot{m}_F$	Fuel mass flow rate (kg/s)
m_H	Heater block effective thermal mass (kg)
m_U	Buffer tank water mass (kg)
m_W	DHW water mass (kg)
$\dot{m}_W$	DHW flow rate (kg/s)
m_X	Heater heat exchanger mass (kg)
N_f	Number of moles of substance f
N_R	Number of occupants
P	Pressure (Pa)
$\dot{Q}_{A0}$	Heat flow rate from inside air to outside air due to infiltration (W)
$\dot{Q}_{B0}$	Heat flow rate from building fabric to outside air (W)
$\dot{Q}_{AB}$	Heat flow rate from inside air to building fabric (W)
$\dot{Q}_{EA}$	Heat flow rate from heat emitters to inside air (W)
$\dot{Q}_C$	Control system target heat generation (W)
$\dot{Q}_H$	Rate of heat generated / heat flow rate into heater block (W)
$\dot{Q}_{Hmax}$	Maximum heat generation capacity of heating unit (W)
$\dot{Q}_{H0}$	Rate of heat loss from heater block to atmosphere (W)
$\dot{Q}_{HX}$	Heat flow rate from heater block into heater heat exchanger (W)
$\dot{Q}_{XE}$	Heat flow rate from heater heat exchanger to heat emitters (W)
$\dot{Q}_{XU}$	Heat flow rate from heater heat exchanger to buffer tank (W)
$\dot{Q}_{UE}$	Heat flow rate from buffer tank to heat emitters (W)
$\dot{Q}_{IB}$	Rate of building fabric gains from solar irradiation (W)
$\dot{Q}_{JA}$	Heat flow rate into inside air from lighting and appliances (W)
$\dot{Q}_{RA}$	Heat flow rate into inside air from occupants (W)
$\dot{Q}_{SU}$	Rate of heat transfer from supplementary burner to buffer tank (W)
$\dot{Q}_{UA}$	Rate of heat loss from buffer tank (gains to inside air) (W)
$\dot{Q}_{WA}$	Rate of heat loss from DHW tank (gains to inside air) (W)
$\dot{Q}_{WR}$	Rate of thermal energy leaving DHW tank as hot water is replaced by cold (W)
$\dot{Q}_{XW}$	Heat flow rate from heater heat exchanger to DHW tank (W)

R	Universal gas constant (J/kgK)
S	Entropy (J/K)
t	Time-step length (s)
t_{WC}	Default time to reheat DHW tank through T_{WX} (s)
T_0	Outside air temperature (K)
T_{0W}	Cold water inlet temperature (K)
T_A	Inside air temperature (K)
T_B	Building fabric temperature (K)
T_{CA}	Control system target inside air temperature after DSM signal (K)
T_{CE}	Target heat emitter flow temperature (K)
T_{DX}	Design condition temperature difference between heat emitter and inside air (K)
T_{DX}	Nominal temperature difference across heater heat exchanger (K)
T_E	Average heat emitter temperature (K)
T_{EC}	Thermostat temperature dead-band (K)
T_{EU}	Heat emitters return temperature (to buffer tank) (K)
T_{EX}	Heat emitters return temperature (to heater heat exchanger) (K)
T_H	Heater block temperature (K)
T_{RA}	Program inside air temperature before DSM signal (K)
T_{Rcold}	Maximum decrease in program temperature acceptable to occupants (K)
T_{Rhot}	Maximum increase in program temperature acceptable to occupants (K)
T_U	Buffer tank temperature (K)
T_{UX}	Buffer tank return temperature (to heater heat exchanger) (K)
T_{UC}	Buffer tank temperature dead-band (K)
T_W	DHW tank temperature (K)
T_{WX}	DHW tank return temperature (to heater heat exchanger) (K)
T_{WC}	DHW tank temperature dead-band (K)
T_X	Heater heat exchanger flow temperature (K)
T_{Z0}	Change to target temperature which would result from free electricity (K)
T_{ZC}	Change in target temperature due to DSM price signal (K)
T_{Zmax}	Change to target temperature which would result from electricity at price z (K)
U	Internal energy (J)

V_W	Daily DHW demand (litre)
$\dot{W}$	Rate of work or electrical power (W)
$\dot{W}_G$	Power generated (by grid) (W)
$\dot{W}_H$	Electrical power flow to heating system (positive is consumption, negative is generation) (W)
$\dot{W}_{Hmax}$	Maximum electrical power flow to heating system (W)
$\dot{W}_J$	Power demand of appliances & lighting (W)
$\dot{W}_L$	Power generated by plant type L (W)
W_{LD}	Electrical energy generated by plant type L to meet demand due to heating (calculated using marginal assumption) (J)
W_{LH}	Electrical energy generated by plant type L to meet demand due to heating (calculated using average mix assumption) (J)
$\dot{W}_S$	Power supplied (by grid) (W)
X	Power fraction: proportion of energy supplied or consumed as electricity
Y_i	"Cost" of electricity at time i
Z_i	"Price" of electricity at time i
Z_{max}	Maximum allowable "price" of electricity
η_e	Electrical efficiency
η_{th}	Thermal efficiency
η_{tot}	Total energy efficiency of device (relative to gross calorific value of fuel)
μ_f	Chemical potential of substance f (V)
ψ	Exergy efficiency of system
ϕ	Ratio of exergy content of fuel to gross calorific value of fuel

10. Appendix C: Journal paper

Thermodynamic efficiency of low-carbon domestic heating systems: heat pumps and micro-cogeneration.